# AUBURN UNIVERSITY

## THERMAL CONDUCTIVITY OF HETEROGENEOUS MIXTURES

## AND

## LUNAR SOILS

Final Report

Contract NAS8-26579

R. I. Vachon, A. G. Prakouras,
R. Crane, and M. S. Khader

**School of Engineering**
**Department of Mechanical Engineering**
**Thermoscience Group**

Under Contract With

George C. Marshall Space Flight Center
National Aeronautics & Space Administration

Administered Through

# ENGINEERING EXPERIMENT STATION
## AUBURN UNIVERSITY
### AUBURN, ALABAMA 36830

October, 1973

# AUBURN UNIVERSITY

THERMAL CONDUCTIVITY OF HETEROGENEOUS MIXTURES

AND

LUNAR SOILS

Final Report

Contract NAS8-26579

by

R. I. Vachon, A. G. Prakouras,
R. Crane, and M. S. Khader

School of Engineering
Department of Mechanical Engineering
Thermoscience Group

Under Contract With

George C. Marshall Space Flight Center
National Aeronautics & Space Administration

Administered Through

ENGINEERING EXPERIMENT STATION
Auburn University
Auburn, Alabama   36830

October, 1973

i

## TABLE OF CONTENTS

TABLE OF CONTENTS (Continued)

LIST OF ILLUSTRATIONS (Concluded)

# LIST OF TABLES

ix

LIST OF TABLES (continued)

# FOREWORD

This document is the final report for Contract NAS8-26579, "Thermal Conductivity of Heterogeneous Mixtures and Lunar Soils." The work was performed by R. I. Vachon, A. G. Prakouras, R. A. Crane and M. S. Khader of Auburn University, Department of Mechanical Engineering, for the National Aeronautics and Space Administration, George C. Marshall Space Flight Center. The period of performance of this study was from October 1970 to October 1973.

ABSTRACT

The heat transport properties of the lunar soil are important
in determining the thermal response of the lunar surface.  This informa-
tion leads toward a wider understanding of the nature of the moon
and ultimately of the universe itself.  The study to be described in
this report concerns itself only with one aspect of the greater problem;
the theoretical evaluation of the effective thermal conductivity of
granular materials.  The basic approarch has been entirely analytical
as others have previously undertaken direct heat transfer measurements.
This work supplements the experimental results of the thermal probe
on the Apollo 17 mission as well as the experiments performed
on lunar samples which have been returned from previous Apollo missions.
Moreover the results are intended as an aid in future evaluation of
the extensive scientific data from both the manned and unmanned
exploratory probes.  The basic formulation is intended to be as general
as possible; this allows application of the final results not only to
terrestial bodies which are yet to be explored but also to a wide
range of non-space related technological applications.  These include
such diverse engineering applications as nuclear power generation,
petroleum production, food processing, chemical production, underground
energy transmission and thermal insulation design.  In addition

analogous diffusion type problems are met in work concerning magnetism, electricity and hydrodynamics.

# NOMENCLATURE

## A. Roman Alphabet

| Symbol | | Dimensional Units |
|---|---|---|
| A | Cross-sectional area | $m^2$ |
| $\bar{a}(T)$ | Rosseland mean absorption coefficient | $m^{-1}$ |
| B | $\left[ k_d/C(k_c - k_d) \right]$ | |
| C | Geometrical constant | |
| d | Particle diameter | m |
| D | One dimensional solid fraction | m |
| $D_a$ | Lower truncation point of granules | m |
| $D_b$ | Upper truncation point of granules | m |
| $D_p$ | Effective pore size | m |
| $(D_p)_c$ | Effective pore size for conduction | m |
| $(D_p)_h$ | Hydraulic diameter | m |
| e | Emissivity | |
| E | Young's modulus | $N/m^2$ |
| F | Ratio of constituent temperature gradients | |
| $F_1$ | Force between particles | N |
| $F_o$ | $k_e/k_o$ | |

| $F_w$ | $(k_e - k_\infty) / (k_0 - k_\infty)$ | |
|---|---|---|
| $F_\infty$ | $k_e/k_\infty$ | |
| $f$ | Frequency function | |
| $f_i$ | Depolarization factor | |
| $g$ | Gravitational acceleration | $m/sec^2$ |
| $g^*$ | Temperature jump distance | m |
| $h_r$ | Coefficient associated with surface microroughness | |
| $k$ | Wiener's constant | |
| $k_c$ | Conductivity of continuous phase | $kcal/m-hr-^{\circ}K$ |
| $k_{c_r}$ | Contact conductivity | $kcal/m-hr-^{\circ}K$ |
| $k_d$ | Conductivity of discontinuous phase | $kcal/m-hr-^{\circ}K$ |
| $k_e$ | Effective conductivity | $kcal/m-hr-^{\circ}K$ |
| $k_g$ | Conductivity of gaseous phase | $kcal/m-hr-^{\circ}K$ |
| $k_g^*$ | Conductivity of gaseous phase at reduced pressures | $kcal/m-hr-^{\circ}K$ |
| $k_k$ | Coefficient associated with microgaps at contact areas | |
| $k_r$ | Radiant conductivity | $kcal/m-hr-^{\circ}K$ |
| $k_s$ | Conductivity of solid phase | $kcal/m-hr-^{\circ}K$ |
| $k_{c_o}$ | Effective conductivity for uniform heat flux | $kcal/m-hr-^{\circ}K$ |
| $k_{e_p}$ | Wiener's parallel phase effective conductivity | $kcal/m-hr-^{\circ}K$ |

| Symbol | Description | Units |
|---|---|---|
| $k_{e_s}$ | Wiener's series phase effective conductivity | kcal/m-hr-°K |
| $k_{c_\infty}$ | Effective conductivity for parallel isotherms | kcal/m-hr-°K |
| Kn | Knudsen number | |
| m | Hamilton's shape factor | |
| M | Measure of sample size | |
| n | Coordination number | |
| N | Grid Size | |
| $N_c$ | Number of contact points per unit volume | |
| p | Pressure | $N/m^2$ |
| pij | Pressure tensor | $N/m^2$ |
| $p_b$ | Breakaway pressure | $N/m^2$ |
| P | Volume fraction of continuous phase (porosity) | |
| $P_1$ | One dimensional solid fraction | |
| Pr | Prandtl number | |
| Q | Total heat transfer | kcal/hr |
| $q_r$ | Radiation heat flux | $kcal/hr-ft^2$ |
| r | Sphere radius | m |
| $r_c$ | Contact area radius | m |
| $R_c$ | Contact resistance | hr-°K/kcal |
| $\overline{R}_c$ | Total conduction thermal resistance | hr-°K/kcal |
| $R_e$ | Effective bulk resistance | hr-°K/kcal |

| $R_i$ | Effective element resistance | hr-$^\circ$K/kcal |
| --- | --- | --- |
| $R_L$ | Resistance to heat flow due to contraction of heat flow lines | hr-$^\circ$K/kcal |
| $R_o$ | Resistance due to oxidizing film | hr-$^\circ$K/kcal |
| $R_s$ | Resistance of solid sphere with two contact areas | hr-$^\circ$K/kcal |
| $R_{s_p}$ | Resistance due to microroughness of solid particles | hr-$^\circ$K/kcal |
| $R_1$ | Solid particle thermal resistance | hr-$^\circ$K/kcal |
| s | Molecular diameter | m |
| S | Two-dimensional solid fraction | |
| T | Temperature | |
| w | Overrelaxation factor | |
| x | Sample dimension | m |
| $x_o$ | Radius of deformed particle | m |
| $V_h$ | Mean void equivalent hole volume | m$^3$ |
| z | Depth below the surface | m |

## B. Greek Alphabet

| $\alpha$ | Thermal accommodation coefficient | |
| --- | --- | --- |
| $\delta_{ij}$ | Kronecker delta | |
| $\varepsilon$ | Local solid fraction | |
| $\bar{\varepsilon}$ | Bulk solid fraction | |
| $\lambda$ | Molecular mean free path | m |
| $\bar{\lambda}$ | Effective molecular mean free path | m |
| $\mu$ | Mode of solid or void fraction | |
| $\mu_1$ | Mode of one-dimensional solid fraction | |

| $\nu$ | Poisson's ratio | |
| $\rho$ | Density | $kgr/m^3$ |
| $\rho_\infty$ | Solid material density | $kgr/m^3$ |
| $\rho_o$ | Surface material density | $kgr/m^3$ |
| $\sigma$ | Standard deviation of solid or void fraction | |
| $\sigma_1$ | Standard deviation of one-dimensional solid fraction | |
| $\sigma_b$ | Stefan-Boltzman constant | $kcal/m^2\text{-}°K^4$ |
| $\phi$ | Local solid fraction | |

# I.  INTRODUCTION AND OUTLINE OF REPORT

Considerable effort has been expended over the past sixty years to find means of calculating the effective thermal conductivity of heterogeneous mixtures from the conductivities of the individual components [1-128].[*] Interests in developing techniques for such calculations have been motivated by the widespread applications of heterogeneous mixtures in such diverse fields as nuclear power generation [21], food processing [76], chemical industry [75], process equipment design [37], geology [23], petroleum production [36], thermal insulation design [26], cryogenics [60] and foundary work [58].

About three years ago researchers at the Marshall Space Flight Center in Huntsville were working on the development of a thermophysical model of the lunar surface. During the course of this development it was found that a method of predicting the effective thermal conductivity of the lunar soil was required. A review of the available literature indicated that application of the proposed correlations to the case of lunar soils resulted in considerable error between analytical and experimental values. As a result, a study was undertaken at Auburn University to determine the causes of failure and develop new correlations. The scope of this study is to extend or develop analytical

---

[*]Numbers in brackets refer to references cited.

1

techniques of predicting the constant thermal conductivity of hetero-
geneous mixtures and include methods for the prediction of variable
thermal conductivity. The techniques developed in this report are
as generally applicable as possible, but specific enough for the
analytical results to be compared with experimental data for many
classes of heterogeneous mixtures, and in particular with the experi-
mental results on basalt powders under vacuum conditions.

The term heterogeneous mixtures encompasses a large number of
single-phase, two-phase or multi-phase physical systems, an excellent
classification of which is given in [70]. The common characteristics
of all these systems, with respect to the conduction of heat, is the
thermal conductivity and volume fraction of each individual phase.
Apart from these characteristics, the conduction of heat in heterogeneous
mixtures in general depends on the following parameters.

1. Particle shape and size distribution;

2. Pore shape and size distribution;

3. Coordination number;

4. Contact resistance.

Obviously, all parameters do not enter the problem for each class of
heterogeneous mixtures. For example, in the determination of the
effective thermal conductivity of emulsions and suspensions the last
three parameters are not relevant. The relevant parameters in each
case can be determined by considering the modes in which heat is
transferred through the mixture. It has been generally agreed by the
investigators that the transfer of energy occurs by three mechanisms
[29, 30, 32].

1. Through the voids by conduction, convection and radiation;

2. Through a series path consisting of an effective solid-path length and void-path length;

3. Through the solid phase, the energy flowing from one particle to the next through the area of contact.

The extent to which each mechanism influences the overall heat transfer process depends on the geometry of the system under consideration, together with the environment the heterogeneous mixture is subjected to, as defined by temperature, pressure, and mechanical loading conditions.

The effective thermal conductivity of a heterogeneous mixture may be defined as the ratio of the overall heat flux to the overall temperature gradient. This approach requires that the material be treated as a continuous single phase so that the temperature distribution predicted by such a model coincides with that of the physical system only "in the large" [4]. This concept has proven to be a very effective tool in predicting the transfer of heat through heterogeneous systems, the dimensions of which are much larger than the dimensions of the individual components.

Construction of a model that represents reasonably well heterogeneous materials has proved to be a difficult problem. Calculation of the effective conductivity of this model has proved to be equally complex. The difficulty does not arise from ignorance of the fundamental laws involved but from complications in applying them [20]. A detailed solution of the conduction problem would require knowledge of the shape, size, location and conductivity of each particle in the system, together with the interactions between particles. Furthermore, a complicated numerical method of solution would be required.

To overcome these difficulties, investigators have generally followed

two methods of approach.

1. A basic repeated structural unit that represents reasonably
well the heterogeneous mixture has been isolated, and equations
have been derived from special geometries of this unit cell based on
the assumption that heat flows in straight lines, normal to parallel
isothermal planes.

2. Based on the assumption of a regular or random distribution
of spherical particles in such small concentrations that there is no
field interaction, the temperature distribution in the system is
determined. Subsequently, the effective thermal conductivity of
the system is evaluated from the Fourier-Biot law.

In this study both methods have been analyzed and refined, so

that they can be applied to many classes of heterogeneous mixtures, over

a wide range of pressures and temperatures. In the proposed developments,

consideration will be primarily directed to two-phase granular systems

and powders for which the following assumptions are valid.

1. The thermal properties of the constituents are both homogeneous
and isotropic;

2. All samples are large in comparison with individual particle
size;

3. All samples contain a sufficient number of particles so that
they can be considered typical of the selected packing;

4. The convective component of heat transfer is sufficiently
small to be neglected.

The first three assumptions are consistent with the concept of the

effective thermal conductivity of granular materials, and permit one

to extend the results obtained from the analysis of a unit cube of the

material to the packing as a whole. The fourth assumption is based on

the studies of Waddams [6] and Wilhelm et al [37] who concluded that

natural convection is negligible for pressures below 10 atmospheres, and

particle diameters less than 3 to 6 mm. Consequently for most granular
materials and powders the transfer of heat by natural convection is
negligibly small.

In Chapter 2 of this report the background information, consisting
of prominent models proposed in the literature, is presented. The
available heat transfer models for heterogeneous systems are classified
as being either flux law models or Ohm's law models. The Ohm's law
models are further classified according to the heat flow assumptions
as being either uniform heat flux models or parallel isotherms models.

In Chapter 3 several representative models have been applied to
172 granular materials, and the calculated values have been compared
to experimental results. The comparisons are presented in a graphical
form. A careful analysis of Figures 3-1 through 3-17 indicates that
the discrepancy between the analytical models and the physical granular
systems can be attributed to one of the following causes.

1.  Failure to account for finite particle contact area;

2.  Failure to utilize a realistic geometry, or a realistic
    distribution of the two phases;

3.  Idealized heat flow assumptions.

As a result of this analysis, the aim of this study has been focused
on an attempt to develop models in which the above three sources of
error are partially or totally eliminated.

The effect of the uniform heat flux and parallel isotherms assump-
tions on the predicted thermal conductivity of randomly packed granular
systems has been investigated in Chapter 4. Special attention has been

directed to the idealized heat flow assumptions, because the possibility of utilizing either one simplifies considerably the problem. However, application of the uniform heat flux assumption to a physically realistic probabilistic model results in calculated effective conductivities that are too low, whereas application of the parallel isotherms assumption results in calculated effective conductivities that are too high. The reason for such behavior is that infinite and zero conductivities in the normal to the heat flow direction are associated with the parallel isotherms and uniform heat flux assumptions respectively.

In Chapter 5 a parallel isotherms probabilistic model has been developed. This model is based upon an extension of concepts originally proposed by Tsao [8], on the basis of which the effective thermal conductivity can be expressed in terms of the mode, $\mu$, and the standard deviation, $\sigma$, of the one dimensional porosity as introduced by Tsao. The mode, $\mu$, has been approximated by the bulk porosity of the granular system, and the standard deviation, $\sigma$, has been correlated to the solid volume fraction only, on the basis of experimental evidence. The resulting equation has been used to determine the effective thermal conductivity of packed beds with solid fractions between 0.30 and 0.70.

The same basic concepts have been applied in the development of the stochastic model of Chapter 6. Noting that the effective conductivity tends to reach a fixed value for $\sigma$ sufficiently large, limiting expressions have been developed for the effective thermal conductivity utilizing both the parallel isotherms and the uniform heat flux assumptions.

Then, rather than assuming both an unrealistic heat flow model and a distorted distribution, an experimentally derived correlation factor has been obtained for each of the limiting expressions. In addition, an experimentally derived weighting factor has been obtained relating both limiting expressions to experimental data.

In Chapter 7, the packing characteristics of random heterogeneous mixtures have been utilized to define the phase distribution in a unit cube of a granular material, by extending the digital simulation technique originally proposed by Baxley and Couper [20]. The temperature distribution in the unit cube was then determined assuming both three-dimensional heat transfer, potential field interaction, and contact resistance between particles. Finally, the effective thermal conductivity of the material was determined by summing heat flows in the direction of the mean heat flow only.

All models discussed up to this point are generally applicable to granular materials at interstitial gas pressures ranging from atmospheric to vacuum. In particular, for a vacuum environment, the basic modes of heat transfer are conduction through the granules and contact areas, and radiation. This situation is analyzed in Chapter 8 on the basis of a parallel isotherms model consisting of an array of spheres. The effect of changes in bulk density and mechanical loading with depth are included, and compared to experimental data on lunar fines.

In Chapters 9 and 10 the results obtained by all models are compared and evaluated with respect to the simplifying assumptions introduced in each model. Moreover, recommendations are made concerning

the extent of the applicability of each model and the areas where more work is required in order to improve the dependability of the predicted effective thermal conductivity values.

The dependence of the effective thermal conductivity on pressure and temperature, at reduced interstitial gas pressures, has been generally recognized and treated extensively in the literature. Reduction of pressure to extremely low values decreases the effective thermal conductivity of the system by one or more orders of magnitude [62]. This has been attributed to the decrease of the apparent gas conductivity when the mean free path of the gas molecules is of the same order of magnitude or larger than the effective pore size, as indicated in Appendix A. Also, at very low pressures, experimental evidence shows that the effective thermal conductivity of the system is very sensitive to temperature changes [3], indicating that radiative heat transfer between particle surfaces is a controlling factor. The aspects of radiation heat transfer are treated in Appendix B.

In the case of heat flow in granular systems "in vacuo", the convergence of the heat flux lines to the contact areas between particles is characterized by the contact resistance, as indicated in Appendix C.

It is evident that for the development of an accurate model for the prediction of the conductivity of granular systems, the geometry of the model should rely heavily on the characteristics of packed beds. A short review of the advances in packing theory is presented in Appendix F. Two of the characteristics of packed beds are of particular

importance to the heat transfer problem. These are the effective pore size and the coordination number, and are treated separately in Appendices D and E respectively.

In summary, the content and results of this report are as follows:

1. A critical review and classification of previously published models is presented together with a review of the parameters associated with the flow of heat through granular systems;

2. Previously published models have been compared to a large number of experimental data, the results have been evaluated with respect to the basic assumptions introduced in the development of each model, and the causes of failure have been summarized;

3. A theoretical development is presented about the effect that the assumptions of uniform heat flux and parallel isotherms have on the calculated effective thermal conductivity, and the theory has been substantiated by experimental evidence;

4. Four new models based on recent results of packing theory have been developed, and have been successfully applied to granular materials for a pressure range from atmospheric to vacuum;

5. The sources of error for all models have been analyzed and related to the geometry and modes of heat transfer;

6. Detailed recommendations with respect to the geometric parameters required for the description of a generalized physically realistic model have been presented;

7. The results of all models have been utilized in the construction of a recommended physically realistic model, which cannot be analyzed

at present due to lack of experimental data required for the determination of a number of the parameters.

## II. BACKGROUND

Because of the broad occurence of systems involving heat transfer in granular materials, considerable attention has been given to the formulation of a model to allow the prediction of the effective thermal conductivity. Unfortunately, the complexity of the mechanisms contributing toward heat flow is such that no truly satisfactory model has been obtained. The continued proliferation of alternate models attests to these difficulties. Nevertheless progress has been made in developing a representative model and it is now possible to determine the effective thermal conductivity of systems whose constituent conductivities are of similar magnitudes.

Available heat transfer models for heterogeneous systems are generally classified as being either flux-law models or Ohm's law models. The flux law model appears to have received the earliest attention and will be discussed first here.

### Flux Law Models

Flux-law models are characterized by their general approach to the determination of the effective thermal conductivity. First a solution is found to the equation describing the temperature field. The heat flow and temperature gradient are also sought. The Fourier-Biot law of heat conduction is then applied to determine the effective

11

thermal conductivity. The principal advantage of this approach lies in the fact that the actual curvature of heat flux lines and isotherms may be taken into account. Most of the methods applicable to heat transfer in heterogeneous materials were originally developed for use in electrical theory, magnetism or hydrodynamics. However each case is applicable to heat transfer in heterogeneous systems in that the same mathematical equations apply.

In considering a cube of heterogeneous material containing a single particle, the fundamental heat conduction equation may be written separately in each of the two phases. It is stipulated that the boundary conditions require a continuous temperature distribution and a continuous heat flux within the field. If each phase is itself isotropic and homogeneous the equations reduce to the form of Laplace's equation. Solutions of this equation are well known.

Maxwell [9] used this technique in finding an expression for the effective conductivity of a suspension of spheres

$$\frac{k_e}{k_c} = \frac{k_d + 2k_c - 2\bar{\varepsilon}(k_c - k_d)}{k_d + 2k_c + \bar{\varepsilon}(k_c - k_d)} \tag{2-1}$$

In the derivation of this equation, it was assumed that the spheres were at sufficient distances from one another that the disturbance of the flux lines around each particle did not extend to neighboring particles. It follows that the geometry of the array of particles does not influence the effective thermal conductivity wherever Equation (2-1) applies.

Several authors have worked to extend the model for dilute suspensions to include solids of alternate geometries. Burgers [10]

and Fricke [11] developed equations for disperse suspensions with ellipsoidal solid particles. Many particle shapes, including flakes, spheres and needles, may be approximated by ellipsoids by properly selecting the relative size of the semi-principal axes. Burgers' equation was

$$k_e = \frac{(1-\bar{\epsilon})k_c + \bar{\epsilon}Fk_d}{(1-\bar{\epsilon}) + \bar{\epsilon}F} \tag{2-2}$$

In this relation F represents the ratio of the overall average temperature gradient in the discontinuous phase to that in the continuous phase. This ratio was found to be given by

$$F = \frac{1}{3} \sum_{i=1}^{3} \left[ 1 + \left( \frac{k_d}{k_c} - 1 \right) f_i \right]^{-1}$$

The factor, $f_i$, referred to as the depolarization factor, depends on the length of the semi-principal axes of the ellipsoid. These factors have been normalized such that $\sum_{i=1}^{3} f_i = 1$. If the three semi-principal axes are equal the particles become spheres and Equation (2-2) reduces to Equation (2-1).

DeVries [12] applied Equation (2-2) to granular materials in calculating the thermal conductivity of soils. He found that if $0 \leq k_d/k_c \leq 10$ then the error obtained from Burgers' equation would be less than 10%. Obviously if the conductivities of the constituent phases are sufficiently close there will be very little disturbance in the flux lines around the particles. Thus the restriction stated by Maxwell is satisfied even though the particles are in close proximity.

Hamilton and Crosser [13] extended Burgers' development to include particles of arbitrary shape. The particle shape was defined in terms of sphericitity, $\psi$, that is in terms of the ratio of the surface area of a sphere compared to that of a particle having the same volume [66]. An empirical relation was developed giving the ratio of the average temperature gradients, F, as a function of the sphericity and the constituent conductivities. The modified Maxwell equation used by Hamilton and Crosser is

$$\frac{k_e}{k_c} = \frac{k_d + (m-1)k_c - (m-1)\,\bar{\varepsilon}\,(k_c - k_d)}{k_d + (m-1)k_c + \bar{\varepsilon}\,(k_c - k_d)} \tag{2-3}$$

where $m = 3/\psi$. It was found that whenever $0 \leq k_d/k_c \leq 100$ the shape of the solid particles had little influence on the overall conductivity of disperse systems. For spherical particles ($\psi = 1$) Equation (2-3) reduces to Maxwell's equation.

Lord Rayleigh [14] considered the case in which the interaction between particles could no longer be neglected. In essence Laplace's equation was solved to find the potential field in and about a single spherical particle. Noting that the Laplace equation is linear it was then possible to utilize the principle of superposition to determine the equivalent field for a given particle distribution. Using a cubic array Lord Rayleigh, with a slight correction given by Runge [15], obtained

$$\frac{k_e}{k_c} = \frac{\left(\frac{2k_c+k_d}{k_c-k_d}\right) - 2\bar{\varepsilon} - 0.525 \left(\frac{3k_c-3k_d}{4k_c+3k_d}\right) \bar{\varepsilon}^{10/3}}{\left(\frac{2k_c+k_d}{k_c-k_d}\right) + \bar{\varepsilon} - 0.525 \left(\frac{3k_c-3k_d}{4k_c+3k_d}\right) \bar{\varepsilon}^{10/3}} \qquad (2\text{-}4)$$

It should be noted that this equation reduces to Maxwell's equation whenever $\bar{\varepsilon}$ is sufficiently small that the last term in the numerator and denominator may be neglected. Meredith and Tobias [16] have followed Lord Rayleigh's development including a larger number of terms from the infinite series defining the temperature field. The equation is

$$\frac{k_e}{k_c} = \frac{\frac{2k_c+k_d}{k_c-k_d} - 2\bar{\varepsilon} + 0.409 \left(\frac{6k_c+3k_d}{4k_c+3k_d}\right) \bar{\varepsilon}^{\frac{7}{3}} - 2.133 \left(\frac{3k_c-3k_d}{4k_c+3k_d}\right) \bar{\varepsilon}^{\frac{10}{3}}}{\frac{2k_c+k_d}{k_c-k_d} + \bar{\varepsilon} + 0.409 \left(\frac{6k_c+3k_d}{4k_c+3k_d}\right) \bar{\varepsilon}^{\frac{7}{3}} - 0.906 \left(\frac{3k_c-3k_d}{4k_c+3k_d}\right) \bar{\varepsilon}^{\frac{10}{3}}} \qquad (2\text{-}5)$$

Both equations compare closely with available experimental results obtained for spheres packed in a cubic geometry. However these equations do not appear applicable to systems with widely differing constituent conductivities [16]. Moreover, results do not compare favorably with those obtained for random packing of spheres. The explanation for this descrepancy is offered by Laubitz [17] that although the mathematics is exact the model is so artificial that it radically departs from real powders.

Bruggeman [18] allowed both for particle size variation and arbitrary particle orientation, by assuming that various elements of the same type have in their neighborhood all possible distributions

of elements of all possible types, in the same frequency in which
the different types are encountered in the two-phase mixture. He
applied Maxwell's equation to find the effective conductivity of an
arbitrary two-phase system, and then using this value as the con-
ductivity of the continuous phase he applied Maxwell's equation again
to find the effective conductivity when one more particle is added
to the system. If this process is repeated indefinitely, for an
infinite particle size range, the effective conductivity approaches
a limit given by

$$1 - \bar{\epsilon} = \frac{k_e - k_d}{k_c - k_d} \left(\frac{k_c}{k_e}\right)^{1/3} \tag{2-6}$$

Using the same basic approach but accounting for only two additions
of the solid particles, Meredith and Tobias [19] obtained a second
relation

$$\frac{k_e}{k_c} = \left[\frac{4k_c + 2k_d - 2\bar{\epsilon}(k_c - k_d)}{4k_c + 2k_d + \bar{\epsilon}(k_c - k_d)}\right]\left[\frac{4k_c + 2k_d - \bar{\epsilon}(4k_c - k_d)}{4k_c + 2k_d - \bar{\epsilon}(k_c - 2k_d)}\right] \tag{2-7}$$

Baxley and Cooper [20] utilized a digital simulation technique
to describe heat transfer in heterogeneous materials. The model
incorporated a random placement technique to arrange solid cubes in
a square array. The Laplace equation was then written for the entire
two phase region and was solved utilizing a numerical relaxation
technique. Once having obtained the proper temperature distribution

for the system, the effective conductivity was obtained by applying the Fourier-Biot law. The resulting equations were given in terms of a computer code. Calculational results obtained from the model appear to correlate data for suspensions with good accuracy. The authors note that solid particles of any shape could be considered by constructing such particles from sufficiently small cubes. The success of this technique has motivated the construction and analysis of a similar model for powders and granular materials, which is one of the subjects of this study.

Summarizing the flux law models it is found that they may be generally categorized as extensions of the Maxwell model or as finite difference models. The models derived from Maxwell's formulation may suffer from one or more of a series of shortcomings as applied to granular systems. Maxwell's original equation failed to account for the interaction of the flux lines around particles. Other equations are restricted to a regular and quite unrealistic array. Each breaks down when applied to systems in which the conductivity of the discontinuous phase is several orders of magnitude larger than that of the continuous phase. Ideally, for systems in which the solid particles touch, $k_e/k_c$ should approach infinity as $k_d/k_c$ approaches infinity; however, this condition is not met in these equations [16]. The reason for this discrepancy appears to be explained by Meredith and Tobias. They suggest that it is due to the neglection of higher order terms in the equation defining the temperature distribution. Thus,

these equations do not appear applicable to the case of granular systems in a medium of extremely low conductivity.

## Ohm's Law Models

The mathematical complexity of the formulation and solution of the flux law model has precluded consideration of anything but the simplest shaped particles and arrangements. Since these formulations have not proved satisfactory in describing most physical systems of randomly packed powders, attention has more recently centered around alternate approaches. Here the Ohm's law model has been used extensively. This model bypasses the determination of the temperature field and seeks instead to evaluate the equivalent thermal resistance for a given array.

Wiener [7] was among the first to apply the electrical analogy to the problem of heat transfer in heterogeneous systems. While he did not obtain an expression for the effective thermal conductivity, it was shown that the value would lie between those predicted by the following formulas:

$$k_{es} = \frac{k_d k_c}{\bar{\varepsilon} k_c + (1-\bar{\varepsilon}) k_d} \tag{2-8}$$

$$k_{ep} = \bar{\varepsilon} k_d + (1-\bar{\varepsilon}) k_c \tag{2-9}$$

These two equations, referred to as Wiener's bounding formulas (Wiernerschen Grenzformeln), represent the cases in which the component resistances are arranged respectively in series, Figure (2-2a), and in parallel, Figure (2-1a) while Equations (7-8) and (2-9) establish

(a) Parallel Model      (b) Loeb's Model
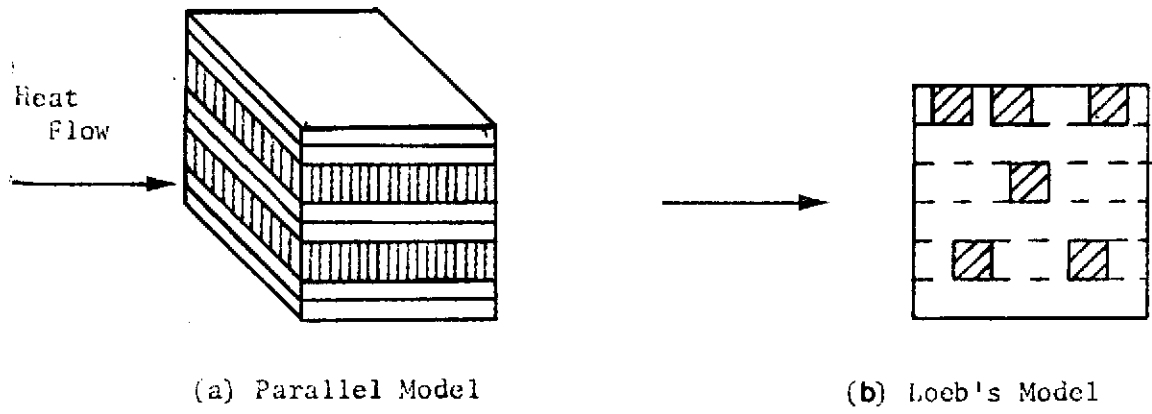
FIGURE 2-1. UNIFORM HEAT FLUX MODELS



(a) Series Model      (b) Jefferson's Model
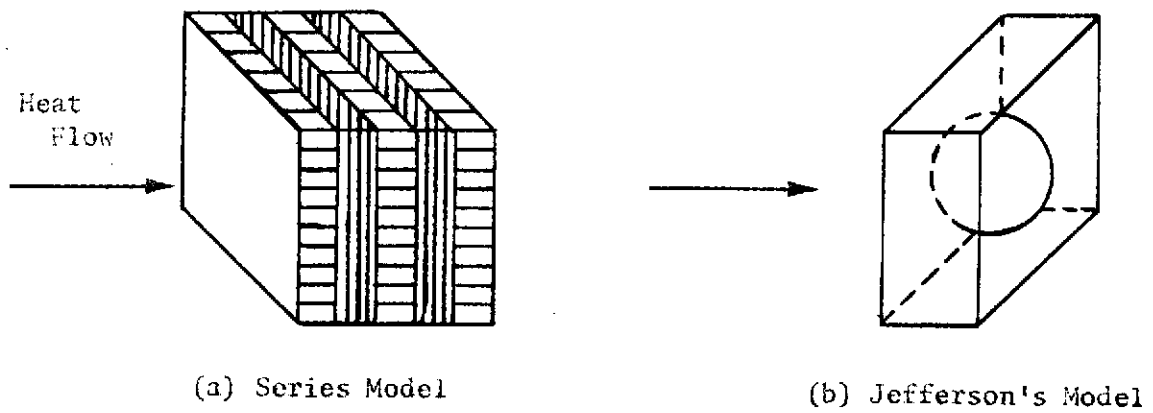
FIGURE 2-2. PARALLEL ISOTHERMS MODELS

upper and lower bounds on the effective conductivity they are not intended to be used to calculate the actual value. This is because the effective conductivity of the system is strongly influenced by the constituent's arrangement [21]. Since neither case corresponds to the actual geometrical arrangement neither formula is satisfactory for such cases.

Several applications have been made of Wiener's results. Note that Equation (2-9) represents the effective thermal conductivity as the weighted arithmetic mean of the constituent conductivities; Equation (2-8) represents the thermal conductivity as the weighted harmonic mean. Lichteneker [22] proposed an equation in which the effective conductivity corresponded to the weighted geometric mean

$$k_e = k_c^{(1-\overline{\varepsilon})} k_d^{\overline{\varepsilon}} \tag{2-10}$$

Woodside and Messmer [23] report that this equation is generally valid for the range $0 < k_d/k_c < 20$. Whenever $k_d/k_c$ exceeds 20 the Lichteneker equation overestimates the effective conductivity.

Bruggeman [18] states that Equation (2-10) allows for random orientation of particles in two directions only. For a truly three-dimensional random dispersion he generalized the Lichteneker equation to obtain

$$k_e = k_c^{[(1-\overline{\varepsilon})(1-k\overline{\varepsilon})]} k_d^{\overline{\varepsilon}[1+k(1-\overline{\varepsilon})]} \tag{2-11}$$

where

$$k = \frac{3}{2} \; \frac{k_d - k_c}{(2\sqrt{k_d} + \sqrt{k_c})(2\sqrt{k_c} + \sqrt{k_d})}$$

Another method of generalizing Wiener's results involves geometrically rearranging the physical system. It would seem reasonable that, since the parallel and series arrangements represent the limiting cases, an equivalent system composed of elements acting partly in parallel and partly in series could be used to represent the physical system.

Several authors have approximated a granular system by representing the solid particles as cubes arranged in a cubic lattice. The uniform spacing between particles is maintained such that the idealized system retains the proper volume fractions. A typical unit cell of this model is represented in Figure (2-3a). It is assumed that the effective thermal conductivity may be determined by considering the equivalent electrical resistances in parallel and in series and by applying Ohm's law.

In taking such an approach, certain additional simplifying assumptions are generally required. The assumption of straight and parallel heat flux lines yields the equivalent electrical network for the cubic array shown in Figure (2-3b). An alternate assumption of straight and parallel isotherms leads to a different equivalent network as shown in Figure (2-3c).

The two networks result in different effective conductivities both of which are approximations to the exact solution. In fact, these two cases represent two bounding solutions to the simplified model. The exact solution will yield an effective conductivity between those given
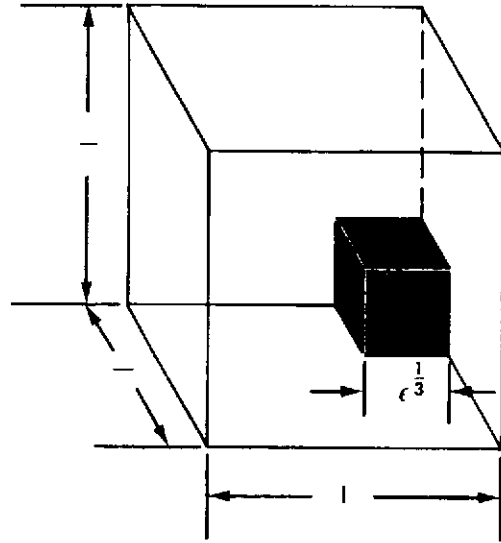
(a)
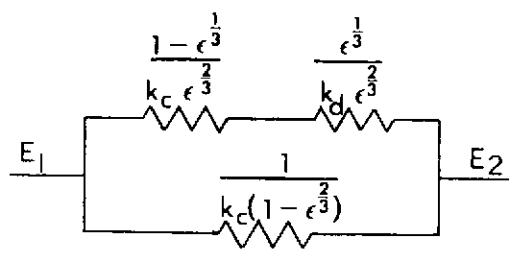
(b)
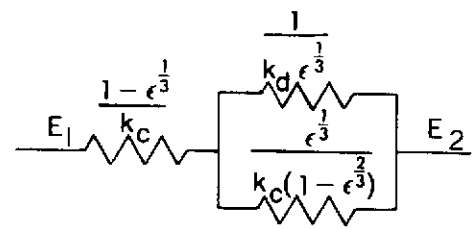
(c)

FIGURE 2-3.  CUBIC LATTICE REPRESENTATION OF GRANULAR
MATERIAL

by the two electrical networks. This is more clearly seen when one considers a nodal point representation of the temperature field in the proposed system. If the resistances normal to the direction of heat flow are assumed to be very large, the heat flow will remain uniform in the direction of the temperature gradient. Conversely, if the lateral resistances are taken as zero the potential will be equal in each lateral plane. Therefore, the assumption of linear and parallel heat flux lines is equivalent to the assumption of infinite lateral resistance; the assumption of parallel isotherms is equivalent to that of zero lateral resistance. The actual laterial resistance will, of course, fall somewhere between zero and infinity so that these two cases form the bounding conditions. Whether the two solutions represent the bounding conditions for the physical system depends upon the suitability of the proposed model.

It is generally assumed that either one or the other bounding condition represents a close approximation to the flow of energy in the proposed model. The suitability of this assumption will be discussed after the respective models have been considered. In compensation for this approximation it has been found possible to consider much more complex geometries than those which are possible using the flux-law model.

## Uniform Heat Flux

Lichteneker [24] and son Frey [25] developed the uniform heat-flux model shown in Figure (2-3b). The effective thermal conductivity is then given as

$$\frac{k_e}{k_c} = \frac{(1 - \bar{\varepsilon}^{\frac{1}{3}} + \bar{\varepsilon}) + \frac{k_c}{k_d}(\bar{\varepsilon}^{\frac{1}{3}} - \bar{\varepsilon})}{(1 - \bar{\varepsilon}^{\frac{1}{3}}) + \frac{k_c}{k_d}\bar{\varepsilon}^{\frac{1}{3}}} \qquad (2\text{-}12)$$

It should be noted that this geometry results in a definite gap between particles and a complete absence of solid to solid contact. While such a model is suitable for dilute suspensions it is doubtful if it could adequately represent granular materials. In cases where the gas conductivity is much less than the solid conductivity, solid to solid heat conduction may, in fact, be the major mode of heat transfer. In such cases it might be anticipated that the proposed model would yield consistently low results, especially in light of the fact that the assumption of linear heat flux lines should lead to low results.

A number of investigators have continued to develop a similar model using various schemes to overcome the problem of the relatively large gap between particles. One such technique is to distort the solid cube, elongating it in the direction of heat flow. Woodside and Messmer [23], Schotte [26], Smith [27] and Willhite, Kunii and Smith [31] developed models assuming such an arrangement. Woodside and Messmer obtained

$$\frac{k_e}{k_c} = \frac{(\bar{\varepsilon} + 0.03)^2 k_d}{0.03 k_d + \bar{\varepsilon} k_c} + 0.97 - \bar{\varepsilon} \qquad (2\text{-}13)$$

The equation of Willhite, Kunii and Smith is

$$\frac{k_e}{k_c} = 1 + \bar{\varepsilon}\left(1 - \frac{k_c}{k_d}\right) + \frac{\gamma}{\alpha}\left(1 - \frac{k_c}{k_d}\right)^2 \bar{\varepsilon} \qquad (2\text{-}14)$$

DIRECTION OF
HEAT FLOW
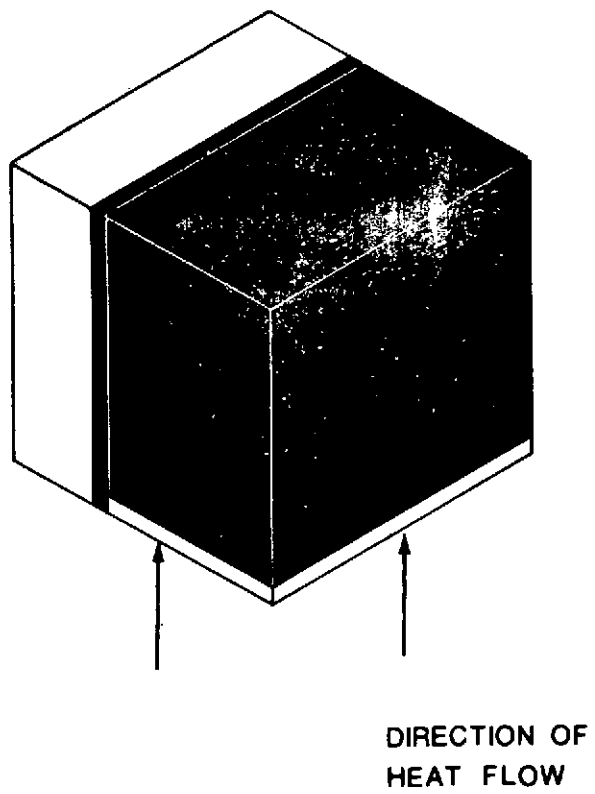
FIGURE 2-4. PARALLELOPIPED REPRESENTATION OF GRANULAR
MATERIAL

where

$$\alpha = \frac{\sin^2\theta}{2} \frac{\left(\frac{k_d-k_c}{k_d}\right)^2 \sin^2\theta}{\ln\left[\frac{k_d}{k_c} - \left(\frac{k_d}{k_c} - 1\right)\cos\theta\right] - \frac{k_d-k_c}{k_d}(1-\cos\theta)}$$

$$\theta = \sin^{-1}\sqrt{\frac{2}{n}}$$

In this relation $n$ is the average number of contact points on the particle. The experimentally derived parameter, $\gamma$, represents the ratio of the effective length of the solid particle to the diameter of the physical particle. The authors state that a value $\gamma \approx 2/3$ correlates a wide range of data.

A number of investigators have continued to develop similar models using various schemes to overcome the problem of the relatively large gap between particles. Bernstein [44] effectively utilized this approach in arranging rectangular particles in a staggered two dimensional array. For high porosity ($\varepsilon \geq 0.5$) systems the solid cube was distorted by lengthening its dimension in the direction of heat flux while decreasing its lateral dimensions to maintain the proper volume fractions. For low porosity systems ($\varepsilon \leq 0.5$) Bernstein interchanged the solid and void regions of the unit cube so that the effective thermal conductivity is given by the equations

$$\frac{k_e}{k_c} = \frac{4\bar{\varepsilon}}{\left(1 + \frac{k_c}{k_d}\right)} + \frac{k_d}{k_c}(1 - 2\bar{\varepsilon}) \qquad (2\text{-}15a)$$

$$\bar{\varepsilon} \leq .50$$

$$\frac{k_e}{k_c} = \frac{4(1-\bar{\varepsilon})}{\left(1 + \frac{k_c}{k_d}\right)} + 2\bar{\varepsilon} - 1 \qquad (2\text{-}15b)$$

$$\bar{\varepsilon} \geq .50$$

A second scheme of reducing the gap between particles considers a portion of the solid phase to pass entirely through the unit cube. This accounts for the residual conductivity of the system in a pure vacuum. A typical element of this type is shown in Figure (2-4). Several authors [28-34] have used this technique to include contact between particles. However, most of these developments have required the inclusion of one or more parameters which must be experimentally obtained for each sample. Generally this information is not available.

Using the same basic assumption of linear heat flux lines Schumann and Voss [35] developed a model using a somewhat different geometry. It was assumed that a unit cell of the material could be replaced by an equivalent geometry in which the two phases are divided by a rectangular hyperbola. Thus the solid phase appears as a somewhat distorted "cylinder" arranged in a square array oriented normal to the direction of heat flux. The varying fraction of the solid phase seems much more representative of the physical system. The effective thermal conductivity obtained by Schumann and Voss is:

$$\frac{k_e}{k_c} = (1-\bar{\varepsilon})^3 + \frac{1 - (1-\bar{\varepsilon})^3}{\left(\frac{k_c}{k_d} + p \frac{k_c}{k_d} - 1\right)} \left\{ 1 + \frac{p(1+p)(k_c-k_d)}{k_c+p(k_c-k_d)} \ln\left[\frac{k_c}{k_d} \frac{(1+p)}{p}\right] \right\}$$

$$(2\text{-}16)$$

where p is implicitly defined by the relation:

$$1 - \bar{\epsilon} = p(p+1) \ln \frac{1+p}{p} - p$$

The inclusion of an implicit relation makes the equation somewhat difficult to solve analytically although a graphical tabulation has been given.

In comparison to the Lichteneker and son Frey model, the model of Schumann and Voss is much more realistic in representing granular systems in that the finite gap between particles has been eliminated. Nevertheless the effective thermal conductivity obtained from this equation still tends to fall below experimentally obtained values. This tendency was noted separately by Preston [36] and Wilhelm [37]. Both authors presented correction terms to the Schumann and Voss equation to bring the calculated value closer to the experimental data. Wilhelm's correlation has been widely used, and its predictions are in good agreement with many experimental data for granular materials since it was constructed from these data. This equation is

$$\log(\Delta \times 10^5) = m + n \left( \frac{k_d}{1-\bar{\epsilon}} \right) \tag{2-17}$$

where $\Delta$ in cal/cm-sec-$^\circ$K is an error term to be added to calculated conductivities according to Schumann and Voss, and the "least squares" values of the constants are

$$m = 0.859 \pm 0.051$$

$$n = 3.12 \pm 0.29 \ (\text{cal/cm-sec-}^\circ\text{K})^{-1}$$

Gorring and Churchill [4] used a development somewhat analogous to Schumann and Voss' for three dimensional particles. In this case, an equivalent geometry was assumed in which the two phases were separated by a parabola of revolution. The solid particles then appear as distorted "spheres" arranged in a square array. For this geometry the effective conductivity is given by

$$\frac{k_e}{k_c} = \frac{\pi}{6\left(1 - \frac{k_c}{k_d}\right)CB} \left\{ \ln\left(\frac{\sqrt{B^2 - Bx_0 + x_0^2}}{B + x_0}\right) + \sqrt{3}\ \tan^{-1}\left(\frac{2x_0 - B}{\sqrt{3}B}\right) \right.$$

$$\left. -\sqrt{3}\ \tan^{-1}\left(\frac{1}{\sqrt{3}}\right) \right\} + \left\{ 1 - \frac{\pi x_0^2}{4} \right\} \qquad (2\text{-}18)$$

where:  $B = \left[\frac{k_c}{C(k_d - k_c)}\right]^{\frac{1}{3}}$

for  $\bar{\epsilon} \leq \frac{\pi}{10}$,  $x_0 = 1.0$

$$C = \frac{10\bar{\epsilon}}{\pi}$$

for  $\bar{\epsilon} \geq \frac{\pi}{10}$,  $x_0 = \frac{1.0}{C^{\frac{1}{3}}}$  $\qquad C = \left[\frac{3\pi}{5\pi - 20\bar{\epsilon}}\right]^{\frac{3}{2}}$

Systems of spherical particles arranged in a square array were studied by Hengst [38] and later by Lyalikov [39] and Kaganer [40]. Kaganer's expression for the effective conductivity of granular systems assumes the form

$$\frac{k_e}{k_c} = \frac{n\bar{\epsilon}k_d}{2(k_d - k_c)} \left[\frac{k_d}{k_d - k_c}\ \ln\left(\frac{k_d}{k_c}\right) - 1\right] \qquad (2\text{-}19)$$

In this expression n is taken as the average number of contacts for each particle. Note that the geometry utilized in this model is precisely the same as that assumed by Lord Rayleigh in the case of touching spheres ($\bar{\epsilon}$ = 0.524). Equation (2-18) is suggested for use with packing fractions greater than 0.524. Physically this is difficult to visualize as denser packings are not possible with the prescribed geometry.

Deissler and Eian [41] accounted for variations in packing fractions in a different manner. Two separate models were developed to account for such variations. One model considered spheres in a cubic array with point contact; the second used cylinders in a square array with line contact. Including the cases in which the material is composed of all solid or all gas, the relation between $k_e/k_c$ and $k_d/k_c$ is then known for four values of $\bar{\epsilon}$. For any other packing fraction the effective conductivity could be found by interpolation. Krupiczka [42] used the same approach but introduced solutions for the spherical and cylindrical arrays based on flux-law models. Krupiczka then curve fitted his solutions together with certain experimental data to obtain

$$\frac{k_e}{k_c} = \left(\frac{k_d}{k_c}\right)^{[0.280 - 0.757 \ln (1-\bar{\epsilon}) - 0.057 \ln (k_d/k_c)]} \tag{2-20}$$

Loeb [69] was one of the first to deviate from an assumed rigid geometry and account for the distribution of the two phases. His basic assumption is that if a unit cube of the two-phase material is subdivided into parallel to the heat flow tubes, the dispersed phase may be arranged to lie completely within a set of tubes (Figure 2-1b). An electrical analogy is then written for each tube, and the conduc-

tance of the unit cube is expressed as the sum of the tube conductances. The final expression for the effective thermal conductivity is

$$k_e = k_c \left[ (1-P_c) + \frac{P_c}{P_L \frac{k_c}{k_d} + (1-P_L)} \right] \tag{2-21}$$

where: $P_c$ = fraction of cross-sectional area occupied by the tubes

$P_L$ = fraction of tube length occupied by discontinuous phase.

## Parallel Isotherms

As previously noted, the development of an Ohm's law model requires first the selection of an equivalent geometry. Then either the assumption of uniform heat flux or parallel isotherms may be used. It is not surprising, then, that frequently models of each type have been developed starting from the same basic configuration.

Russell [43] selected the same cubic array of cubical particles as Lichteneker and son Frey. Assuming parallel isotherms, Russell obtained

$$\frac{k_e}{k_c} = \frac{\varepsilon^{\frac{2}{3}} + \frac{k_c}{k_d} (1-\varepsilon^{\frac{2}{3}})}{\varepsilon^{\frac{2}{3}} - \varepsilon + \frac{k_c}{k_d} (1 - \varepsilon^{\frac{2}{3}} + \varepsilon)} \tag{2-22}$$

Here again, the model does not consider solid to solid contact so that it might be anticipated that results would tend to fall below experimental values. Laubitz [17] reported that Russell's equation typically gave results which were low by about a factor of two.

Jefferson [78] derived an expression for spherical particles, each enclosed in a unit cube of the continuous phase. His derivation

is based on one-half such unit (Figure 2-2b), and the resulting equations are

$$k_e = k_c \left[ 1 - \frac{\pi}{4(1+2n)^2} \right] + \frac{\pi}{4(1+2n)^2} \left[ \frac{(0.5+n) \, k_a \, k_c}{0.5 \, k_c + n \, k_a} \right]$$

(2-23)

$$k_a = k_c \cdot k_d \left[ \frac{2k_d}{(k_d - k_c)^2} \, \ln \left( \frac{k_d}{k_c} \right) - \frac{2}{k_d - k_c} \right]$$

$$n = 0.403 \, ( \overline{\varepsilon} )^{-1/3} - 0.5$$

Baxley and Couper [20] report that for suspensions and emulsions the average error of Equation (2-22) is 21%.

Godbee and Ziegler [45] developed a parallel isotherm model analogous to that proposed by Woodside and Messmer. The solid particles in a heterogeneous system were replaced by a pore free parallelopiped within the representative material cube. The authors have obtained an expression relating the dimensions of the solid region to the material volume fractions and the particle size distribution so that the effective thermal conductivity is given by the relation

$$\frac{k_e}{k_c} = \frac{1}{\left\{ \frac{D/x}{\left( 1 - \frac{S}{x^2} \right) + \frac{k_d}{k_c} \left( \frac{S}{x^2} \right)} + \left( 1 + \frac{D}{x} \right) \right\}}$$

(2-24)

where

$$S = \frac{D^2}{2} \int_{D_a}^{D_b} e^{-u^2/2} \, du$$

$$x = \left(\frac{SD}{1-\bar{\epsilon}}\right)^{1/3}$$

Topper [46], Webb [47] and Woodside [48] proposed models incorporating spherical particles arranged in a cubic lattice similar to that of Hengst. The introduction of spherical particles will tend to reduce the gap between particles. Unfortunately the method is restricted by the requirement that the spheres do not overlap, i.e. the solid fraction must be less than 0.524. Most granular materials tend to pack to a higher density so that this model is of restricted application. The formula developed by Woodside is

$$\frac{k_e}{k_c} = \frac{1}{1 - \left[\frac{6\bar{\epsilon}}{\pi}\right]^{\frac{1}{3}} \left[1 - \left(\frac{a^2-1}{a}\right) \ln\left(\frac{a+1}{a-1}\right)\right]} \qquad (2\text{-}25)$$

where:

$$a = \left[1 + \frac{4}{\pi\left(\frac{k_d}{k_c} - 1\right)\left(\frac{6\bar{\epsilon}}{\pi}\right)^{\frac{2}{3}}}\right]^{\frac{1}{2}}$$

$$0 \leq \bar{\epsilon} \leq 0.524$$

Tsao [8] was able to overcome the problem of introducing solid to solid contact while simultaneously introducing a truly randomly packed array. The development of the stochastic model is indicated in Figure (2-5a). Considering a typical unit cube, the heterogeneous material was divided into a large number of laminae oriented normal to the direction of heat flow. By taking the laminae sufficiently thin the area of each phase will remain essentially constant across the element. Thus the two phases may be viewed as acting in parallel across the laminae. The arrangement of the parallel resistances do not affect the overall resistance so that the element may be replaced by one in which the two phases have been segregated as shown in Figure (2-5b). Similarly since each of the laminae may be viewed as a resistance acting in series the order of the laminae may be arbitrarily changed. For simplicity Tsao arranged the elements in order of decreasing solid fraction. This final arrangement is shown in Figure (3c). Probability theory was then used to develop an expression for the shape of the distribution curve. The final expression is given in terms of the experimentally obtained solid distribution parameters $\mu_1$ and $\sigma_1$

$$k_e = \cfrac{1}{\displaystyle\int_0^1 \cfrac{dP_1}{k_c + \cfrac{(k_d - k_c)}{\sigma_1 \sqrt{2\pi}} \displaystyle\int_{P_1}^1 e^{-1/2\left[\frac{x-u_1}{\sigma_1}\right]^2} dx}} \qquad (2-26)$$
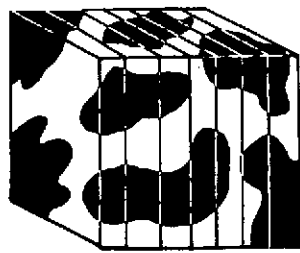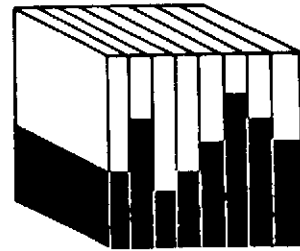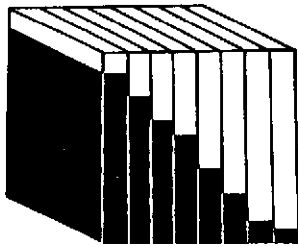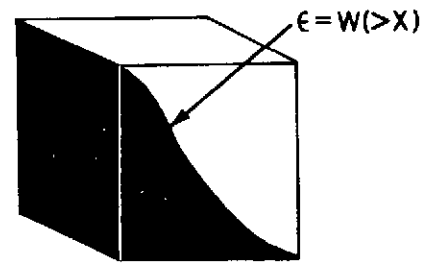
FIGURE 2-5. EQUIVALENT GEOMETRIES FOR LINEAR ISOTHERMS

Here $\mu_1$ represents the mean solid fraction and $\sigma_1$ represents the standard deviation of the solid fraction in the horizontal laminae of the re-distributed element shown in Figure (2-5d); these laminae are chosen parallel to the direction of heat flow as opposed to the vertical laminae used in the redistribution. A considerable amount of theoretical and experimental work has been done on material distributions in packed beds [49-51]. These studies show that the mean solid-area fraction is equal to the bulk solid fraction but thus far no data is given to evaluate the standard deviation in solid area fraction of these redistributed elements. Furthermore, it does not appear possible to evaluate this parameter directly.

Warren and Messmer [52] noted that Tsao failed to normalize the frequency distribution used in Equation (2-26). This is not a serious fault provided that $\mu_1$ is sufficiently small. Under the conditions $3\sigma_1 < \bar{\varepsilon}$ and $3\sigma_1 < (1-\bar{\varepsilon})$ the normalized distribution reduces to that used in Tsao's correlation.

One important contribution by Tsao was to show how random distributions could be analyzed without resorting to the regular arrays assumed by each of the previous investigations. Furthermore, this correlation is applicable to granules of any shape and size distribution. Thus Tsao's correlation is one of the most general equations presented thus far.

Summarizing the Ohm's law models, it is found that they are characterized by unrealistic assumptions regarding the lateral conductivity of the mixture. Frequently these models retain the same

unrealistic geometries common to the flux law models. However, more realistic geometries can and have been used with this type of analysis.

Equations have been developed to predict the thermal conductivity for special cases. Very dilute suspensions and emulsions are represented quite adequately by the Maxwell equation. However, each of the proposed models retains one or more approximations which greatly limits their utility and accuracy when applied to granular materials. The purpose of this study is to derive a general set of equations which will predict the effective thermal conductivity of a two phase granular system while overcoming these specific objections.

III.   COMPARISON OF PUBLISHED MODELS AND CRITIQUE


Before an attempt can be made to develop models that improve the
predicted effective thermal conductivity values, an investigation of
when and why already published models fail should be made.  To accomplish
this, a number of the models presented in Chapter 2 have been applied
to the granular systems listed in Table 6-I.  The models chosen are
those which are most widely used in the current literature and in
present engineering practice.  In cases where the development of two
models is only slightly different, one of the two is chosen.

The results are presented in Figures (3-1) through (3-18) and
summarized in Table 3-I.  The figures are classified according to the
categories mentioned in Chapter 2 as follows:

1.  Figures (3-1) through (3-4) present flux law models;

2.  Figures (3-5) through (3-13) present Ohm's Law, uniform
    heat flux models;

3.  Figures (3-13) through (3-16) present Ohm's Law, parallel
    isotherms models;

4.  Figures (3-17) and (3-18) present Lichtenecker's weighted
    equations.

Figures 3-1 through 3-4 indicate that the flux law models are
in good agreement with experimental measurements at low constituent

38

conductivity ratios, but predict considerably lower values at high constituent conductivity ratios. There is a number of reasons to explain this behavior. First, the heat flow path from particle to particle is neglected due to the absence of a finite particle contact area. Thus an important mode of heat transfer at high conductivity ratios is not taken into account. Second, the idealized particle shape and geometry utilized in the models do not provide a sufficiently close approximation to the geometry of most granular materials. Finally, with the exception of Bruggeman's equation, the flux law models have been extrapolated beyond the porosity range for which they are theoretically applicable ( $\frac{\pi}{6} \leq P \leq 1$ ).

It should be noted that whereas the conductivities predicted by Lord Rayleigh's and Meredith and Tobias' equations are comparable, Bruggeman's equation represents a considerable improvement of the calculated values. This is probably an indication that the geometry of any future flux law model should not radically depart from the geometry of real granular systems.

Figures 3-5 through 3-13 indicate that in general uniform heat flux models predict low effective thermal conductivities and the discrepancy increases with the ratio of constituent conductivities. As it will be discussed in detail in Chapter 4, the uniform heat flux assumption necessitates that the conductivity of the constituents in the normal to the heat flow direction be zero. Consequently, the low predicted thermal conductivities are an expected result of the linear

heat flow assumption. However, the equation of Woodside and Messmer predicts high values at low constituent conductivity ratios, but when $k_d/k_c$ increases beyond a certain limit the calculated values become low. The explanation of this behavior lies on the geometry assumptions introduced in the model. In the Woodside and Messmer model the solid phase is elongated in the direction of heat flow, thus rendering the calculated effective conductivity high at low values of $k_d/k_c$. However, when $k_d/k_c$ increases, the absence of finite contact areas between particles and the linear heat flow assumption come into effect, and as a result the calculated effective conductivities are low.

It is seen that the equations of Preston, Wilhelm et al, and Krupiczka, which include correlation terms, are in very good agreement with the experimental data for granular materials and powders at atmospheric pressures.

Figures 3-14 through 3-16 indicate that parallel isotherms models generally predict high values for the effective thermal con-ductivity. Again, this is due to the introduction of infinite con-ductivity in the normal to the heat flow direction, necessitated by the heat flow assumption. Russell's model is an exception to this conclusion, since it predicts low values at high ratios of constituent conductivities. This is probably due to the simplified geometry of the model, and to the relatively large gaps between particles. It appears that the influence of the simplified geometry and the absence of contact areas between particles dominate over the influence of the heat flow assumption.

In Figures (3-17) and (3-18) Lichtenecker's weighted equations are compared to experimental data. Evidently the values predicted by these equations are in error, indicating that any such future attempt should rely heavily on experimental evidence.

Summarizing the comparison of published models, it is found that the major sources of error can be attributed to the following causes.

1. Distorted or idealized geometry;

2. Idealized heat flow;

3. Absence of finite particle contact area.

Not all sources of error are applicable to each one of the models discussed. Typically, one or more are applicable in each case. However, it is difficult to isolate a prior source of error for a particular model. It appears that the discrepancy between calculated and experimental values is due to an interaction of all sources, each source dominating over a particular range of $k_d/k_c$ depending on the geometry and heat flow assumptions. Consequently, in any more refined model the influence of each of the above sources of error should be minimized, especially if it is expected that the model should be applicable to granular materials having large ratios of constituent conductivities. Such an attempt has been undertaken in the models that will be described in the rest of this study. First, however, the effects of the uniform heat flux and parallel isotherms assumptions will be investigated, because if it were possible to utilize either

assumption, the problem of finding the effective thermal conductivity of granular materials would be simplified considerably.
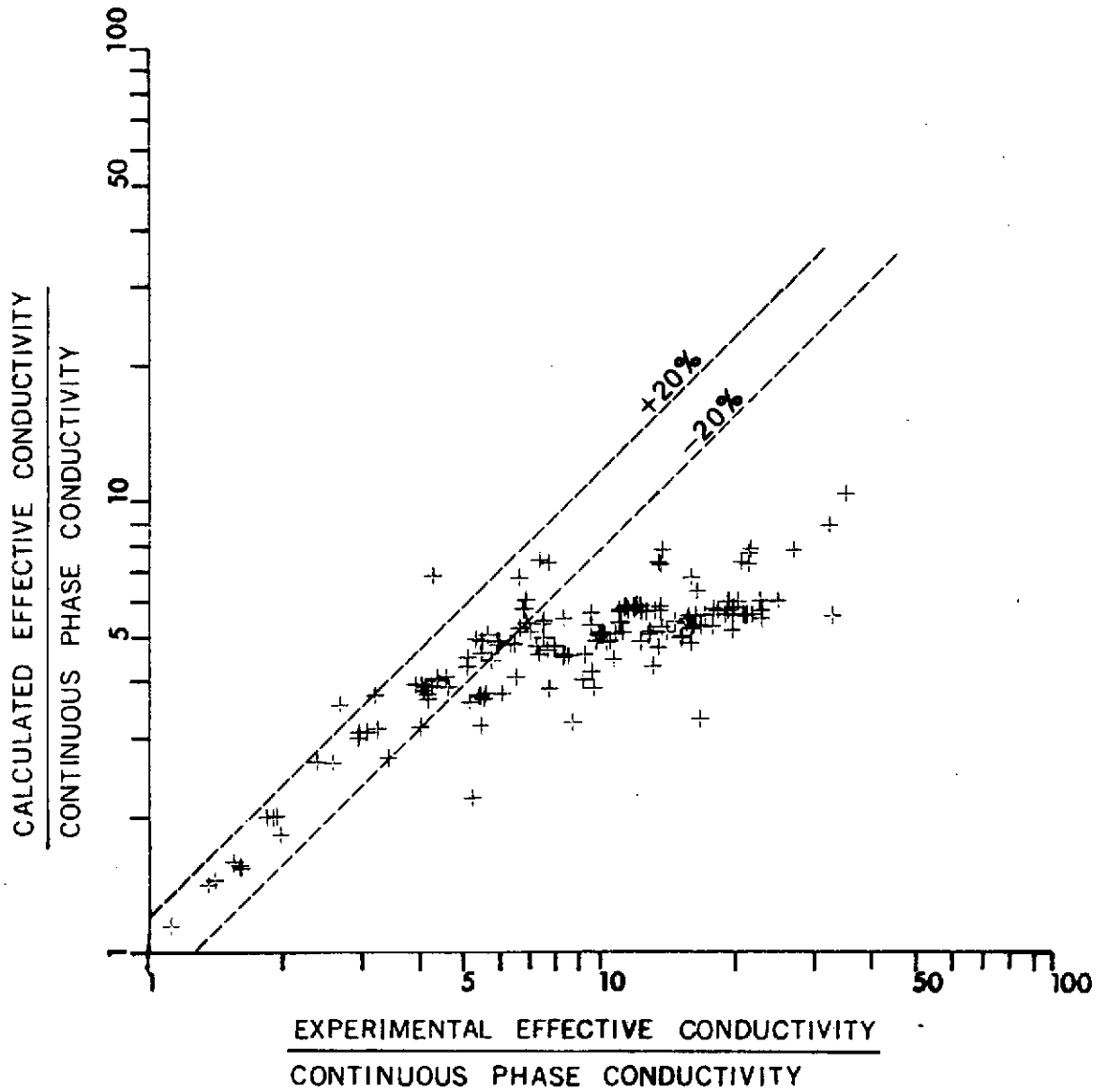
FIGURE 3-1. COMPARISON OF EXPERIMENTAL RESULTS WITH CALCULATED CONDUCTIVITY FOR THE MAXWELL EQUATION.
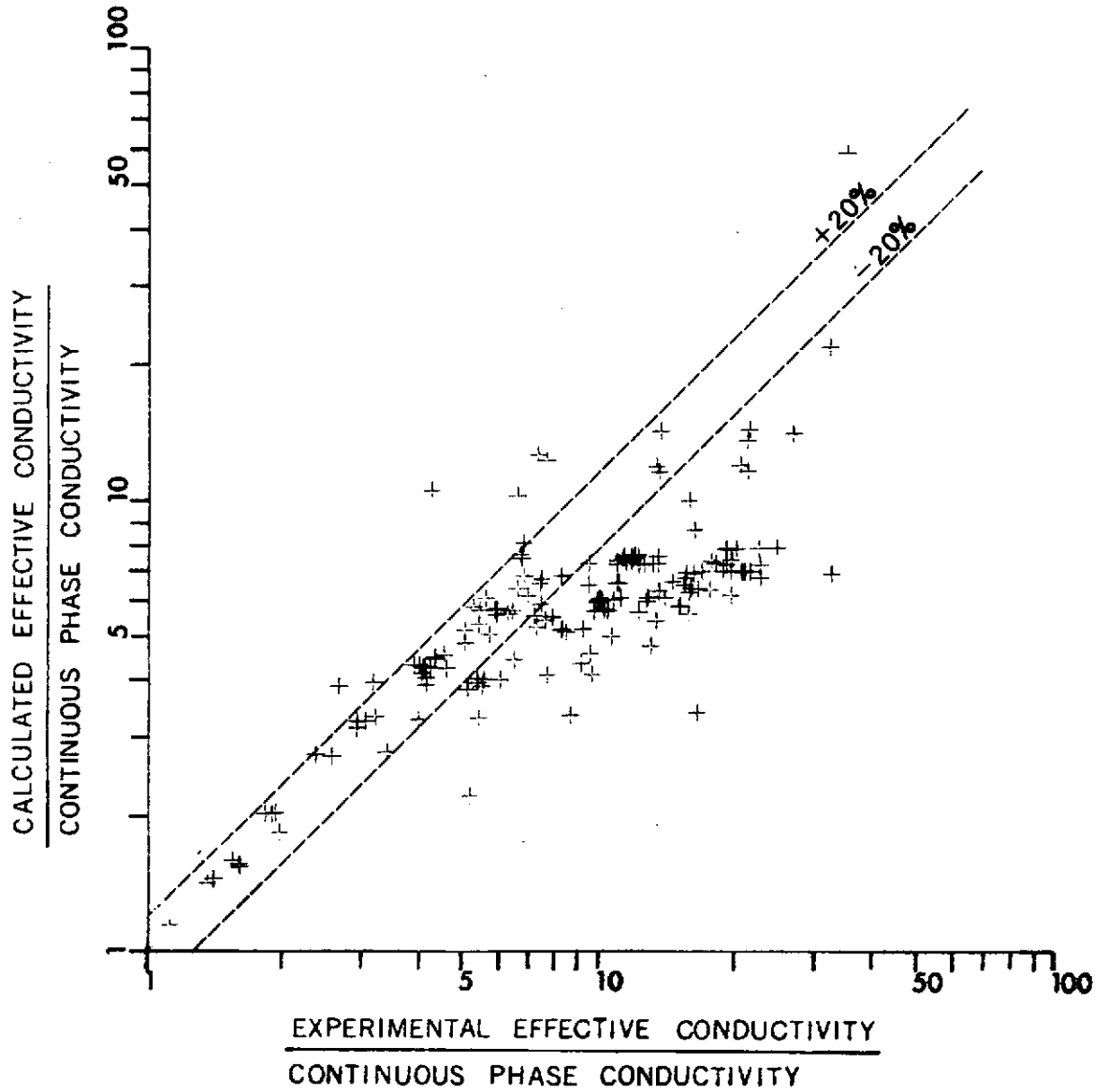
FIGURE 3-2. COMPARISON OF EXPERIMENTAL RESULTS WITH CALCULATED CONDUCTIVITY FOR THE LORD RAYLEIGH EQUATION.
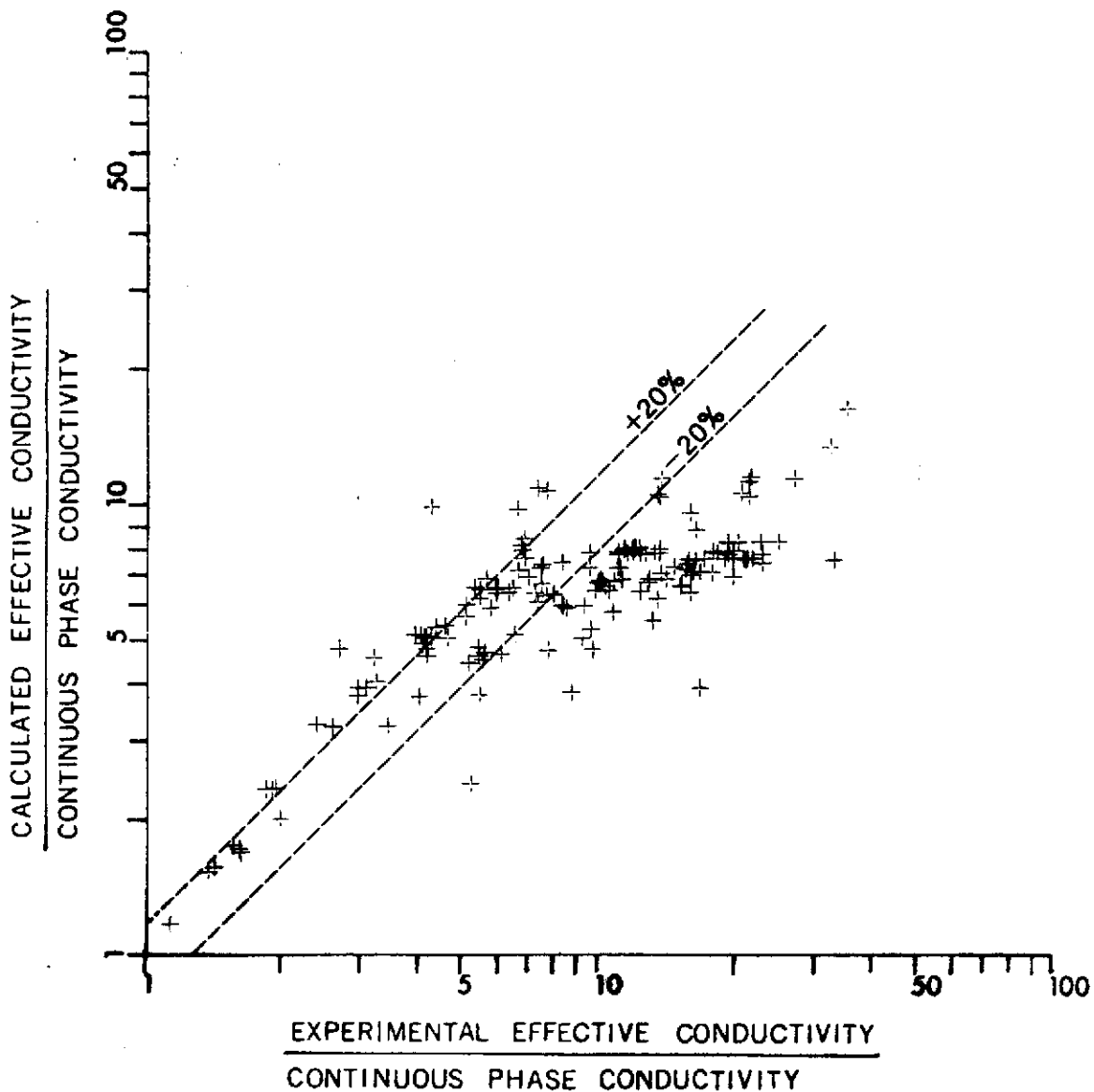
FIGURE 3-3. COMPARISON OF EXPERIMENTAL RESULTS WITH CALCULATED CONDUCTIVITY FOR THE MEREDITH AND TOBIAS EQUATION.
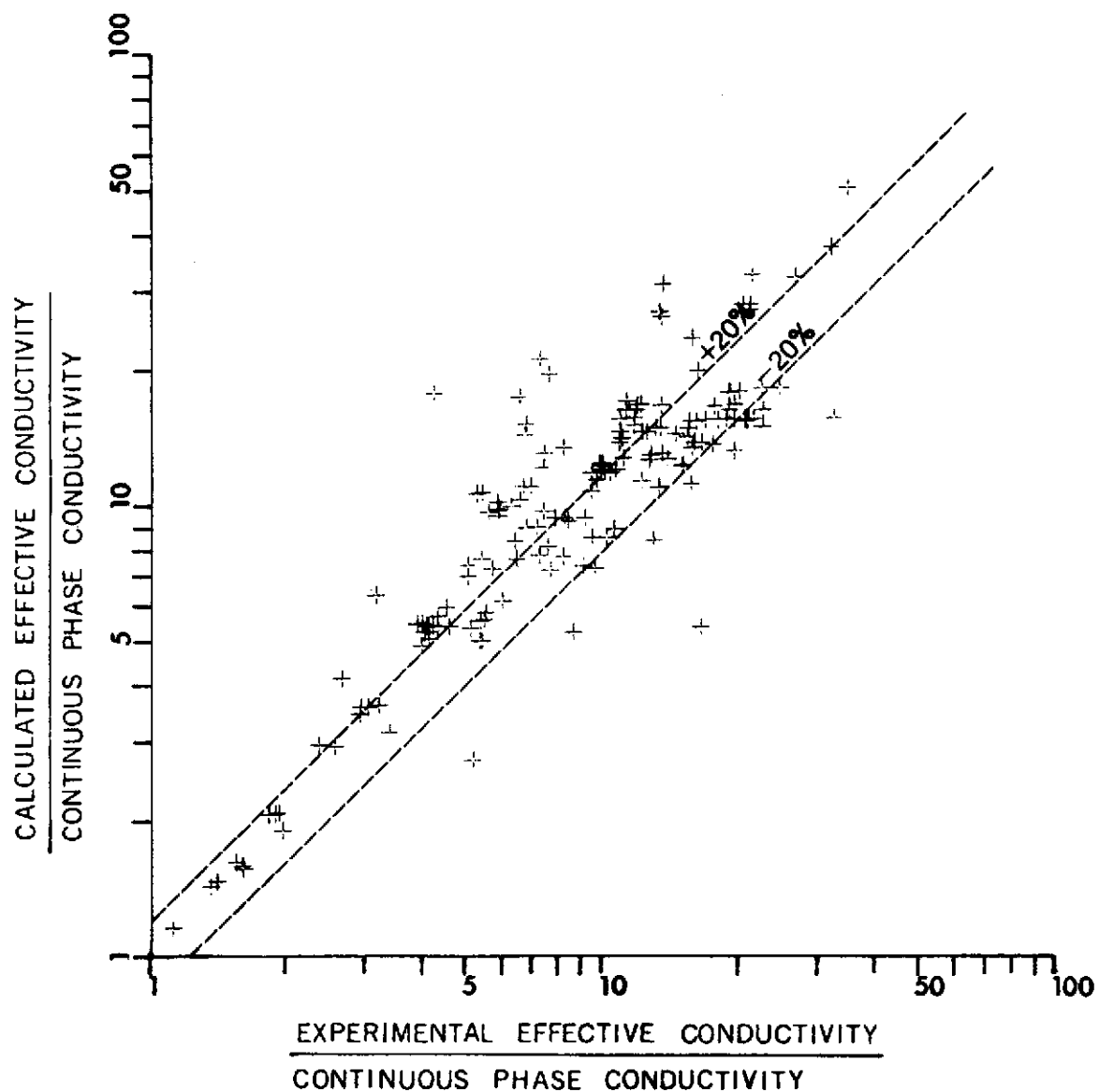
FIGURE 3-4. COMPARISON OF EXPERIMENTAL RESULTS WITH CALCULATED CONDUCTIVITY FOR THE BRUGGEMAN EQUATION.
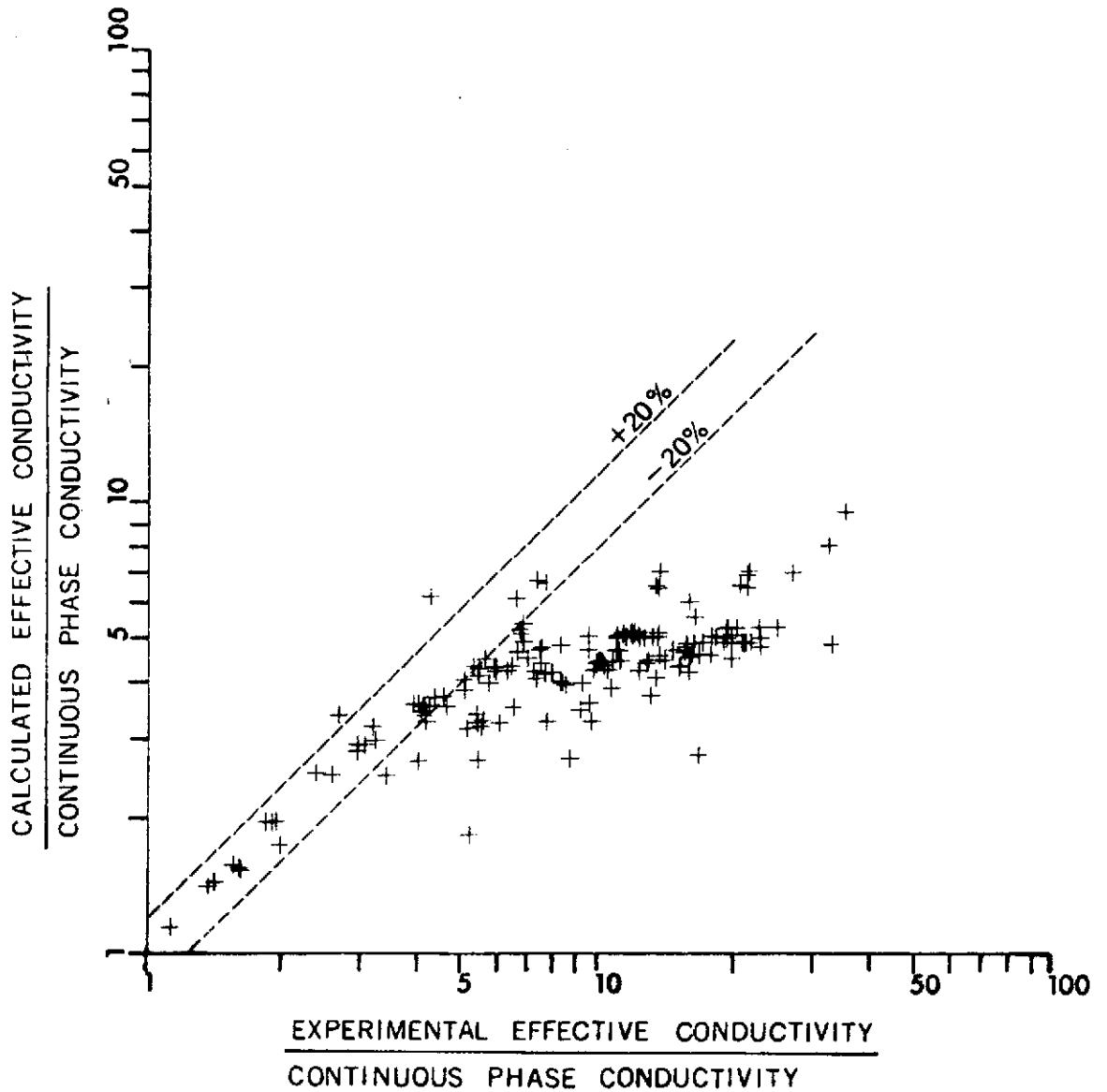
FIGURE 3-5. COMPARISON OF EXPERIMENTAL RESULTS WITH CALCULATED CONDUCTIVITY FOR THE SON FREY EQUATION.
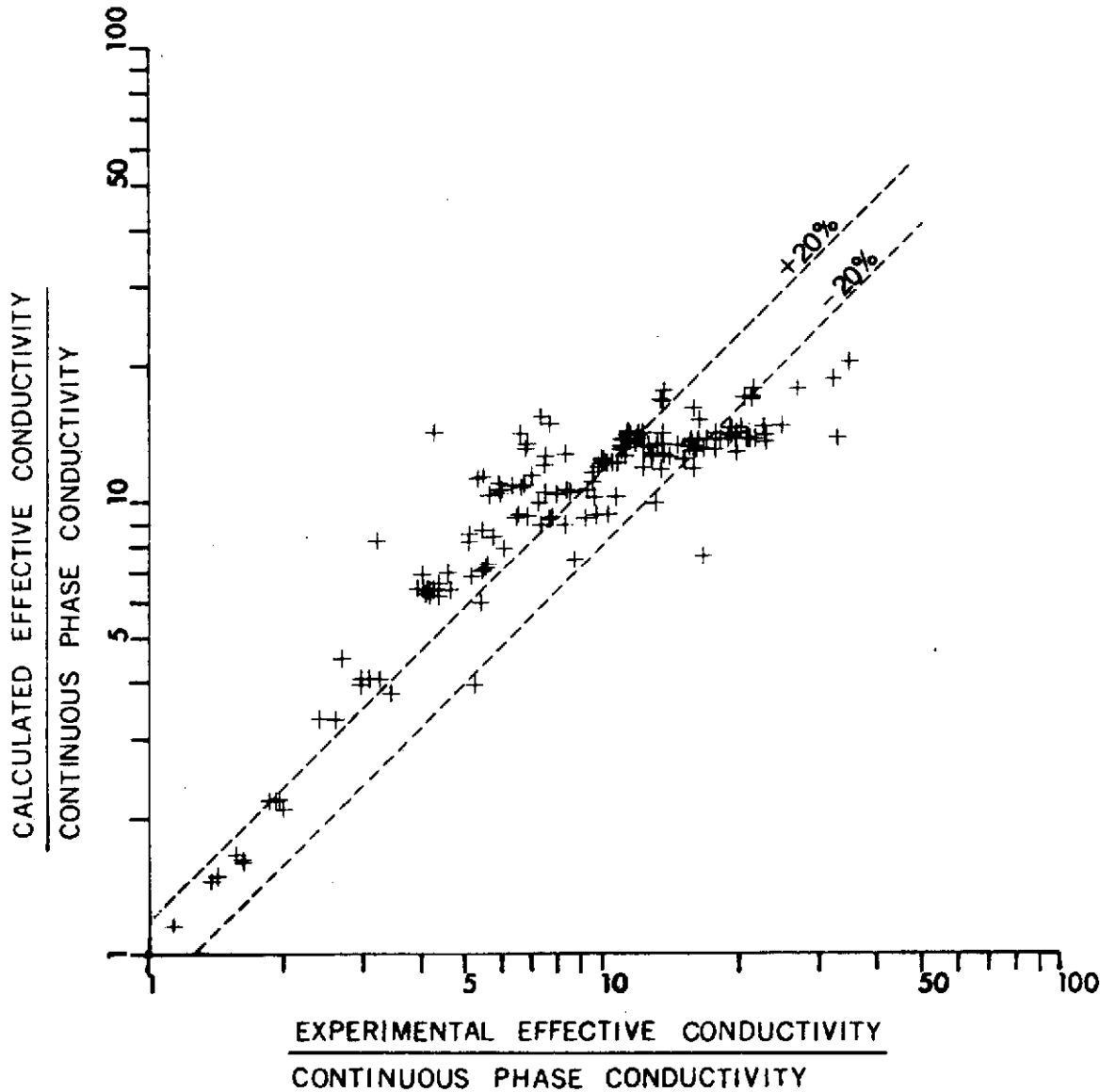
FIGURE 3-6. COMPARISON OF EXPERIMENTAL RESULTS WITH CALCULATED CONDUCTIVITY FOR THE WOODSIDE AND MESSMER EQUATION.
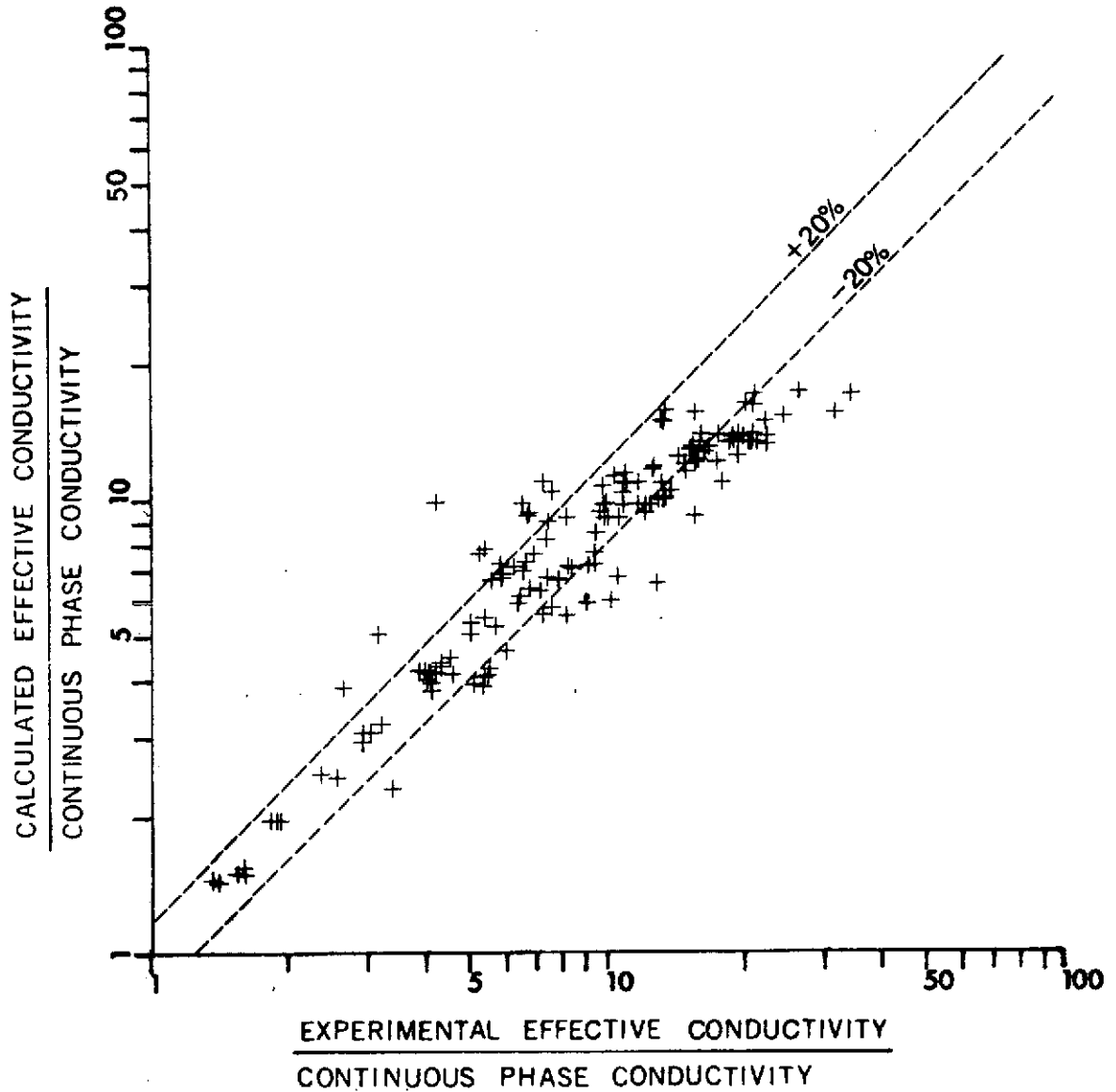
FIGURE 3-7. COMPARISON OF EXPERIMENTAL RESULTS WITH
CALCULATED CONDUCTIVITY FOR THE KANAGER
EQUATION.
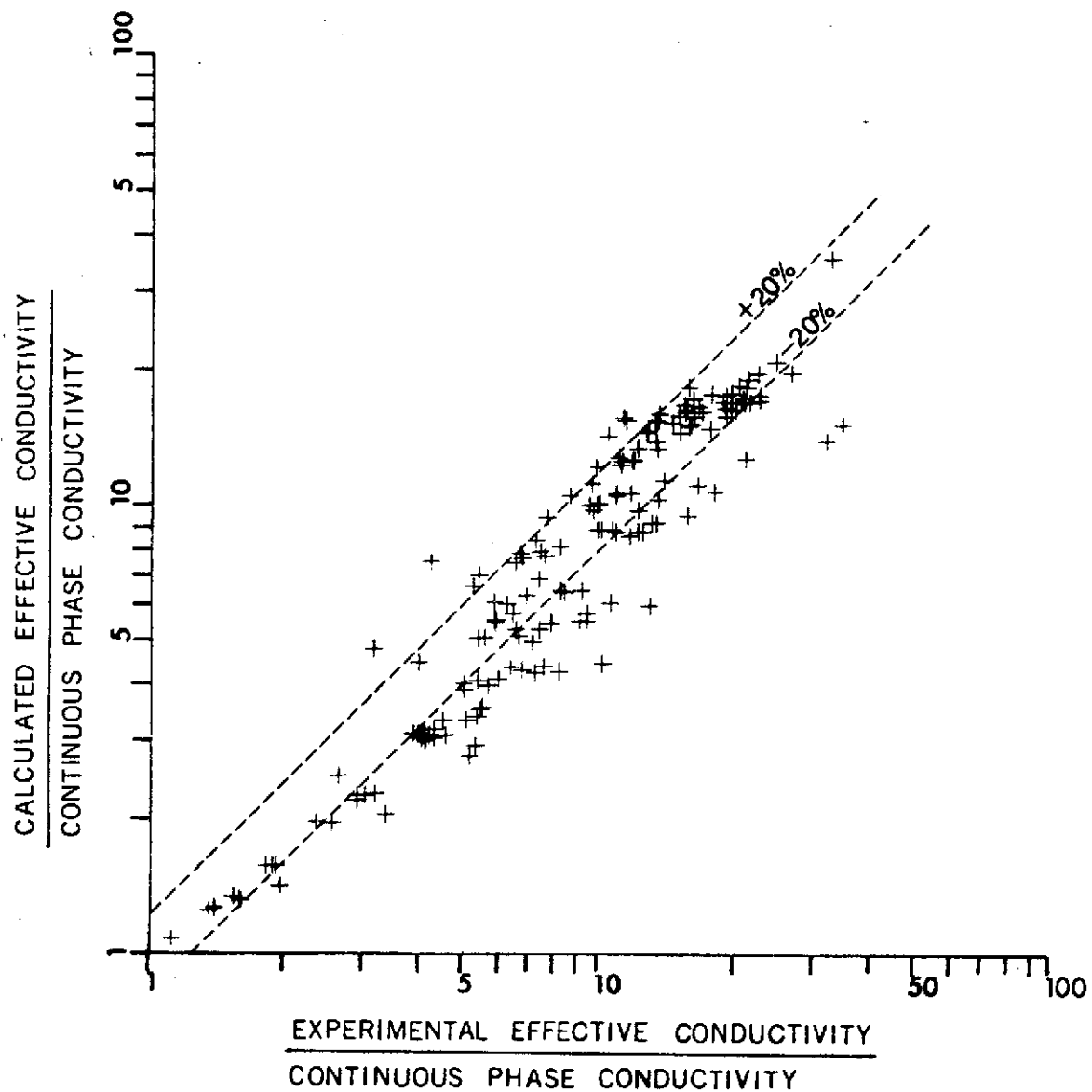
FIGURE 3-8. COMPARISON OF EXPERIMENTAL RESULTS WITH
CALCULATED CONDUCTIVITY FOR THE GORRING
AND CHURCHILL EQUATION.
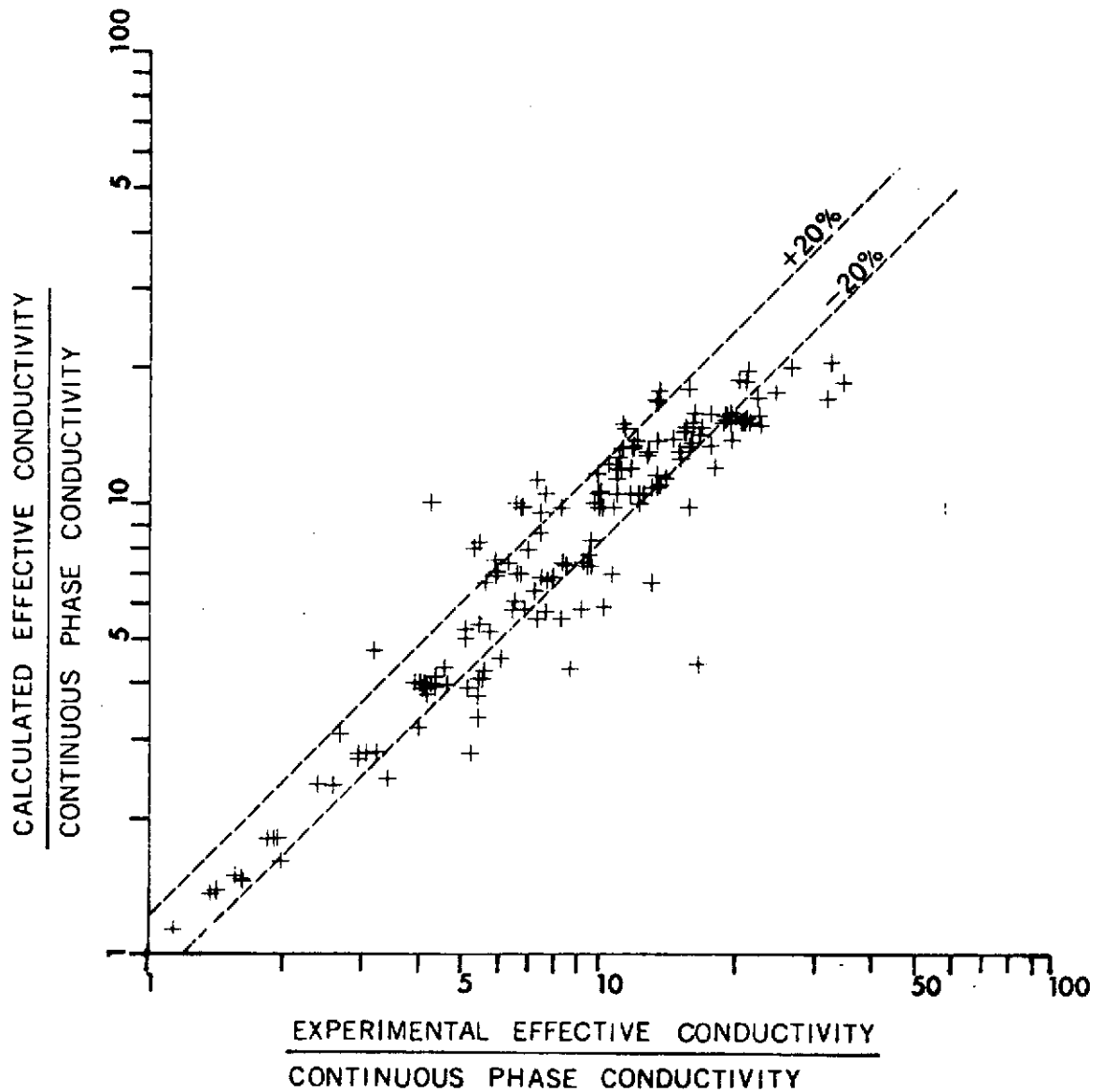
FIGURE 3-9. COMPARISON OF EXPERIMENTAL RESULTS WITH CALCULATED CONDUCTIVITY FOR THE WILLHITE, KUNII AND SMITH EQUATION.
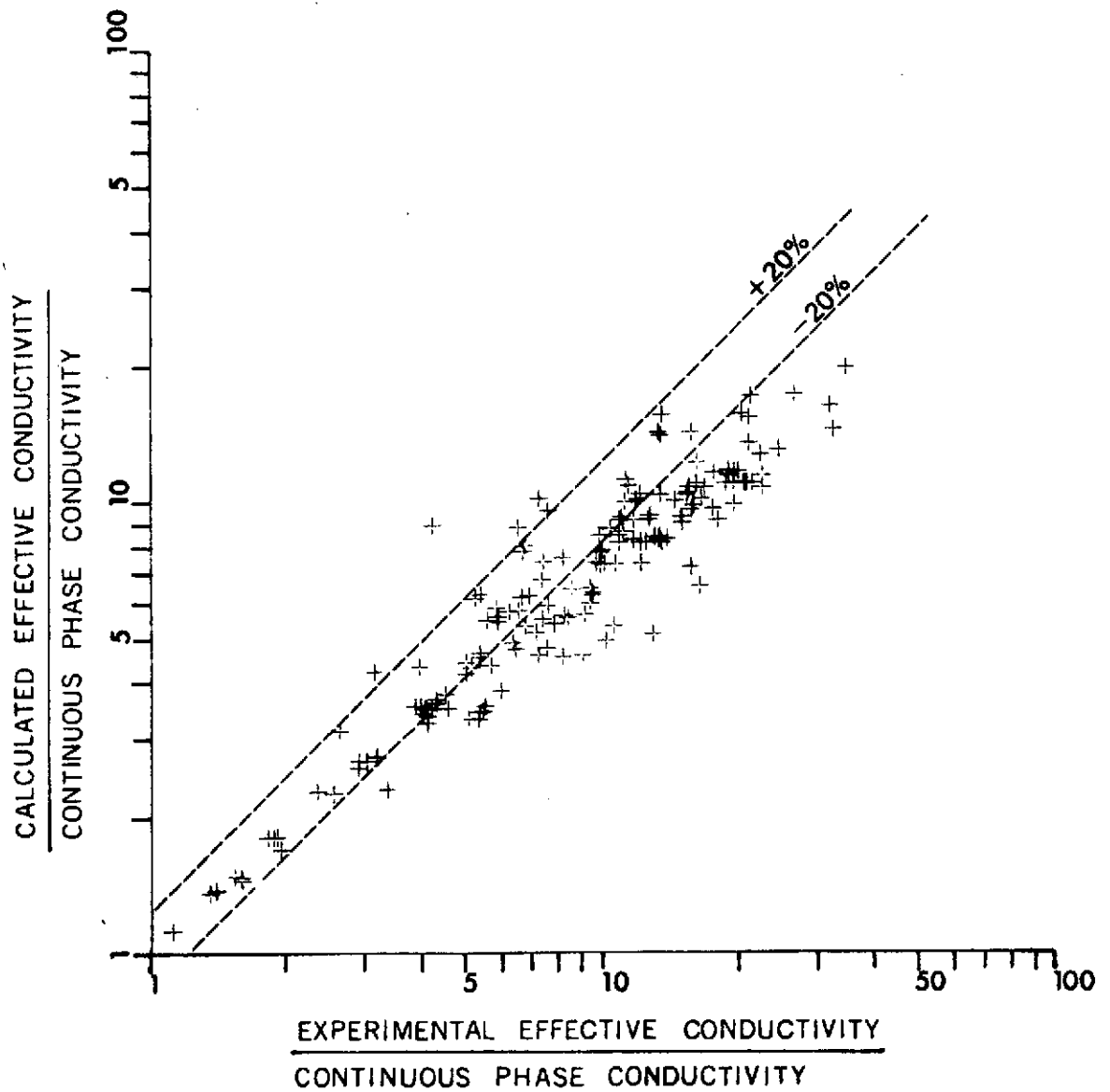
FIGURE 3-10. COMPARISON OF EXPERIMENTAL RESULTS WITH CALCULATED CONDUCTIVITY FOR THE SCHUMANN AND VOSS EQUATION.
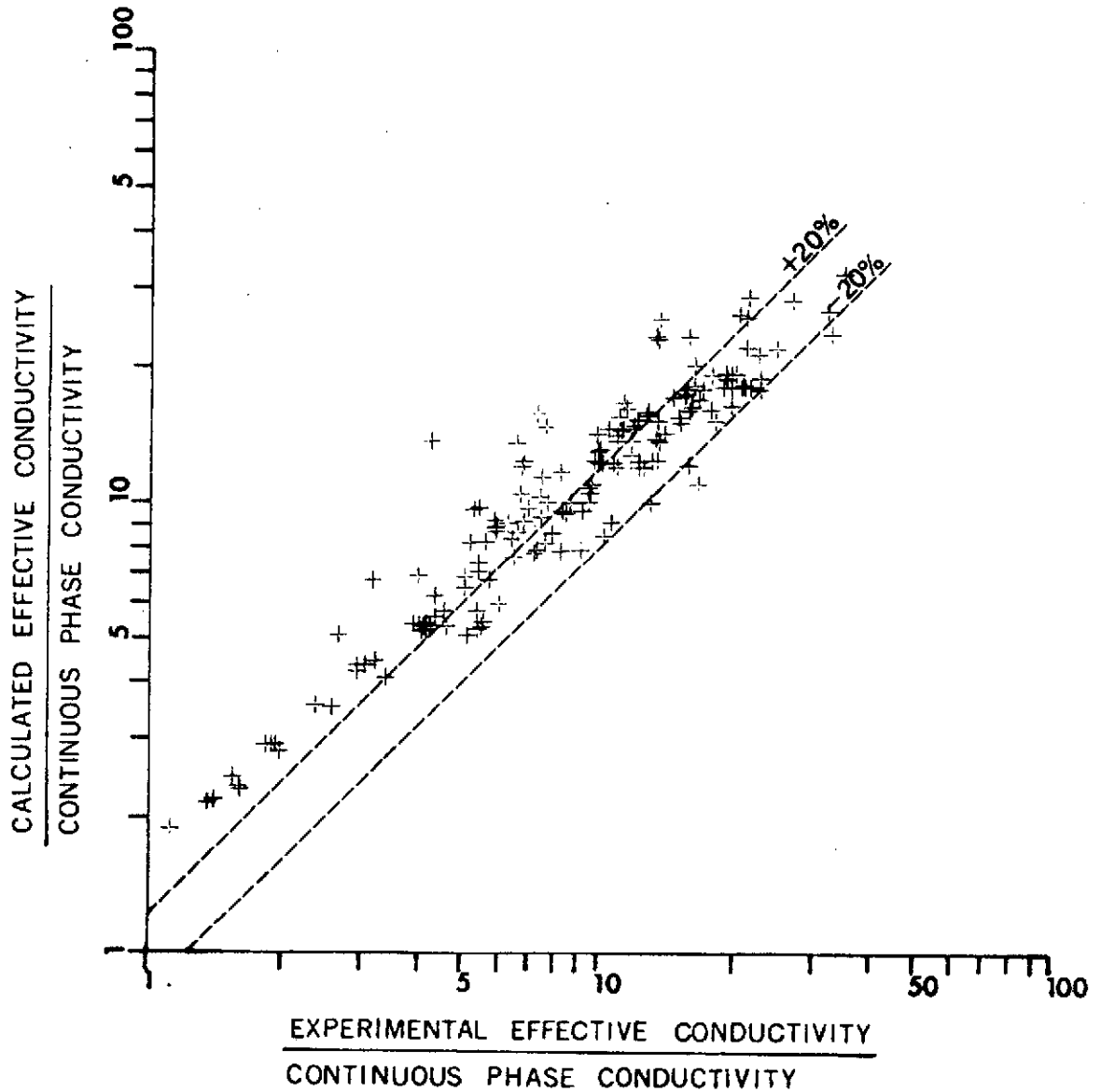
FIGURE 3-11. COMPARISON OF EXPERIMENTAL RESULTS WITH CALCULATED CONDUCTIVITY FOR THE PRESTON EQUATION.
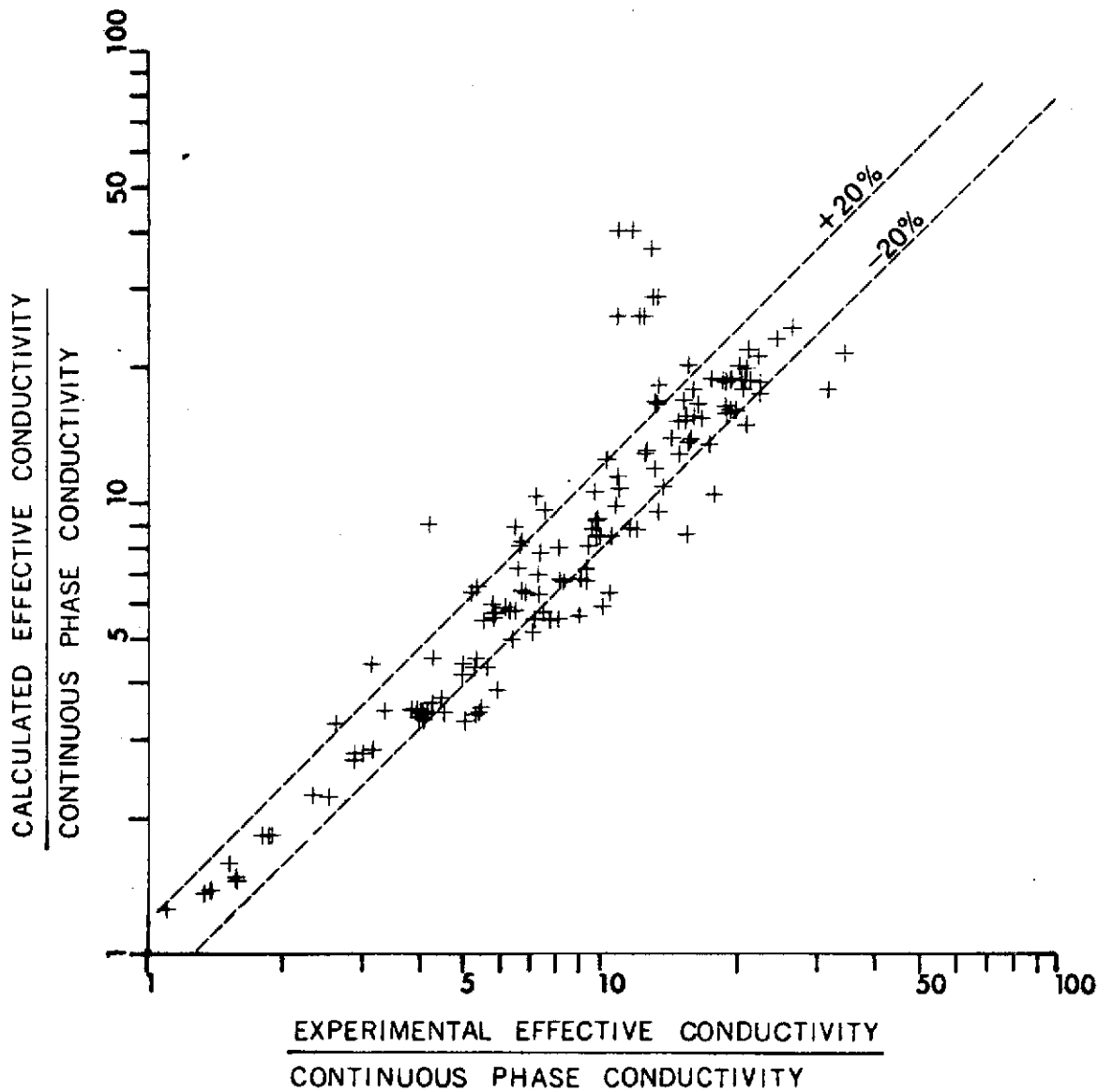
FIGURE 3-12. COMPARISON OF EXPERIMENTAL RESULTS WITH CALCULATED CONDUCTIVITY FOR THE WILHELM ET AL EQUATION.
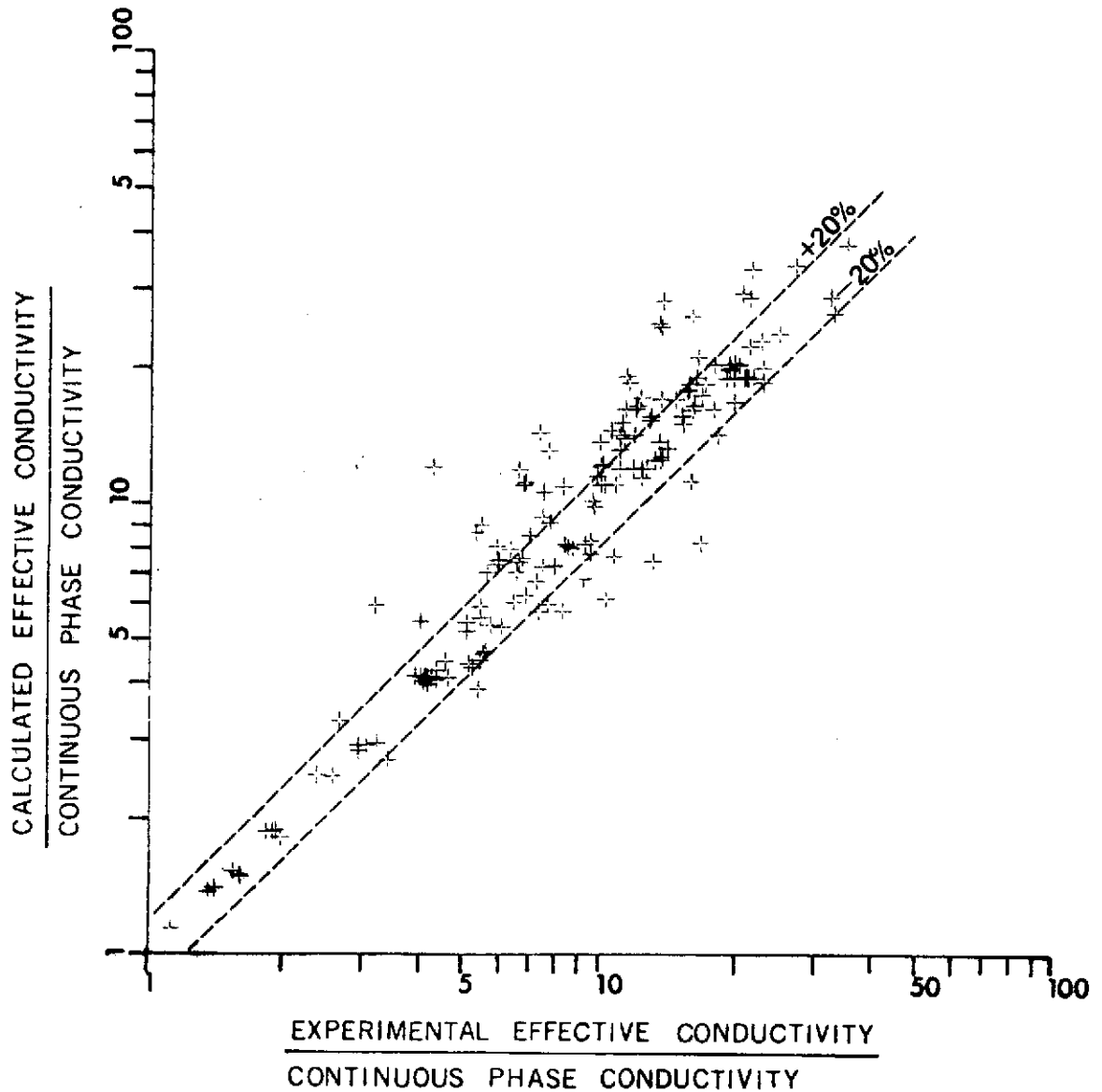
FIGURE 3-13. COMPARISON OF EXPERIMENTAL RESULTS WITH
CALCULATED CONDUCTIVITY FOR THE KRUPICZKA
EQUATION.
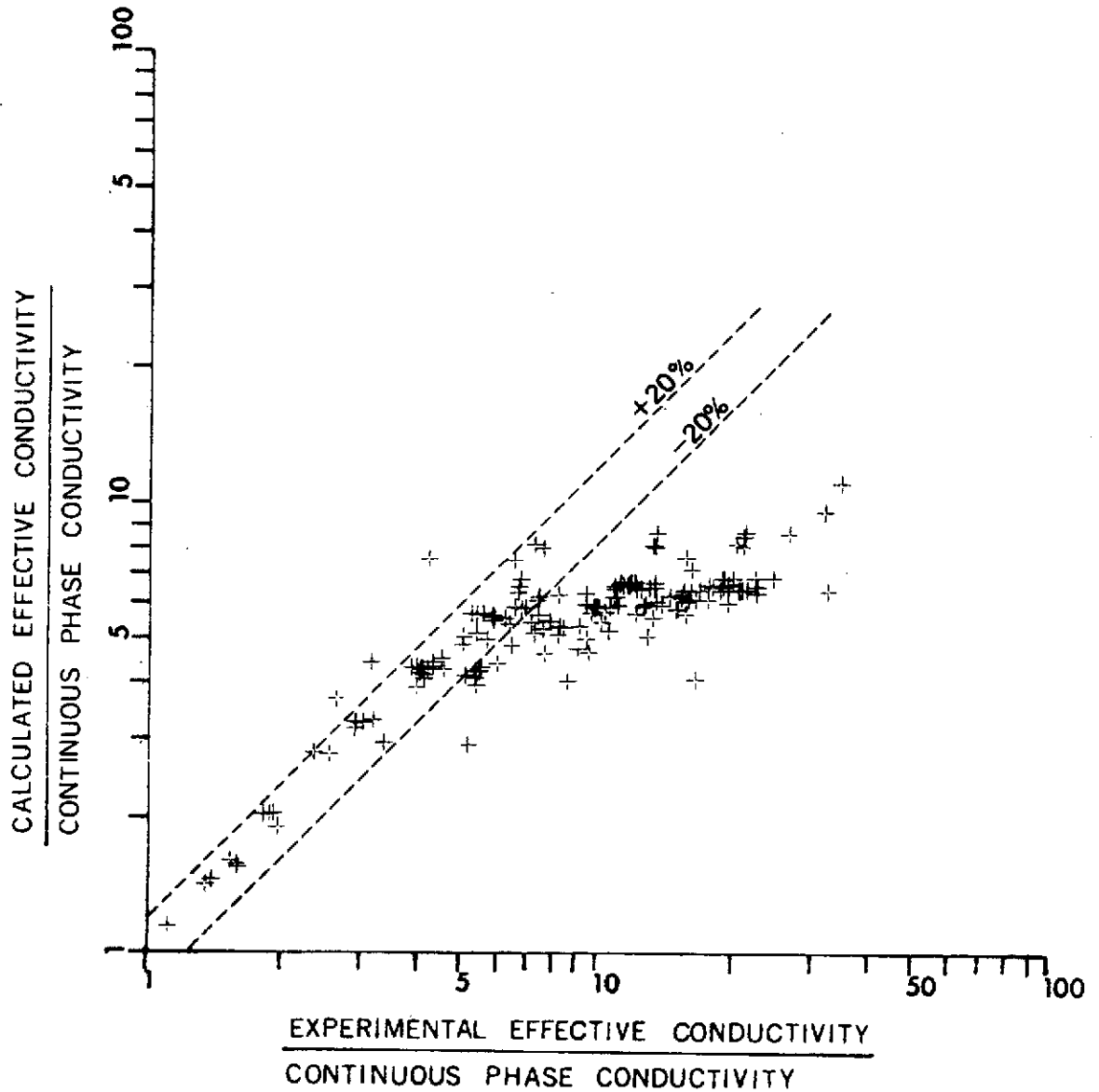
FIGURE 3-14. COMPARISON OF EXPERIMENTAL RESULTS WITH CALCULATED CONDUCTIVITY FOR THE RUSSELL EQUATION.
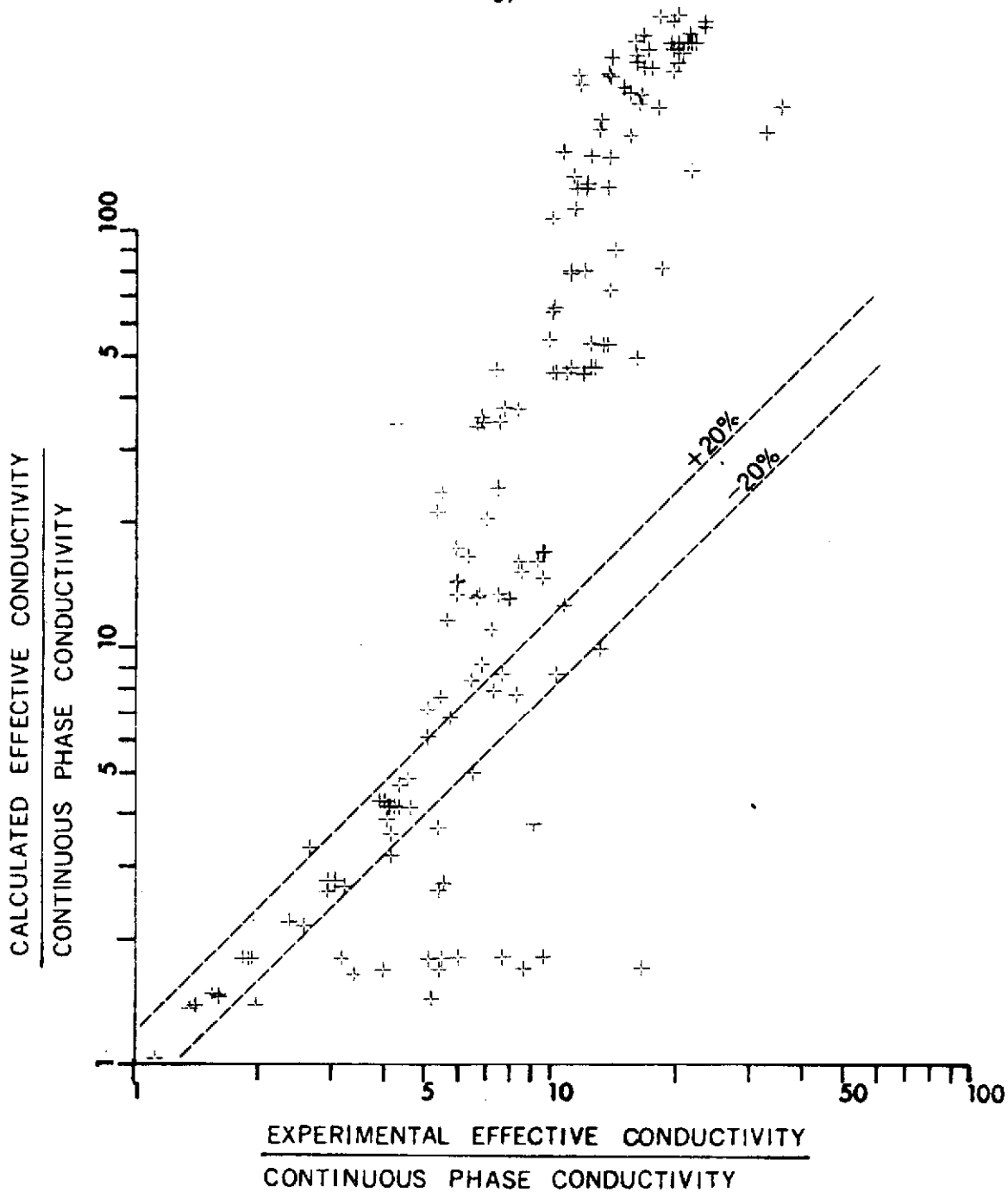
FIGURE 3-15. COMPARISON OF EXPERIMENTAL RESULTS WITH CALCULATED CONDUCTIVITY FOR THE BERNSTEIN EQUATION.
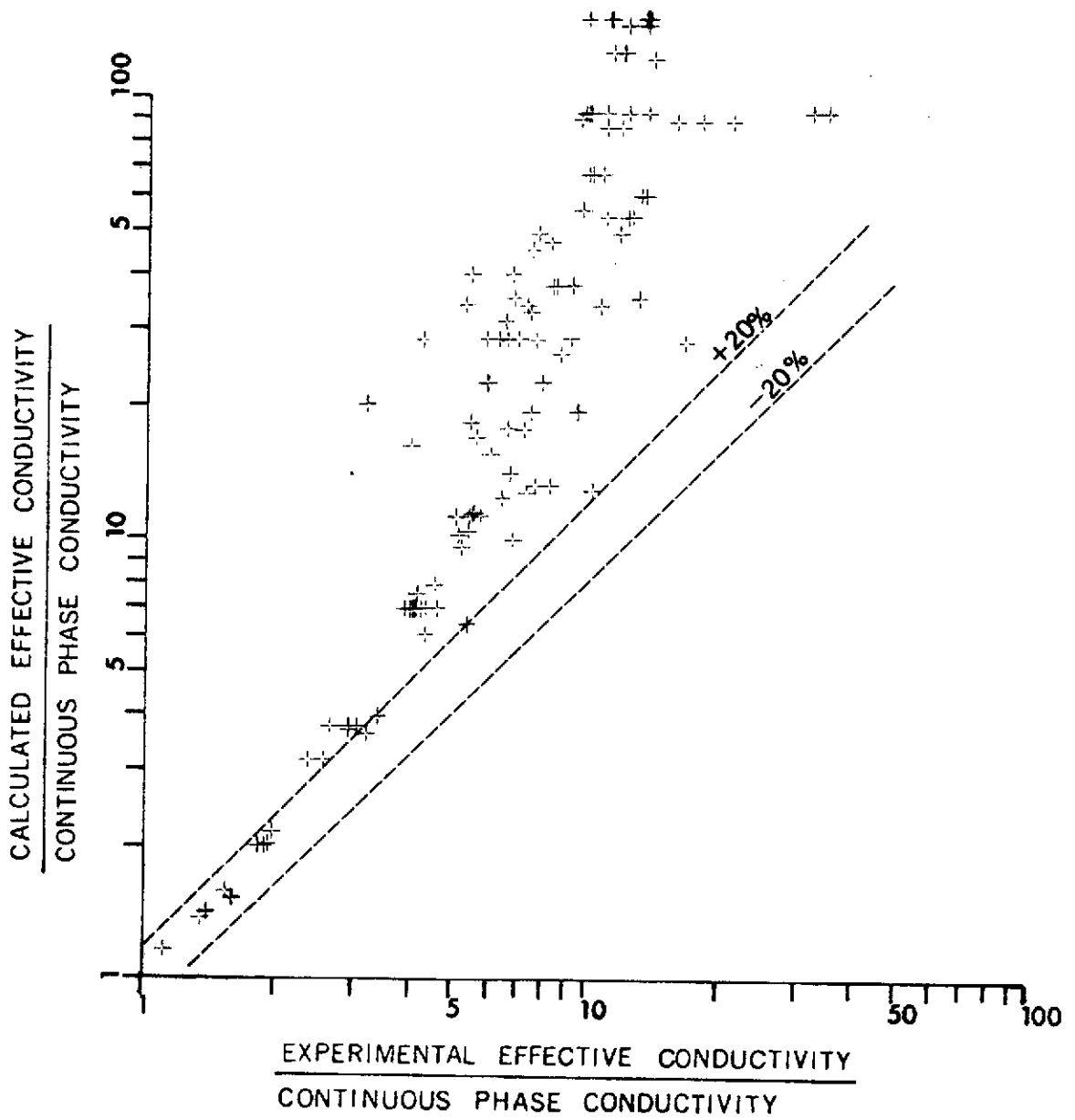
FIGURE 3-16. COMPARISON OF EXPERIMENTAL RESULTS WITH CALCULATED CONDUCTIVITY FOR THE WOODSIDE EQUATION.
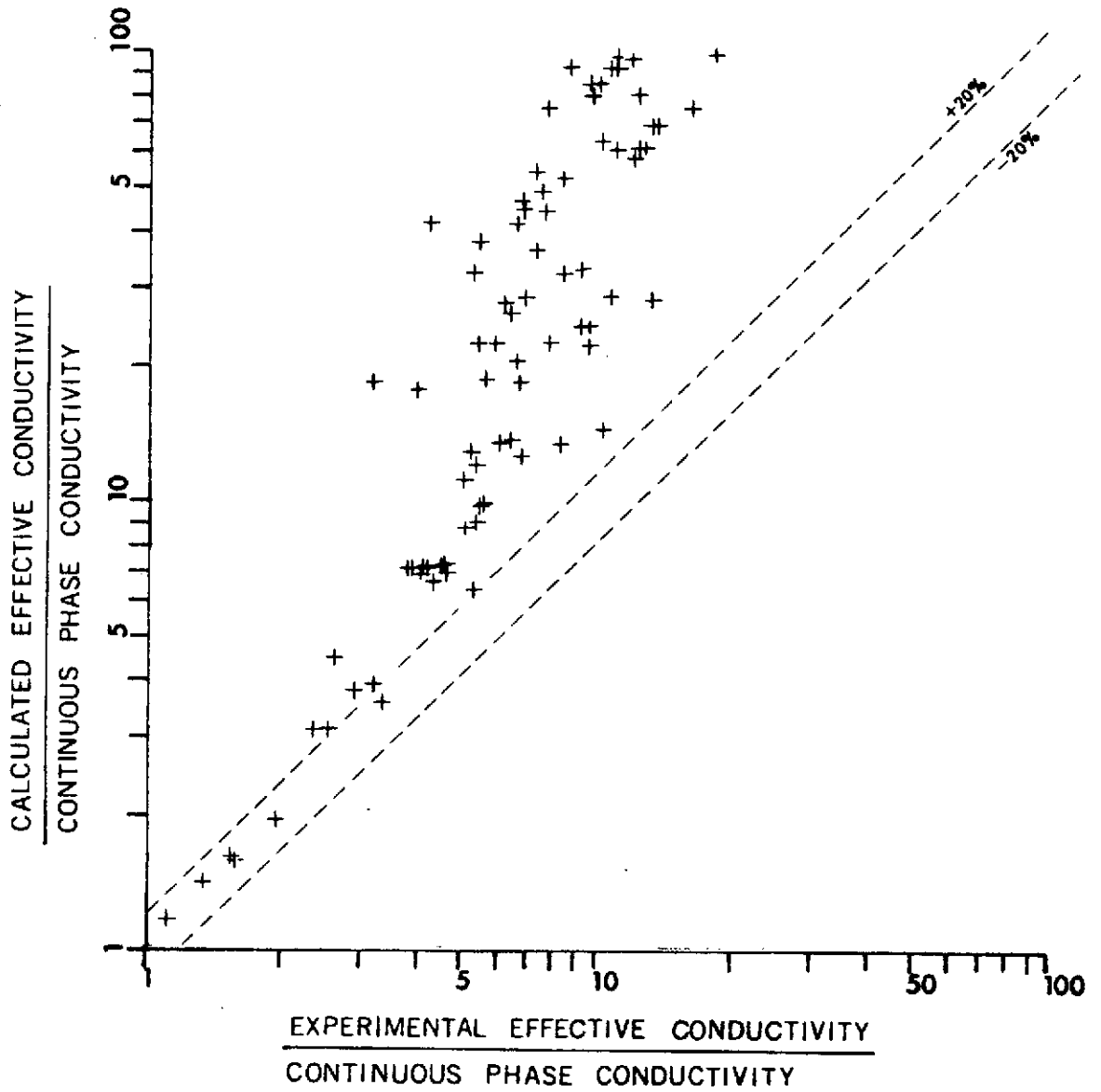
FIGURE 3-17. COMPARISON OF EXPERIMENTAL RESULTS WITH
CALCULATED CONDUCTIVITY FOR THE LICHTENECKER
3-D EQUATION.
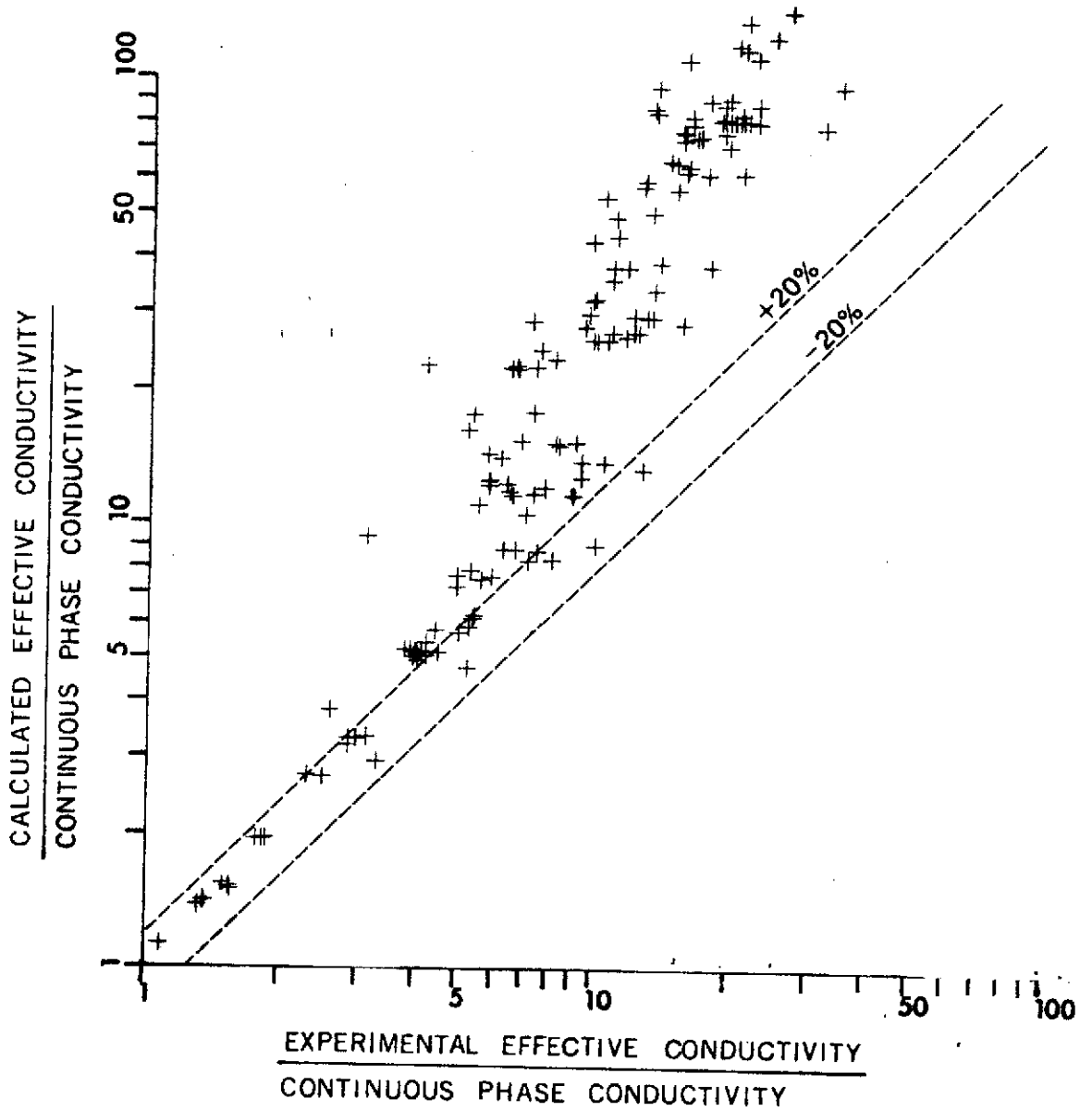
FIGURE 3-18. COMPARISON OF EXPERIMENTAL RESULTS WITH CALCULATED CONDUCTIVITY FOR THE LICHTENECKER 2-D EQUATION.

TABLE 3-I.  AVERAGE ERROR, AVERAGE BIAS AND
ERROR VARIANCE OF CALCULATED THERMAL
CONDUCTIVITY AT ATMOSPHERIC PRESSURE
BASED ON SELECTED MODELS

|  | Av. Bias % | Av. Error % | Error Var. |
|---|---|---|---|
| **A. Flux Law Models** | | | |
| 1. Maxwell | -37.9 | 40.2 | 0.0606 |
| 2. Lord Rayleigh | -24.8 | 33.7 | 0.0594 |
| 3. Meredith and Tobias | -18.7 | 34.4 | 0.0416 |
| 4. Bruggeman | 23.8 | 32.9 | 0.1540 |
| **B. Uniform Heat Flux Models** | | | |
| 1. son Frey | -43.8 | 45.1 | 0.0599 |
| 2. Woodside and Messmer | 20.9 | 34.8 | 0.0992 |
| 3. Kanager | -6.7 | 18.9 | 0.0286 |
| 4. Gorring and Churchill | -10.7 | 20.0 | 0.0192 |
| 5. Willhite, Kunii and Smith | -3.6 | 17.8 | 0.0268 |
| 6. Schumann and Voss | -21.1 | 25.8 | 0.0260 |
| 7. Preston | 26.6 | 30.5 | 0.0875 |
| 8. Wilhelm et al | -2.1 | 19.7 | 0.0373 |
| 9. Krupiczka | 13.2 | 21.2 | 0.0693 |
| **C. Parallel Isotherm Models** | | | |
| 1. Russell | -30.3 | 35.0 | 0.0566 |
| 2. Bernstein | 677.9 | 686.1 | 85.05 |
| 3. Woodside | 670.3 | 670.4 | 55.16 |

TABLE 3-I. Continued

D. Weighted Ohm's Law Models

| | | | | |
|---|---|---|---|---|
| 1. | Lichtenecker 3-D | 701.1 | 701.2 | 48.70 |
| 2. | Lichtenecker 2-D | 194.5 | 195.0 | 2.98 |

# IV.  CHARACTERISTICS OF PROBABILISTIC MODELS

As indicated in Chapter 2, almost all methods proposed to determine the thermal conductivities of two-phase systems may be grouped into two general classes.  The first classification consists of the Ohm's law model equations derived from some special geometries, usually some orderly array of spheres or cubes distributed in a continuous medium.

The second classification consists of the flux law model equations which account for non-linear heat flow. However, most of these equations are based on the assumption that the concentration of particles is small enough so that the field surrounding one particle is not affected by the presence of other particles.

As indicated in [68], published correlations for the thermal conductivity of granular materials, are not applicable to systems composed of different materials for which the thermal conductivities are highly different.  This is the case, because the approximations inherent to the assumptions of both classifications mentioned above are no longer valid when the ratio of the component conductivities becomes exceedingly high. The object of this study is the development of a model that will account for non-linear heat flow, that can be extended to a large range of the ratio of thermal conductivities,

and will include the following parameters:

1. Volume fraction of one phase;

2. Particle shape;

3. Particle size distribution;

4. Contact resistance.

The description and analysis of such models is preceded by the development of two Ohm's law models based on the assumption of parallel isotherms and uniform heat flux respectively. Both these models are an outgrowth of Tsao's [8] and Loeb's [69] models supplemented by recent results on the structural properties of packed beds [49, 51]. It should be noted that apart from the heat flow assumptions, the basic proposition utilized in the development of the models is that a granular material can be considered as a random mixture of two phases, in which all particles of the same size and shape have the same probability to occupy each unit volume of the mixture. The validity of this proposition together with its limitations have been discussed extensively by Debbas and Rumpf [51], and it has been utilized in Tsao's [8] model.

The purpose of these preliminary developments is two-fold. First, to indicate that Ohm's law models with realistic geometries provide an upper and lower bound to the effective conductivity of granular materials. Second, to illustrate the need for a probabilistic flux law model that includes particle interaction, so that the unrealistic assumptions concerning the value of the thermal conductivity in the direction perpendicular to the heat flow can be overcome.

## Ohm's Law Model - Parallel Isotherms

Consider a unit cube of a granular material subdivided into $N^3$ cubicles by a three-dimensional grid. Assume that the grid is fine enough, and the two phases are arranged in such a manner that each cubicle is occupied either by the continuous or the discontinuous phase. It has been shown [51] that most granular materials can be thought of as a random mixture of the two phases. Accordingly, the probability that a cubicle is occupied by the continuous phase is P, the volume fraction of the continuous phase. It has been also shown [8, 53] that due to the parallel isotherms assumption, the conductivity of each lamina perpendicular to the heat flow direction depends on the volume fraction of the continuous phase present in the lamina, but is independent of the manner in which the two phases are arranged. Consequently, the effective thermal conductivity of each lamina does not change if the continuous phase is arranged as indicated in Figure (4-1b). Also, since the laminae can be thought of as series resistances to the flow of heat, the effective conductivity of the unit cube does not change if the laminae are rearranged according to decreasing height of the continuous phase as indicated in Figure (4-1c), approximated by a continuous distribution curve indicated in Figure (4-1d). Summation of the series resistances yields the following expression for $k_e$, the effective conductivity of the unit cube

(a)

(c)

(b)

(d)

Y

X

Z
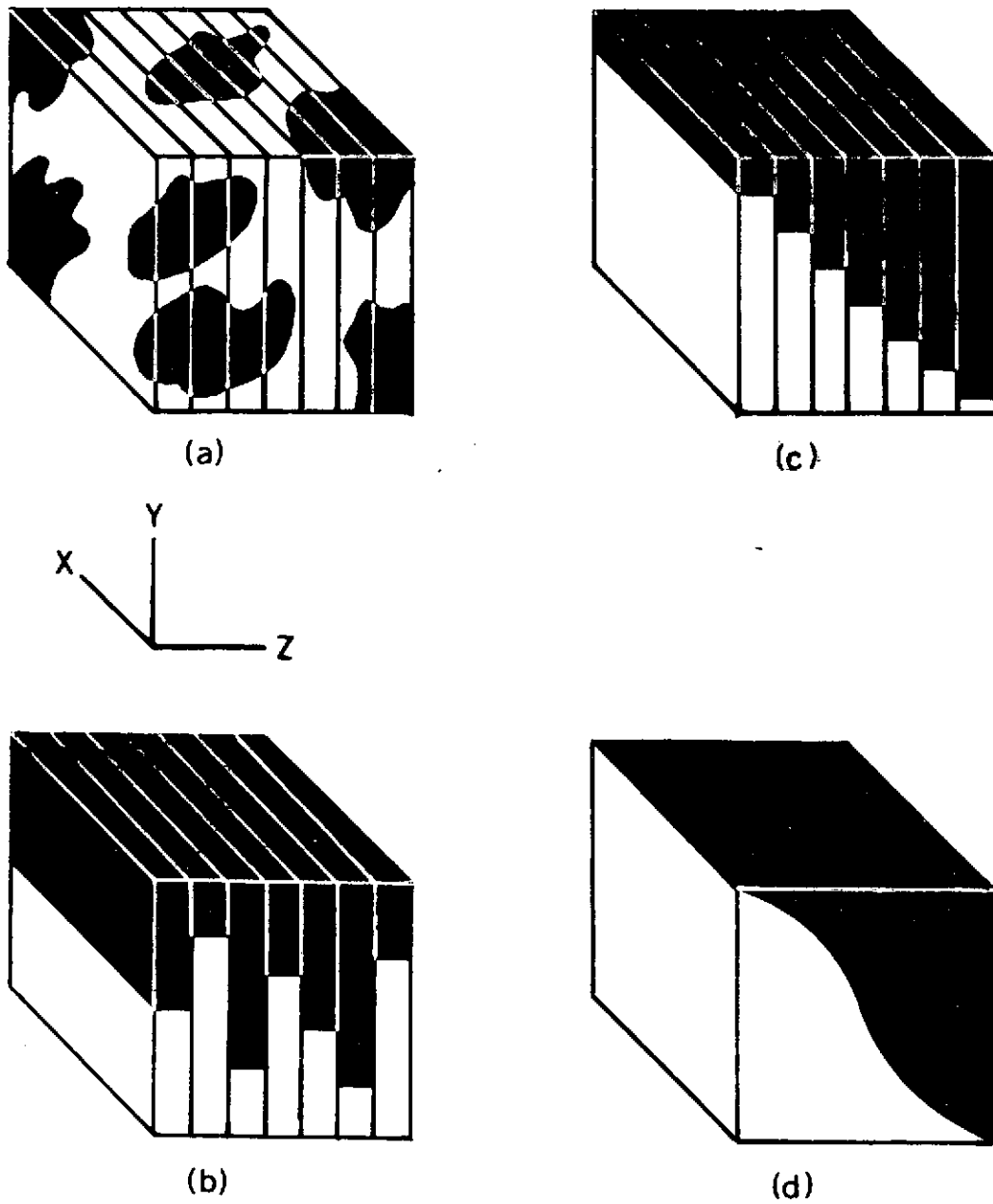
FIGURE 4-1. OHM'S MODEL — LINEAR ISOTHERMS

$$k_e = \frac{1}{\int_0^1 \frac{dz}{k_d + (k_c - k_d)\, y}} \tag{4-1}$$

A number of attempts have been made to determine a functional relationship between y and z by either expressing y as a function of z, $\mu$, and $\sigma$, where $\mu$ is the mean value of z and $\sigma$ is the standard deviation of z [8, 53], or by approximating the phase distribution curve by a curve by a parabolic function [70]. The method proposed in this study is based on the initial assumption of randomness.

Consider one of the laminae that is perpendicular to the mean heat flow. The probability that exactly $rN$ cubicles, out of the $N^2$ cubicles present in the lamina, are occupied by the continuous phase is given by the binomial distribution:

$$\Pi(rN) = \frac{(N^2)!}{(N^2)!\,(N^2 - rN)!}\; P^{rN}\, Q^{N^2 - rN} \tag{4-2}$$

where

$$Q = 1 - P \tag{4-3}$$

Suppose that the height of the continuous phase in the $m^{th}$ lamina is $r/N$ after the laminae have been rearranged according to decreasing height of the continuous phase, as indicated in Figure 4-1c. It

follows that there are m laminae in which the height of the contin-
uous phase is equal to or greater than r/N, and consequently

$$m = N \sum_{rN}^{N^2} \Pi(rN) \qquad (4-4)$$

If $N^2$ is large enough, $\Pi(rn)$ can be approximated by the normal
distribution [71],

$$f(rN) = \frac{1}{\sqrt{2\pi} \; \sqrt{N^2 PQ}} \cdot e^{-\frac{(rN-PN^2)^2}{2(N^2 PQ)}} \qquad (4-5)$$

Substitution of Equation (4-5) into Equation (4-4), and noting that
and r/N = y, it follows that

$$z = \frac{1}{2}(1 - \mathrm{erf}\, t) \; , \quad t = \frac{N^2 (y - P)}{\sqrt{2N^2 PQ}} \qquad (4-6)$$

Equation (4-6) is an expression for z as a function of y in terms
of the parameters P and N. The continuous phase volume fraction
P is assumed to be known since it is reported in all experimental
investigations of granular materials. N is a measure of the fineness
of the three-dimensional grid. In other words, it is a measure of
the sample size. Although, there is no analytical method to determine
N if the size of the cubicles is not selected, a lower bound for N

can be found by the constraint that the total number of cubicles in the unit cube occupied by the continuous phase must be equal to $PN^3$. In other words

$$\int_0^1 z \, dy = P \tag{4-7}$$

Equation (4-7) is satisfied when $N^2$ is larger than $8/P$ and $8/Q$. It can be also shown that under this condition, the approximation of the binomial distribution by the normal distribution is also valid.

In view of the discussion above, Equations (4-1) and (4-6) constitute a solution for the effective thermal conductivity of granular materials, provided the model and the assumptions associated with it constitute a realistic approximation of the system. However, it should be noted that the additional resistance to the heat flow from one particle to the other, introduced due to the contact surface of two particles, has not been taken into account in the development. This assumption is certainly justified for unconsolidated porous media, but induces large errors in the case of granular materials [34]. To overcome this discrepancy, an additional term will be introduced in Equation (4-1) to account for contact resistance.

Let $N_c$ be the total number of contact areas in a unit cube. Assuming that these contact areas are randomly distributed and oriented, the number of contact areas in the z-direction, $N_{cz}$ is $N_c/3$. These contact resistances can be distributed over the

laminae shown in Figure (4-1c) in such a manner that the number of contact resistances in a lamina $\dot{n}_{cz}$ is proportional to the discontinuous phase present in the lamina. That is:

$$\frac{(1 - y) \ (1/N)}{(1 - P)} = \frac{n_{cz}}{N_{cz}} \qquad (4-8)$$

Now, taking into account that each lamina is composed of continuous phase cubicles, discontinuous phase cubicles, and cubicles containing contact areas as given by Equation (4-8), summation over the thermal resistances present in each lamina, and integration over all laminae, yields a modified form of Equation (4-1).

$$k_e = \frac{1}{\int\limits_0^1 \dfrac{dz}{k_d + (k_c - k_d)y - \dfrac{(1-y)}{(1-P)} \dfrac{N_{cz}}{N^3} (k_d - k_{cr})}} \qquad (4-9)$$

In Equation (4-9), $k_{cr}$ is the contact thermal conductivity associated with a contact area. In the calculations, an expression for $k_{cr}$ is taken from Luikov [34].

It is still necessary to find an expression for the total number of contact areas per unit cube, in order to determine $N_{cz}$. This can be accomplished by assigning a characteristic volume to each particle and considering the coordination number n which is the average number of contact points per particle. As indicated in [66] the

characteristic volume of each particle is $\epsilon_v d^3$, where $\epsilon_v$ is an experimentally determined volumetric parameter that depends on the particle shape, and d is a characteristic particle size obtained from the sieve data. It follows then that the number of particles per unit volume is $\frac{1-P}{\epsilon_v d^3}$. The coordination number is given in [49] as

$$n = 39.39 \ (0.571 - P) \tag{4-10}$$

For spherical particles $\epsilon_v$ is equal to $\pi/6$. Combination of these expressions yields, for spherical particles

$$N_{cz} = \frac{12.54 \ (0.571 - P)}{d^3} \ (1 - P) \tag{4-11}$$

Combination of Equations (4-1), (4-9), (4-11) constitute a solution for the effective thermal conductivity of granular materials in terms of the conductivities of the components, the porosity, and the parameters mentioned. The equations have been solved and compared to a number of experimentally determined values. It should be noted that the value of N chosen for each case satisfied the lower bounds mentioned, and was such that the cubicles were smaller than the particles and the voids.

## Ohm's Law Model - Uniform Heat Flux

Again, consider a unit cube of a granular material subdivided into $N^3$ cubicles by a three-dimensional grid. Looking at the parallel-

to-the-heat-flow rectangular tubes, it can be seen that they include
continuous phase and discontinuous phase cubicles. Under the
assumption of uniform heat flux, the effective thermal conductivity
of the rectangular tubes does not change if the cubicles are
rearranged in such a manner that the continuous phase is pushed
forward [69], as indicated in Figure (4-2b).

The effective thermal resistance of each tube is due to the
thermal resistance of the continuous phase and the thermal resistance
of the discontinuous phase present in the tube, acting in series.
Moreover, since the effective thermal resistances of all tubes are
in parallel, summation of all the thermal conductances of the tubes
gives the effective thermal conductance of the unit cube. Assuming
that the summation can be approximated by integration, the effective
thermal conductivity of the unit cube is

$$k_e = \int_0^1 \int_0^1 \frac{dx\, dy}{\frac{1-z}{k_d} + \frac{z}{k_c}} \tag{4-12}$$

where $z$ is the height of the discontinuous phase at $(x,y)$. To
integrate Equation (4-12), it is necessary to know $z$ as a function of
$x$ and $y$. This can be accomplished by a rearrangement of the rectangular
tubes that are parallel to the heat flow as follows:

1.  In each parallel to the heat flow x-z lamina, the tubes are
    rearranged according to decreasing height of the continuous
    phase in the x-direction (Figure 4-2c).

2.  The x-z laminae are rearranged according to the total amount of continuous phase present in each lamina. Further, the rearrangement is such that the continuous phase void fraction of each lamina decreases with $y$ (Figure 4-2d).

This rearrangement of the rectangular tubes does not affect the effective thermal conductivity of the unit cube, since the height of the continuous phase in each tube remains the same, but permits one to express the distribution of the phases in the unit cube by continuous functions. The arguments leading to these distribution functions are the same as the ones presented for the development of Equation (4-6), and will not be repeated here. The results are the following. For each lamina at $y$, and having thickness $dy$,

$$x = \tfrac{1}{2}(1 - \text{erf}\,t), \qquad t = \frac{N(z - P_y)}{\sqrt{2N\,P_y\,Q_y}} \qquad (4\text{-}13)$$

where $P_y$ is the ratio of the volume of the continuous phase present in the lamina to the total volume of the lamina, and $Q_y = 1 - P_y$. Analysis of Figure (4-2d) gives,

$$y = \tfrac{1}{2}(1 - \text{erf}\,u), \qquad u = \frac{N^2(P_y - P)}{\sqrt{2N^2 PQ}} \qquad (4\text{-}14)$$

Again, the constraint that the total number of cubicles in the unit cube, occupied by the continuous phase, must be equal to $PN^3$ is satisfied when $N$ is larger than $8/P$ and $8/Q$. Under these conditions
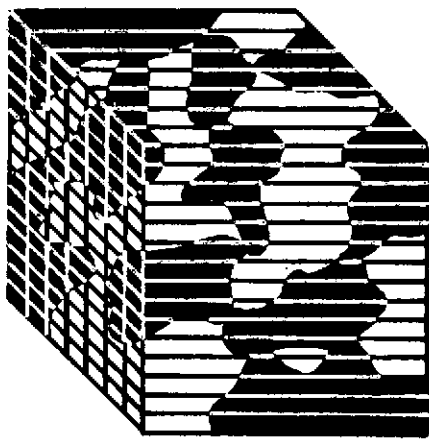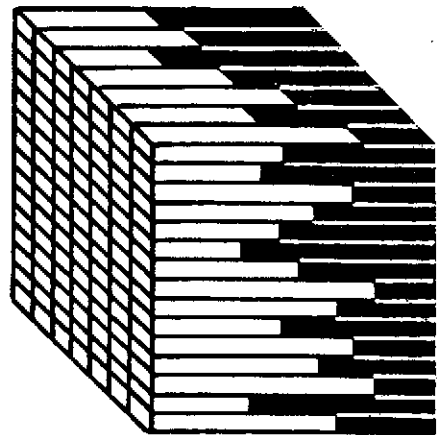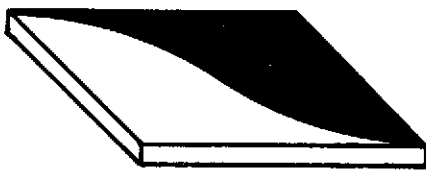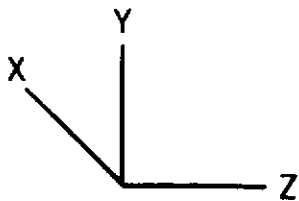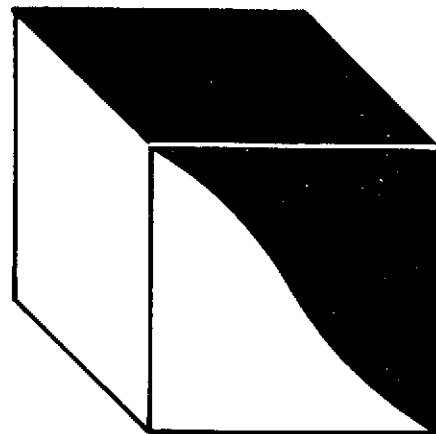
FIGURE 4-2. EQUIVALENT GEOMETRIES FOR UNIFORM HEAT FLUX.

the approximation of the binomial distribution by the normal distribution is also valid.

Combination of Equations (4-12), (4-13) and (4-14) constitutes a solution for the effective thermal conductivity of granular materials in terms of the conductivities of the components and the porosity. The equations have been solved and compared to a number of experimentally determined values. Again, the value of N chosen for each case satisfied the lower bounds mentioned, and was such that the cubicles were smaller than the particles and the voids. It should be noted that in this model the thermal contact resistance, due to the contact areas between particles, has not been introduced. The reason is that the uniform heat flux assumption renders the calculated effective conductivity smaller than the experimental one, and introduction of the contact thermal resistance will increase the discrepancy between calculated and experimental values.

## Comparison of the Ohm's Law Models

Equations (4-9) and (4-12) have been obtained to predict the effective thermal conductivity of granular materials as a function of the constituent conductivities, porosity, and the parameters indicated. In both models, a representative unit cube of the granular material has been considered. The basic assumption utilized in order to obtain the distribution of the two phases in the unit cube is that a granular material can be considered a

random mixture of two phases. In view of the evidence given by Debbas and Rumpf [51] and Baxley and Cooper [20], this assumption is in good agreement with experimental results, and consequently it can be concluded that the assumed geometry of the unit cube is quite accurate for most granular materials.

Equations (4-9) and (4-12) have been solved for a number of cases, and some of the results are presented in Figures (4-3) and (4-4), representing granular systems with porosities 0.42 and 0.38, respectively. Wiener's upper and lower bounds are also indicated. The experimentally determined values have been obtained from references [6, 21, 23, 36]. It can be seen that the parallel isotherms model grossly overpredicts the effective thermal conductivity of granular materials, while the uniform heat flux model predicts lower values. The discrepancy increases with the ratio of the constituent conductivities. Although, the region between the upper and lower bounds thus defined is smaller than the region defined by Wiener's bounds, the specific values obtained from Equations (4-9) and (4-12) leave much to be desired.

This difference between calculated and true effective thermal conductivity values can be explained by Laubitz's [17] observation that in the uniform heat flux model it is effectively assumed that the thermal conductivity of the medium in the normal to the heat flow directions is infinite, while in the parallel isotherms model it is
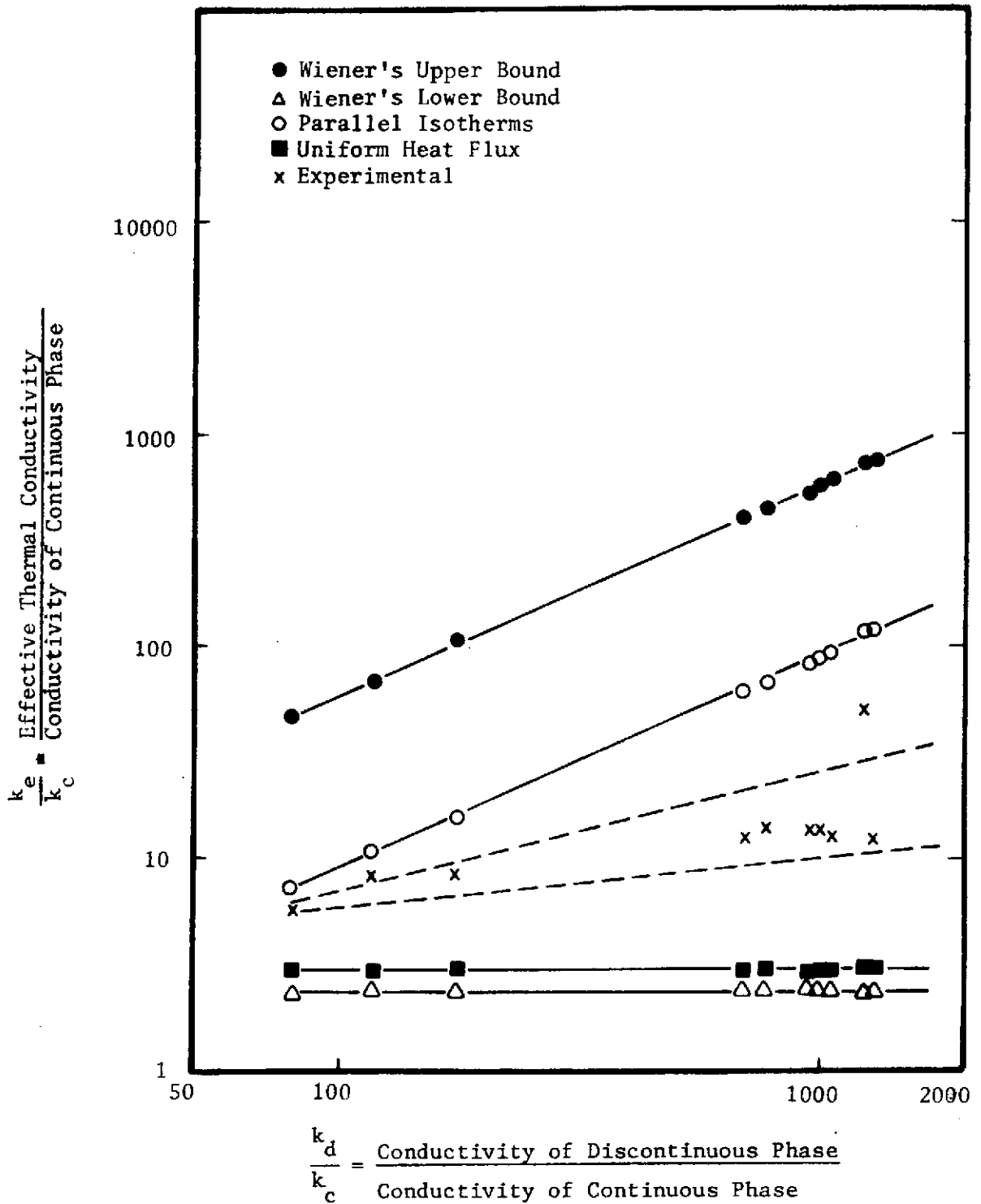
FIGURE 4-3. COMPARISON OF BOUNDING CONDUCTIVITIES WITH EXPERIMENTAL DATA FOR A POROSITY OF 0.42.
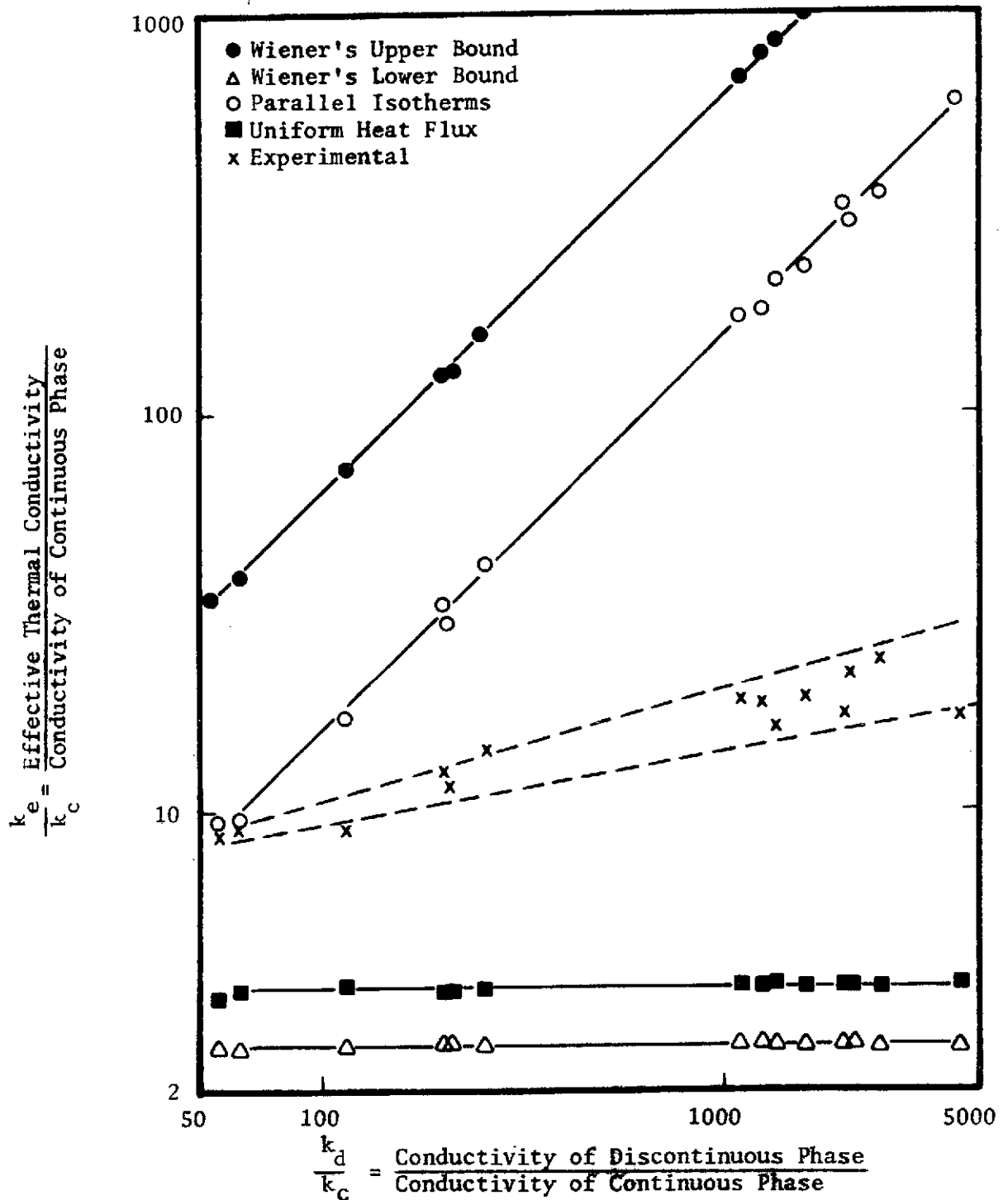
FIGURE 4-4. COMPARISON OF BOUNDING CONDUCTIVITIES WITH
EXPERIMENTAL DATA FOR A POROSITY OF 0.38.

vanishingly small. It also provides an explanation as to why previous Ohm's Law models, based upon an assumed regular array, have generally not been successful at higher constituent conductivity ratios. Some of the discrepancy due to the heat flow assumptions has been countered in previous Ohm's law models by assuming a somewhat distorted array. However, at high constituent conductivity ratios, the effect of the heat flow assumptions prevails, and the calculated values continually deviate from the true effective thermal conductivity values.

Since the lateral conductivity of granular materials falls between the limits of zero and infinite lateral conductivity, it can be concluded that Equations (4-9) and (4-12) constitute an upper and lower bound to the true effective thermal conductivity. Numerous correlation forms have been developed in the literature [18] associating the true conductivity of the granular material to the bounding values. However, it does not appear possible to select the correlation which is more consistent with the physical system. Consequently, an alternate approach is suggested, where the geometry of the granular system is the same, while no assumption is made with respect to the heat flow. This constitutes the basic model of this study, and it differs from the Ohm's law models presented in that both the geometry and the heat flow assumptions are realistic. The Ohm's law models will be utilized in the discussion that follows as a criterion for the selection of a number of parameters such as contact resistance, coordination number, etc.

# V    PARALLEL ISOTHERMS MODEL

The approach specified in this chapter is based upon an extension
of the approach originally proposed by Wiener [7] and later extended,
first by Russell [43], and later by Tsao [8]. The effective thermal
conductivity of the heterogeneous system is determined using the
electrical analogy. Probability techniques are used to describe the
random distribution of the particles within the system as introduced
in Tsao's model. Two statistical parameters are introduced and are
determined based upon bulk physical properties.

Consider a unit cube of the heterogeneous system shown in
Figure (2-5a). The system is to be divided into a series of fine
laminae oriented normal to the direction of heat flux. These elements
are sufficiently thin that the cross-sectional area of the solid
particles are essentially constant throughout its width. Assuming
parallel isotherms within the unit cube, the discontinuous (solid) and
continuous phases will act as resistances in parallel within each
lamina. The order of the parallel resistances may be changed arbitrarily
without affecting the overall resistance of the parallel circuit. Thus
the resistances of the solid elements may be combined into a single
solid resistance at the bottom of the laminae as shown in Figure (2-5b).

A simple calculation then shows that the equivalent resistance is given by the equation

$$k_e = \frac{1}{\sum_{m=1}^{h} \frac{1}{k_c + (k_d - k_c)\bar{\epsilon}_m}} \tag{5-1}$$

In this equation the fraction of solid in the $m^{th}$ lamina is given by $\bar{\epsilon}_m$ and the width of each lamina is $\Delta x$.

Note that the laminae act as resistances in series. Again the order of the resistances does not affect the overall thermal resistance so that the elements may be rearranged in order of decreasing solid fraction as shown in Figure (2-5c). If the width of the laminae is allowed to approach zero then the effective thermal conductivity for Figure (2-5d) becomes

$$k_e = \frac{1}{\int_0^1 \frac{dx}{k_c + (k_d - k_c)\,\bar{\epsilon}}} \tag{5-2}$$

The solution of this equation requires the knowledge of a relationship between the solid area fraction $\bar{\epsilon}$ and the position x. Such a relationship is given in the form

$$\bar{\epsilon} = \frac{\int_x^1 e^{-1/2\left(\frac{\rho - \mu}{\sigma}\right)^2} d\rho}{\int_0^1 e^{-1/2\left(\frac{\rho - \mu}{\sigma}\right)^2} d\rho} \tag{5-3}$$

In this expression $\mu$ and $\sigma$ represent the mode and the standard deviation of the one dimensional porosity as introduced by Tsao. For the case at hand the mode, $\mu$, will be very close to the bulk solid fraction. The standard deviation, $\sigma$, is unknown. In general, it will be a function of the particle shape, size distribution and volume fraction. By restricting consideration to uniform sized particles which are either spherical or semi-spherical the standard deviation becomes a function of the volume fractions only. Or

$$\sigma = f( \bar{\epsilon} ) \tag{5-4}$$

Using the experimental data available from the literature, Equations (5-2) and (5-3) may be solved to determine $\sigma$ for each case. These data have been curve fitted using a least squares technique to obtain the relation

$$\sigma = 0.32248 \ (1 - \bar{\epsilon}) - 0.092543 \ (1 - \bar{\epsilon})^2 \tag{5-5}$$

The resulting equations may be used to determine the effective thermal conductivity of packed beds with solid fractions between 0.3 to 0.7. Beyond these limits the assumption of random packing of semi-spherical particles no longer holds.

## Results

Data describing the effective thermal conductivity of packed beds have been compiled from the literature. Generally, results obtained from Equation (5-2) fall within ± 20% of the reported values, provided that radiation may be neglected. A representative sample of data

taken from several sources [6, 35, 37, 58] is shown in Figure (5-1). A more extensive comparison between predicted and experimentally determined values for granular materials at atmospheric pressure is included in Chapter 6.

The model has also been extended to the case of particulate basalt in a simulated lunar environment, and the results are shown in Figure (5-2). It is noted that the model predicts a slightly greater dependence of the effective conductivity on packing fraction than is indicated by the experimental data. This could be off-set to some extent by modifying the empirical distribution function used in the correlation; such a modification would be difficult to justify on theoretical grounds and therefore has not been undertaken.
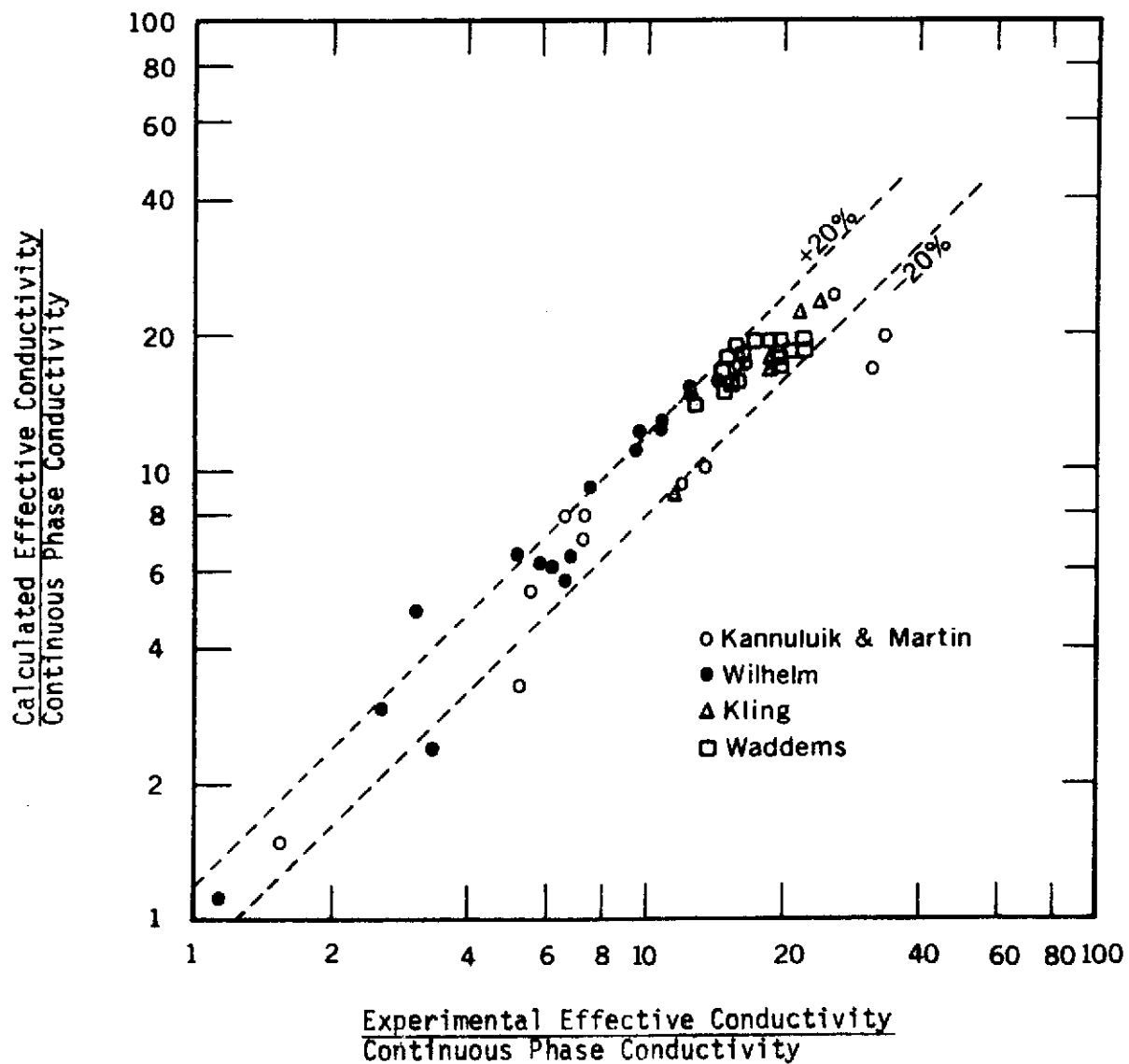
FIGURE 5-1. COMPARISON OF EXPERIMENTAL AND MODEL PREDICTED THERMAL CONDUCTIVITIES.
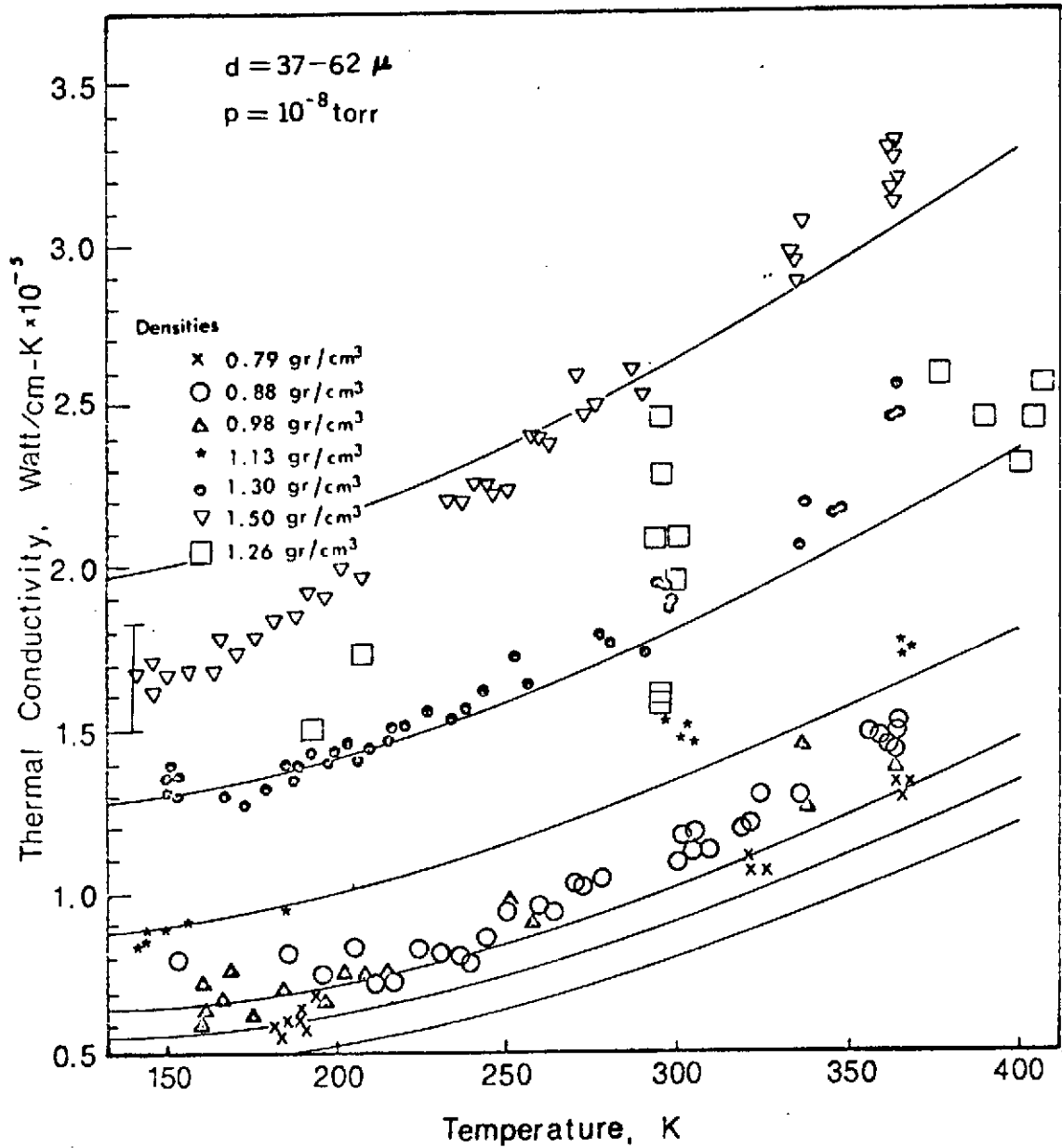
FIGURE 5-2. COMPARISON BETWEEN MODEL PREDICTED AND
EXPERIMENTAL THERMAL CONDUCTIVITIES FOR
BASALT IN SIMULATED LUNAR ENVIRONMENT.

# VI. STOCHASTIC MODEL

Over the past sixty years [7] numerous Ohm's law models have been introduced. Most of these models are based upon a rough approximation of granular materials in terms of solid parallelopipeds or cubically arrayed spheres. Neither geometry bears a close relation to the random dispersions commonly found in nature. The approach described herein avoids these unnatural arrays and unrealistic geometries by assuming a random distribution of arbitrarily shaped solid particles.

As noted in the literature survey, those models incorporating Ohm's law almost universally utilize assumptions of zero or infinite lateral conductivity. In any real substance the lateral conductivity will fall between these two extremes. Consequently these two assumptions lead toward a set of bounding equations for the effective thermal conductivity of the model. These bounding equations set much narrower limits than those originally proposed by Wiener [7]. A comparison of the two sets of equations is shown in Figure (6-1). The effective conductivity of a square array of uniform spheres ($\overline{\epsilon}$ = 0.5236) is represented. Note that at a constituent conductivity ratio of $10^6$, these new bounding conditions are approximately one order of magnitude above the lower bound and a factor of five below the upper bound established by Wiener. Therefore, a set of such equations, applicable to any packing geometry would represent a considerable improvement over Wiener's formulation.
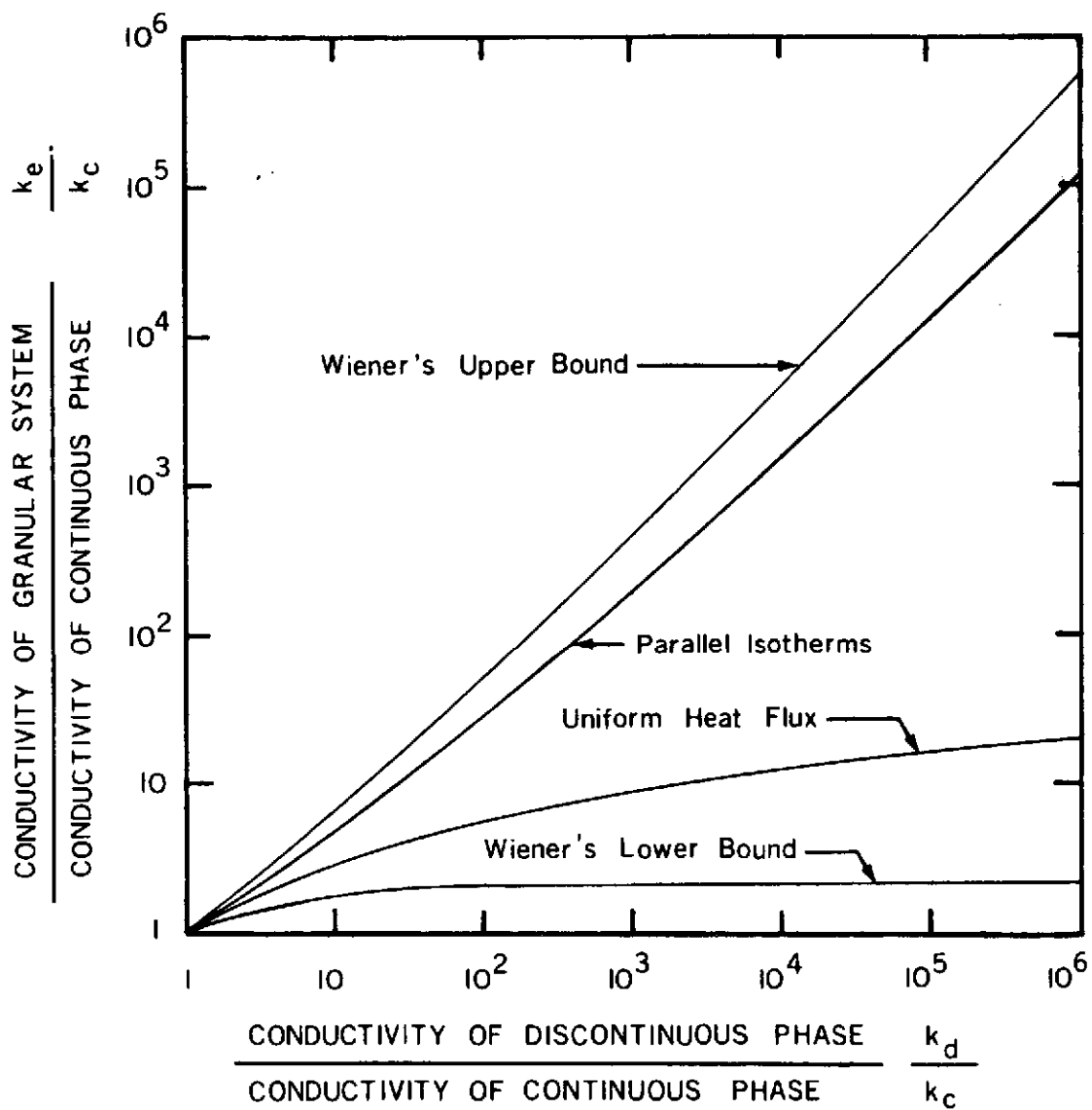
FIGURE 6-1. BOUNDING EQUATIONS FOR A CUBIC ARRAY OF SPHERES

Herein will be developed a set of such equations, generally applicable to any shape particle.

Consider a typical unit cell of the heterogeneous system shown in Figure (6-2a). Divide the unit cell into uniform sized channels by passing both vertical and horizontal planes through the element. These planes are to be oriented parallel to the direction of heat flux and are to be equispaced. If the channels are sufficiently small compared to the dimensions of the solid particles, they will appear as consisting of sections of the continuous and discontinuous phases placed in series. Assuming a uniform heat flux in each channel, the order of the series resistances does not influence the overall resistance. Consequently, the two components may be separated as shown in Figure (6-2b). The resistance of the channel is then given by

$$R_i = \frac{\varepsilon_i}{k_d \Delta A} + \frac{(1-\varepsilon_i)}{k_c \Delta A} \tag{6-1}$$

The channels behave as resistances in parallel. The overall resistance is then given as:

$$\frac{1}{R_e} = \frac{1}{R_1} + \frac{1}{R_2} + \ldots + \frac{1}{R_n} \tag{6-2}$$

The order of these channels and their shape may be altered so long as the individual channel resistances remain unchanged. They may then be distorted to a unit width by changing the vertical dimension while retaining the unit length. They are then arranged in order of decreasing

solid fraction. This geometry is shown in Figure (6-2c). The effective

thermal conductivity for the specified element is

$$k_{e_0} = \frac{k_c k_d \Delta A}{\sum_{i=1}^{n} k_c \epsilon_i + k_d (1-\epsilon_i)} \tag{6-3}$$

If the area of the channels is allowed to approach zero as the number

of channels approaches infinity the summation in Equation (26) may be

replaced by an integral.

$$k_{e_0} = \int_A \frac{k_c k_d}{k_c \epsilon + k_d (1-\epsilon)} \, dA \tag{6-4}$$

or,

$$k_{e_0} = \int_0^1 \int_0^1 \frac{k_c k_d}{k_d + \epsilon (k_c - k_d)} \, dx dy$$

$$= \int_0^1 \frac{k_c k_d}{k_d + \epsilon (k_c - k_d)} \, dx \tag{6-5}$$

since the integrand is constant in the horizontal direction. The

corresponding geometry is shown in Figure (6-2d).

In a similar manner the effective conductivity has been found

assuming infinite lateral conductivity [8, 53]:
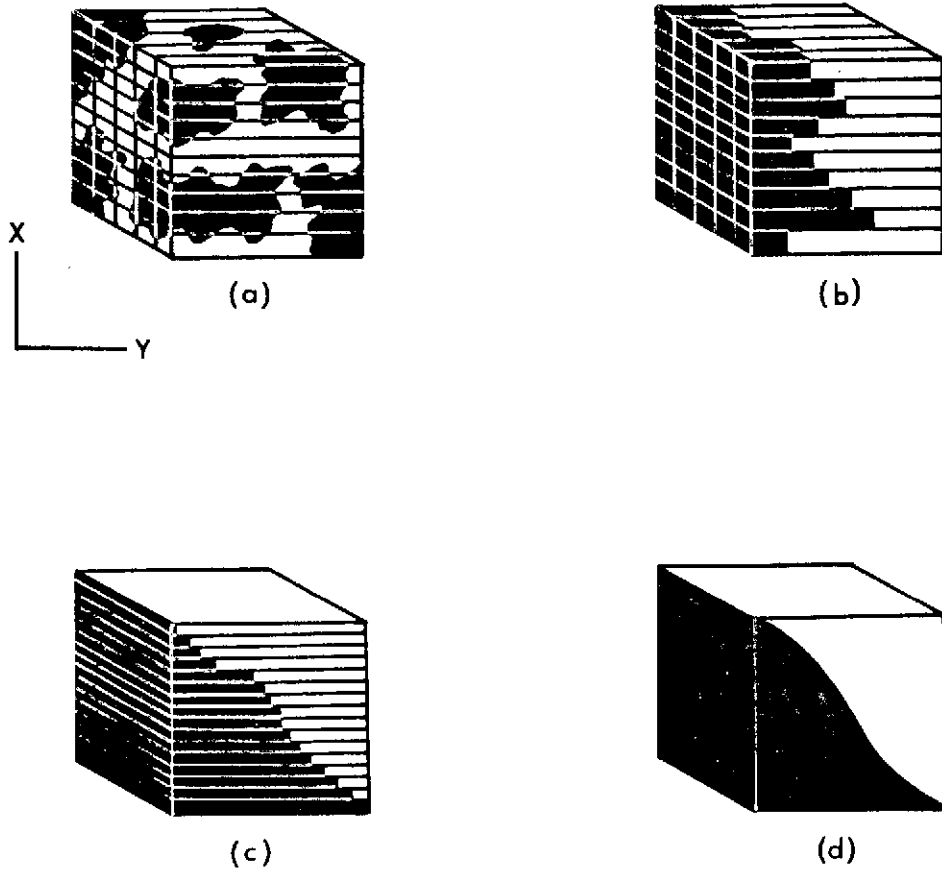
FIGURE 6-2. EQUIVALENT GEOMETRIES FOR UNIFORM HEAT FLUX

$$\frac{1}{k_{e_\infty}} = \int_0^1 \frac{dx}{k_c + \epsilon(k_d - k_c)} \tag{6-6}$$

Both equations for zero and infinite lateral conductivity require a knowledge of the functional relation between the solid area fraction, $\epsilon$, and the position, $x$, to solve the integral. Consider the arbitrary material distribution shown in Figure (6-2c). The verticle position of each lamina is determined by its solid fraction. The portion of the elements below a particular element is then equal to the portion of elements having larger solid fractions.

$$x = P(\epsilon_i > \epsilon)$$

$$= \int_\epsilon^1 f(\phi)d\phi \tag{6-7}$$

Differentiating this equation,

$$dx = -f(\epsilon)d\epsilon \tag{6-8}$$

This relationship may be substituted into Equations (6-5) and (6-6) for the thermal conductivity with uniform heat flux and parallel isotherms. The limits of integration must be changed accordingly

$$k_{e_0} = \int_1^0 \frac{k_c k_d f(\epsilon)}{k_d + \epsilon(k_c - k_d)} d\epsilon \tag{6-9}$$

$$\frac{1}{k_{e_\infty}} = \int_1^0 \frac{f(\varepsilon)}{k_c + \varepsilon(k_d - k_c)}\, d\varepsilon \qquad (6\text{-}10)$$

Equations (6-9) and (6-10) are entirely general in that no assumptions have yet been made regarding the particle shape or size distribution. The effects of these parameters on the solid area fraction were studied by Debbas and Rumph [51] and Haughey and Beveridge [49]. These sources found experimentally that the distribution of the solid area fraction is Gaussian for most packings. A notable exception occurs after prolonged vibration of a sample. This packing produces large regions of ordered distribution and strong anisotropic effects. Similarly large particle size variations tend to allow sifting of smaller particles into the lower regions of a given sample. This produces a definite bulk porosity gradient in the vertical direction. In such cases the radial distribution remains normal. Neglecting all such non-normal distributions the frequency distribution may be taken as Gaussian.

$$f(t) = \frac{e^{-\frac{1}{2}t^2}}{\displaystyle\int_a^b e^{-\frac{1}{2}t^2}\, dt} \qquad (6\text{-}11)$$

The integral in the denominator serves to normalize the truncated Gaussian distribution. By replacing the standardized random variable Equation (6-11) may be written in the form:

$$f(\epsilon) = \frac{+e^{-\frac{1}{2}\left(\frac{\epsilon-\mu}{\sigma}\right)^2}}{\frac{\sigma\sqrt{\pi}}{\sqrt{2}}\left[\text{erf}\left(\frac{1-\mu}{\sigma\sqrt{2}}\right) - \text{erf}\left(\frac{0-\mu}{\sigma\sqrt{2}}\right)\right]} \tag{6-12}$$

The mode of the distribution, $\mu$, and the standard deviation of the solid area fraction, $\sigma$, remain to be evaluated. The mode may be defined implicitly in terms of the standard deviation from the basic geometry of the mixture. The total solid volume is equal to the sum of the elemental solid volumes.

$$\bar{\epsilon} = \int_0^1 \epsilon \, dx \tag{6-13}$$

Using the results of Equation (6-8) this expression may be written:

$$\bar{\epsilon} = \int_1^0 -\epsilon \, f(\epsilon) \, d\epsilon \tag{6-14}$$

Determination of an exact expression for the standard deviation is difficult. Stange [50] reports that the standard deviation is given by the relation,

$$\sigma = \frac{\text{constant}}{\sqrt{M}} \tag{6-15}$$

where M is a measure of the sample size.

The exact value of the standard deviation is difficult to evaluate. However, it may be noted from Figure (6-3) that the effective conductivity tends to reach a fixed value for $\sigma$ sufficiently large. Consequently a sufficiently large value of $\sigma$ may be selected for analysis.

## Development of an Effective Conductivity Correlation

Equations (6-9) and (6-10) have been obtained to predict the effective thermal conductivity of a two phase mixture as a function of the constituent conductivities and the volume fractions. These expressions are based upon the assumptions of zero and infinite lateral conductivity, respectively. Since the lateral conductivity of the mixture falls between these limits the two equations form a set of bounding limits for the physical case. As noted in the review of literature, numerous authors have proposed correlations which effectively imply that one of these two assumptions is sufficiently close to the physical system that it may be used in obtaining an effective conductivity expression. In spite of arguments presented for proponents of both methods, it does not appear possible to select, a priori, the correlation which is more consistant with physical system. Results from both correlations are then to be compared with experimental results.

Such a comparison has been made and the results are shown graphically in Figures (6-4),(6-5) and (6-6). These figures represent granular systems with porosities of 0.31, 0.43 and 0.58 respectively. The selected values represent a range of packing fractions so that they may be considered as representative of all random packings. The non-dimensionalized effective conductivity is given as a function of the constituent conductivity ratios. The experimental values are taken from a number of independent sources and
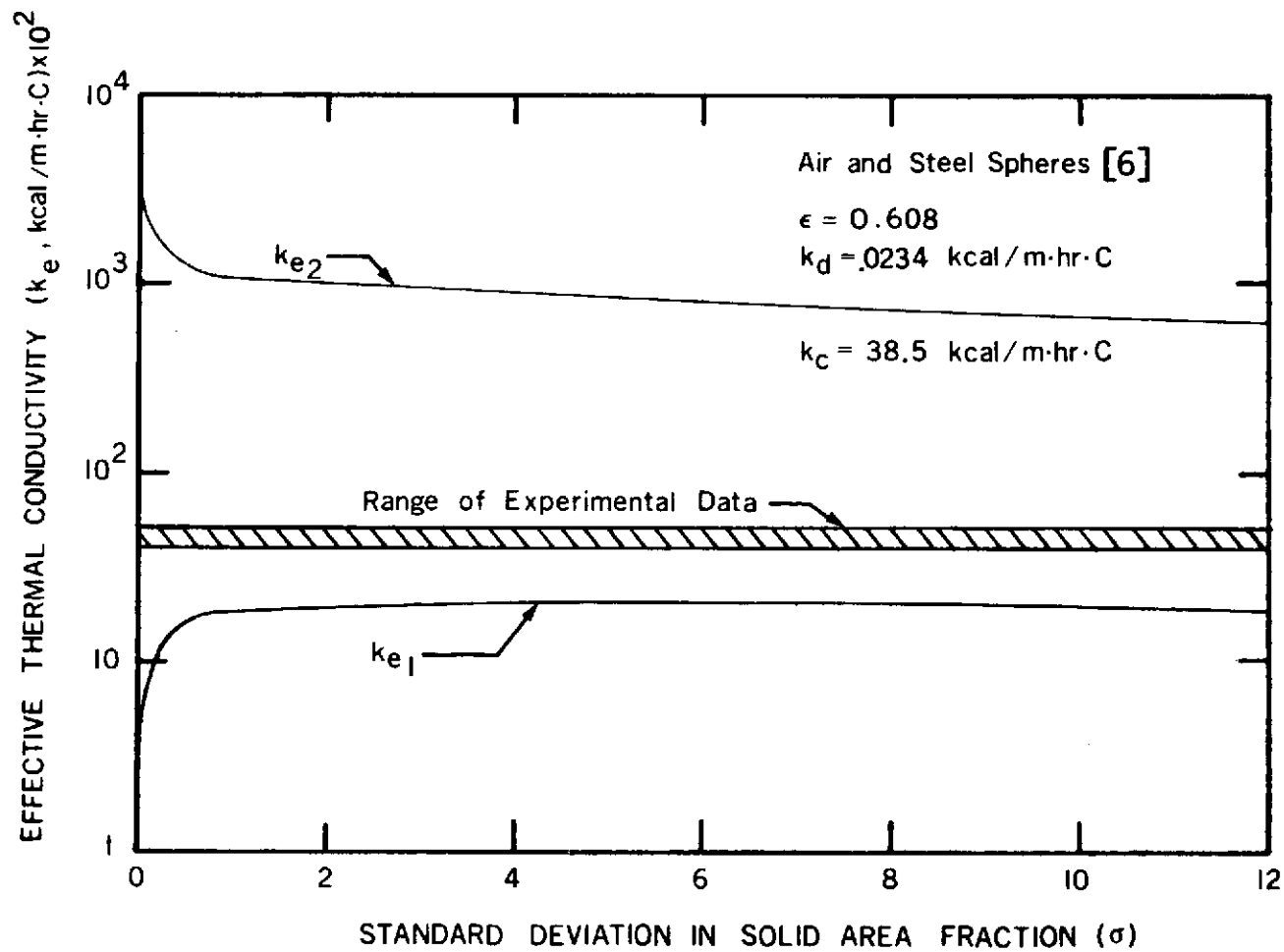
FIGURE 6-3. EFFECT OF STANDARD DEVIATION IN AREA FRACTION UPON EFFECTIVE CONDUCTIVITY
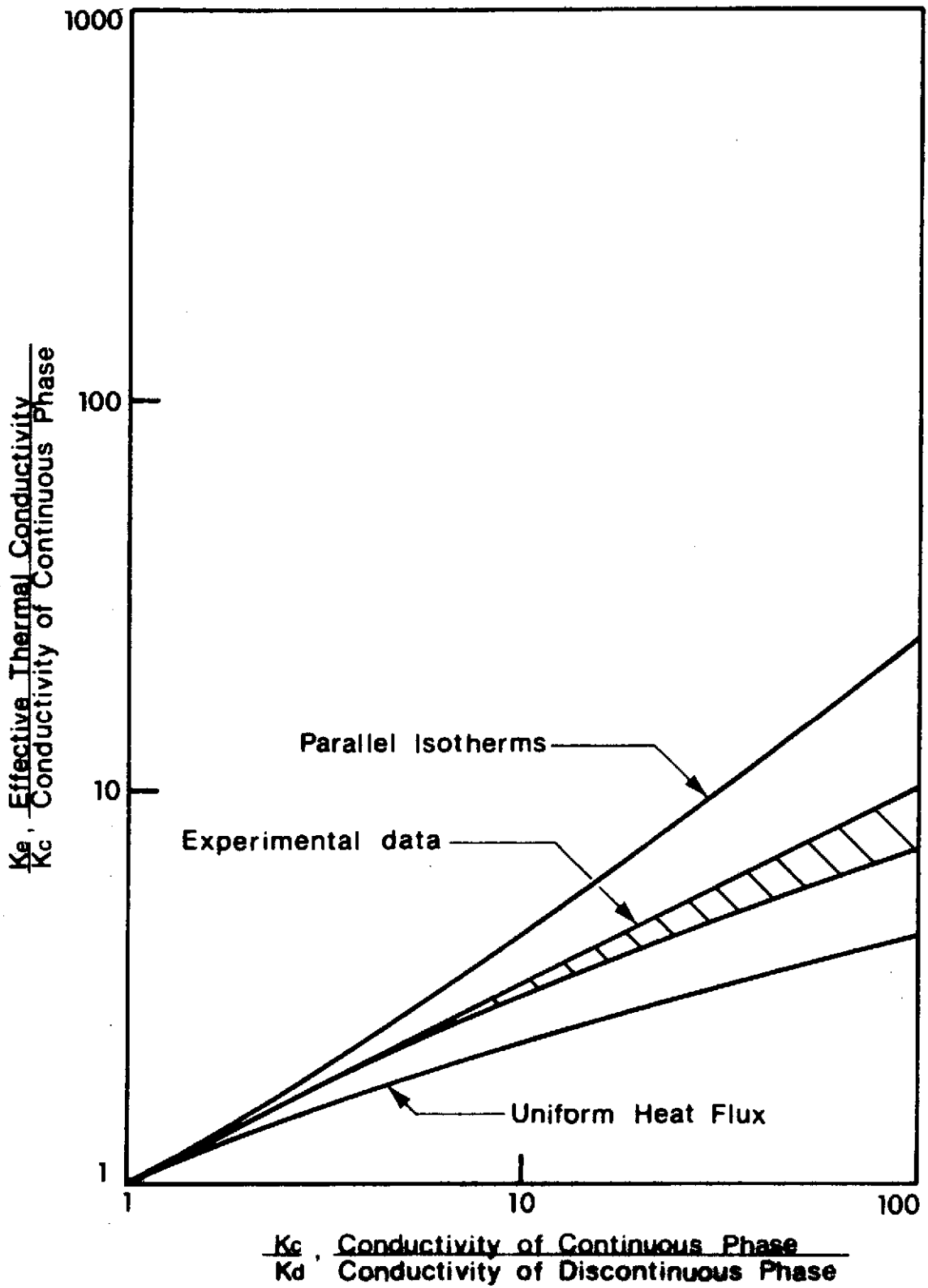
FIGURE 6-4.   COMPARISON OF BOUNDING CONDUCTIVITIES WITH
EXPERIMENTAL DATA FOR A POROSITY OF 0.31
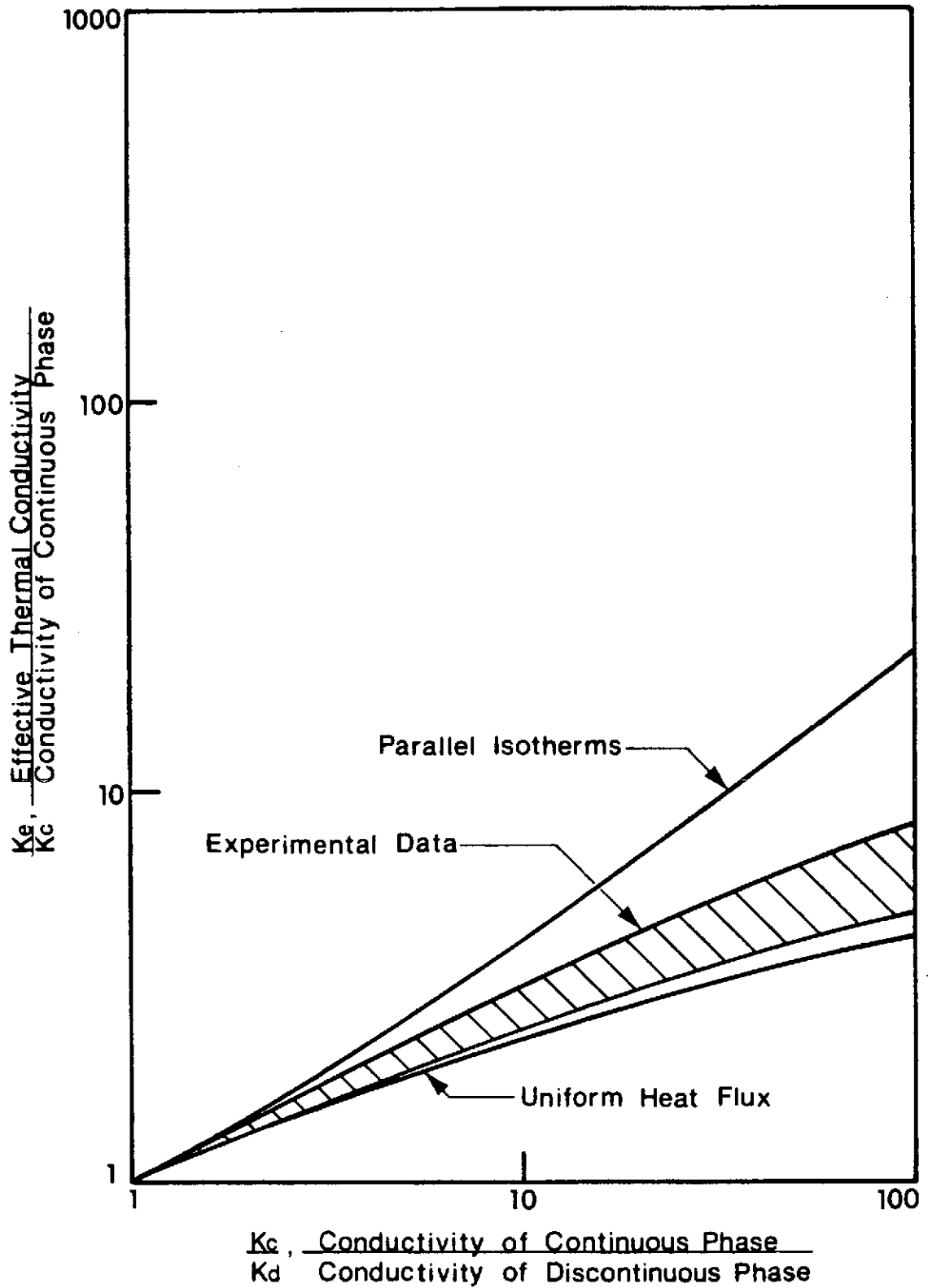
FIGURE 6-5. COMPARISON OF BOUNDING CONDUCTIVITIES WITH EXPERIMENTAL DATA FOR A POROSITY OF 0. 43
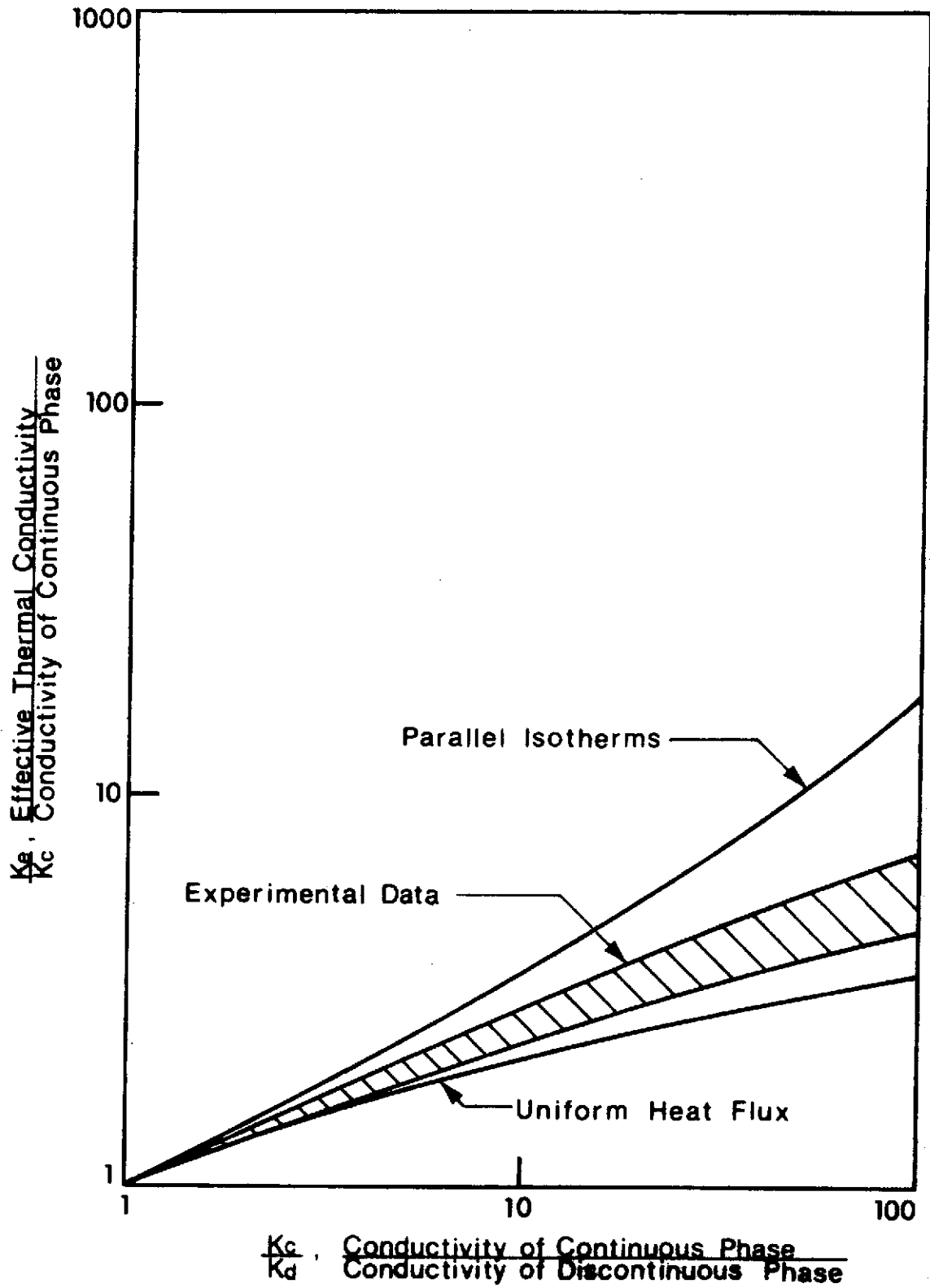
FIGURE 6-6.  COMPARISON OF BOUNDING CONDUCTIVITIES WITH
EXPERIMENTAL DATA FOR A POROSITY OF 0.58

are listed in Table 6-I. Note that the bulk of these data fall between the two bounding curves as would be anticipated. For a constituent conductivity ratio, $k_d/k_c < 10$ either bounding equation gives reasonably accurate results. For $k_d/k_c > 100$ both bounding equations deviate significantly from the experimental data. This indicates the reason why previous Ohm's law models, based upon an assumed regular array, have generally not been successful at higher constituent conductivity ratios. No doubt, some of the discrepancy has been countered by assuming a somewhat distorted array. Uniform heat flux models have been developed such that an inordinate amount of the higher conductivity material is arranged in series with itself. Thus the calculated conductivities have been raised above the lower bounding curve. Similarly for parallel isotherm models an excessive amount of the higher conductivity material is placed in parallel with itself and in series with the low conductivity phase. This distortion tends to result in a lower calculated conductivity than that of the upper bound.

Rather than assuming both an unrealistic heat flow model and a distorted distribution, three alternate approaches are suggested here. A uniform heat flux model and a parallel isotherm model were developed based upon a theoretical distribution of the granular material which has been experimentally verified. Since only the heat flow model is simplified, an experimentally derived correction factor for the heat flow shall be obtained for each correlation. In addition, an experimentally derived weighting factor shall be obtained for the two correlations. The effective thermal conductivity will then by given by:

$$k_{eff} = F_\infty \, k_\infty \qquad\qquad (6\text{-}16)$$

$$k_{eff} = F_0 \, k_0 \qquad\qquad (6\text{-}17)$$

$$k_{eff} = k_\infty - F_w(k_\infty - k_0) \qquad\qquad (6\text{-}18)$$

where:

$F_\infty$ = Correction factor for nonparallel isotherms

$F_0$ = Correction factor for nonuniform heat flux

$F_w$ = Weighting factor for bounding equations

These correction factors are considered to be, in general, functions of the material solid fraction, constituent conductivity ratio, particle shape and particle size distribution. Unfortunately, previous attempts to describe arbitrary particle shapes with a single parameter have been largely unsuccessful [13]. Various statistical techniques have been proposed for accounting for particle size distribution [45, 54] but sufficient experimental data are not yet available to consider this parameter at this time. For this reason the correction factors are treated as functions of the conductivity ratios and the solid fractions only.

Equations (6-16) through 18) may be solved together with available experimental data to obtain the empirical values of the correction factors. This has been done for a wide range of data from the several sources as listed in Table 6-I. The correction factors listed do, of course, include both experimental error and data scatter. To obtain an easily usuable correlation these factors have been correlated into a polynomial function using a least-squares technique [55]. The fitted correction factors have

been found to be represented by the functional relations:

$$\ln(F_\infty) = 6.038 + 0.28697 \ln(k_d/k_c) - 0.079693 [\ln(k_c/k_d)]^2$$
$$- 42.035(1-\bar{\varepsilon}) + 94.701(1-\bar{\varepsilon})^2 - 0.91135(1-\bar{\varepsilon}) \ln(k_d/k_c)$$
$$+ 0.0029629 [\ln(k_d/k_c)]^3 + 0.0040281(1-\bar{\varepsilon}) [\ln(k_d/k_c)]^2$$
$$+ 0180897(1-\bar{\varepsilon})^2 \ln(k_d/d_c) - 69.049(1-\bar{\varepsilon})^3 \qquad (6-19)$$

$$\ln(F_o) = -2.4006 + 0.83611 \ln(k_d/k_c) - 0.0036959 [\ln(k_d/k_c)]^2$$
$$+ 12.426(1-\bar{\varepsilon}) - 16.278(1-\bar{\varepsilon})^2 - 3.0926(1-\bar{\varepsilon}) \ln(k_d/k_c)$$
$$+ 0.0019151 [\ln(k_d/k_c)]^3 - 0.034069(1-\varepsilon) [\ln(k_d/k_c)]^2$$
$$+ 3.3197(1-\bar{\varepsilon})^2 \ln(k_d/k_c) + 2.5768(1-\bar{\varepsilon})^3 \qquad (6-20)$$

$$F_w = 1.5287 + 0.064259 \ln(k_d k_c) - 0.0064623 [\ln(k_d/k_c)]^2$$
$$- 6.1759\bar{\varepsilon} + 11.059\bar{\varepsilon}^2 + 0.22176\bar{\varepsilon} \ln(k_d/k_c)$$
$$+ 0.00015041 [\ln(k_d/k_c)]^3 - 0.0042453 \bar{\varepsilon} [\ln(k_d/k_c)]^2$$
$$- 0.10921 \bar{\varepsilon}^2 \ln(k_d/k_c) - 7.2252 \bar{\varepsilon}^3 \qquad (6-21)$$

In conclusion, three correlations have been proposed for evaluating the effective thermal conductivity of granular systems. There appears to be no theoretical basis for selecting one solution in preference to the others. Thus, selection of the best correlation must be made solely on the basis of a comparison with experimental results.

## Comparison of Available Heat Transfer Models

A number of proposed heat transfer models have been presented in the literature survey. No doubt a number of other correlations may be found through a more exhaustive search of the literature. Nevertheless, the equations which have been presented represent those models which are most prominently used in the current literature and in present engineering practice. Moreover, many of the models are somewhat redundant in that they represent only slight variations of the same basic geometrical assumptions.

The approach to be used in making a comparison of these correlations is to select models representing varying basic geometries and varying heat flow assumptions. Where two models of the same type are particularly well known both are included. Certain prominent models require the input of parameters which are generally unknown; these are, of necessity, excluded from the comparison.

Table 6-II includes a representative sample of correlations based on flux law models. Tables 6-III and 6-IV present Ohm's law models utilizing the assumption of uniform heat flux. Table 6-V presents those Ohm's law models based upon an assumption of parallel isotherms. Table 6-VI includes those Ohm's law models which include a weighting factor or a correction factor to circumvent the simplifying heat flow assumptions. Figure (6-7) presents the results of Equation (5-2) in a graphical form. Figures (6-8) through (6-10) present the results of Equations (6-16) through (6-18)

It should be noted that several of these equations have been extrapolated or extended beyond the range for which they are theoretically applicable. The correlations by Lord Rayleigh, Hengst, and Woodside were derived based on the assumption of a cubical array of uniform sized spheres. The geometrical limits on the solid fraction are then such that $0 \leq \bar{\epsilon} \leq \pi/6$. Similarly the equation presented by Schumann and Voss and by Preston are limited to solid fractions of $0.5 \leq \bar{\epsilon} \leq 1$. In order to compare these correlations with the remaining correlations over the same number of cases it was necessary to extrapolate the derived equation beyond its theoretical limits; where extrapolation was not possible, the closest possible value of the solid fraction was taken.

Initial results indicated that the correlation by Gorring and Churchill [4] was in considerable error. It was suspected that a typographical error may have existed in the correlation as published. Following the approach described by the authors Equation (2-17) was rederived and the corrected form of the equation was found to be:

$$\frac{k_e}{k_c} = \frac{\pi}{6\left(1 - \frac{k_c}{k_d}\right)CB}\left[\ln\left(\frac{\sqrt{B^2 - Bx_o + x_o^2}}{B + x_o}\right) + \sqrt{3}\,\tan^{-1}\left(\frac{2x_o - B}{B\sqrt{3}}\right)\right.$$

$$\left. -\sqrt{3}\,\tan^{-1}\left(\frac{-1}{\sqrt{3}}\right)\right] + \left[1 - \frac{\pi x_o}{4}\right] \tag{2-17a}$$

This equation was found to fit the experimental data much more closely.

In summarizing the results obtained from each correlation, it is found that the major sources of error can be attributed to the following causes:

1. Distorted particle geometry

2. Idealized heat flow

3. Absence of a finite particle contact area.

Not every source of error applies to each correlation. Typically one source will dominate depending upon the ratio of the constituent conductivities, $k_d/k_c$. It is difficult to define an exact range of $k_d/k_c$ over which one source will dominate as the range will vary between models. However, it is possible to discuss relative ranges.

A system composed of materials of equal conductivities will itself have a conductivity equal to that of the constituents. This is true regardless of the distribution or contact areas. Moreover the assumptions of uniform heat flux and parallel isotherms are both valid for such a system. Consequently each model should be equally valid for $k_d/k_c = 1$. If the ratio $k_d/k_c$ is increased beyond 1.0 the effects of a distorted particle geometry appear as the dominant source of error. At still higher values of $k_d/k_c$ the effects of the heat flow assumption become dominant. At yet higher values of $k_d/k_c$ the effects of the particle contact area predominate.

The tendency of the particle contact area to predominate as a source of error at high constituent conductivity ratios is clearly demonstrated. In granular systems with extremely low gaseous conductivities direct particle to particle conductions will be a major mode of heat

transfer. The effective conductivity of any idealized system having no finite particle contact will approach zero as the conductivity of the gaseous phase approaches zero. An example of such action is shown in the results for a simulated lunar soil. These data are listed in the Tables as cases 159 to 164. The bulk of the correlations yield results far below the experimental values. Those correlations based upon an assumed Gaussian distribution of the two phases are the exception. The reason for this action is attributed to the fact that, while the normalized Gaussian distribution allows only point contact, the granules are in close proximity over a larger area.

The assumption of a uniform heat flux tends to yield results somewhat smaller than the experimental value while the assumption of parallel isotherms tends to yield values which are overly large. This tendency can be offset by a distortion of the material distribution so that the effects are somewhat self compensating. However, the effects of these two factors are not the same overall ranges of $k_d/k_c$. Therefore, calculational results tend to be high or low depending on which factor predominates.

The results of the comparison between the models is summarized in Table 6-VII. Here a nondimensionalized variance is listed for the results of each model calculated over all 172 cases of Table 6-I. The formula used in determining the variance is:

$$\text{Variance} = \sum_{n=1}^{172} \left( \frac{k_{eff} - k_{exp}}{k_h} \right)^2$$

where $k_h$ is equal to either $k_{eff}$ or $k_{exp}$, whichever is greater. This method of comparing the variance ensures that calculational results which are either high or low by the same factor are penalized equally for the difference.

It should be noted from Table 6-VII that Equation (5-2) equation together with the Equations (6-16), (6-17) and (6-18) result in the least variance. It is therefore concluded that these equations represent the closest estimation of the experimentally derived effective thermal conductivity.

The major source of error in these formulations is expected to be the failure to account for particle size distribution and shape. Additional experimental work in these areas would provide data from which Equations (6-19), (6-20) and (6-21) could be rederived to more closely fit the actual effect of bending of the heat flux lines.

Failure to account for the contact resistance between particles may or may not be an important source of error. If contact resistance were an important parameter it would be anticipated that the effective thermal conductivity of a system would be a definite function of particle size. Systems of small particles would then have a lower conductivity than systems of large particles, all other parameters being equal. While sufficient data of the necessary kind is not available to draw a definite conclusion, comparisons can be made. Waddams [6] lists the thermal conductivity of 1/8 inch steel spheres in air (Case 84, Table 6-I) as 0.517 kcal/m-hr-K while that of 7/32 inch steel spheres (Case 107, Table 6-I) is given as only 0.403 kcal/m-hr-K; the smaller

diameter, lower density particles are reported to have the larger

conductivity in this case. Other data may show similar or opposite

trends. Further experimental work will be required before a definite

conclusion may be drawn.

The results of Table 6-VI and Table 6-VII indicate that the proposed

models each perform well over the range of constituent conductivity

ratios of $0 \leq k_d/k_c \leq 10^9$. Further, it is seen that most previous

models fail at much lower conductivity ratios. Thus the correlations

described herein represent a significant extrapolation of previous

models.

TABLE 6-I.  COMPARISON OF BOUNDING CONDUCTIVITIES TO EXPERIMENTAL CONDUCTIVITIES

| Case | Conductivity, $(k_{cal}/m\text{-}hr\text{-}k) \times 100$ | | | | | $(k_d/k_c)$ | $1-\bar{\epsilon}$ | Ref. |
| | Fluid Phase | Solid Phase | Experiment | Uniform Heat Flux | Parallel Isotherms | | | |
|---|---|---|---|---|---|---|---|---|
| 1 | Air 2.41 | Calcite 310 | 21.4 | 12.1 | 64.8 | 128.63 | .493 | 6 |
| 2 | Air 2.41 | Steel 1650 | 22.4 | 16.1 | 261.1 | 684.647 | .489 | 36 |
| 3 | Helium 11.95 | Steel 1650 | 75.5 | 60.48 | 341.2 | 138.075 | .489 | 36 |
| 4 | Glycerin 45.4 | Steel 1650 | 246 | 170.6 | 456.4 | 36.343 | .489 | 36 |
| 5 | Water 51.6 | Steel 1650 | 272 | 187.4 | 471.9 | 31.976 | .489 | 36 |
| 6 | $CO_2$ .08016 | Basalt 10.76 | 1.015 | .0047 | 2.259 | 134.177 | .470 | 3 |
| 7 | EtOH 15.7 | Calcite 310 | 63.6 | 49.9 | 101 | 19.745 | .465 | 56 |
| 8 | Air 2.41 | Calcite 310 | 25 | 11.9 | 65.7 | 128.63 | .458 | 6 |
| 9 | Air 2.13 | Calcite 310 | 17.5 | 10.6 | 65.7 | 145.54 | .454 | 56 |

TABLE 6-I.  Continued

| 10 | EtOH<br>15.7 | Calcite<br>310. | 63.5 | 48.7 | 10.3 | 19.7452 | .454 | 56 |
| 11 | Water<br>50.5 | Calcite<br>310 | 127 | 103.8 | 154.3 | 6.1386 | .453 | 42 |
| 12 | Air<br>2.12 | Calcite<br>310 | 19 | 10.7 | 64.7 | 146.2264 | .451 | 42 |
| 13 | Air<br>2.13 | Calcite<br>310 | 17.2 | 10.6 | 65.6 | 145.54 | .451 | 42 |
| 14 | Air<br>2.34 | Lead<br>2950 | 30.4 | 16.1 | 455 | 1260.6841 | .450 | 6 |
| 15 | Water<br>50.8 | Calcite<br>310 | 118 | 104.4 | 154.3 | 6.1024 | .447 | 42 |
| 16 | Air<br>2.38 | Quartz<br>950.1 | 36.5 | 14.0 | 170.1 | 398.7498 | .440 | 56 |
| 17 | Air<br>2.34 | Lead<br>2950 | 23.85 | 15.4 | 475.7 | 1260.6841 | .439 | 6 |
| 18 | Water<br>54.5 | Silica<br>973.9 | 216.0 | 154.3 | 356.0 | 17.8689 | .439 | 36 |
| 19 | Air<br>2.25 | Quartz<br>945 | 26.8 | 12.7 | 176.3 | 420 | .438 | 35 |
| 20 | Air<br>2.25 | Coal<br>36 | 11.8 | 6.2 | 13.6 | 16 | .437 | 35 |
| 21 | Hydrogen<br>16.6 | Coal<br>36 | 25.3 | 21.8 | 27.7 | 2.1687 | .437 | 35 |

TABLE 6-I. Continued

| | | | | | | | |
|---|---|---|---|---|---|---|---|
| 22 | Air 2.308 | Silica 973.9 | 21.89 | 13.0 | 181.7 | 421.9353 | .437 | 36 |
| 23 | Air 2.34 | Steel 3350 | 34.1 | 15.8 | 604.7 | 1645.2996 | .435 | 6 |
| 24 | EtOH 29.34 | Silica 973.9 | 144.7 | 98.4 | 302.0 | 33.198 | .434 | 36 |
| 25 | Air 2.34 | Lead 2950 | 34.4 | 15.4 | 475.7 | 1260.6841 | .433 | 6 |
| 26 | Water 54.5 | Silica 973.9 | 244.9 | 154.3 | 356.1 | 17.8689 | .431 | 36 |
| 27 | IC8 12.29 | Glass 93.96 | 35.14 | 26.5 | 44.6 | 7.6485 | .431 | 36 |
| 28 | Oil 15.4 | Lead 2410 | 81.5 | 73.1 | 533.3 | 156.4935 | .430 | 42 |
| 29 | Water 54.5 | Silica 973.9 | 224.9 | 154.3 | 356.1 | 17.8689 | .430 | 36 |
| 30 | Water 54.5 | Silica 973.9 | 217.4 | 154.3 | 356.1 | 17.8689 | .430 | 36 |
| 31 | Water 54.5 | Silica 973.9 | 218.9 | 154.3 | 356.1 | 17.8689 | .430 | 36 |
| 32 | Water 54.5 | Silica 973.9 | 218.9 | 154.3 | 356.1 | 17.8689 | .430 | 36 |

TABLE 6-I. Continued

| 33 | H₂ 14.85 | SiC 1550 | 91 | 65 | 371.3 | 104.3771 | .429 | 37 |
|----|-------|------|------|------|-------|-----------|------|----|
| 34 | Air 2.08 | SiC 1550 | 20 | 12.8 | 266.2 | 745.1921 | .429 | 37 |
| 35 | CO₂ 1.26 | SiC 1550 | 15.6 | 8.3 | 250.6 | 1230.1594 | .429 | 37 |
| 36 | IC8 12.29 | Silica 973.9 | 94.4 | 50.6 | 247.0 | 79.2727 | .428 | 36 |
| 37 | IC8 12.29 | Silica 973.9 | 94.0 | 50.7 | 247 | 79.2727 | .428 | 36 |
| 38 | Glycerin 46.3 | Glass 94 | 73.3 | 29.1 | 73.3 | 2.0289 | .428 | 36 |
| 39 | Water 54.5 | Silica 973.9 | 207.0 | 156.7 | 350.5 | 17.8689 | .426 | 36 |
| 40 | Water 54.5 | Silica 973.9 | 212.9 | 153.4 | 358.0 | 17.8689 | .426 | 36 |
| 41 | Air 2.31 | Silica 973.9 | 22.3 | 13 | 182.6 | 421.9353 | .426 | 36 |
| 42 | IC8 12.29 | Silica 973.9 | 70.9 | 50.4 | 248.4 | 79.2727 | .426 | 36 |
| 43 | Air 2.31 | Glass 94.0 | 18.5 | 8.1 | 27.9 | 40.7097 | .426 | 36 |

TABLE 6-I. Continued

| | | | | | | | |
|---|---|---|---|---|---|---|---|
| 44 | Helium 11.95 | SiC 1550 | 61.5 | 54.4 | 357.5 | 129.7071 | .425 | 3 |
| 45 | Hydrogen 14.85 | SiC 1550 | 85 | 64.7 | 373.3 | 104.3771 | .425 | 37 |
| 46 | Air 2.08 | SiC 1550 | 22.6 | 12.7 | 267.7 | 745.1921 | .425 | 37 |
| 47 | CO₂ 1.26 | SiC 1550 | 14.7 | 8.2 | 252 | 1230.1594 | .425 | 37 |
| 48 | Air 2.31 | Silica 973.9 | 22.6 | 13 | 182.6 | 421.9353 | .424 | 36 |
| 49 | CO₂ 1.2 | SiO 700 | 16.3 | 7.1 | 125 | 583.3333 | .424 | 36 |
| 50 | Air 2.41 | SiO 700 | 23.8 | 12.8 | 139.5 | 290.4563 | .424 | 36 |
| 51 | Air 2.41 | SiO 700 | 23.4 | 12.8 | 139.5 | 290.4563 | .424 | 36 |
| 52 | Air 2.41 | SiO 700 | 25.2 | 12.8 | 139.5 | 290.4563 | .424 | 36 |
| 53 | Glycerin 26.3 | Silica 973.9 | 205.5 | 136.6 | 342.2 | 21.0289 | .424 | 36 |
| 54 | Air 2.34 | Steel 3850 | 44.6 | 15.7 | 608 | 1645.2996 | .423 | 6 |

112

TABLE 6-I.  Continued

| | | | | | | | | |
|---|---|---|---|---|---|---|---|---|
| 55 | EtOH 29.3 | Silica 973.9 | 163.8 | 97.9 | 303.6 | 33.1980 | .423 | 36 |
| 56 | EtOH 29.3 | Glass 94.0 | 55.4 | 45.3 | 61.7 | 3.2030 | .423 | 36 |
| 57 | Air 2.34 | Lead 2950 | 36 | 15.3 | 478.3 | 1260.6841 | .420 | 6 |
| 58 | Air 2.41 | Glass 93.5 | 17.1 | 8.4 | 28.1 | 38.7967 | .420 | 36 |
| 59 | Helium 11.95 | Glass 93.5 | 34.2 | 25.9 | 44.3 | 7.8243 | .420 | 36 |
| 60 | Helium 11.95 | Glass 93.5 | 35.6 | 25.9 | 44.3 | 7.8243 | .420 | 36 |
| 61 | EtOH 29.6 | Glass 93.5 | 53.3 | 45.5 | 61.8 | 3.1588 | .420 | 36 |
| 62 | EtOH 29.6 | Glass 93.5 | 55 | 45.5 | 61.8 | 3.1588 | .420 | 36 |
| 63 | Glycerol 45.4 | Glass 93.5 | 71.4 | 58.1 | 73.8 | 2.0595 | .420 | 36 |
| 64 | Water 51.6 | Glass 93.5 | 71.6 | 62.3 | 78.1 | 1.8120 | .428 | 36 |
| 65 | Water 51.6 | Glass 93.5 | 71.4 | 62.3 | 78.1 | 1.8120 | .420 | 36 |

TABLE 6-I. Continued

| | | | | | | | | |
|---|---|---|---|---|---|---|---|---|
| 66 | Water 51.1 | Lead 3000 | 358 | 196.1 | 816.9 | 58.7084 | .420 | 42 |
| 67 | IC8 12.3 | Silica 973.9 | 70.7 | 50.4 | 248.4 | 79.2727 | .420 | 36 |
| 68 | IC8 12.3 | Silica 973.9 | 71.3 | 50.4 | 248.4 | 79.2727 | .419 | 36 |
| 69 | EtOH 29.3 | Silica 973.9 | 144.4 | 97.9 | 303.6 | 33.198 | .418 | 36 |
| 70 | Air 2.34 | Steel 3850 | 37.8 | 15.7 | 608 | 1645.2996 | .417 | 6 |
| 71 | Air 2.48 | Lead 2950 | 42.5 | 16.1 | 481.4 | 1189.5161 | .417 | 57 |
| 72 | Air 2.25 | Quartz 945 | 29.7 | 12.7 | 177.3 | 420 | .416 | 35 |
| 73 | Air 2.34 | Lead 2950 | 36.4 | 15.3 | 478.3 | 1260.6841 | .416 | 6 |
| 74 | Air 2.308 | Glass 94.0 | 17.1 | 8.1 | 27.9 | 40.7097 | .414 | 36 |
| 75 | Water 54.5 | Silica 973.9 | 230.8 | 153.4 | 358.0 | 17.8689 | .414 | 36 |
| 76 | Air 2.34 | Steel 3850 | 35.1 | 15.7 | 608 | 1645.2996 | .413 | 6 |

114

TABLE 6-I. Continued

| | | | | | | | | |
|---|---|---|---|---|---|---|---|---|
| 77 | Hydrogen 14.85 | SiC 1550 | 100.7 | 64.7 | 373.3 | 104.3771 | .410 | 37 |
| 78 | Air 2.08 | SiC 1550 | 22.4 | 12.7 | 267.7 | 745.1921 | .410 | 37 |
| 79 | $CO_2$ 1.26 | SiC 1550 | 17.8 | 82.1 | 252 | 1230.1594 | .410 | 37 |
| 80 | Air 2.86 | Sand 187.5 | 20.7 | 11.3 | 49.9 | 65.6250 | .410 | 29 |
| 81 | EtOH 29.3 | Silica 973.9 | 154.9 | 97.9 | 303.6 | 33.1980 | .410 | 36 |
| 82 | Water 54.5 | Glass 94 | 73.1 | 64.3 | 80.2 | 1.7240 | .408 | 36 |
| 83 | Air 2.31 | Silica 973.9 | 24.6 | 13 | 182.6 | 421.9353 | .408 | 36 |
| 84 | Air 2.34 | Steel 3850 | 51.7 | 15.7 | 608 | 1645.2996 | .406 | 6 |
| 85 | Air 2.14 | Lead 3000 | 32.3 | 14.1 | 481.1 | 1401.8694 | .406 | 42 |
| 86 | Air 2.48 | Copper 32950 | 78.6 | 18.4 | 4700 | 13313.2539 | .403 | 56 |
| 87 | Air 2.34 | Steel 3850 | 36.8 | 15.7 | 608 | 1645.2996 | .402 | 6 |

TABLE 6-I. Continued

| | | | | | | | | |
|---|---|---|---|---|---|---|---|---|
| 88 | Air 2.34 | Steel 3850. | 47.5 | 15.7 | 608.0 | 1645.3 | .401 | 6 |
| 89 | Air 2.14 | Lead 3000. | 32.5 | 14.1 | 481.1 | 1401.9 | .401 | 42 |
| 90 | Air 2.25 | Lead 3030. | 37.0 | 14.8 | 487.9 | 1346.7 | .400 | 35 |
| 91 | Hydrogen 16.6 | Lead 3030. | 120.6 | 80.8 | 655.2 | 182.5 | .400 | 35 |
| 92 | Water 54.5 | Lead 3030. | 298.0 | 206.5 | 835.3 | 55.6 | .400 | 35 |
| 93 | Glycerin 24.4 | Lead 3030. | 176.0 | 110.1 | 704.9 | 124.2 | .400 | 35 |
| 94 | Hydrogen 12.6 | Glass 93.5 | 39.6 | 26.7 | 45.1 | 7.42 | .400 | 57 |
| 95 | Air 2.48 | Glass 93.5 | 15.5 | 8.6 | 28.3 | 37.7 | .400 | 57 |
| 96 | Air 2.91 | Steel 4500. | 53.2 | 19.4 | 714.8 | 1546.4 | .400 | 29 |
| 97 | Air 2.91 | Steel 4500. | 55.4 | 19.4 | 714.8 | 1546.4 | .400 | 29 |
| 98 | Air 2.91 | Steel 4500. | 58.5 | 19.4 | 714.8 | 1546.4 | .400 | 29 |

TABLE 6-I. Continued

| | | | | | | | | |
|---|---|---|---|---|---|---|---|---|
| 99 | Air 2.91 | Steel 4500. · | 59.5 | 19.4 | 714.8 | 1546.4 | .400 | 29 |
| 100 | Air 2.91 | Steel 4500. | 61.1 | 19.4 | 714.8 | 1546.4 | .400 | 29 |
| 101 | Air 2.34 | Cellite 92.0 | 23.4 | 8.2 | 27.5 | 39.3 | .400 | 42 |
| 102 | Air 2.41 | Coal 36.0 | 10.2 | 6.4 | 13.9 | 14.9 | .400 | 42 |
| 103 | EtOH 15.7 | Lead 3000. | 126.0 | 77.0 | 643.3 | 191.1 | .397 | 36 |
| 104 | Air 2.34 | Steel 3850. | 43.5 | 15.7 | 608.0 | 1645.3 | .394 | 6 |
| 105 | Air 2.34 | Steel 3850. | 51.7 | 15.7 | 608.0 | 1645.3 | .394 | 6 |
| 106 | EtOH 29.3 | Copper 33163. | 327.6 | 198.4 | 5197.1 | 1130.5 | .392 | 36 |
| 107 | Air 2.34 | Steel 3850. | 40.3 | 16.0 | 597.1 | 1645.3 | .391 | 6 |
| 108 | Water 50.9 | Lead 3000. | 327.0 | 193.5 | 824.8 | 58.9 | .391 | 42 |
| 109 | Air 2.34 | Steel 3850. | 44.6 | 15.6 | 614.4 | 1645.3 | .390 | 6 |

117

TABLE 6-I. Continued

| | | | | | | | | |
|---|---|---|---|---|---|---|---|---|
| 110 | Air<br>2.85 | Sand<br>187.6 | 26.3 | 11.1 | 50.4 | 65.6 | .390 | 29 |
| 111 | Air<br>2.38 | Quartz<br>950.1 | 41.8 | 13.2 | 181.7 | 398.7 | .390 | 56 |
| 112 | EtOH<br>29.8 | Copper<br>11500. | 318.0 | 163.7 | 2210.0 | 385.9 | .388 | 36 |
| 113 | EtOH<br>29.8 | Copper<br>11500. | 342.0 | 163.7 | 2210.0 | 385.9 | .388 | 36 |
| 114 | Glycerin<br>45.4 | Copper<br>11500. | 580.0 | 232.2 | 2370.0 | 253.3 | .388 | 36 |
| 115 | Glycerin<br>45.4 | Copper<br>11500. | 595.0 | 232.2 | 2370.0 | 253.3 | .388 | 36 |
| 116 | Water<br>51.6 | Copper<br>11500. | 550.0 | 257.8 | 2424.0 | 222.9 | .388 | 36 |
| 117 | Water<br>51.6 | Copper<br>11500. | 615.0 | 257.8 | 2424.0 | 222.9 | .388 | 36 |
| 118 | Water<br>51.6 | Copper<br>11500. | 630.0 | 257.8 | 2424.0 | 222.9 | .388 | 36 |
| 119 | Water<br>54.5 | Copper<br>33163. | 629.9 | 321.2 | 5950.6 | 608.5 | .387 | 36 |
| 120 | Water<br>54.5 | Copper<br>33163. | 597.1 | 321.2 | 5950.6 | 608.5 | .387 | 36 |

TABLE 6-I. Continued

| | | | | | | | | |
|---|---|---|---|---|---|---|---|---|
| 121 | EtOH 29.33 | Copper 33163. | 323.1 | 321.2 | 5950.6 | 1130.5 | .386 | 36 |
| 122 | Glycerin 46.3 | Copper 33163. | 607.6 | 321.2 | 5950.6 | 716.1 | .386 | 36 |
| 123 | Glycerin 46.3 | Copper 33163. | 549.5 | 187.5 | 5499.4 | 716.1 | .385 | 36 |
| 124 | Water 54.5 | Copper 33163. | 634.4 | 279.4 | 5818.1 | 608.5 | .384 | 36 |
| 125 | Air 2.43 | Steel 3030. | 45.0 | 15.7 | 497.1 | 1246.9 | .380 | 58 |
| 126 | Methane 3.0 | Steel 3300. | 55.8 | 19.1 | 548.9 | 1100.0 | .380 | 58 |
| 127 | Propane 1.6 | Steel 3300. | 35.0 | 10.9 | 516.5 | 2062.5 | .380 | 58 |
| 128 | $CO_2$ 1.35 | Steel 3300. | 32.4 | 9.3 | 509.8 | 2444.4 | .380 | 58 |
| 129 | Hydrogen 16.4 | Steel 3300. | 188.0 | 80.4 | 708.4 | 201.2 | .380 | 58 |
| 130 | Air 2.34 | Steel 2850. | 45.7 | 15.1 | 468.7 | 1217.9 | .380 | 6 |
| 131 | Oil 15.4 | Lead 2410. | 101.0 | 72.0 | 541.9 | 156.5 | .380 | 57 |

TABLE 6-I. Continued

| | | | | | | | | |
|---|---|---|---|---|---|---|---|---|
| 132 | Air 2.86 | Sand 187.6 | 26.4 | 11.1 | 50.4 | 65.6 | .370 | 29 |
| 133 | Air 2.25 | Steel 2250. | 35.6 | 14.2 | 378.4 | 1000.0 | .365 | 35 |
| 134 | Hydrogen 16.6 | Steel 2250. | 110.0 | 75.5 | 520.0 | 135.5 | .365 | 35 |
| 135 | Helium 11.95 | Glass 93.5 | 31.1 | 25.6 | 44.8 | 7.8 | .350 | 37 |
| 136 | Air 2.12 | Glass 93.5 | 13.8 | 7.5 | 27.5 | 44.1 | .350 | 37 |
| 137 | Air 2.08 | Glass 59.1 | 13.8 | 6.61 | 19.4 | 28.3 | .349 | 59 |
| 138 | Air 2.23 | Lead 3030. | 34.2 | 14.5 | 492.6 | 1358.7 | .346 | 12 |
| 139 | Hydrogen 14.9 | SiC 1548.7 | 95.4 | 64.1 | 377.2 | 104.0 | .328 | 59 |
| 140 | Air 2.08 | SiC 1548.7 | 27.3 | 12.6 | 270.4 | 742.8 | .328 | 59 |
| 141 | $CO_2$ 1.27 | SiC 1548.7 | 26.2 | 8.2 | 254.6 | 1223.5 | .328 | 59 |
| 142 | Hydrogen 14.9 | SiC 1548.7 | 61.7 | 64.1 | 377.2 | 104.0 | .325 | 59 |

TABLE 6-I. Continued

| | | | | | | | | |
|------|----------|--------|-------|-------|-------|--------|------|----|
| 143 | Air | SiC | | | | | | |
| | 2.08 | 1548.7 | 27.0 | 12.6 | 270.4 | 742.9 | .325 | 59 |
| 144 | $CO_2$ | SiC | | | | | | |
| | 1.27 | 1548.7 | 25.2 | 8.2 | 254.6 | 1223.5 | .325 | 59 |
| 145 | Air | Quartz | | | | | | |
| | 2.38 | 950.1 | 49.0 | 13.4 | 178.1 | 398.7 | .310 | 56 |
| 146 | Hydrogen | SiC | | | | | | |
| | 14.9 | 1548.7 | 110.8 | 62.5 | 386.4 | 104.0 | .308 | 59 |
| 147 | Air | SiC | | | | | | |
| | 2.08 | 1548.7 | 27.5 | 12.3 | 277.0 | 742.9 | .308 | 59 |
| 148 | $CO_2$ | SiC | | | | | | |
| | 1.27 | 1548.7 | 26.4 | 7.97 | 260.7 | 1223.5 | .308 | 59 |
| 149 | Helium | SiC | | | | | | |
| | 12.0 | 1548.7 | 85.2 | 52.7 | 260.7 | 129.2 | .308 | 59 |
| 150 | Air | Lead | | | | | | |
| | 2.25 | 3030. | 58.4 | 14.3 | 505.1 | 1346.7 | .310 | 35 |
| 151 | Air | Quartz | | | | | | |
| | 2.25 | 945.0 | 70.0 | 12.2 | 183.5 | 420.0 | .276 | 37 |
| 152 | Air | Quartz | | | | | | |
| | 2.25 | 945.0 | 76.0 | 12.2 | 183.5 | 420.0 | .241 | 37 |
| 153 | Water | S.S. | | | | | | |
| | 54.5 | 1795.9 | 272.5 | 195.8 | 496.8 | 33.0 | .501 | 36 |

TABLE 6-I. Continued

| | | | | | | | | |
|---|---|---|---|---|---|---|---|---|
| 154 | Glycerin 46.3 | S.S. 1795.9 | 248.7 | 172.9 | 475.5 | 38.8 | .502 | 36 |
| 155 | EtOH 29.3 | S.S. 1795.9 | 172.7 | 120.7 | 422.3 | 61.2 | .505 | 36 |
| 156 | Hydrogen 14.85 | $(C_6H_5)_2NH$ 18.9 | 16.5 | 16.7 | 16.7 | 1.3 | .513 | 37 |
| 157 | Air 2.08 | $(C_6H_5)_2NH$ 18.9 | 6.9 | 5.1 | 7.5 | 9.1 | .513 | 37 |
| 158 | Hydrogen 14.85 | SiC 1550. | 46. | 68.3 | 322.1 | 104.4 | .518 | 37 |
| 159 | $CO_2$ $.1578x10^{-7}$ | Basalt 90.7 | .1061 | $.1280x10$ | 10.53 | $5.75x10$ | .540 | 3 |
| 160 | $CO_2$ $.1856x10^{-7}$ | Basalt 90.7 | .08183 | $.1760x10$ | 9.0 | $4.89x10$ | .600 | 3 |
| 161 | $CO_2$ $.2373x10^{-7}$ | Basalt 90.7 | .05598 | $.1933x10$ | 10.47 | $3.82x10$ | .654 | 3 |
| 162 | $CO_2$ $.2967x10^{-7}$ | Basalt 90.7 | .0511 | $.2747x10$ | 8.90 | $3.16x10$ | .683 | 3 |
| 163 | $CO_2$ $.4764x10^{-7}$ | Basalt 90.7 | .0414 | $.181x10$ | 19.15 | $2.23x10$ | .721 | 3 |
| 164 | $CO_2$ $.1464x10^{-7}$ | Basalt 90.7 | .1404 | $.652x10$ | 19.15 | $6.19x10$ | .470 | 37 |

TABLE 6-I Continued

| 165 | Air<br>2.08 | SiC<br>1550. | 15.6 | 12.7 | 218.9 | 745.2 | .518 | 37 |
|-----|-------------|--------------|------|------|-------|-------|------|-----|
| 166 | $CO_2$<br>1.26 | SiC<br>1550. | 11.85 | 8.1 | 205.6 | 1230.2 | .518 | 37 |
| 167 | Air<br>2.47 | Iron<br>5628.9 | 39.9 | 13.2 | 584.0 | 2277.1 | .575 | 56 |
| 168 | Oil<br>15.4 | Copper<br>32000. | 130. | 80.6 | 3365. | 2077.9 | .580 | 57 |
| 169 | Oil<br>15.4 | Steel<br>3500. | 81.5 | 62.2 | 512.8 | 227.3 | .580 | 42 |
| 170 | Oil<br>15.4 | Glass<br>61.2 | 29.8 | 25.2 | 31.2 | 3.974 | .580 | 42 |
| 171 | Oil<br>15.4 | Lead<br>2410. | 60. | 58.7 | 381.7 | 156.5 | .580 | 42 |
| 172 | $CO_2$<br>.2013 | Basalt<br>96.8 | 1.024 | .602 | 18.28 | 480.7 | .720 | 3 |

123

# TABLE 5-11 COMPARISON OF SELECTED FLUX LAW MODELS

| DATA | | EFFECTIVE THERMAL CONDUCTIVITY (KCAL/M-HR-K) X 10 | | | |
|------|------|------|------|------|------|
| CASE | EXPERIMENTAL | MAXWELL | RAYLEIGH | MEREDITH & TOBIAS | BRUGGEMAN |
| 1 | 21.39999 | 9.51694 | 10.32832 | 11.92574 | 17.31554 |
| 2 | 22.39999 | 9.89817 | 10.85322 | 12.47304 | 19.95781 |
| 3 | 75.5 | 47.83798 | 52.1409 | 60.15923 | 88.51478 |
| 4 | 246. | 166.67621 | 173.89758 | 208.61894 | 254.99024 |
| 5 | 272. | 186.62283 | 199.79781 | 233.31593 | 278.58374 |
| 6 | 1.15 | .53894 | .37632 | .43272 | .65405 |
| 7 | 63.59999 | 56.91492 | 60.14163 | 70.91235 | 77.23344 |
| 8 | 25. | 10.54335 | 11.85223 | 13.59271 | 20.83421 |
| 9 | 17.5 | 9.47892 | 10.72303 | 12.25495 | 19.18465 |
| 10 | 63.5 | 57.55986 | 62.29413 | 73.55556 | 80.01877 |
| 11 | 127. | 130.42792 | 134.33577 | 158.94153 | 143.49553 |
| 12 | 15. | 9.52291 | 10.81323 | 12.34107 | 19.42204 |
| 13 | 17.2 | 9.56628 | 10.86201 | 12.39723 | 19.50473 |
| 14 | 5.39999 | 10.87432 | 12.47522 | 14.11478 | 25.07587 |

# TABLE 6-II CONTINUED

| DATA | | EFFECTIVE THERMAL CONDUCTIVITY (KCAL/M-HR-K) X 10⁶ | | | |
|------|--------------|-----------|-----------|--------------------|-----------|
| CASE | EXPERIMENTAL | MAXWELL | RAYLEIGH | MEREDITH & TOBIAS | BRUGGEMAN |
| 15 | 113. | 132.23315 | 136.36444 | 161.78436 | 145.45194 |
| 16 | 36.5 | 11.31429 | 13.12894 | 14.79832 | 25.97957 |
| 17 | 23.84999 | 11.26248 | 13.12744 | 14.74412 | 26.96909 |
| 18 | 316. | 213.2 45 | 221.36946 | 262.35938 | 278.50317 |
| 19 | 26.79999 | 10.77165 | 12.53937 | 14.11154 | 24.89319 |
| 20 | 11.8 | 8.21585 | 8.91648 | 10.59934 | 10.98189 |
| 21 | 25.29999 | 25.93337 | 26.71422 | 28.59103 | 26.13719 |
| 22 | 21.89 | 11.08524 | 12.92428 | 14.53338 | 25.78222 |
| 23 | 34.9999 | 11.41934 | 13.39832 | 14.99745 | 27.84776 |
| 24 | 144.7 | 123.8436 | 139.13130 | 161.94485 | 198.32906 |
| 25 | 34.39999 | 11.48218 | 13.51769 | 15.13701 | 28.05673 |
| 26 | 244.89999 | 207.31269 | 227.28255 | 269.50562 | 285.59204 |
| 27 | 35.14 | 36.06357 | 37.77673 | 45.36514 | 41.25337 |
| 28 | 61.5 | 74.01193 | 86.59778 | 97.54688 | 160.52133 |

# TABLE 6-II CONTINUED

| DATA CASE | EXPERIMENTAL | MAXWELL | RAYLEIGH | MEREDITH & TOBIAS | BRUGGEMAN |
|---|---|---|---|---|---|
| | | | EFFECTIVE THERMAL CONDUCTIVITY (KCAL/M-HR-K) X 100 | | |
| 29 | 224.89999 | 207.82314 | 228.04282 | 270.41699 | 286.40747 |
| 30 | 217.39999 | 207.82314 | 228.04282 | 270.41699 | 286.35205 |
| 31 | 216.89999 | 207.82314 | 228.04282 | 270.41699 | 286.36499 |
| 32 | 213.89999 | 207.82314 | 228.04282 | 270.41699 | 286.36499 |
| 33 | 91.00000 | 70.38913 | 82.01788 | 92.81613 | 144.37750 |
| 34 | 20.00000 | 10.03813 | 12.19656 | 13.60151 | 25.16855 |
| 35 | 15.60000 | 6.26272 | 7.41785 | 8.26378 | 15.52164 |
| 36 | 94.39999 | 57.51353 | 66.76503 | 75.87054 | 112.61105 |
| 37 | 94.39999 | 57.51353 | 66.76503 | 75.87054 | 112.61105 |
| 38 | 73.29999 | 70.08798 | 70.25729 | 76.85007 | 70.51149 |
| 39 | 207.00000 | 209.92138 | 231.12563 | 274.10352 | 289.76667 |
| 40 | 212.89999 | 209.92138 | 231.12563 | 274.10352 | 289.84961 |
| 41 | 22.29999 | 11.49383 | 13.64746 | 15.20180 | 27.59543 |
| 42 | 70.89999 | 57.86711 | 67.37192 | 76.46379 | 113.76636 |

# TABLE 6-II. CONTINUED

| DATA CASE | EXPERIMENTAL | MAXWELL | RAYLEIGH | MEREDITH & TOBIAS | BRUGGEMAN |
|---|---|---|---|---|---|
| 43 | 16.5 | 1.24156 | 11.69946 | 13.5178 | 17.37811 |
| 44 | 61.5 | 57.93112 | 68.15116 | 76.65494 | 124.1643 |
| 45 | 35. | 71.2794 | 83.55272 | 94.28964 | 147.49832 |
| 46 | 22.59999 | 1.4432 | 12.44179 | 13.82354 | 25.86356 |
| 47 | 15.7 | 6.34491 | 7.56726 | 8.39893 | 15.94831 |
| 48 | 22.59999 | 11.56858 | 13.77651 | 15.32526 | 27.95589 |
| 49 | 16.39999 | 6.3185 | 7.19293 | 7.9974 | 14.83859 |
| 50 | 23.79999 | 11.99753 | 14.25591 | 15.89282 | 28.22928 |
| 51 | 23.39999 | 11.99753 | 14.25591 | 15.89282 | 28.22726 |
| 52 | 25.2 | 11.99753 | 14.25591 | 15.89282 | 28.233 |
| 53 | 25.5 | 185.74664 | 216.64229 | 243.69996 | 267.73511 |
| 54 | 44.59999 | 11.87461 | 14.2193 | 15.74392 | 3.24588 |
| 55 | 163.79999 | 127.58 | 145.15849 | 168.41991 | 2 7.2396 |
| 56 | 55.39999 | 57.76314 | 58.43582 | 67.42899 | 59.36821 |

# TABLE 6-II. CONTINUED

| DATA CASE | EXPERIMENTAL | EFFECTIVE THERMAL CONDUCTIVITY (KCAL/M-HR-K) X 100 | | | |
| | | MAXWELL | RAYLEIGH | MEREDITH & TOBIAS | BRUGGEMAN |
|---|---|---|---|---|---|
| 57 | 36.  | 11.97962 | 14.4178 | 15.9213 | 3.67448 |
| 58 | 17. 9999 | 1 .8 734 | 12.42 18 | 14.31884 | 18.3 139 |
| 59 | 34.2 | 36.13893 | 38. 7352 | 45.94 64 | 41.589 |
| 6 | 35.59999 | 36.13893 | 38. 7352 | 45.94 64 | 41.591.45 |
| 61 | 53.29999 | 5 . 6 36 | 58.721 7 | 67.75734 | 59.6 811 |
| 62 | 55. | 53. 6 36 | 58.721 7 | 67.75734 | 59.6 846 |
| 63 | 71.39999 | 6 .69447 | 69.89546 | 76.79613 | 7 .13710 |
| 64 | 71.59999 | 73.42126 | 73.53889 | 79.45315 | 73.66144 |
| 65 | 71.39999 | 73.42126 | 73.53889 | 79.45815 | 73.683 7 |
| 66 | 358.  | 23 .48276 | 279.155 3 | 317.83447 | 447.21973 |
| 67 | 7 .7 | 58.99115 | 69.3 759 | 78.34 39 | 117.3372 |
| 68 | 71.29999 | 59.17392 | 69.63153 | 78.64911 | 117.93312 |
| 69 | 1 4.39999 | 129.4 219 | 149.14 | 171.56953 | 21 .78299 |
| 7 | 37.79999 | 12.11177 | 14.66577 | 16.1357 | 31.52858 |

# TABLE 6-II. CONTINUED

| DATA CASE | EXPERIMENTAL | MAXWELL | RAYLEIGH | MEREDITH & TOBIAS | BRUGGEMAN |
|-----------|--------------|---------|----------|-------------------|-----------|
| | | EFFECTIVE THERMAL CONDUCTIVITY (KCAL/M-HR-K) X 1·· | | | |
| 71 | 42.5 | 12.81913 | 15.51392 | 17.·7814 | 33.·92··7 |
| 72 | 29.7 | 11.56561 | 13.·7361 | 15.42·64 | 28.67444 |
| 73 | 36.29999 | 12.13889 | 14.72·56 | 16.18491 | 31.54257 |
| 74 | 17.·9999 | 1·.59676 | 12.3··149 | 14.11691 | 18.3·182 |
| 75 | 23·.79·99 | 216.39837 | 24·.84163 | 285.57251 | 3···.92358 |
| 76 | 35.·9999 | 12.27368 | 14.·7375 | 16.4·419 | 32.44339 |
| 77 | 1··.7 | 74.72·79 | 89.82399 | 1··.·9573 | 159.95567 |
| 78 | 22.39999 | 1·.972·8 | 13.·4718 | 14.7··5· | 28.6317· |
| 79 | 17.79999 | 6.66732 | 8.16226 | 8.93278 | 17.7·522 |
| 8· | 2··.7·· | 13.94991 | 16.5717·· | 18.67726 | 27.15118 |
| 81 | 154.·9999 | 132.39192 | 153.15465 | 176.77412 | 217.64229 |
| 82 | 73.·9999 | 75.78534 | 75.89779 | 81.73167 | 75.99522 |
| 83 | 24.59999 | 12.19252 | 14.9653· | 16.36278 | 31.·6195 |
| 84 | 51.7··· | 12.56468 | 15.55835 | 16.88557 | 34.·9999 |

# TABLE 6-II. CONTINUED

| DATA | | EFFECTIVE THERMAL CONDUCTIVITY (KCAL/M-HR-K) X 1. | | | |
| CASE | EXPERIMENTAL | MAXWELL | RAYLEIGH | MEREDITH & TOBIAS | BRUGGEMAN |
| 85 | 32.29999 | 11.46351 | 14.21559 | 15.43543 | 31.72811 |
| 86 | 76.59999 | 13.49535 | 16.94593 | 18.18315 | 37.76892 |
| 87 | 36.79999 | 12.73554 | 15.91930 | 17.17470 | 35.05396 |
| 88 | 47.50000 | 12.77873 | 15.99943 | 17.24638 | 35.24092 |
| 89 | 32.50000 | 11.67903 | 14.61817 | 15.76233 | 32.19775 |
| 90 | 37.70000 | 12.31887 | 15.45297 | 16.63954 | 34.05927 |
| 91 | 120.59999 | 88.33647 | 109.36789 | 119.34586 | 212.08203 |
| 92 | 298.40000 | 271.12842 | 324.58243 | 364.70020 | 514.50122 |
| 93 | 176.40000 | 127.89821 | 157.29483 | 172.79655 | 289.11646 |
| 94 | 38.59999 | 38.75138 | 41.05339 | 49.93776 | 44.29501 |
| 95 | 15.50000 | 11.74639 | 13.87323 | 15.83732 | 24.21743 |
| 96 | 53.20000 | 15.94177 | 20.00313 | 21.53299 | 44.20741 |
| 97 | 55.39999 | 15.94177 | 20.00313 | 21.53299 | 44.18983 |
| 98 | 58.50000 | 15.94177 | 20.00313 | 21.53299 | 44.10741 |

# TABLE 6-II. CONTINUED

EFFECTIVE THERMAL CONDUCTIVITY (KCAL/M-HR-K) X 1⁰⁰

| DATA CASE | EXPERIMENTAL | MAXWELL | RAYLEIGH | MEREDITH & TOBIAS | BRUGGEMAN |
|---|---|---|---|---|---|
| 99 | 59.6 | 15.94177 | 2?.??313 | 21.5320? | 44.?7?76 |
| ? | 61.?999 | 15.94177 | 2?.??313 | 21.5329? | 44.2261? |
| 1?1 | 23.39999 | 11.14626 | 13.19173 | 15.?31?6 | 19.4?2?5 |
| 1?2 | 1?.2??? | 9.46?87 | 1?.544?5 | 12.59192 | 12.64756 |
| 1?3 | 126.? | 84.5?438 | 1?5.37512 | 114.45631 | 2?5.92126 |
| 1?4 | 4?.5??? | 13.?8748 | 16.6591? | 17.76472 | 37.21918 |
| 1?5 | 51.7?? | 13.?8748 | 16.6591? | 17.76472 | 37.22635 |
| 1?6 | 327.5?985 | 164.718?3 | 21?.52751 | 223.961?3 | 466.13599 |
| 1?7 | 4?.29?99 | 13.23317 | 16.95822 | 17.9933? | 37.98?55 |
| 1?8 | 327.??? | 26?.924?7 | 319.54712 | ?55.12183 | 511.55884 |
| 1?9 | 44.59?99 | 13.26886 | 17.?6?26 | 18.?7?39 | 38.34334 |
| 11? | 26.29999 | 14.8?45? | 19.24736 | 2?.16972 | 29.88664 |
| 111 | 4?.79?99 | 13.336?3 | 17.?4173 | 18.?6583 | 35.99596 |
| 112 | 318.???? | 168.?3546 | 215.?4771 | 229.?7646 | 454.3?2?3 |

131

# TABLE 6-II. CONTINUED

| DATA CASE | EFFECTIVE THERMAL CONDUCTIVITY (KCAL/M-HR-K) X 100 | | | | |
|---|---|---|---|---|---|
| | EXPERIMENTAL | MAXWELL | RAYLEIGH | MEREDITH & TOBIAS | BRUGGEMAN |
| 113 | 342. | 168. 3546 | 215.74771 | 229.27646 | 454.94434 |
| 114 | 58. | 253. 84285 | 324.5 | 346.4 30 8 | 658.8944 |
| 115 | 595. | 253. 84285 | 324.5 | 346.4 3 8 | 658.91260 |
| 116 | 55. | 287. 54614 | 366.958 1 | 392.414 6 | 733.746 9 |
| 117 | 615. | 287. 54614 | 366.958 1 | 392.414 6 | 734.41235 |
| 118 | 63 . | 287. 54614 | 366.958 1 | 392.414 6 | 734.46753 |
| 119 | 629.8999 | 31 .217 4 | 40 .58 6 | 423.5835 | 87 .687 1 |
| 120 | 597. 9985 | 31 .217 4 | 4 .58 8 | 423.5835 | 869.529 5 |
| 121 | 323. 9985 | 166.33691 | 218.5 92 | 23 . 2142 | 489. 3589 |
| 122 | 6 7.59985 | 265. 3931 | 343.4292 | 362.18555 | 754.622 7 |
| 123 | 549.5 | 265. 95825 | 345.538 9 | 363.74438 | 759. 3125 |
| 124 | 634.3999 | 313.45 44 | 4 7.99486 | 429. 7178 | 889.40552 |
| 125 | 45. | 14.2493 | 15.81113 | 19.568 4 | 42.45663 |
| 126 | 55.79999 | 17.57947 | 23.198 9 | 24.14169 | 52.1 484 |

# TABLE 6-II. CONTINUED

| DATA | EFFECTIVE THERMAL CONDUCTIVITY (KCAL/M-HR-K) X 10 | | | | |
|------|--------------|---------|----------|---------------------|-----------|
| CASE | EXPERIMENTAL | MAXWELL | RAYLEIGH | MEREDITH & TOBIAS | BRUGGEMAN |
| 127 | 35.    | 9.4 169 | 12.42641 | 12.91 25 | 28.43169 |
| 128 | 32.39999 | 7.9365 | 1 .49296 | 1 .89927 | 24. 1172 |
| 129 | 188.    | 93.6284 | 121.76 38 | 128.65332 | 241.37253 |
| 13  | 45.7     | 13.71985 | 18.11 89 | 18.841 2 | 4 .93221 |
| 131 | 1 1.     | 87.13061 | 112.76949 | 119.75 14 | 215.79996 |
| 132 | 26.39999 | 15.8399 | 2 .41969 | 21.97133 | 33. 451 |
| 133 | 35.59999 | 13.59732 | 19.2 981 | 19.328 6 | 43.73842 |
| 134 | 11.     | 98.25 16 | 132.1279 | 136.81972 | 246.3 835 |
| 135 | 3 . 4999 | 41.46146 | 45 4. 475 | 56.1776 | 48. 9766 |
| 136 | 13.9    | 11.97224 | 15.84873 | 16.92 73 | 22.85 46 |
| 137 | 13.8    | 1 .941 9 | 13.93198 | 15.45854 | 18.13 58 |
| 138 | 34.2    | 14.795 1 | 22. 3165 | 2 .9122 | 51.26269 |
| 139 | 95.39990 | 9. 739 | 151. 283 | 142.69764 | 253.6 451 |
| 14  | 27.2 099 | 14 7.9 4 | 23.81555 | 21.12596 | 53.26739 |

# TABLE 6-II. CONTINUED

DATA :   EFFECTIVE THERMAL CONDUCTIVITY (KCAL/M-HR-K) X 100

| CASE | EXPERIMENTAL | MAXWELL | RAYLEIGH | MEREDITH & TOBIAS | BRUGGEMAN |
|------|--------------|---------|----------|-------------------|-----------|
| 141 | 20.2 | 9.01769 | 14.66218 | 12.94813 | 33.74352 |
| 142 | 51.7 | 177.59858 | 154.81660 | 144.67279 | 258.38135 |
| 143 | 27.4 | 14.88107 | 24.50314 | 21.42986 | 54.60304 |
| 144 | 25.2 | 9.12357 | 15.58942 | 13.13482 | 34.50200 |
| 145 | 49.0 | 17.89517 | 32.05487 | 26.13341 | 64.99879 |
| 146 | 110.79999 | 166.64850 | 190.67283 | 156.68053 | 284.81616 |
| 147 | 27.5 | 15.91846 | 29.30002 | 23.27493 | 63.02864 |
| 148 | 26.39999 | 9.76224 | 18.07634 | 14.26836 | 40.26196 |
| 149 | 85.2 | 87.16588 | 157.16927 | 127.94313 | 248.04050 |
| 15 | 56.39999 | 17.16690 | 31.34285 | 25.04462 | 77.51279 |
| 151 | 7. | 19.60879 | 48.68428 | 29.47662 | 82.06227 |
| 152 | 76. | 22.89493 | 137.57375 | 35.69896 | 110.92848 |
| 153 | 272.5 | 191.64548 | 203.74248 | 237.47173 | 283.51660 |
| 154 | 248.7 | 165.27722 | 176.08318 | 204.93089 | 251.63412 |

# TABLE 6-II. CONTINUED

| CASE | EXPERIMENTAL | MAXWELL | RAYLEIGH | MEREDITH & TOBIAS | BRUGGEMAN |
|------|--------------|---------|----------|-------------------|-----------|
| | | EFFECTIVE THERMAL CONDUCTIVITY (KCAL/M-HR-K) X 1 | | | |
| 155 | 172.7. | 1 7.73157 | 115.24449 | 133.64227 | 175.524 2 |
| 156 | 16.9 | 16.73445 | 16.73523 | 17. 769 | 16.7366 |
| 157 | 6.9 | 5.5177. | 5.66798 | 6.58252 | 6.36967 |
| 158 | 46. | 54.1 468 | 57.62999 | 66.59724 | 91.57744 |
| 159 | .1 61 | | | .9 3 | |
| 160 | .818 | | | | |
| 161 | . 5593 | | | | |
| 162 | . 511 | | | | |
| 163 | . 414 | | | | |
| 164 | .14 4 | .4 | | | |
| 165 | 15.6 | 7.84149 | 8.39758 | 9.67169 | 14.6 451 |
| 166 | 11. 5 | 4.75 8 | 5.1 28 | 5.87268 | 8.93119 |
| 167 | 35.59999 | 7.93444 | 8.23735 | 9. 89 | 12.91767 |
| 168 | 3 . | 3.772 5 | 5 .52993 | 37. 6246 | 78.35597 |

# TABLE 6-II. CONTINUED

| DATA CASE | EXPERIMENTAL | EFFECTIVE THERMAL CONDUCTIVITY (KCAL/M-HR-K) X 10⁰ | | | |
|---|---|---|---|---|---|
| | | MAXWELL | RAYLEIGH | MEREDITH & TOBIAS | BRUGGEMAN |
| 169 | 81.5 | 48.10748 | 49.77625 | 56.79597 | 74.95113 |
| 17 | 29.79599 | 27.61348 | 27.74528 | 30.30795 | 28.56239 |
| 171 | 67. | 47.778 9 | 49.40659 | 56.37567 | 73.31424 |
| 172 | 1.024 | 0.43413 | 0.43656 | 0.47197 | 0.53364 |

# TABLE 5-III. COMPARISON OF SELECTED UNIFORM HEAT FLUX MODELS

| DATA CASE | EXPERIMENTAL | EFFECTIVE THERMAL CONDUCTIVITY (KCAL/M-HR-K) X 1⁰⁰ | | | |
|---|---|---|---|---|---|
| | | SCHUFFEY | WOODSIDE & MESSMER | HENGST | GORRING & CHURCHILL |
| 1 | 21.39599 | 3.216 5 | 21.59131 | 27.81955 | 9.68224 |
| 2 | 22.85604 | 8.6 7 7 | 24.04747 | 39.61765 | 17.98637 |
| 3 | 75.5 | 41.33388 | 1⁰9.26635 | 141.4⁰97⁰ | 49.78612 |
| 4 | 346. | 146.78638 | 322.41919 | 372.84497 | 114.44376 |
| 5 | 273. | 164.86118 | 252.13623 | 4⁰6.8⁰713 | 123.79⁰3⁰ |
| 6 | 1. 15 | .29447 | .77575 | ⁰.97724 | ⁰.34656 |
| 7 | 63.50599 | 5 .47438 | 94.6.92⁰ | 1⁰9.921⁰7 | 32.43243 |
| 8 | 25. | 9.1⁰536 | 24.⁰7825 | 2⁰.74⁰⁰4 | 1⁰.55274 |
| 9 | 17.5 | 8.26423 | 21.84⁰9⁰ | 27.26914 | 9.36445 |
| 1⁰ | 63.5 | 52. 2 31 | 97.⁰⁰682 | 112.18112 | 33.⁰⁰687 |
| 11 | 127. | 123.41541 | 162.52831 | 22⁰.49751 | 63.22⁰73 |
| 12 | 19.⁰ | 8.3 843 | 21.54783 | 27.32⁰34 | 9.9⁰542 |
| 13 | 17.⁰ | 8.34694 | 22.⁰4125 | 27.41888 | 9.93447 |
| 14 | 5⁰.39599 | 9.43198 | 26.84637 | 45.⁰9⁰91 | 24.⁰5783 |

137

# TABLE 5-III. CONTINUED

| DATA | EFFECTIVE THERMAL CONDUCTIVITY (KCAL/M-HR-K) X 10⁻⁰ | | | | |
|------|--------------|------------|-----------------------|-----------|----------------------|
| CASE | EXPERIMENTAL | SCHUMANN-FREY | WOODSIDE & MESSMER | HENGST | GORRING & CHURCHILL |
| 15 | 118.____ | 125.67723 | 164.3205_ | 226.6629_ | 63.6421 3 |
| 16 | 36.5___ | 9.85696 | 27.358 6 | 38.78313 | 16.59296 |
| 17 | 23.84999 | 9.79678 | 27.8 275 | 46.825 4 | 24.77 10 |
| 18 | 216.___ | 184.86432 | 332.35 59 | 385.83325 | 112.37578 |
| 19 | 26.79 99 | 9.358 4 | 26. 8 46 | 37.15984 | 16. 6 78 |
| 2_ | 11.8 __ | 7.5 753 | 13. 5321 | 15.34 29 | 4.4349 |
| 21 | 25.2999 | 25.674 7 | 26.91245 | 43.9 685 | 1 .63655 |
| 22 | 21.89 __ | 9.66385 | 26.84 93 | 38.22 3 | 16.54385 |
| 23 | 34. 9999 | 9.94242 | 28.24911 | 49.18425 | 27.51242 |
| 24 | 144.7 _ | 11 .79633 | 233.35 6 | 259.31 55 | 79.22112 |
| 25 | 34.9999 | 1 . 4 9 | 28.33229 | 47.32585 | 25.15863 |
| 26 | 244.89999 | 198.96 85 | 338. 5981 | 391.33496 | 113.71243 |
| 27 | 35.14 _ | 34. 186 | 47.15613 | 62.53662 | 17.38632 |
| 28 | 81.5 | 64.91 23 | 17 .95238 | 2 9.34 68 | 77.48856 |

138

# TABLE 6-III. CONTINUED

| DATA CASE | EXPERIMENTAL | SUN FREY | WOODSIDE & MESSMER | HENGST | GORRING & CHURCHILL |
|-----------|--------------|----------|--------------------|---------|---------------------|
| 29 | 224.86990 | 189.4815 | 338.77515 | 392.12271 | 113.87953 |
| 30 | 217.39999 | 189.4815 | 338.77515 | 392.12271 | 113.87953 |
| 31 | 218.99999 | 189.4816 | 338.77515 | 392.12271 | 113.87953 |
| 32 | 218.99999 | 189.4815 | 338.77515 | 392.12271 | 113.87953 |
| 33 | 91. | 61.94331 | 157.14453 | 193.37791 | 64.07443 |
| 34 | 2. | 3.99619 | 25.24947 | 38.78304 | 18.76709 |
| 35 | 15.6 | 5.46259 | 15.44203 | 25.56157 | 13.56719 |
| 36 | 94.39999 | 5.77246 | 124.56232 | 141.57391 | 47.70506 |
| 37 | 94.39999 | 5.77246 | 124.56232 | 141.57391 | 47.70596 |
| 38 | 73.29999 | 69.527 | 72.25192 | 119.72414 | 27.08932 |
| 39 | 27. | 191.5834 | 341.64139 | 394.77393 | 114.54784 |
| 40 | 212.84999 | 191.5834 | 341.6438 | 394.77393 | 114.54784 |
| 41 | 22.05999 | 1.0515 | 27.78610 | 38.99496 | 17.00264 |
| 42 | 7.09999 | 51.91237 | 125.25269 | 142.08886 | 47.90417 |

# TABLE 6-III. CONTINUED

| DATA CASE | EXPERIMENTAL | SUM FREY | WOODSIDE & MESSMER | HENGST | GORRING & CHURCHILL |
|---|---|---|---|---|---|
| | | EFFECTIVE THERMAL CONDUCTIVITY (KCAL/M-HR-K) X 1?? | | | |
| 43 | 18.5? | 9.1437 | 2?.?2167 | 22.?7112 | 6.?836? |
| 44 | 5?.5? | 5?.94296 | 131.74925 | 156.75896 | 56.577?9 |
| -5 | 35.??? | 62.7872 | 158.93935 | 134.66257 | 64.62695 |
| 46 | 22.5?9?9 | 9.12391 | 25.56296 | 39.?5473 | 18.8927? |
| 47 | 1?.7 | 5.5435 | 15.6349? | 25.74?63 | 13.7?532 |
| 4? | 22.5?9?9 | 1?.121?1 | 27.95563 | 39.12391 | 17.?8449 |
| 49 | 16.?9?9? | 5.2734? | 14.69415 | 21.6?397 | 9.99637 |
| ?? | 23.7?9?? | 1?.5?79? | 28.62161 | 37.89958 | 15.52456 |
| ?1 | 23.3?9?? | 1?.5?79? | 28.62161 | 37.89958 | 15.52456 |
| ?? | 25.2 | 1?.5?79? | 28.62161 | 37.89958 | 15.52456 |
| ?? | 2?5.5 | 168.7?114 | 314.546?8 | 356.984?4 | 1?4.8?246 |
| ?4 | 44.5?9?9 | 1?.37231 | 29.32655 | 5?.22885 | 28.37459 |
| ?? | 1?3.?4?99 | 114.46762 | 239.46548 | 264.1?522 | ?9.71844 |
| ?? | 55.3?9?9 | 56.55273 | 62.95?51 | 98.81178 | 25.57965 |

# TABLE 6-III. CONTINUED

| DATA CASE | EXPERIMENTAL | SON FREY | WOODSIDE & MESSMER | HENGST | GORRING & CHURCHILL |
|---|---|---|---|---|---|
| 57 | 36. | 1.4748 | 29.498 | 48.41 9 | 26. 40 |
| 58 | 17. 999 | 9.67121 | 2 .89 2 | 22.92738 | 7.11912 |
| 59 | 34. | 34.12347 | 47.36348 | 62.62257 | 17.25584 |
| 6 | 35.59 99 | 34.12347 | 47.36348 | 62.62257 | 17.25584 |
| 61 | 52.2 99 | 5 .8 24 | 6 .1 475 | 99.5 975 | 25.53238 |
| 62 | 55. | 5 .88243 | 63.1 475 | 99.5 975 | 25.53238 |
| 63 | 71. 9 99 | 69.12439 | 71.91624 | 12 . 4 74 | 26.61925 |
| 64 | 71.59 99 | 73. 1462 | 74.96863 | 126.46695 | 25. 4327 |
| 65 | 71.3 99 | 73. 1462 | 74.96863 | 126.46695 | 25. 4327 |
| 66 | 358. | 212.72653 | 96.72485 | 549.67188 | 178.83778 |
| 67 | 7 .7 | 52.1 13 | 127.4174 | 143.63 56 | 48.5 255 |
| 68 | 71.29 99 | 52.3673 | 127.76588 | 143.88718 | 48.621 9 |
| 69 | 44.3 99 | 116.256 3 | 242.3562 | 266.3938 | 81.4279 |
| 7 | 37.79 99 | 1 .59711 | 2 .87333 | 5 .75116 | 28.8 548 |

141

# TABLE 6-III. CONTINUED

| DATA | EFFECTIVE THERMAL CONDUCTIVITY (KCAL/M-HR-K) X 10° | | | |
|---|---|---|---|---|
| CASE | EXPERIMENTAL | SON FREY | WOODSIDE & MESSMER | HENGST | GORRING & CHURCHILL |

| CASE | EXPERIMENTAL | SON FREY | WOODSIDE & MESSMER | HENGST | GORRING & CHURCHILL |
|---|---|---|---|---|---|
| 71 | 42.5 | 11.21879 | 31.52399 | 51.58989 | 27.19503 |
| 72 | 29.7 | 1.14100 | 27.89072 | 38.61450 | 16.93538 |
| 73 | 36.36999 | 10.62590 | 29.86176 | 48.74478 | 26.25940 |
| 74 | 17.09999 | 9.4887 | 20.61638 | 22.51954 | 7.03276 |
| 75 | 231.79999 | 176.06493 | 351.27002 | 403.02715 | 116.55283 |
| 76 | 35.9999 | 10.75003 | 31.24095 | 51.09940 | 29.09288 |
| 77 | 110.70000 | 66.10103 | 165.75314 | 189.47987 | 66.69872 |
| 78 | 22.79999 | 9.62626 | 26.75684 | 40.07353 | 19.59247 |
| 79 | 17.79999 | 5.84626 | 16.36954 | 26.41212 | 14.22331 |
| 80 | 20.7 | 12.40590 | 29.27657 | 32.27780 | 17.67211 |
| 81 | 154.69999 | 119.19699 | 247.00516 | 277.05542 | 82.56298 |
| 82 | 73.09999 | 75.44955 | 77.09415 | 132.34380 | 23.03883 |
| 83 | 24.59999 | 10.71463 | 29.33125 | 40.21684 | 17.73851 |
| 84 | 51.7 | 11.02745 | 31.89000 | 51.70874 | 29.59578 |

# TABLE 6-III. CONTINUED

| DATA CASE | EXPERIMENTAL | SON FREY | WOODSIDE & MESSNER | HENGST | GORRING & CHURCHILL |
|---|---|---|---|---|---|
| 85 | 32.29999 | 1..7968 | 28.19328 | 46.1178? | 25.56139 |
| 86 | 72.59999 | 11.84763 | 33.375?9 | 72.95583 | 65.64183 |
| 87 | 36.79999 | 11.19.?? | 31.26418 | 52.?5698 | 29.883?9 |
| 88 | 47.5???? | 11.23128 | 31.358?9 | 52.1440? | 29.95494 |
| 89 | 32.5??? | 1?.2659? | 28.62??? | 46.5?6?? | 25.87??7 |
| 90 | 37.??? | 1?.83176 | 3?.16437 | 48.6662? | 26.87482 |
| 91 | 12?.59999 | 78.?5263 | 2?4.?7242 | 246.?298? | 94.633?9 |
| 92 | 298.???? | 241.48158 | 55?.44?43 | 597.11328 | 193.8?983 |
| 93 | 176.???? | 113.29666 | 287.?6?79 | 33?.49585 | 119.78264 |
| 94 | 39.59999 | 36.9?632 | 49.77415 | 66.7126? | 18.??235 |
| 95 | 15.5???? | 1?.57513 | 22.35555 | 24.19?51 | 7.49979 |
| 96 | 53.2???? | 14.?1585 | 39.?8441 | 64.33?81 | 36.52295 |
| 97 | 55.39999 | 14.?1585 | 39.?8441 | 64.33?81 | 36.52295 |
| 98 | 58.5???? | 14.?1585 | 39.?8441 | 64.33?81 | 36.52295 |

# TABLE 6-III. CONTINUED

| DATA | | EFFECTIVE THERMAL CONDUCTIVITY (KCAL/M-HR-K) X 1?? | | | |
|------|--------------|----------|---------------------|--------|----------------------|
| CASE | EXPERIMENTAL | SUN FREY | WOODSIDE & MESSNER | HENGST | GORRING & CHURCHILL |
| 99 | 59.5? | 14.?1545 | 39.?8441 | 64.33?81 | 36.52295 |
| ? | 61.9595 | 14.?1585 | 39.?8441 | 64.33?81 | 36.52295 |
| 1?1 | 23.39999 | 1?.?2616 | 21.38562 | 23.12411 | 7.2?296 |
| 1?2 | 1?.2? | 8.74336 | 14.523?5 | 17.?592? | 4.84294 |
| 1?3 | 126.? | 74.71269 | 195.49753 | 236.26627 | 91.67732 |
| 1?4 | 43.5? | 11.52577 | 32.?1976 | 52.75337 | 3?.45782 |
| 1?5 | 61.7? | 11.52577 | 32.?1976 | 52.75337 | 3?.45782 |
| 1?6 | ?27.5?9?5 | 145.1?892 | 4?1.15942 | 624.39941 | 334.98853 |
| 1?7 | 4?.2?999 | 1?.65537 | 32.3?559 | 53.?1453 | 3?.67331 |
| 1?8 | ?27. | 2?3.63?85 | 533.677?? | 575.53516 | 188.54?97 |
| 1?9 | 44.5?999 | 11.699?3 | 32.4?115 | 53.1?158 | 3?.74516 |
| 11? | 2?.?4999 | 13.23942 | 3?.75471 | 33.29242 | 11.?6783 |
| 11? | 41.79?99 | 11.78?71 | 31.77673 | 42.24588 | 18.65?44 |
| 11? | ?1?. | 148.55?2? | 399.52?? 8 | 527.19482 | 231.6???94 |

# TABLE 6-III. CONTINUED

| DATA CASE | EXPERIMENTAL | SON FREY | WOODSIDE & MESSMER | HENGST | GORRING & CHURCHILL |
|---|---|---|---|---|---|
| 113 | 342.    | 148.55 2  | 399.528 8 | 527.19482 | 231.6  04 |
| 114 | 58. 6   | 224.72 38 | 5 3.5 537 | 737.2 19  | 3 1. 1343 |
| 115 | 595.    | 2 4.72 3  | 5 3.5 537 | 737.2 19  | 3 1. 1343 |
| 116 | 55 .    | 2 4.6 652 | 667.9458  | 815.22581 | 325.8 2   |
| 117 | 615.    | 254.69652 | 667.9458  | 815.22681 | 325.8 2   |
| 118 | 63 .    | 254.69652 | 667.9458  | 815.22681 | 325.8 2   |
| 119 | 629.8999 | 274. 5371 | 746.15283 | 1 52.25757 | 5 2.66479 |
| 12  | 597. 9965 | 274. 5371 | 746.15283 | 1 52.25757 | 5 2.66479 |
| 121 | 323. 9995 | 148.63745 | 4 8.7 557 | 631.1 156 | 339.873 5 |
| 122 | 6 7.59985 | 234.15 19 | 63 .17944 | 922.36353 | 454.59473 |
| 123 | 549.5    | 235. 3 56 | 641. 4  4 | 923.86597 | 455.61694 |
| 124 | 634.3999 | 277.15299 | 752.66563 | 1 57.4 674 | 5 6. 3979 |
| 125 | 45.      | 12.6 28  | 34.515 1 | 53.64485 | 29.57269 |
| 126 | 55.79999 | 15.54993 | 42.52 84 | 64.93873 | 34.89153 |

# TABLE 6-III. CONTINUED

| DATA | EFFECTIVE THERMAL CONDUCTIVITY (KCAL/M-HR-K) X 10² | | | | |
|------|-----|-----|-----|-----|-----|
| CASE | EXPERIMENTAL | SON FREY | WOODSIDE & MESSMER | HENGST | GORRING & CHURCHILL |
| 127 | 35. | 8.31253 | 22.86977 | 38.19576 | 23.32364 |
| 128 | 32.39999 | 7.1661 | 19.32559 | 33.4791 | 20.91578 |
| 129 | 138. | 83.1662 | 215.19414 | 256.68701 | 161.24123 |
| 13 | 45.7 | 12.13477 | 33.22412 | 51.46205 | 28.23676 |
| 131 | 1 1. | 77.5923 | 196.97273 | 227.7387 | 86.22366 |
| 132 | 26.39999 | 14.24709 | 32.42883 | 34.47119 | 11.56709 |
| 133 | 35.59999 | 12.34881 | 33.23314 | 49.6239 | 26.13159 |
| 134 | 11. | 87.8669 | 217.2074 | 243.02867 | 90.48083 |
| 135 | 31.4699 | 39.66171 | 52.69141 | 70.18048 | 18.27229 |
| 136 | 13.8 | 1.89926 | 22.5916 | 23.57623 | 7.46199 |
| 137 | 13.8 | 1.5478 | 18.89433 | 20.09761 | 6.03471 |
| 138 | 34.2 | 13.21836 | 34.93280 | 52.64954 | 30.15294 |
| 139 | 95.29999 | 89.7282 | 205.80371 | 216.31229 | 78.15236 |
| 14 | 27.29999 | 13.22277 | 33.78964 | 45.63637 | 23.41751 |

# TABLE 6-III. CONTINUED

| DATA CASE | EXPERIMENTAL | SON FREY | WOODSIDE & MESSMER | HENGST | GORRING & CHURCHILL |
|---|---|---|---|---|---|
| 141 | 26.2 | 8.1 2 6 | 2 .86414 | 3 .27881 | 17.13559 |
| 142 | 61.7 | 9 .8 51 | 2 7.32312 | 217.27795 | 78.56728 |
| 143 | 27. | 13.3 986 | 34. 6313 | 45.84 1 | 23.55 45 |
| 144 | 25.2 | 8.2 482 | 21. 3415 | 3 .41397 | 17.23967 |
| 145 | 49. | 16.19675 | 39.55229 | 47.78639 | 21.94421 |
| 146 | 11 .79999 | 97.25 7 | 216. 243 | 222.75 18 | 8 .93 69 |
| 147 | 27.5 | 1 .39 46 | 35.63449 | 46.99461 | 24.34775 |
| 148 | 26.39999 | 8.82587 | 22. 11 2 | 31.17998 | 17.83273 |
| 149 | 35.2 | 79.34776 | 18 .23277 | 189.21664 | 71.22829 |
| 15 | 58.39999 | 15.5 932 | 3 .85716 | 55.96614 | 32.62816 |
| 151 | 7 . | 17.84613 | 4 .87521 | 47.87144 | 22.66267 |
| 152 | 76. | 21.18156 | 44.51111 | 5 .18568 | 24.55772 |
| 153 | 272.5 | 163.7 651 | 363.51343 | 423.66528 | 129.13 16 |
| 154 | 248.7 | 144.91 72 | 323.16113 | 378.1731 | 116.45776 |

# TABLE 6-III. CONTINUED

| DATA CASE | EXPERIMENTAL | SON FREY | WOODSIDE & MESSMER | HENGST | GORRING & CHURCHILL |
|---|---|---|---|---|---|
| | | EFFECTIVE THERMAL CONDUCTIVITY (KCAL/M-HR-K) X 1°° | | | |
| 155 | 172.7 | 93.6`571 | 226.`15`9 | 272.27515 | 86.89446 |
| 156 | 16.5 | 16.71394 | 16.7916 | 24.55`05 | 3.55`39 |
| 157 | 6.9 | 5.`867` | 7.65523 | 9.76947 | 2.93787 |
| 158 | 46.` | 46.57545 | 119.69844 | 154.79541 | 51.782`6 |
| 159 | `.1 61 | | | `.`` | `.`````2 |
| 160 | .`9193 | | | `.`````` | `.```2 |
| 161 | `.`6593 | | | `.```` | `.`````1 |
| 162 | .`511` | | | `.```` | `.`````1 |
| 163 | .`414` | | | `.`````` | `.`````1 |
| 164 | `.`4`4` | | `.``````` | `.`````` | `.`````3 |
| 165 | 15.6 | 6.694`9 | 18.9`675 | 32.738`7 | 14.55421 |
| 166 | 11.85` | 4.`6198 | 11.46297 | 21.57736 | 1`.49382 |
| 167 | 29.89999 | 6.69278 | 18.28589 | 41.`2341 | 2`.55`72 |
| 168 | 13.`` | 41.1`8`6 | 111.72429 | 249.32`14 | 121.63942 |

148

# TABLE 6-III. CONTINUED

| DATA CASE | EXPERIMENTAL | SUN FREY | WOODSIDE & MESSMER | HENGST | GORRING & CHURCHILL |
|---|---|---|---|---|---|
| | | | EFFECTIVE THERMAL CONDUCTIVITY (KCAL/M-HR-K) X 100 | | |
| 169 | 81.5 | 4.71188 | 116.39820 | 167.68166 | 58.07501 |
| 17 | 29.79999 | 25.41213 | 31.45314 | 42.29439 | 15.41329 |
| 171 | 6.  . | 4.51416 | 113.88419 | 154.25796 | 51.28328 |
| 172 | 1.24 | .36333 | .77145 | 1.69970 | .44762 |

# TABLE 6-IV. COMPARISON OF SELECTED UNIFORM HEAT FLUX MODELS

| DATA | | EFFECTIVE THERMAL CONDUCTIVITY (KCAL/M-HR-K) X 100 | | | |
|---|---|---|---|---|---|
| CASE | EXPERIMENTAL | WILLHITE, KUNII & SMITH | SCHUMANN & VOSS | PRESTON | KRUPICZKA |
| 1 | 21.39999 | 30.58623 | 10.94355 | 18.70827 | 16.19852 |
| 2 | 22.39999 | 47.55049 | 14.85457 | 25.07813 | 24.24138 |
| 3 | 75.50000 | 163.22572 | 55.93527 | 89.43590 | 82.96129 |
| 4 | 246.00000 | 400.29590 | 158.42358 | 242.72166 | 209.98410 |
| 5 | 272.00000 | 432.23389 | 174.36879 | 266.10303 | 228.48177 |
| 6 | 1.01500 | 1.37111 | 0.40426 | 0.79117 | 0.58865 |
| 7 | 63.59999 | 133.01194 | 50.24249 | 80.68788 | 61.53003 |
| 8 | 25.00000 | 46.32814 | 12.68302 | 21.55121 | 18.21974 |
| 9 | 17.50000 | 44.25276 | 11.69747 | 19.94258 | 16.93826 |
| 10 | 63.50000 | 146.90202 | 51.59330 | 83.38252 | 62.99168 |
| 11 | 127.00000 | 224.19444 | 112.45572 | 174.73199 | 124.08296 |
| 12 | 19.00000 | 45.44478 | 11.80254 | 20.11433 | 17.06645 |
| 13 | 17.20000 | 45.59529 | 11.84647 | 20.18613 | 17.12315 |
| 14 | 30.39999 | 83.85543 | 19.15024 | 31.99532 | 31.86885 |

# TABLE 6-IV. CONTINUED

| DATA | EFFECTIVE THERMAL CONDUCTIVITY (KCAL/M-HR-K) X 100 | | | | |
|------|--------------|--------------------------|-------------------|-----------|-----------|
| CASE | EXPERIMENTAL | WILLHITE, KUNII & SMITH | SCHUMANN & VOSS | PRESTON | KRUPICZKA |
| 15 | 118.00000 | 232.31764 | 114.24954 | 177.40428 | 125.47821 |
| 16 | 36.50000 | 74.12903 | 16.92627 | 28.42311 | 26.38243 |
| 17 | 23.84999 | 93.82394 | 20.22913 | 33.72197 | 33.77486 |
| 18 | 216.00000 | 541.22119 | 183.03313 | 278.77075 | 217.02795 |
| 19 | 26.79999 | 72.28341 | 16.30099 | 27.41541 | 25.49240 |
| 20 | 11.80000 | 21.24489 | 7.33154 | 12.74100 | 8.59804 |
| 21 | 25.29999 | 31.74640 | 24.32825 | 40.24960 | 25.07823 |
| 22 | 21.89000 | 74.93779 | 16.81395 | 28.24219 | 26.29956 |
| 23 | 34.09999 | 102.45132 | 21.47824 | 35.71642 | 36.33392 |
| 24 | 144.70000 | 418.10156 | 120.99857 | 187.44221 | 150.96895 |
| 25 | 34.39999 | 99.40473 | 20.84666 | 34.70860 | 34.88362 |
| 26 | 244.89999 | 572.65503 | 187.48227 | 285.26611 | 220.84439 |
| 27 | 35.14000 | 73.13052 | 31.21465 | 51.11766 | 34.42345 |
| 28 | 81.50000 | 408.71387 | 95.18149 | 148.90633 | 136.89030 |

# TABLE 6-IV. CONTINUED

| DATA | | EFFECTIVE THERMAL CONDUCTIVITY (KCAL/M-HR-K) X 100 | | | |
| --- | --- | --- | --- | --- | --- |
| CASE | EXPERIMENTAL | WILLHITE, KUNII & SMITH | SCHUMANN & VOSS | PRESTON | KRUPICZKA |
| 29 | 224.89999 | 576.60229 | 188.04678 | 286.08984 | 221.33124 |
| 30 | 217.39999 | 576.60229 | 188.04678 | 286.08984 | 221.33124 |
| 31 | 218.89999 | 576.60229 | 188.04678 | 286.08984 | 221.33124 |
| 32 | 218.89999 | 576.60229 | 188.04678 | 286.08984 | 221.33124 |
| 33 | 91.00000 | 349.10938 | 84.12898 | 132.28313 | 116.49580 |
| 34 | 20.00000 | 82.54218 | 17.37775 | 29.14975 | 28.26201 |
| 35 | 15.60000 | 55.29848 | 11.40983 | 19.47205 | 19.10077 |
| 36 | 94.39999 | 264.32520 | 65.42412 | 103.93791 | 88.21062 |
| 37 | 94.39999 | 264.32520 | 65.42412 | 103.93791 | 88.21062 |
| 38 | 73.29999 | 84.76138 | 66.28185 | 105.24437 | 67.93713 |
| 39 | 207.00000 | 592.43018 | 190.32243 | 289.40918 | 223.30064 |
| 40 | 212.89999 | 592.43018 | 190.32243 | 289.40918 | 223.30064 |
| 41 | 22.29999 | 82.85297 | 17.72032 | 29.70062 | 27.68407 |
| 42 | 70.89999 | 268.62280 | 65.94923 | 104.73782 | 88.80655 |

# TABLE 6-IV. CONTINUED

| DATA | | EFFECTIVE THERMAL CONDUCTIVITY (KCAL/M-HR-K) X 100 | | | |
|------|--------------|--------------------------|------------------|-----------|-----------|
| CASE | EXPERIMENTAL | WILLHITE, KUNII & SMITH | SCHUMANN & VOSS | PRESTON | KRUPICZKA |
| 43 | 18.50000 | 38.45332 | 10.38729 | 17.79535 | 13.12635 |
| 44 | 61.50000 | 311.97437 | 72.38222 | 114.51656 | 102.07315 |
| 45 | 85.00000 | 360.78979 | 85.53532 | 134.40306 | 118.17538 |
| 46 | 22.59999 | 85.55513 | 17.72148 | 29.70250 | 28.84357 |
| 47 | 15.70000 | 57.34253 | 11.64175 | 19.85146 | 19.52393 |
| 48 | 22.59999 | 84.30673 | 17.88850 | 29.97090 | 27.94415 |
| 49 | 16.29999 | 47.21161 | 9.85118 | 16.91360 | 15.76856 |
| 50 | 23.79999 | 80.12569 | 17.38402 | 29.15985 | 26.34326 |
| 51 | 23.39999 | 80.12569 | 17.38402 | 29.15985 | 26.34326 |
| 52 | 25.20000 | 80.12569 | 17.38402 | 29.15985 | 26.34326 |
| 53 | 205.50000 | 560.34937 | 171.63145 | 262.09570 | 203.90205 |
| 54 | 44.59999 | 114.48170 | 22.88257 | 37.95303 | 38.89476 |
| 55 | 163.79999 | 453.54956 | 125.76273 | 194.51445 | 155.36868 |
| 56 | 55.39999 | 85.36807 | 52.36089 | 83.94774 | 54.60246 |

# TABLE 6-IV. CONTINUED

| DATA | EFFECTIVE THERMAL CONDUCTIVITY (KCAL/M-HR-K) X 100 | | | | |
|---|---|---|---|---|---|
| CASE | EXPERIMENTAL | WILLHITE, KUNII & SMITH | SCHUMANN & VOSS | PRESTON | KRUPICZKA |
| 57 | 36.00000 | 111.82214 | 22.29712 | 37.02130 | 37.47093 |
| 58 | 17.09999 | 41.02596 | 10.93644 | 18.69662 | 13.68109 |
| 59 | 34.20000 | 76.87021 | 31.42694 | 51.45102 | 34.42252 |
| 60 | 35.59999 | 76.87021 | 31.42694 | 51.45102 | 34.42252 |
| 61 | 53.29999 | 85.84662 | 52.72963 | 84.51462 | 54.87790 |
| 62 | 55.00000 | 85.84662 | 52.72963 | 84.51462 | 54.87790 |
| 63 | 71.39999 | 85.76227 | 65.91762 | 104.68968 | 67.41853 |
| 64 | 71.59999 | 85.66153 | 70.29794 | 111.35236 | 71.57538 |
| 65 | 71.39999 | 85.66153 | 70.29794 | 111.35236 | 71.57538 |
| 66 | 358.00000 | 1041.73608 | 260.21729 | 390.65063 | 338.67065 |
| 67 | 70.70000 | 281.75488 | 67.68922 | 107.38646 | 90.68391 |
| 68 | 71.29999 | 283.93408 | 67.95511 | 107.79092 | 90.99518 |
| 69 | 144.39999 | 469.97510 | 127.91452 | 197.70503 | 157.51139 |
| 70 | 37.79999 | 120.64456 | 23.57863 | 39.05948 | 40.27139 |

# TABLE 6-IV. CONTINUED

| DATA CASE | EXPERIMENTAL | EFFECTIVE THERMAL CONDUCTIVITY (KCAL/M-HR-K) X 100 | | | |
| --- | --- | --- | --- | --- | --- |
| | | WILLHITE, KUNII & SMITH | SCHUMANN & VOSS | PRESTON | KRUPICZKA |
| 71 | 42.50000 | 120.25105 | 23.76529 | 39.35597 | 39.88403 |
| 72 | 29.70000 | 87.76758 | 18.10641 | 30.32092 | 28.23933 |
| 73 | 36.39999 | 115.72844 | 22.74287 | 37.73077 | 38.32213 |
| 74 | 17.09999 | 41.93744 | 10.84972 | 18.55441 | 13.58416 |
| 75 | 230.79999 | 640.26025 | 197.46478 | 299.81689 | 229.43102 |
| 76 | 35.09999 | 124.80501 | 24.05841 | 39.82138 | 41.22763 |
| 77 | 100.70000 | 405.39233 | 91.10527 | 142.78535 | 124.84547 |
| 78 | 22.39999 | 97.12326 | 19.09396 | 31.90515 | 31.18739 |
| 79 | 17.75999 | 65.19725 | 12.56905 | 21.36546 | 21.23581 |
| 80 | 20.70000 | 65.61769 | 15.58228 | 26.25514 | 20.38972 |
| 81 | 154.85999 | 496.46704 | 131.46788 | 202.96892 | 161.05682 |
| 82 | 73.09999 | 87.70724 | 73.14787 | 115.67809 | 74.00459 |
| 83 | 24.59999 | 96.18216 | 19.31223 | 32.25484 | 30.16379 |
| 84 | 51.70000 | 132.18263 | 24.92836 | 41.20128 | 42.97977 |

# TABLE 6-IV CONTINUED

DATA            EFFECTIVE THERMAL CONDUCTIVITY (KCAL/M-HR-K) X 100

| CASE | EXPERIMENTAL | WILLHITE, KUNII & SMITH | SCHUMANN & VOSS | PRESTON | KRUPICZKA |
|------|-------------|-------------------------|-----------------|---------|-----------|
| 85 | 32.29999 | 117.29691 | 22.23698 | 36.92557 | 37.98433 |
| 86 | 78.59999 | 159.33517 | 35.51990 | 57.86070 | 64.84431 |
| 87 | 36.79999 | 136.45222 | 25.44284 | 42.01639 | 44.02840 |
| 88 | 47.50000 | 137.52550 | 25.57341 | 42.22316 | 44.29619 |
| 89 | 32.50000 | 122.02280 | 22.80809 | 37.83456 | 39.12225 |
| 90 | 37.00000 | 128.29848 | 23.94914 | 39.64790 | 41.00870 |
| 91 | 120.59999 | 584.87109 | 121.11996 | 187.62265 | 174.98882 |
| 92 | 298.00000 | 1251.81348 | 294.91113 | 440.46875 | 377.66968 |
| 93 | 176.00000 | 760.24341 | 162.79938 | 249.14752 | 226.25079 |
| 94 | 39.59999 | 85.96399 | 33.90945 | 55.34254 | 36.56947 |
| 95 | 15.50000 | 47.73401 | 11.97573 | 20.39729 | 14.75896 |
| 96 | 53.20000 | 170.37206 | 31.65918 | 51.81555 | 54.68451 |
| 97 | 55.39999 | 170.37206 | 31.65918 | 51.81555 | 54.68451 |
| 98 | 58.50000 | 170.37206 | 31.65918 | 51.81555 | 54.68451 |

156

# TABLE 6-IV. CONTINUED

| DATA | EFFECTIVE THERMAL CONDUCTIVITY (KCAL/M-HR-K) X 100 | | | |
|------|--------------|----------------------------|-------------------|-----------|
| CASE | EXPERIMENTAL | WILLHITE, KUNII & SMITH | SCHUMANN & VOSS | PRESTON | KRUPICZKA |
| 99  | 59.50000  | 170.37206  | 31.65918  | 51.81555  | 54.68451  |
| 100 | 61.09999  | 170.37206  | 31.65918  | 51.81555  | 54.68451  |
| 101 | 23.39999  | 45.95647   | 11.44436  | 19.52858  | 14.16165  |
| 102 | 10.20000  | 27.48444   | 8.53562   | 14.74131  | 9.68186   |
| 103 | 126.00000 | 573.10449  | 117.28314 | 181.91917 | 170.16017 |
| 104 | 43.50000  | 145.10443  | 26.51057  | 43.70592  | 46.23676  |
| 105 | 51.70000  | 145.10443  | 26.51057  | 43.70592  | 46.23676  |
| 106 | 327.59985 | 1715.02881 | 315.72998 | 470.24634 | 537.74292 |
| 107 | 40.29999  | 148.38657  | 26.92435  | 44.35989  | 47.10522  |
| 108 | 327.00000 | 1271.44189 | 289.85645 | 433.22607 | 371.82324 |
| 109 | 44.59999  | 149.48515  | 27.06407  | 44.58066  | 47.39987  |
| 110 | 26.29999  | 75.03748   | 16.80733  | 28.23152  | 21.79857  |
| 111 | 41.79999  | 111.82056  | 21.44038  | 35.65605  | 33.45587  |
| 112 | 318.00000 | 1407.88379 | 269.20239 | 403.57739 | 418.94873 |

# TABLE 6-IV. CONTINUED

| DATA | EFFECTIVE THERMAL CONDUCTIVITY (KCAL/M-HR-K) X 100 | | | |
| CASE | EXPERIMENTAL | WILLHITE, KUNII & SMITH | SCHUMANN & VOSS | PRESTON | KRUPICZKA |
|---|---|---|---|---|---|
| 113 | 342.00000 | 1407.88379 | 269.20239 | 403.57739 | 418.94873 |
| 114 | 580.00000 | 1916.31787 | 375.79736 | 555.72754 | 560.92163 |
| 115 | 595.00000 | 1916.31787 | 375.79736 | 555.72754 | 560.92163 |
| 116 | 550.00000 | 2099.59497 | 415.35303 | 611.70728 | 611.90381 |
| 117 | 615.00000 | 2099.59497 | 415.35303 | 611.70728 | 611.90381 |
| 118 | 630.00000 | 2099.59497 | 415.35303 | 611.70728 | 611.90381 |
| 119 | 629.99990 | 2894.58716 | 540.02856 | 786.80811 | 877.19165 |
| 120 | 597.09985 | 2894.58716 | 540.02856 | 786.80811 | 877.19165 |
| 121 | 323.09985 | 1792.87500 | 325.79004 | 484.60596 | 557.69434 |
| 122 | 607.59985 | 2570.67017 | 475.26123 | 696.08081 | 783.57446 |
| 123 | 549.50000 | 2588.86743 | 477.62915 | 699.40625 | 787.97876 |
| 124 | 634.39990 | 2956.20654 | 548.06128 | 798.02905 | 891.69800 |
| 125 | 45.00000 | 158.02725 | 28.29333 | 46.52072 | 49.08374 |
| 126 | 55.79999 | 190.22292 | 34.20032 | 55.79771 | 58.74028 |

# TABLE 6-IV. CONTINUED

| DATA | EFFECTIVE THERMAL CONDUCTIVITY (KCAL/M-HR-K) X 100 | | | |
| CASE | EXPERIMENTAL | WILLHITE, KUNII & SMITH | SCHUMANN & VOSS | PRESTON | KRUPICZKA |
|------|--------------|-------------------------|-----------------|----------|-----------|
| 127 | 35.00000 | 114.50127 | 20.19646 | 33.66980 | 36.33409 |
| 128 | 32.39999 | 99.59148 | 17.48831 | 29.32759 | 31.80313 |
| 129 | 188.00000 | 683.11768 | 133.78758 | 206.40227 | 195.06731 |
| 130 | 45.70000 | 151.46167 | 27.13866 | 44.69846 | 46.99364 |
| 131 | 101.00000 | 593.08423 | 118.45277 | 183.65854 | 168.09543 |
| 132 | 26.39999 | 84.99678 | 18.23677 | 30.53023 | 23.48619 |
| 133 | 35.59999 | 154.58116 | 27.24794 | 44.87105 | 47.12100 |
| 134 | 110.00000 | 669.15698 | 131.65253 | 203.24222 | 183.83636 |
| 135 | 31.04999 | 105.88724 | 36.88158 | 59.98622 | 38.93994 |
| 136 | 13.80000 | 58.70363 | 12.93406 | 21.96014 | 15.85690 |
| 137 | 13.80000 | 45.93121 | 10.94369 | 18.70853 | 12.81330 |
| 138 | 34.20000 | 183.41197 | 31.51228 | 51.58502 | 57.44498 |
| 139 | 95.39999 | 668.09253 | 129.35771 | 199.84351 | 175.85689 |
| 140 | 27.29999 | 166.50456 | 28.89240 | 47.46490 | 50.64946 |

# TABLE 6-IV. CONTINUED

| DATA | EFFECTIVE THERMAL CONDUCTIVITY (KCAL/M-HR-K) X 100 | | | |
| CASE | EXPERIMENTAL | WILLHITE, KUNII & SMITH | SCHUMANN & VOSS | PRESTON | KRUPICZKA |
|---|---|---|---|---|---|
| 141 | 26.20000 | 113.17999 | 19.36655 | 32.34183 | 35.98036 |
| 142 | 61.70000 | 678.12842 | 131.05650 | 202.35971 | 178.34129 |
| 143 | 27.00000 | 169.20699 | 29.34781 | 48.18216 | 51.67146 |
| 144 | 25.20000 | 115.03691 | 19.68065 | 32.84468 | 36.76106 |
| 145 | 49.00000 | 179.21666 | 31.78062 | 52.00621 | 52.57718 |
| 146 | 110.79999 | 735.47827 | 141.22476 | 217.39323 | 193.58580 |
| 147 | 27.50000 | 184.69882 | 32.10506 | 52.51523 | 58.07330 |
| 148 | 26.39999 | 125.68794 | 21.58565 | 35.88768 | 41.67722 |
| 149 | 85.20000 | 642.29883 | 121.19238 | 187.73024 | 171.18640 |
| 150 | 58.39999 | 224.99965 | 38.52536 | 62.54784 | 75.00726 |
| 151 | 70.00000 | 201.06511 | 36.36180 | 59.17522 | 63.78119 |
| 152 | 76.00000 | 232.15498 | 44.17183 | 71.31412 | 83.49115 |
| 153 | 272.50000 | 399.69238 | 178.60139 | 272.29443 | 237.12428 |
| 154 | 248.70000 | 356.15112 | 157.72446 | 241.69421 | 212.07919 |

# TABLE 6-IV. CONTINUED

| DATA | | EFFECTIVE THERMAL CONDUCTIVITY (KCAL/M-HR-K) X 100 | | | |
|------|--------------|----------------------------|-------------------|-----------|-----------|
| CASE | EXPERIMENTAL | WILLHITE,<br>KUNII & SMITH | SCHUMANN<br>& VOSS | PRESTON | KRUPICZKA |
| 155 | 172.70000 | 252.44057 | 110.58070 | 171.93726 | 153.71112 |
| 156 | 16.50000 | 16.85527 | 16.46114 | 27.67363 | 16.72668 |
| 157 | 6.90000 | 7.48778 | 4.74239 | 8.39002 | 5.55099 |
| 158 | 46.00000 | 121.25670 | 62.07175 | 98.82504 | 87.33781 |
| 159 | 0.10610 | 0.00000 | 0.00000 | 0.00000 | 0.00000 |
| 160 | 0.08183 | 0.00000 | 0.00000 | 0.00000 | 0.00000 |
| 161 | 0.05598 | 0.00000 | 0.00000 | 0.00000 | 0.00000 |
| 162 | 0.05110 | 0.00000 | 0.00000 | 0.00000 | 0.00000 |
| 163 | 0.04140 | 0.00000 | 0.00000 | 0.00000 | 0.00000 |
| 164 | 0.14040 | 0.00000 | 0.00000 | 0.00000 | 0.00000 |
| 165 | 15.60000 | 25.68503 | 12.15019 | 20.68217 | 18.75803 |
| 166 | 11.85000 | 16.91458 | 7.90069 | 13.68808 | 12.28974 |
| 167 | 39.89999 | 10.58609 | 15.94372 | 26.83890 | 20.00317 |
| 168 | 130.00000 | 64.80984 | 97.74626 | 152.75218 | 121.11963 |

## TABLE 6-IV. CONTINUED

| DATA | EFFECTIVE THERMAL CONDUCTIVITY (KCAL/M-HR-K) X 100 | | | | |
|------|--------------|----------------------|-------------------|-----------|-----------|
| CASE | EXPERIMENTAL | WILLHITE, KUNII & SMITH | SCHUMANN & VOSS | PRESTCN | KRUPICZKA |
| 169 | 81.50000 | 50.49634 | 70.56497 | 111.75790 | 89.70921 |
| 170 | 29.79999 | 24.32439 | 25.85866 | 42.67471 | 27.67903 |
| 171 | 60.00000 | 48.08287 | 66.04495 | 104.88356 | 83.26828 |
| 172 | 1.02400 | 0.54938 | 0.85596 | 1.62444 | 0.85991 |

# TABLE 6-V. COMPARISON OF SELECTED PARALLEL ISOTHERMS MODELS

| DATA CASE | EFFECTIVE THERMAL CONDUCTIVITY (KCAL/M-HR-K) X 1∩∩ | | | | |
|---|---|---|---|---|---|
| | EXPERIMENTAL | RUSSELL | BERNSTEIN | WOODSIDE | Equation 5-2 |
| 1 | 21.39999 | 11.35∩34 | 9.∩5587 | 34.11279 | 13.3∩∩4∩ |
| 2 | 22.39∩99 | 11.91∩25 | 41.∩∩717 | 1∩7.35464 | 23.42773 |
| 3 | 75.5∩∩∩∩ | 57.∩2879 | 59.5∩623 | 185.24553 | 68.∩7611 |
| 4 | 246.∩∩∩∩∩ | 193.6767∩ | 122.72449 | 257.73462 | 173.96∩13 |
| 5 | 272.∩∩∩∩∩ | 215.93658 | 134.169∩4 | 265.81763 | 19∩.39352 |
| 6 | 1.∩15∩∩ | ∩.4∩1∩∩ | ∩.79519 | 1.3951∩ | ∩.47514 |
| 7 | 63.59999 | 63.∩55∩5 | 49.49434 | 58.13519 | 52.52979 |
| 8 | 25.∩∩∩∩∩ | 12.4119∩ | 3∩.421∩8 | 4∩.47348 | 14.54256 |
| 9 | 17.5∩∩∩∩ | 11.149∩3 | 32.36168 | 39.668∩6 | 13.51∩∩1 |
| 1∩ | 63.5∩∩∩∩ | 64.579∩9 | 55.65683 | 58.13519 | 53.69958 |
| 11 | 127.∩∩∩∩∩ | 137.792∩8 | 1∩7.82751 | 78.63356 | 115.7∩479 |
| 12 | 19.∩∩∩∩∩ | 11.18736 | 34.17848 | 39.63994 | 13.57578 |
| 13 | 17.2∩∩∩∩ | 11.23781 | 34.1963∩ | 39.668∩6 | 13.61926 |
| 14 | 3∩.39999 | 12.88216 | 299.2∩85∩ | 279.977∩5 | 32.7∩816 |

# TABLE 5-V. CONTINUED

EFFECTIVE THERMAL CONDUCTIVITY (KCAL/M-HR-K) X 10⁰

| DATA CASE | EXPERIMENTAL | RUSSELL | BERNSTEIN | WOODSIDE | Equation 5-2 |
|---|---|---|---|---|---|
| 15 | 118. | 139.49962 | 11 .9 158 | 78.77 39 | 117.15749 |
| 16 | 36.5 | 13.31256 | 118.19 25 | 1 4.51558 | 22. 1546 |
| 17 | 33. 4 39 | 13.27931 | 364. 586 | 279. 77 5 | 33.94925 |
| 18 | 216. | 225.7 9 7 | 2 9.44612 | 186.88631 | 186. 587 |
| 19 | 6.79 9 | 12.66572 | 121.11266 | 1 3.21956 | 21.32 31 |
| 2 | 11.0 | 9. 7 18 | 8.23765 | 7. 9 29 | 7.43614 |
| 21 | 25.29 9 | 26.19 4 | 24.39537 | 12.93435 | 24.85637 |
| 22 | 21.89 | 13. 2 19 | 126.73624 | 1 6.34 9 | 21.97264 |
| 23 | 34. 9 9 | 13.44579 | 5 4. 6934 | 354.25293 | 38.64723 |
| 24 | 144.7 | 14 .56415 | 177.9995 | 163.15637 | 123.339 4 |
| 25 | 34.35 99 | 13.5 4 8 | 3 9.34961 | 279.977 5 | 34.65524 |
| 26 | 244.89999 | 22 .76244 | 223.37694 | 186.88631 | 189.11176 |
| 27 | 35.14 | 38.36937 | 31.7 35 | 22.33326 | 31.64961 |
| 28 | 61.5 | 86.25 27 | 363.71973 | 3 4.82275 | 1 6.79 85 |

164

# TABLE 6-V. CONTINUED

| DATA CASE | EXPERIMENTAL | EFFECTIVE THERMAL CONDUCTIVITY (KCAL/M-HR-K) X 150 | | | |
| --- | --- | --- | --- | --- | --- |
| | | RUSSELL | BERNSTEIN | WOODSIDE | Equation 5-2 |
| 29 | 224.89999 | 230.26491 | 225.11832 | 186.88631 | 189.49945 |
| 30 | 217.39999 | 230.26491 | 225.11832 | 186.88631 | 189.49945 |
| 31 | 218.89999 | 230.26491 | 225.11832 | 186.88631 | 189.49945 |
| 32 | 218.89999 | 230.26491 | 225.11832 | 186.88631 | 189.49945 |
| 33 | 91.6 | 81.64751 | 245.34085 | 219.56784 | 90.58546 |
| 34 | 20. | 12.09319 | 223.66454 | 156.78442 | 25.14748 |
| 35 | 15.6 | 7.35292 | 222.26050 | 147.33360 | 18.72270 |
| 36 | 94.39999 | 66.42775 | 161.01988 | 138.11543 | 68.85420 |
| 37 | 94.39999 | 66.42775 | 161.01988 | 138.11543 | 68.85420 |
| 38 | 73.29999 | 70.64775 | 66.64334 | 34.64285 | 67.55347 |
| 39 | 207. | 232.29062 | 232.08362 | 186.88631 | 191.06364 |
| 40 | 212.89999 | 232.29062 | 232.08362 | 186.88631 | 191.06364 |
| 41 | 22.29999 | 13.44735 | 148.76400 | 176.31741 | 22.73305 |
| 42 | 70.89999 | 66.78267 | 164.81833 | 138.11543 | 69.21696 |

# TABLE 6-V. CONTINUED

| DATA CASE | EXPERIMENTAL | EFFECTIVE THERMAL CONDUCTIVITY (KCAL/M-HR-K) X 10⁰ RUSSELL | BERNSTEIN | WOODSIDE | Equation 5-2 |
|---|---|---|---|---|---|
| 43 | 18.5 | 11.65616 | 17.75331 | 15.11711 | 17.54553 |
| 44 | 61.5 | 67.25276 | 252.65945 | 252.77339 | 79.14689 |
| 45 | 85. | 92.53639 | 257.57537 | 259.56784 | 91.57344 |
| 46 | 22.59999 | 12.23790 | 236.73130 | 156.78442 | 25.47903 |
| 47 | 15.7 | 7.43690 | 234.64637 | 147.33360 | 18.98404 |
| 48 | 22.59999 | 13.52346 | 151.94125 | 136.31741 | 22.87326 |
| 49 | 16.29999 | 7.05777 | 178.43170 | 73.16948 | 13.40702 |
| 50 | 23.79999 | 14.70364 | 117.47327 | 87.59071 | 25.91824 |
| 51 | 23.29999 | 14.70364 | 117.47327 | 87.59071 | 25.91824 |
| 52 | 25.2 | 14.70364 | 117.47327 | 87.59071 | 25.91824 |
| 53 | 25.5 | 276.76819 | 222.99376 | 187.73682 | 172.75056 |
| 54 | 44.59999 | 13.91775 | 596.85693 | 354.25293 | 47.33075 |
| 55 | 163.79999 | 144.22986 | 198.17822 | 163.17674 | 126.37257 |
| 56 | 55.39999 | 59.71576 | 52.27781 | 29.37241 | 53.32962 |

# TABLE 6-V. CONTINUED

| DATA CASE | EXPERIMENTAL | EFFECTIVE THERMAL CONDUCTIVITY (KCAL/M-HR-K) X 100 | | | |
| | | RUSSELL | BERNSTEIN | WOODSIDE | Equation 5-2 |
| --- | --- | --- | --- | --- | --- |
| 57 | 36.0    | 14. 1232 | 475.92822 | 279.97705 | 36.25958 |
| 58 | 17. 9999 | 12.25793 | 18.9 7 6 | 15.17392 | 1 .99409 |
| 59 | 34.2     | 38.4 248 | 32.76 91 | 22.13 75 | 31.61661 |
| 6  | 35.59999 | 38.4 248 | 32.76 91 | 22.13 75 | 31.61661 |
| 61 | 53.29999 | 59.26619 | 52.73 62 | 29.3 298 | 53.66516 |
| 62 | 55.      | 59.26619 | 52.73 62 | 29.3 299 | 53.66516 |
| 63 | 71.39999 | 7 .25677 | 66.3 217 | 34.26784 | 67. 7533 |
| 64 | 71.59999 | 73.81848 | 7 .82 22 | 36. 4248 | 71.438 3 |
| 65 | 71.39999 | 73.81848 | 7 .82 22 | 36. 4248 | 71.438 3 |
| 66 | 358.     | 274.26123 | 564.41 16 | 449.33862 | 265.78369 |
| 67 | 7 .7     | 67.916 6 | 176.23 3 | 138.13518 | 7 .36467 |
| 68 | 71.29999 | 68. 9929 | 178.12949 | 138.13518 | 7 .55255 |
| 69 | 144.39999 | 146. 2 61 | 2 7.27832 | 163.1 674 | 127.853 1 |
| 7  | 37.79999 | 14.15291 | 642.99976 | 354.25293 | 41.21 1 |

# TABLE 6-V.  CONTINUED

| DATA CASE | EXPERIMENTAL | EFFECTIVE THERMAL CONDUCTIVITY (KCAL/M-HR-K) X 10° | | | |
| | | RUSSELL | BERNSTEIN | WOODSIDE | Equation 5-2 |
|---|---|---|---|---|---|
| 71 | 42.5 | 14.97444 | 493.83391 | 281.79614 | 37.97573 |
| 72 | 29.7 | 13.47485 | 162.49513 | 103.21956 | 22.89739 |
| 73 | 36.39999 | 14.17487 | 499.49072 | 279.07775 | 36.77461 |
| 74 | 17.99999 | 12.00739 | 19.89945 | 15.10771 | 19.84907 |
| 75 | 231.79999 | 238.52497 | 252.97986 | 186.88631 | 195.99224 |
| 76 | 35.09999 | 14.31813 | 673.76245 | 354.25293 | 41.81262 |
| 77 | 110.79999 | 86.00999 | 303.12256 | 279.55384 | 95.44077 |
| 78 | 22.39999 | 12.77026 | 282.40649 | 156.78442 | 26.78778 |
| 79 | 17.79999 | 7.76587 | 281.06470 | 147.33367 | 23.01439 |
| 80 | 20.7 | 15.94651 | 28.36993 | 27.51408 | 15.81591 |
| 81 | 154.89999 | 148.95731 | 221.95050 | 163.10674 | 130.28931 |
| 82 | 73.09999 | 76.11324 | 73.59721 | 36.96539 | 74.01647 |
| 83 | 24.59999 | 14.15834 | 182.95847 | 106.31741 | 24.04616 |
| 84 | 51.7 | 14.61435 | 727.59741 | 354.25293 | 42.89624 |

# TABLE 6-V. CONTINUED

| DATA CASE | EXPERIMENTAL | EFFECTIVE THERMAL CONDUCTIVITY (KCAL/M-HR-K) X 10⁶ | | | |
|---|---|---|---|---|---|
| | | RUSSELL | BERNSTEIN | WOODSIDE | Equation 5-2 |
| 85 | 32.29999 | 13.35525 | 567.47256 | 280.96582 | 36.51816 |
| 86 | 78.59999 | 15.68976 | 6396.29297 | 2443.18774 | 145.43269 |
| 87 | 36.79999 | 14.78839 | 758.36511 | 354.25293 | 43.53212 |
| 88 | 47.5 | 14.83294 | 766.85029 | 354.25293 | 43.69395 |
| 89 | 32.5 | 13.55441 | 597.42969 | 280.96582 | 37.18903 |
| 90 | 37. | 14.29047 | 609.59668 | 284.89160 | 38.55194 |
| 91 | 120.59999 | 101.81012 | 632.41534 | 374.02499 | 132.07474 |
| 92 | 299. | 306.62988 | 691.65918 | 458.49316 | 293.43774 |
| 93 | 176. | 146.91357 | 644.72803 | 397.89697 | 170.77969 |
| 94 | 39.59999 | 40.90118 | 36.46587 | 22.46028 | 33.77589 |
| 95 | 15.5 | 13.21395 | 22.56546 | 15.26178 | 11.77022 |
| 96 | 53.2 | 18.49570 | 904.65259 | 416.99780 | 53.03323 |
| 97 | 55.39999 | 18.49570 | 904.65259 | 416.99780 | 53.03323 |
| 98 | 58.5 | 18.49570 | 904.65259 | 416.99780 | 53.03323 |

# TABLE 6-V. CONTINUED

| DATA CASE | EXPERIMENTAL | EFFECTIVE THERMAL CONDUCTIVITY (KCAL/M-HR-K) X 100 RUSSELL | BERNSTEIN | WOODSIDE | Equation 5-2 |
|---|---|---|---|---|---|
| 65 | 59.5 | 18.4957 | 974.65259 | 416.99787 | 53.03323 |
| 1 | 61.59999 | 18.49577 | 974.65259 | 416.99780 | 53.03323 |
| 1 1 | 23.39969 | 12.55259 | 22.75112 | 14.89795 | 11.25840 |
| 1 2 | 17.7 | 17.39619 | 17.81456 | 7.20878 | 8.38487 |
| 1 3 | 126. | 97.31678 | 642.80176 | 367.71703 | 127.09695 |
| 1 4 | 43.5 | 15.14726 | 819.88511 | 354.25293 | 44.84630 |
| 1 5 | 51.7 | 15.14726 | 819.88511 | 354.25293 | 44.84630 |
| 1 6 | 327.59985 | 197.41057 | 7209.19938 | 3185.29442 | 478.98633 |
| 1 7 | 41.29999 | 15.28532 | 842.95728 | 354.25293 | 45.35347 |
| 1 8 | 327. | 295.4907 | 732.27954 | 449.02368 | 286.15188 |
| 1 9 | 44.59999 | 15.33187 | 857.64722 | 354.25293 | 45.52478 |
| 11 | 26.29999 | 15.79286 | 45.65143 | 27.51696 | 16.65929 |
| 111 | 43.79999 | 15.36889 | 212.72542 | 174.51558 | 25.72656 |
| 112 | 318. | 193.46812 | 2622.12915 | 1270.93921 | 320.17505 |

# TABLE 6-V. CONTINUED

| DATA CASE | EXPERIMENTAL | EFFECTIVE THERMAL CONDUCTIVITY (KCAL/M-HR-K) X 1^^ | | | |
| | | RUSSELL | BERNSTEIN | WOODSIDE | Equation 5-2 |
|---|---|---|---|---|---|
| 113 | 342.????? | 193.468?2 | 2622.12915 | 127?.93921 | 32?.17505 |
| 114 | 58?.????? | 291.728?3 | 2646.18384 | 135?.791?2 | 419.15674 |
| 115 | 595.????? | 291.728?3 | 2646.18384 | 135?.791?2 | 419.15674 |
| 116 | 55?.?? ??? | 33?.22461 | 2655.72559 | 1376.92456 | 455.653^8 |
| 117 | 615.???? ? | 33?.22461 | 2655.72559 | 1376.92456 | 455.653?8 |
| 118 | 63?.?? ?? | 33?.22461 | 2655.72559 | 1376.92456 | 455.653?8 |
| 119 | 629.8999? | 357.48779 | 7579.?8594 | 3446.13?13 | 7??.1?938 |
| 12? | 557.?9985 | 357.48779 | 7579.?8594 | 3446.13?13 | 7??.1?938 |
| 12? | 323.?9985 | 194.11241 | 76?6.42578 | 3188.54565 | 489.9248? |
| 122 | 6?7.59985 | 3?5.4?4?5 | 7632.61719 | 3374.64258 | 637.7832? |
| 123 | 549.5??? | 3?6.3374? | 7698.75781 | 3374.64258 | 64?.?4639 |
| 124 | 634.3?9?? | 36?.76929 | 7777.414?6 | 3446.13?13 | 7?7.4350?6 |
| 125 | 45.?? ??? | 16.39252 | 73?.88989 | 287.87524 | 43.33?41 |
| 126 | 55.79999 | 2?.22?55 | 796.55566 | 318.1?571 | 5?.62471 |

# TABLE 6-V. CONTINUED

| DATA CASE | EXPERIMENTAL | EFFECTIVE THERMAL CONDUCTIVITY (KCAL/M-HR-K) X 10⁻⁴ | | | |
| | | RUSSELL | BERNSTEIN | WOODSIDE | Equation 5-2 |
|---|---|---|---|---|---|
| 127 | 35.     | 1 .82 55 | 794.43 18 | 295.87476 | 35.92 18 |
| 128 | 32.39599 | 9.13533 | 794. 5 78 | 289.8210 4 | 32.87917 |
| 129 | 1 8.    | 1 7.1  872 | 816.8 444 | 4 1.246 9 | 143.295 3 |
| 13  | 4 .7   | 15.783    | 687.55298 | 271.42334 | 41.29378 |
| 13  | 1 1.    | 99.49986 | 6 1.65919 | 3 4.82275 | 123.51195 |
| 132 | 26.39599 | 17.82768 | 52.94521 | 27.52713 | 17.66586 |
| 13  | 3 .59599 | 15.88542 | 61 .76149 | 219.37628 | 38.53224 |
| 13  | 11 .     | 111.38135 | 631.55811 | 291.23584 | 132.75174 |
| 13  | 31. 4 99 | 43.4 933 | 42.384 8 | 22.13 75 | 35.75244 |
| 136 | 13.8     | 13.27157 | 3 .95219 | 14.79249 | 12.118 6 |
| 137 | 13.9     | 11. 9142 | 2 .65315 | 1 .2289 | 1 .22176 |
| 13  | 34.2 | 16.78769 | 936.32373 | 284.83989 | 47.14157 |
| 13  | 95.29999 | 11 .33 95 | 552.11499 | 2 9.51463 | 122.22845 |
| 14  | 27.29599 | 16.55669 | 535.47754 | 156.78442 | 36.2 37 |

# TABLE 6-V. CONTINUED

| DATA CASE | EXPERIMENTAL | RUSSELL | BERNSTEIN | WOODSIDE | Equation 5-2 |
|---|---|---|---|---|---|
| | | | EFFECTIVE THERMAL CONDUCTIVITY (KCAL/M-HR-K) X 100 | | |
| 141 | 26.2 | 1.15738 | 534.41724 | 147.54761 | 27.48863 |
| 142 | 61.7 | 111.41758 | 561.22998 | 209.51463 | 123.41405 |
| 143 | 27.0 | 16.73 3 | 544.74463 | 156.78442 | 36.64189 |
| 144 | 25.20 | 1.26433 | 543.69434 | 147.54761 | 27.82973 |
| 145 | 49. | 19.97 25 | 363.98169 | 104.51558 | 34.28934 |
| 146 | 11.79999 | 117.936. 8 | 612.88218 | 209.51463 | 130.50111 |
| 147 | 27.5 | 17.77635 | 597.25952 | 156.78442 | 39.28493 |
| 148 | 25.30999 | 1.9.893 | 596.26392 | 147.54761 | 29.88408 |
| 149 | 35.2 | 96.59285 | 609.37085 | 202.07487 | 113.45471 |
| 15 | 58.39999 | 19.2 45 | 1154.18774 | 284.89160 | 54.95262 |
| 151 | 7. | 21.48741 | 425.83789 | 103.21956 | 38.16228 |
| 152 | 76. | 24.38144 | 491.67358 | 103.21956 | 44.83087 |
| 153 | 272.5 | 222.07977 | 105.69698 | 274.77612 | 197.92854 |
| 154 | 248.7 | 193.4 34 | 90.09673 | 261.72681 | 175.95125 |

# TABLE 6-V. CONTINUED

| DATA CASE | EXPERIMENTAL | EFFECTIVE THERMAL CONDUCTIVITY (KCAL/M-HR-K) X 10^? | | | |
|---|---|---|---|---|---|
| | | RUSSELL | BERNSTEIN | WOODSIDE | Equation 5-2 |
| 155 | 172.7 | 127.75555 | 57.37563 | 226.?8?69 | 126.26?59 |
| 156 | 15.5 | 16.7538 | 16.58563 | 8.49812 | 16.65686 |
| 157 | 6.5? | 5.?422? | 3.7?421 | 4.?6507 | 4.99119 |
| 158 | 46.??? | 65.1?677 | 28.89358 | 149.47769 | 72.52258 |
| 159 | ?.1?61? | .?? ??? | ?.??????? | ?.?????? | ?.1?854 |
| 16? | ?.?183 | ?.??? | ?.????? | ?.?????? | ?.?7389 |
| 161 | ?.?558 | .??? ? | ?.?????? | ?.??????? | ?.?5266 |
| 162 | ?.?51? | .?????? | ?.?????? | ?.????? | ?.?4411 |
| 163 | ?.?414? | ?.? ?.??? | ?.??? ? | ?.?????? | ?.?3523 |
| 164 | ?.14?4? | ?.?? ?? | 5.442?? | ?.??906 | ?.17131 |
| 165 | 15.6?? | ?.5?66? | 4.?7?74 | 51.?482? | 19.17526 |
| 166 | 11.?6? | 5.?7?7 | 2.47266 | 35.?6?68 | 14.?3751 |
| 167 | 35.?????? | 9.93?2 | 4.55765 | 34.1132? | 29.69441 |
| 168 | 13?.??? | 61.17?55 | 28.32355 | 2?1.181?? | 175.598?1 |

174

# TABLE 6-V. CONTINUED

| DATA CASE | EXPERIMENTAL | EFFECTIVE THERMAL CONDUCTIVITY (KCAL/M-HR-K) X 100 | | | Equation 5-2 |
|---|---|---|---|---|---|
| | | RUSSELL | BERNSTEIN | WOODSIDE | |
| 169 | 81.5 | 59.92964 | 28.22266 | 14.48741 | 81.95348 |
| 17 | 29.79999 | 28.95757 | 23.13467 | 16.43518 | 25.34375 |
| 171 | 65.4 | 59.32135 | 28.17171 | 124.2811 | 73.52748 |
| 172 | 1.24 | .57686 | .31356 | .95478 | 3.90038 |

# TABLE 6-VI   COMPARISON OF SELECTED WEIGHTED OHM'S LAW MODELS

DATA EFFECTIVE THERMAL CONDUCTIVITY (KCAL/M-HR-K) X 100

| CASE | EXPERIMENTAL | EQUATION 6-16 | EQUATION 6-17 | EQUATION 6-18 | LICHTENKER |
|------|-------------|---------------|---------------|---------------|------------|
| 1  | 21.40000  | 18.26809  | 17.83623  | 20.88347  | 59.00730  |
| 2  | 22.40000  | 23.24886  | 27.50689  | 30.67581  | 206.36506 |
| 3  | 75.50000  | 93.65003  | 91.99059  | 107.58758 | 314.29590 |
| 4  | 246.00000 | 232.27410 | 241.86344 | 252.00923 | 448.36002 |
| 5  | 272.00000 | 252.41523 | 264.36643 | 272.00594 | 464.56322 |
| 6  | 1.01500   | 0.66111   | 0.67820   | 0.77075   | 2.26094   |
| 7  | 63.60000  | 67.37439  | 75.83169  | 72.35299  | 107.45101 |
| 8  | 25.00000  | 20.38193  | 21.50933  | 23.97093  | 69.58905  |
| 9  | 17.50000  | 18.96925  | 20.11296  | 22.43993  | 68.91376  |
| 10 | 63.50000  | 68.78856  | 79.14794  | 74.64435  | 110.90501 |
| 11 | 127.00000 | 132.90186 | 158.07349 | 135.94636 | 155.17180 |
| 12 | 19.00000  | 19.10030  | 20.38149  | 22.64880  | 69.81630  |
| 13 | 17.20000  | 19.16223  | 20.45052  | 22.72027  | 69.89026  |
| 14 | 30.40000  | 39.26373  | 40.27656  | 33.26539  | 408.71057 |

# TABLE 6-VI. CONTINUED

| DATA | | EFFECTIVE THERMAL CONDUCTIVITY (KCAL/M-HR-K) X 100 | | | |
|------|--------------|----------------|----------------|----------------|-----------|
| CASE | EXPERIMENTAL | EQUATION 6-16 | EQUATION 6-17 | EQUATION 6-18 | LICHTENKER |
| 15 | 118.00000 | 133.97484 | 161.11842 | 137.83734 | 157.10994 |
| 16 | 36.50000 | 30.15233 | 32.32900 | 35.23028 | 181.32992 |
| 17 | 23.85000 | 41.26558 | 43.65939 | 35.34461 | 439.41410 |
| 18 | 216.00000 | 235.94091 | 279.92522 | 258.02148 | 372.71004 |
| 19 | 26.80000 | 29.16821 | 31.40180 | 33.97493 | 180.36430 |
| 20 | 11.80000 | 9.33043 | 11.14216 | 10.15881 | 14.24098 |
| 21 | 25.30000 | 25.78623 | 31.08171 | 25.81932 | 26.30080 |
| 22 | 21.89000 | 30.10430 | 32.44405 | 35.05504 | 186.72458 |
| 23 | 34.10000 | 45.50702 | 48.14179 | 31.81032 | 554.84475 |
| 24 | 144.70000 | 165.32420 | 192.19444 | 186.89323 | 326.60048 |
| 25 | 34.40000 | 42.16504 | 45.30069 | 36.36206 | 456.89007 |
| 26 | 244.90000 | 238.63294 | 285.40920 | 261.98245 | 380.91525 |
| 27 | 35.14000 | 36.77445 | 44.65680 | 38.57387 | 45.87782 |
| 28 | 81.50000 | 152.07631 | 166.76405 | 181.94245 | 589.76435 |

# TABLE 6-VI. CONTINUED

| DATA CASE | EXPERIMENTAL | EFFECTIVE THERMAL CONDUCTIVITY (KCAL/M-HR-K) X 100 | | | |
|---|---|---|---|---|---|
| | | EQUATION 6-16 | EQUATION 6-17 | EQUATION 6-18 | LICHTENKER |
| 29 | 224.90000 | 242.84768 | 281.59641 | 262.72258 | 381.94926 |
| 30 | 217.40000 | 243.84827 | 280.68852 | 262.89725 | 381.94926 |
| 31 | 218.90000 | 246.64020 | 277.63526 | 263.15639 | 381.94926 |
| 32 | 218.90000 | 242.37366 | 282.55591 | 262.87220 | 381.94926 |
| 33 | 91.00000 | 129.46813 | 141.89911 | 152.53862 | 414.18049 |
| 34 | 20.00000 | 32.98888 | 35.18421 | 34.81148 | 275.61703 |
| 35 | 15.60000 | 23.07759 | 24.45273 | 20.01663 | 247.63950 |
| 36 | 94.40000 | 97.42206 | 107.97547 | 113.73614 | 276.64474 |
| 37 | 94.40000 | 97.42206 | 107.97547 | 113.73614 | 276.64474 |
| 38 | 73.30000 | 69.88891 | 82.74999 | 69.85542 | 70.84719 |
| 39 | 207.00000 | 257.25429 | 267.99600 | 265.11636 | 386.10388 |
| 40 | 212.90000 | 257.25429 | 267.99600 | 265.11636 | 386.10388 |
| 41 | 22.30000 | 33.17131 | 31.66056 | 36.50809 | 198.39167 |
| 42 | 70.90000 | 103.75744 | 102.17270 | 114.86331 | 278.87070 |

# TABLE 6-VI. CONTINUED

| DATA CASE | EXPERIMENTAL | EFFECTIVE THERMAL CONDUCTIVITY (KCAL/M-HR-K) X 100 | | | |
|---|---|---|---|---|---|
| | | EQUATION 6-16 | EQUATION 6-17 | EQUATION 6-18 | LICHTENKER |
| 43 | 18.50000 | 15.25530 | 15.40108 | 16.37681 | 30.95555 |
| 44 | 61.50000 | 114.81826 | 120.61396 | 133.78939 | 403.13726 |
| 45 | 85.00000 | 135.23735 | 137.66891 | 154.02988 | 421.27522 |
| 46 | 22.60000 | 35.39034 | 33.52736 | 35.34213 | 282.25755 |
| 47 | 15.70000 | 24.76877 | 23.33712 | 20.18501 | 254.04953 |
| 48 | 22.60000 | 33.36160 | 31.75435 | 36.66610 | 200.56221 |
| 49 | 16.30000 | 19.03756 | 18.10594 | 20.06048 | 134.88290 |
| 50 | 23.60000 | 31.17224 | 29.72937 | 35.05696 | 155.47729 |
| 51 | 23.40000 | 31.17224 | 29.72937 | 35.05696 | 155.47729 |
| 52 | 25.20000 | 31.17224 | 29.72937 | 35.05696 | 155.47729 |
| 53 | 205.50000 | 235.25228 | 242.43308 | 243.88625 | 373.68603 |
| 54 | 44.60000 | 50.14001 | 47.26900 | 32.66897 | 601.03429 |
| 55 | 163.80000 | 179.51593 | 182.11988 | 190.52539 | 338.40064 |
| 56 | 55.40000 | 60.50910 | 64.11924 | 58.35769 | 60.60930 |

# TABLE 6-VI. CONTINUED

| DATA CASE | EXPERIMENTAL | EFFECTIVE THERMAL CONDUCTIVITY (KCAL/M-HR-K) X 100 | | | |
|---|---|---|---|---|---|
| | | EQUATION 6-16 | EQUATION 6-17 | EQUATION 6-18 | LICHTENKER |
| 57 | 36.00000 | 46.42386 | 44.45473 | 37.65998 | 496.56298 |
| 58 | 17.10000 | 15.68087 | 15.89289 | 16.80524 | 31.74458 |
| 59 | 34.20000 | 38.77132 | 41.26020 | 38.53062 | 46.34372 |
| 60 | 35.60000 | 38.77132 | 41.26020 | 38.53062 | 46.34372 |
| 61 | 53.30000 | 60.48748 | 64.27804 | 58.47467 | 60.80183 |
| 62 | 55.00000 | 60.48748 | 64.27804 | 58.47467 | 60.80183 |
| 63 | 71.40000 | 73.26926 | 76.86735 | 70.64043 | 70.49702 |
| 64 | 71.60000 | 77.41596 | 80.76813 | 74.73293 | 73.88966 |
| 65 | 71.40000 | 77.41596 | 80.76813 | 74.73293 | 73.88966 |
| 66 | 358.00000 | 388.95095 | 388.27393 | 425.23792 | 934.81427 |
| 67 | 70.70000 | 104.28636 | 103.06313 | 115.53438 | 285.66888 |
| 68 | 71.30000 | 104.28372 | 103.25560 | 115.60843 | 286.80489 |
| 69 | 144.40000 | 179.31822 | 183.37059 | 190.95476 | 343.90477 |
| 70 | 37.80000 | 50.29769 | 48.41836 | 33.46267 | 625.19866 |

# TABLE I-VI. CONTINUED

| DATA CASE | EXPERIMENTAL | EFFECTIVE THERMAL CONDUCTIVITY (KCAL/M-HR-K) X 100 | | | |
|---|---|---|---|---|---|
| | | EQUATION 6-16 | EQUATION 6-17 | EQUATION 6-18 | LICHTENKER |
| 71 | 42.50000 | 48.44803 | 46.88942 | 40.97817 | 512.13830 |
| 72 | 29.70000 | 32.53211 | 31.63679 | 36.06000 | 203.35508 |
| 73 | 36.40000 | 46.52268 | 45.14170 | 38.15535 | 509.27668 |
| 74 | 17.10000 | 15.29368 | 15.61938 | 16.48975 | 32.23886 |
| 75 | 230.80000 | 257.46974 | 270.49073 | 266.56968 | 398.74598 |
| 76 | 35.10000 | 50.43168 | 49.22279 | 34.06481 | 641.71144 |
| 77 | 100.70000 | 138.76442 | 138.65102 | 156.33456 | 448.62784 |
| 78 | 22.40000 | 35.63231 | 35.29717 | 36.38001 | 308.21786 |
| 79 | 17.80000 | 24.97200 | 24.71508 | 21.10048 | 279.20431 |
| 80 | 20.70000 | 22.67456 | 22.93893 | 25.06121 | 59.33500 |
| 81 | 154.90000 | 179.21011 | 185.36218 | 191.69065 | 352.83431 |
| 82 | 73.10000 | 78.77325 | 82.64781 | 76.88286 | 76.15786 |
| 83 | 24.60000 | 33.57004 | 33.32753 | 37.49713 | 218.55021 |
| 84 | 51.70000 | 50.72692 | 50.70768 | 35.26633 | 671.39497 |

# TABLE 5-VI. CONTINUED

| DATA CASE | EFFECTIVE THERMAL CONDUCTIVITY (KCAL/M-HR-K) X 100 | | | | |
|---|---|---|---|---|---|
| | EXPERIMENTAL | EQUATION 6-16 | EQUATION 6-17 | EQUATION 6-18 | LICHTENKER |
| 85 | 32.30000 | 44.22812 | 44.29449 | 34.89893 | 539.94730 |
| 86 | 78.60000 | 101.09844 | 107.61176 | 25.89379 | 3839.37706 |
| 87 | 36.80000 | 49.60256 | 53.10404 | 36.21983 | 688.81107 |
| 88 | 47.50000 | 51.67617 | 51.35218 | 36.27270 | 693.21712 |
| 89 | 32.50000 | 47.99164 | 42.17589 | 35.85984 | 557.12542 |
| 90 | 37.00000 | 56.05673 | 39.32221 | 39.14365 | 570.58757 |
| 91 | 120.60000 | 227.28975 | 157.62872 | 228.19567 | 825.91706 |
| 92 | 298.00000 | 493.66227 | 349.73652 | 471.72746 | 1026.50052 |
| 93 | 176.00000 | 294.26019 | 204.87509 | 292.15431 | 885.54253 |
| 94 | 39.60000 | 47.86938 | 35.61040 | 41.92740 | 48.82971 |
| 95 | 15.50000 | 19.33748 | 13.85331 | 18.10140 | 34.11394 |
| 96 | 53.20000 | 75.55705 | 52.95738 | 47.29458 | 825.22139 |
| 97 | 55.40000 | 75.55705 | 52.95738 | 47.29458 | 825.22139 |
| 98 | 58.50000 | 75.55705 | 52.95738 | 47.29458 | 825.22139 |

182

# TABLE 6-VI. CONTINUED

| DATA CASE | EXPERIMENTAL | EFFECTIVE THERMAL CONDUCTIVITY (KCAL/M-HR-K) X 100 | | | |
|---|---|---|---|---|---|
| | | EQUATION 6-16 | EQUATION 6-17 | EQUATION 6-18 | LICHTENKER |
| 99 | 59.50000 | 75.55705 | 52.95738 | 47.29458 | 825.22139 |
| 100 | 61.10000 | 75.55705 | 52.95738 | 47.29458 | 825.22139 |
| 101 | 23.40000 | 18.55058 | 13.27307 | 17.40321 | 33.29460 |
| 102 | 10.20000 | 12.71516 | 9.34998 | 11.38894 | 15.90991 |
| 103 | 126.00000 | 194.07769 | 172.08793 | 212.10419 | 822.21901 |
| 104 | 43.50000 | 55.37533 | 50.30533 | 37.92990 | 724.64669 |
| 105 | 51.70000 | 55.37533 | 50.30533 | 37.92990 | 724.64669 |
| 106 | 327.60000 | 621.64499 | 568.03096 | 542.55222 | 6773.54644 |
| 107 | 40.30000 | 55.61382 | 51.00951 | 38.71766 | 738.43325 |
| 108 | 327.00000 | 420.38800 | 382.06988 | 440.48026 | 1038.46366 |
| 109 | 44.60000 | 55.69790 | 51.24874 | 38.99000 | 743.07128 |
| 110 | 26.30000 | 24.54554 | 22.27846 | 25.86402 | 63.90143 |
| 111 | 41.80000 | 37.21594 | 33.64014 | 40.32416 | 236.51583 |
| 112 | 318.00000 | 462.40538 | 419.48245 | 502.89521 | 2909.23004 |

# TABLE 6-VI. CONTINUED

| DATA | | EFFECTIVE THERMAL CONDUCTIVITY (KCAL/M-HR-K) X 100 | | | |
|------|--------------|---------------|---------------|---------------|-------------|
| CASE | EXPERIMENTAL | EQUATION 6-16 | EQUATION 6-17 | EQUATION 6-18 | LICHTENKER |
| 113 | 342.00000 | 462.40538 | 419.48245 | 502.89521 | 2909.23004 |
| 114 | 580.00000 | 619.09245 | 558.39753 | 680.84295 | 3128.44173 |
| 115 | 595.00000 | 619.09245 | 558.39753 | 680.84295 | 3128.44173 |
| 116 | 550.00000 | 675.81458 | 608.94645 | 743.07338 | 3197.92937 |
| 117 | 615.00000 | 675.81458 | 608.94645 | 743.07338 | 3197.92937 |
| 118 | 630.00000 | 675.81458 | 608.94645 | 743.07338 | 3197.92937 |
| 119 | 629.90000 | 969.77173 | 889.60602 | 1011.09310 | 7789.99876 |
| 120 | 597.10000 | 969.77173 | 889.60602 | 1011.09310 | 7789.99876 |
| 121 | 323.10000 | 627.66939 | 583.42334 | 558.45987 | 7020.76531 |
| 122 | 607.60000 | 866.10024 | 799.05327 | 880.03270 | 7612.86973 |
| 123 | 549.50000 | 867.41892 | 802.21736 | 882.93277 | 7655.19008 |
| 124 | 634.40000 | 974.09676 | 892.78815 | 1020.03510 | 7917.56551 |
| 125 | 45.00000 | 54.11049 | 51.20005 | 47.10982 | 653.27948 |
| 126 | 55.80000 | 64.34005 | 60.76265 | 58.97540 | 727.19873 |

# TABLE 6-VI. CONTINUED

| DATA CASE | EXPERIMENTAL | EFFECTIVE THERMAL CONDUCTIVITY (KCAL/M-HR-K) X 100 | | | |
|---|---|---|---|---|---|
| | | EQUATION 6-16 | EQUATION 6-17 | EQUATION 6-18 | LICHTENKER |
| 127 | 35.00000 | 41.54685 | 39.44183 | 24.98846 | 651.05339 |
| 128 | 32.40000 | 36.98011 | 35.08021 | 17.48121 | 631.57698 |
| 129 | 188.00000 | 210.03414 | 191.43568 | 231.29989 | 968.31840 |
| 130 | 45.70000 | 51.73979 | 48.94081 | 45.52054 | 616.99663 |
| 131 | 101.00000 | 181.62449 | 165.29476 | 198.75663 | 737.09537 |
| 132 | 26.40000 | 25.17274 | 23.15149 | 26.44550 | 68.74687 |
| 133 | 35.60000 | 48.45411 | 47.33002 | 47.83672 | 548.95760 |
| 134 | 110.00000 | 191.22090 | 176.21498 | 207.79861 | 749.89525 |
| 135 | 31.05000 | 43.00424 | 39.24361 | 40.23275 | 52.95140 |
| 136 | 13.80000 | 16.63020 | 15.22358 | 16.81157 | 39.01617 |
| 137 | 13.80000 | 13.63439 | 12.47190 | 13.43961 | 26.49543 |
| 138 | 34.20000 | 55.90693 | 57.34914 | 54.08713 | 784.56546 |
| 139 | 95.40000 | 173.82155 | 156.94868 | 178.85411 | 618.86684 |
| 140 | 27.30000 | 46.56551 | 47.08640 | 51.44201 | 480.59426 |

# TABLE 6VI.   CONTINUED

| DATA CASE | EXPERIMENTAL | EFFECTIVE THERMAL CONDUCTIVITY (KCAL/M-HR-K) X 100 | | | |
|---|---|---|---|---|---|
| | | EQUATION 6-16 | EQUATION 6-17 | EQUATION 6-18 | LICHTENKER |
| 141 | 26.20000 | 33.16844 | 34.68392 | 35.04215 | 449.82873 |
| 142 | 61.70000 | 175.90408 | 158.08702 | 179.92768 | 625.75569 |
| 143 | 27.00000 | 47.21751 | 47.79587 | 52.29997 | 487.91652 |
| 144 | 25.20000 | 33.64918 | 35.27914 | 35.85971 | 457.15207 |
| 145 | 49.00000 | 47.89173 | 45.75384 | 52.19388 | 347.16633 |
| 146 | 110.80000 | 190.25043 | 164.78573 | 186.60326 | 665.64385 |
| 147 | 27.50000 | 51.67708 | 52.16730 | 57.69110 | 530.74884 |
| 148 | 26.40000 | 36.93366 | 38.97973 | 41.00819 | 500.11590 |
| 149 | 85.20000 | 165.94268 | 145.43751 | 165.60189 | 649.41849 |
| 150 | 58.40000 | 66.74942 | 71.02539 | 73.34132 | 956.51049 |
| 151 | 70.00000 | 58.07241 | 51.68107 | 59.01005 | 398.32499 |
| 152 | 76.00000 | 81.74598 | 61.62668 | 70.87885 | 459.77048 |
| 153 | 272.50000 | 262.01689 | 267.10996 | 280.01328 | 480.93223 |
| 154 | 248.70000 | 234.70536 | 237.01759 | 252.82006 | 457.18135 |

# TABLE 6-VI. CONTINUED

| DATA | EFFECTIVE THERMAL CONDUCTIVITY (KCAL/M-HR-K) X 100 | | | |
| CASE | EXPERIMENTAL | EQUATION 6-16 | EQUATION 6-17 | EQUATION 6-18 | LICHTENKER |
|---|---|---|---|---|---|
| 155 | 172.70000 | 171.02733 | 168.08607 | 188.14054 | 396.68016 |
| 156 | 16.50000 | 18.09448 | 17.80534 | 16.71334 | 16.74108 |
| 157 | 6.90000 | 6.07512 | 6.30359 | 6.00097 | 7.36559 |
| 158 | 46.00000 | 97.87946 | 91.63376 | 109.30790 | 277.44236 |
| 159 | 0.10610 | 0.08101 | 0.08228 | 0.03170 | 0.03203 |
| 160 | 0.08183 | 0.06274 | 0.04555 | 0.04203 | 0.00773 |
| 161 | 0.05598 | 0.06051 | 0.03174 | 0.08234 | 0.00207 |
| 162 | 0.05110 | 0.02694 | 0.05470 | 0.04489 | 0.00105 |
| 163 | 0.04140 | 0.03160 | 0.02755 | 0.02220 | 0.00046 |
| 164 | 0.14040 | 0.10830 | 0.13498 | 0.17819 | 0.15300 |
| 165 | 15.60000 | 23.09515 | 20.32662 | 23.63961 | 156.30005 |
| 166 | 11.95000 | 15.94027 | 13.75262 | 13.68524 | 134.58651 |
| 167 | 39.90000 | 29.98027 | 22.82285 | 16.35257 | 253.52111 |
| 168 | 130.00000 | 181.94301 | 137.55627 | 110.98691 | 1428.90519 |

# TABLE 6-VI. CONTINUED

| DATA | EFFECTIVE THERMAL CONDUCTIVITY (KCAL/M-HR-K) X 100 | | | | |
|------|-------------|---------------|---------------|---------------|-------------|
| CASE | EXPERIMENTAL | EQUATION 6-16 | EQUATION 6-17 | EQUATION 6-18 | LICHTENKER |
| 169 | 81.50000 | 103.96177 | 85.07619 | 116.02943 | 349.59322 |
| 170 | 29.80000 | 29.54646 | 25.51770 | 28.03818 | 29.64116 |
| 171 | 60.00000 | 94.51779 | 78.11311 | 104.96805 | 275.08724 |
| 172 | 1.02400 | 1.08128 | 0.97622 | 0.97847 | 2.61458 |

## TABLE 6-VII. DIMENSIONLESS VARIANCE OF CALCULATED THERMAL CONDUCTIVITY BASED ON SELECTED MODELS

A. Flux Law Models
   1. Maxwell                           42.9
   2. Lord Rayleigh                     32.1
   3. Meredith and Tobias               29.8
   4. Bruggemen                         17.8

B. Uniform Heat Flux Models
   1. son Frey                          50.2
   2. Woodside and Messmer              19.2
   3. Kanager                           13.1
   4. Gorring and Churchill             14.8
   5. Willhite, Kunii and Smith         13.3
   6. Schumann and Voss                 20.1
   7. Preston                           16.4
   8. Wilhelm et al                     13.8
   9. Krupiczka                         13.1

C. Parallel Isotherm Models
   1. Russell                           35.2
   2. Bernstein                         87.4
   3. Woodside                          70.7
   4. Equation 5-2                       7.0

D. Weighted Ohm's Law Models
   1. Equation 6-16                     10.6
   2. Equation 6-17                      9.7
   3. Equation 6-18                     13.0
   4. Lichtenecker 3-D                  98.4
   5. Lichtenecker 2-D                  56.8
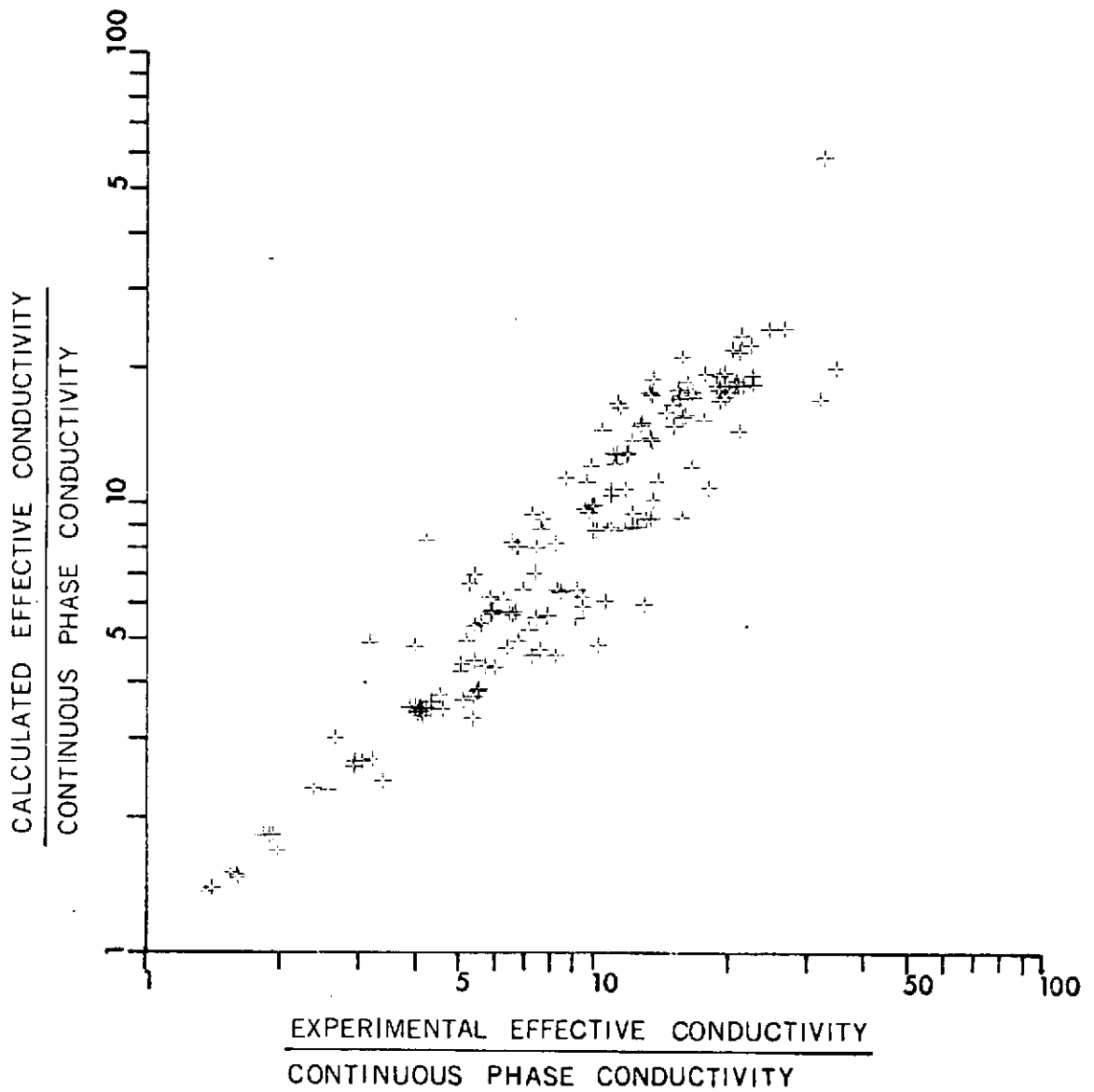
FIGURE 6-7. COMPARISON OF EXPERIMENTAL RESULTS WITH CALCULATED CONDUCTIVITY FOR EQUATION 5-2.
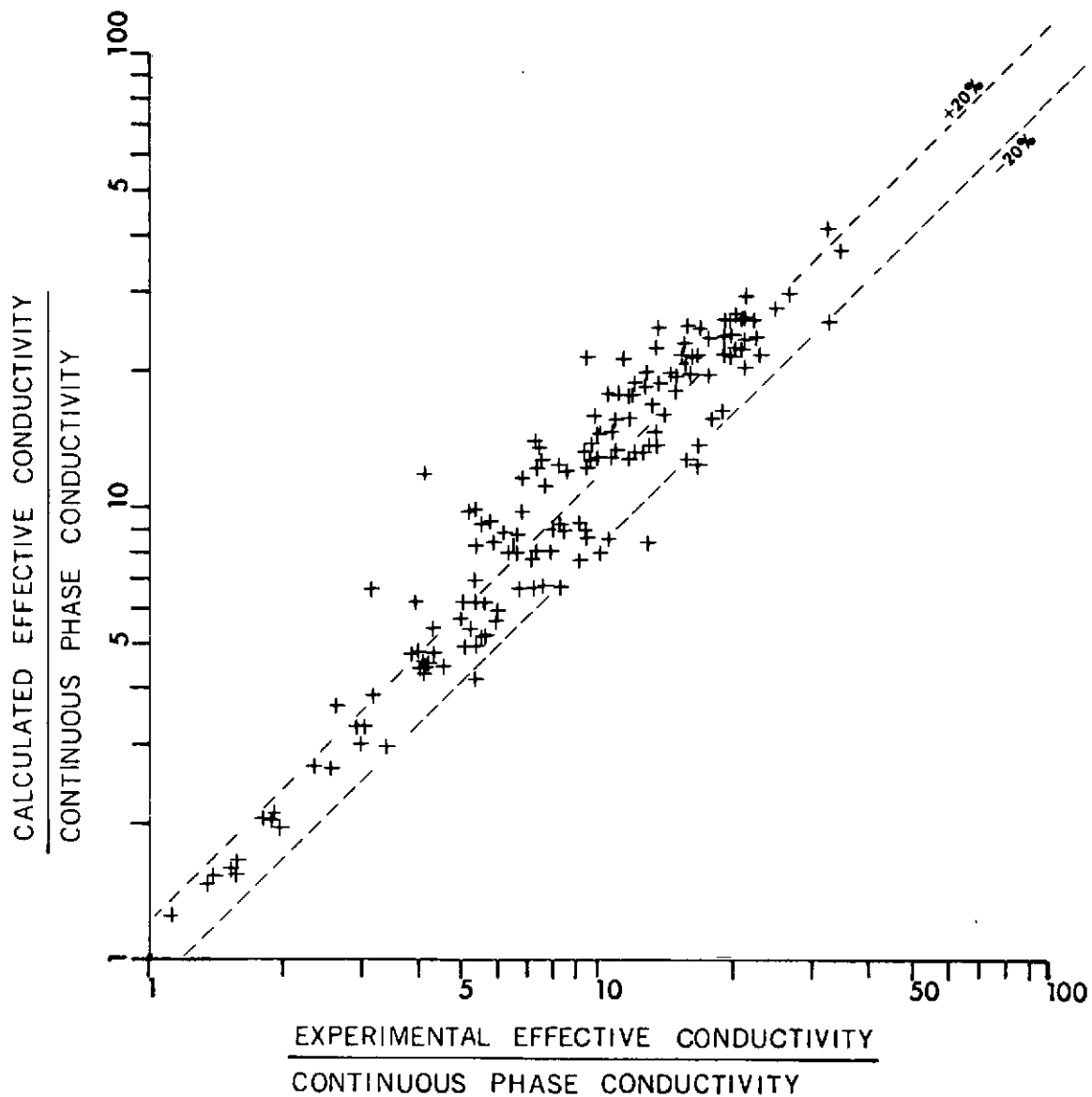
FIGURE 6-8. COMPARISON OF EXPERIMENTAL RESULTS WITH CALCULATED CONDUCTIVITY FOR EQUATION 6-16.
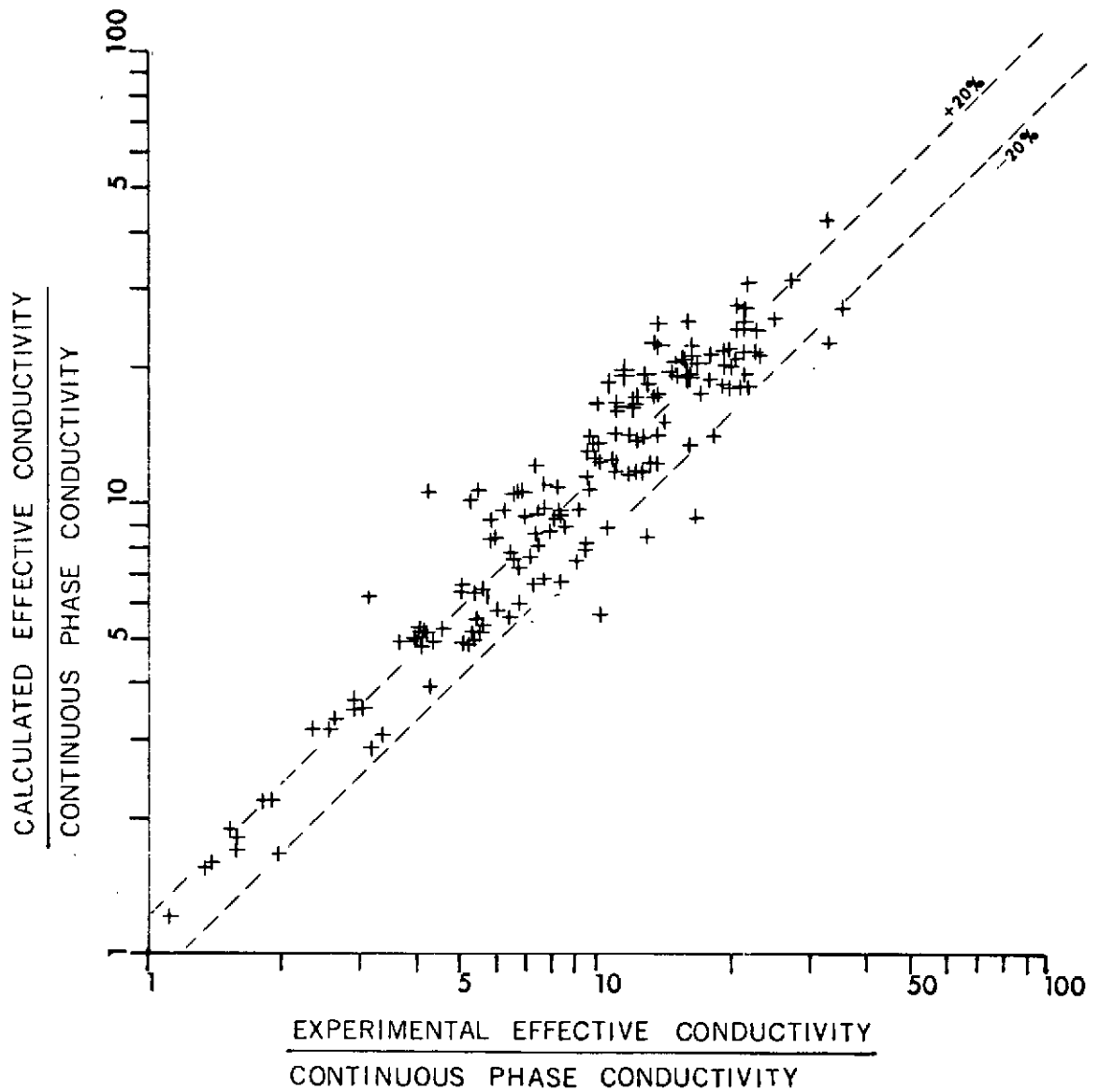
FIGURE 6-9. COMPARISON OF EXPERIMENTAL RESULTS WITH
CALCULATED CONDUCTIVITY FOR EQUATION 6-17.
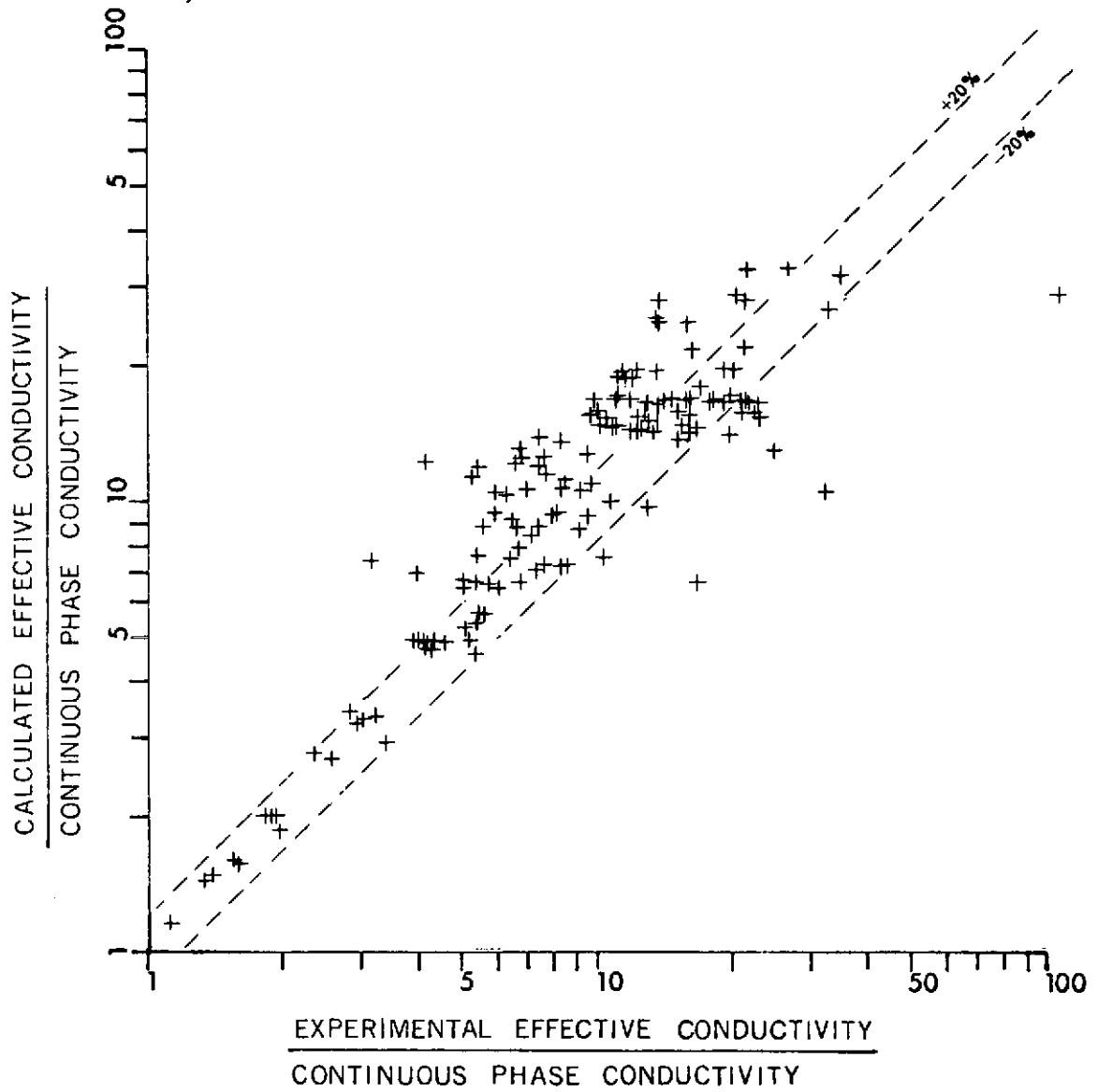
FIGURE 6-10. COMPARISON OF EXPERIMENTAL RESULTS WITH
CALCULATED CONDUCTIVITY FOR EQUATION 6-18.

# VII. MODEL BASED ON NON-LINEAR HEAT FLOW

Consider a representative unit cube of the granular material, subdivided by a three-dimensional grid into $N^3$ cubicles, as indicated in Figure (7-1a). Assume that the two faces normal to the z-direction are isothermal, and the other four faces are insulated, so that application of a constant temperature potential gives rise to a net conduction heat transfer in the z-direction. In order to determine the effective thermal conductivity of such a system, without any additional simplifying assumptions regarding the flow of heat, it is first necessary to find the temperature distribution in the unit cube. Once this has been accomplished, the heat flow rate in the z-direction can be determined, and an effective thermal conductivity can be assigned to the material by the Fourier-Biot law.

The solution proposed in this study consists of the following steps:

1. System synthesis;

2. Determination of the average working thermal conductivities;

3. Computation of the actual temperature distribution;

4. Determination of the heat flows and the effective thermal conductivity.

The above four steps will now be discussed in detail.

## System Synthesis

A representative unit cube of a granular material is shown in Figure (7-1a) and in Figure (7-1b). The distribution of the continuous and discontinuous phases is modified is such a manner that each cubicle is occupied either by the continuous or the discontinuous phase. Effectively, any irregular shaped particle can be built to any degree of approximation by arranging a number of cubicles according to a predetermined format, as indicated in [20]. These particles can then be placed in the unit cube according to a specified statistical distribution. This way, the basic assumption of a regularly repeated elementary cell of spatial configuration, common to most previous models, is avoided.

The method of placing continuous phase cubicles in the unit cube, is based on the assumption that the granular material can be considered as a random mixture of the two phases. Then, in order to place a continuous phase cubicle in the system, three random numbers are generated by the 0-1.0 constant density function random number generator, and these random numbers are associated with three coordinates, defining the position of a cubicle in the system. If the cubicle thus defined, is already occupied by the continuous phase, another triplet of random numbers is generated. This process continues until the total number of continuous phase cubicles is equal to the continuous phase solid fraction of the granular system times the total number of cubicles in the unit cube. The geometry
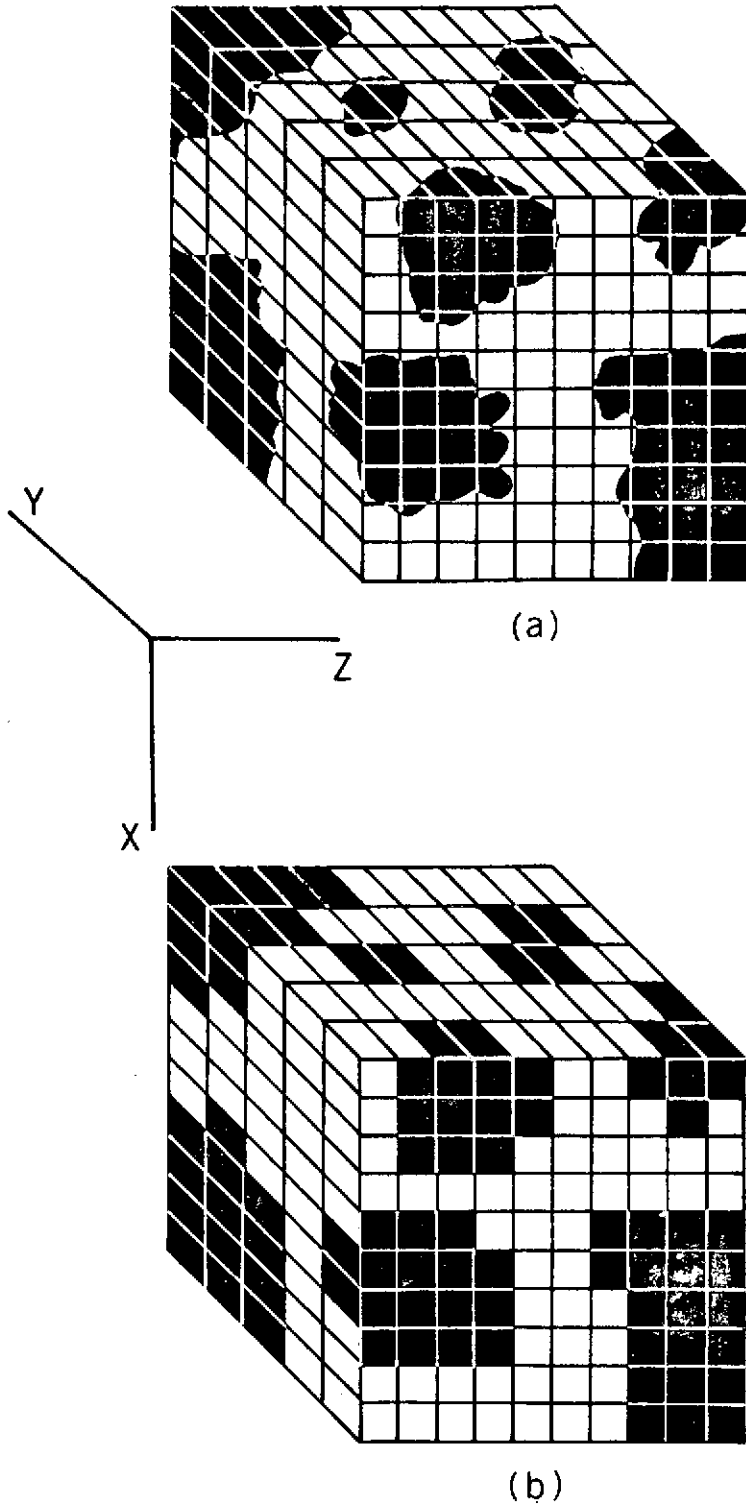
FIGURE 7-1. EQUVALENT GEOMETRIES FOR UNIT CUBE.

of the system thus defined, represents a random mixture of two phases, and, effectively, in this system the probability that a particular cubicle is occupied by the continuous phase is equal to the volume fraction of the continuous phase.

## Determination of the Average Working Thermal Conductivities

As illustrated by Trezek and Witwer [72], there are a number of choices in selecting the average working conductivities between adjacent cubicles, but the series model yields the most accurate results on each side of the interface. According to [72] then,

$$k_{ij} = k_i k_j / (0.5 \ k_i + 0.5 \ k_j) \qquad (7\text{-}1)$$

where $k_{ij}$ is the average working thermal conductivity between the adjacent cubicles i and j. $k_i$ and $k_j$ are the conductivities of the cubicles. A scanning process can now be defined such that looking at a particular cubicle the composition of its neighbors can be determined, and consequently it is possible to assign an average working thermal conductivity between any two adjacent cubicles.

At this point, it should be noted that the working thermal conductivities thus defined, require that the adjacent cubicles are in perfect contact with each other. However, physical granular systems contain randomly distributed and oriented contact areas between neighboring particles that provide additional resistance to the heat flow from one particle to the other. Further, when the voids between particles are evacuated, these contact areas provide the only path

of heat transfer, other than radiation heat transfer, from one particle to the other. Consequently, as indicated in [34], failure to account for these contact areas induces large errors in the calculation of the effective thermal conductivity of granular materials, especially when the ratio of the constituent conductivities is high.

In order to incorporate the effect that these contact areas have on the flow of heat in the physical model presented, it is necessary to associate a contact conductivity with each contact area, and to know the number of contact points in the unit cube. As indicated in the Literature Review, a number of expressions have been developed relating the contact resistance to the contact area between two particles. In the calculations, the expressions given in reference [34] have been used because they are in good agreement with Kanager's [73] analytical development. The number of contact points in the cube, $N_c$, can be determined, as indicated in the Ohm's Law Models section, as a function of the unit cube size, a characteristic particle size obtained from sieve analysis of the granular material, and the coordination number.

To complete the determination of the working thermal conductivities, it is necessary to randomly distribute $N_c$ contact conductivities between adjacent cubicles occupied by the discontinuous phase. Again a triplet of random numbers is generated, and is associated with three coordinates, defining the position of a cubicle in the system. If the cubicle is occupied by the discontinuous phase, the

composition of its neighbors is determined, and the working conductivity between the first pair of solid cubicles is replaced by $k_{cr}$. The process is repeated until $N_c$ such replacements have been executed. A point of importance is that since contact points at the boundaries of the unit cube should also be included, it is necessary to determine the composition of the cubicles surrounding the six faces of the unit cube.

## Determination of the Actual Temperature Distribution

When a steady-state temperature field is desired for a region in which the thermal conductivity is dependent upon the spatial location, a solution must be obtained for the following equation

$$\nabla(k\nabla T) = 0 \tag{7-2}$$

When each cubicle is considered separately, the condition which must be met is the Laplace equation

$$\frac{\partial^2 T}{\partial x^2} + \frac{\partial^2 T}{\partial y^2} + \frac{\partial^2 T}{\partial z^2} = 0 \tag{7-3}$$

Also, each temperature in the unit cube must be bounded by the temperatures applied at the two opposite faces of the unit cube. Laplace's equation requires that the temperature at every cubicle remain constant. That is the net heat accumulation in each cubicle should be equal to zero. In order to write a conduction heat balance for each cubicle, it is first assumed that the cubicle is

isothermal and is lumped into a single node, and all the nodes are connected by the average working thermal conductivities described in the previous paragraph. The basic system unit around which each heat balance is written is shown in Figure (7-2). Under the assumption that heat flow to the center cube is positive, the resulting heat balance is

$$\sum_{i=1}^{6} k_{i7} (T_i - T_7) A/L = R_7 \tag{7-4}$$

Application of Equation (7-4) to all cubicles results in $N^3 = m$ simultaneous, linear equations. The coefficients of this system of linear equations are functions of the average working conductivities, and the unknowns are the node temperatures. As indicated in [74] one of the most efficient methods of solving such a system of equations is a successive overrelaxation technique in conjunction with an iterative scheme. The steps involved in this method are the following.

Consider the system of linear equations

$$b_{11} x_1 + b_{12} x_2 + \cdots \cdots \cdots + b_{1m} x_m = u_1$$
$$b_{21} x_1 + b_{22} x_2 + \cdots \cdots \cdots + b_{2m} x_m = u_2$$
$$\vdots \qquad\qquad\qquad\qquad \vdots \tag{7-5}$$
$$b_{m1} x_1 + b_{m2} x_2 + \cdots \cdots \cdots + b_{mm} x_m = u_m$$
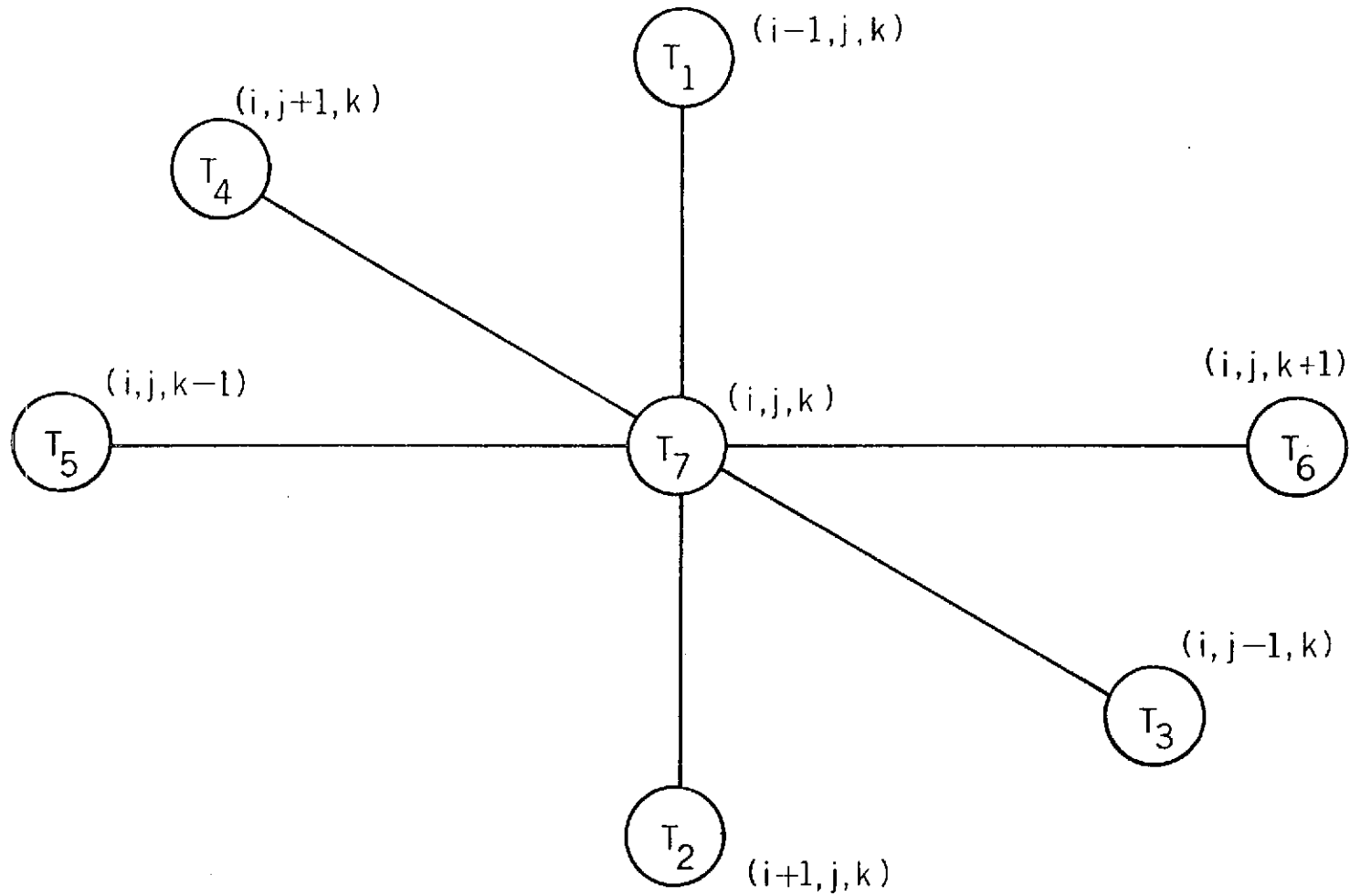
FIGURE 7-2. HEAT BALANCE BASIC NODAL ORIENTATION

or

$$[B] \ \bar{x} = \bar{u} \tag{7-6}$$

First define the ith component of an auxilliary vector iterate $\bar{x}'^n$ by

$$b_{ii} \ x'_i^{n+1} = - \sum_{j=1}^{i-1} b_{ij} \ x_j^{n+1} - \sum_{j=i+1}^{m} b_{ij} \ x_j^n + u_i \tag{7-7}$$

Then, the (n+1) approximation of the ith component of the solution vector for the successive overrelaxation method is defined from

$$x_i^{n+1} = x_i^n + w \ [x'_i^{n+1} - x_i^n] = (1-w) \ x_i^n + wx'_i^{n+1} \tag{7-8}$$

The quantity w is called the overrelaxation factor, and $1 < w < 2$. It is seen from Equation (7-8) that $x_i^{n+1}$ is a weighted mean of $x_i^n$ and $x'_i^{n+1}$, the weights depending only on w. Combination of Equations (7-7) and (7-8) into a single equation yields

$$b_{ii} \ x_i^{n+1} = b_{ii} \ x_i^n + w \left[ - \sum_{j=1}^{i-1} b_{ij} \ x_j^{n+1} - \sum_{j+1}^{m} b_{ij} \ x_j^n \right.$$

$$\left. + u_i - b_{ii} \ x_i^n \right] \tag{7-9}$$

Then, from Equation (7-9) the (n+1) approximation of the ith component of the solution vector is

$$x_i^{n+1} = x_i^n + \frac{w}{b_{ii}} \left[ - \sum_{j=1}^{i-1} b_{ij} \ x_j^{n+1} - \sum_{j+1}^{m} b_{ij} \ x_j^n \right.$$

$$\left. + u_i - b_{ii} \ x_i^n \right] \tag{7-10}$$

It is seen that in the iterations, the newly-computed components of the $\bar{x}$ vector are always used in the righthand sides as soon as they are obtained.

Comparison of Equation (7-10) with the heat balance equation for each cubicle indicates that the term in brackets is equal to the negative of the thermal residue. Also, $b_{ii}$ is the negative of the sum of the average working conductivities between the node at which heat balance is executed and the surrounding nodes. As a result, for the particular problem in question, Equation (7-10) takes the form

$$T^{n+1} = T^n + \frac{w}{\sum\limits_{i=1}^{i=6} k_{i7}} \left[ \sum\limits_{i=1}^{i=6} k_{i7} (T_i - T_7) \right] \tag{7-11}$$

Equation (7-11) gives a better estimate of the temperature at each node in terms of previous estimates. It can be seen that a positive thermal residue, resulting from $T_7$ being too low, will increase the new value of $T_7$.

Exactly the same iterative scheme can be obtained by writing the finite-difference representation of Equation (7-2), and treating the conductivity variation according to Equation (7-1).

The steady-state temperature field in the unit cube can now be obtained, provided that an initial temperature field is defined. A reasonable selection for the initial temperature field is to assume

that planes of nodes normal to the direction of the heat flow are isothermal, and the temperature of each plane is proportional to its distance from the surface of the cube. Also, the imposed boundary conditions dictate that the temperatures of the nodes on the front and back faces, which are normal to the direction of the heat flow, remain constant, and the heat flow away from nodes associated with the other four faces is zero. Application of Equation (7-11) coupled with the assumed initial temperature distribution and the boundary conditions, gives the actual temperature distribution in the unit cube. In the calculations, the iteration process cut-off point is when the sum of the absolute values of the thermal residues becomes less than or equal to 1.0.

### Determination of the Heat Flows and the Effective Thermal Conductivity

After the steady-state temperature field has been determined, three orthogonal heat flux vectors can be defined at each node. However, since the net heat flow is in the z-direction only, this is the rate of heat flow on which the effective thermal conductivity should be based. To find the rate of heat flow Q in the z-direction, the heat flows in the z-direction between all nodes in any two successive planes are summed. This process is repeated for all successive planes, and Q is the average value of these sums. The effective thermal conductivity of the granular material,

as defined by the Fourier-Biot law, is given by:

$$k_e = \frac{Q}{N\Delta T} \qquad (7\text{-}12)$$

where $\Delta T$ is the difference between the temperatures of the back and front faces of the unit cube that are normal to the net heat flow direction.

The method of solution described in the preceding paragraphs can be applied to any granular system for which the fluid in the voids is at atmospheric pressure. In this case, the solid particles and the voids are approximated by the arrangement of a number of cubicles according to the statistical distribution chosen; heat balances at each node should give the temperature distribution since both phases are in the domain of a continuum. However, when the medium in the voids is a rarefied gas, which is the case for both lunar and martian environments, a dominant mode of heat transfer in the voids may be radiation between particle surfaces [1], as shown in Fig. (7-3). Also, when the molecular mean free path is greater than the void diameter, conduction in the voids takes place by direct exchange of energy between particle surfaces. Consequently, for extremely rarefied gases it is not possible to determine a working effective conductivity between nodes that belong to gaseous cubicles located in the same void. However, if the chosen grid size is coarse enough so that the volume of each cubicle is equal to the mean void equivalent hole volume, then each void is approximated by a cubicle and the working effective con-
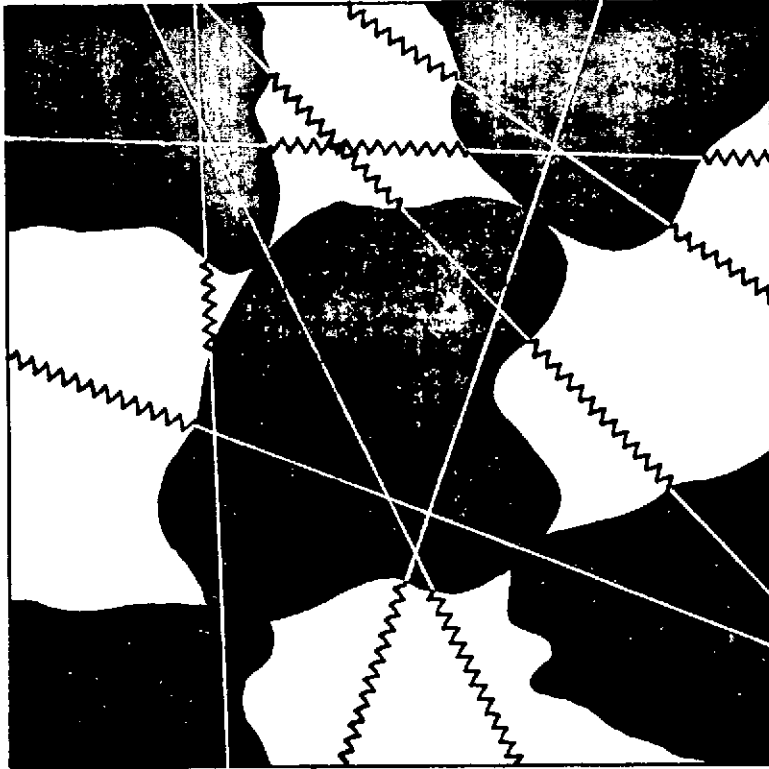
FIGURE 7-3. HEAT CONDUCTED THROUGH GRAINS AND TRANSFERRED
BY CONDUCTION AND RADIATION AT BOUNDRIES.

ductivity of each cubicle occupied by the continuous phase can be approximated by the effective radiative and gaseous conductivities discussed in the literature survey.

## Comparison of Calculated Effective Conductivity to Experimental Data.

The effective thermal conductivity has been calculated and compared to experimentally determined values for a number of granular materials at atmospheric pressures, as indicated on Table 7-I. The range of porosities and constituent conductivities is 0.31 - 0.59 and 1.67 - 2444.4 respectively. For all these cases the conductivities of the constituents were assumed to be constant, independent of temperature distribution in the unit cube. The mechanical properties of the solid phase, required for the calculation of the contact resistance, are shown on Table 7-IX.

In addition to the model presented in this study, the effective conductivity predicted by a number of selected models was also determined, and the calculated values are presented in Tables 7-II and 7-III. The column "Case" in these Tables refers to the granular system described in Table 7-I. It should be noted that a number of these models, such as the Maxwell, Rayleigh and Jefferson models, have been extended to porosities beyond the range for which they are theoretically applicable.

The percentage error between experimental thermal conductivities and those predicted by all selected models is shown on Tables 7-IV and 7-V. Table 7-VI summarizes the mean error, mean bias and the variance of percentage error between the experimental and model

predicted thermal conductivities. From this Table it is seen that the model of this study predicts the experimental thermal conductivities with a mean of 15.8%, an error variance of 1.63, and is biased below the experimental values by 5.8%. This is slightly better than the Krupiczka model, for which a mean error of 17.5% has been calculated. The mean error of all other models is in the range of 30.1% - 42.2%. A graphical representation of the effective thermal conductivity predicted by the model described in this study is shown in Figure (7-4).

It is interesting to observe the performance of some of the models as compared to the assumptions introduced in their developments. It would be expected that models utilizing the parallel isotherm assumption would overpredict the effective thermal conductivity. Jefferson's model (6 in Table 7-VI) generally conforms to this expectation. However Russel's model (5 in Table 7-VI) predicts lower conductivities than the experimental ones, and the discrepancy increases with the ratio of constituent conductivities. The most probably explanation for this behavior is that the effects of the assumed simplified geometry, and the absence of contact areas between particles, dominate over the assumption of infinite conductivity in the lateral-to-the-heat-flow direction, thus rendering the calculated conductivities low.

On the other hand, it would be expected that models utilizing the uniform heat flux assumption would predict low values for the effective thermal conductivity. This is the case for Lichtenecker's

model (8 in Table 7-VI) which, as expected, predicts lower values than Russell's model. However, the Krupiczka and Woodside and Messmer models (7 and 9 in Table 7-VI) are generally biased above the experimental effective thermal conductivity, thus strengthening the indication that the effects of particle shape and spatial distribution, and the bending of the heat flow lines in granular materials are too complex to be analyzed separately, and should be incorporated in a single unified model. Therefore, an analysis of a simplified geometrical configuration or an unrealistic heat flow assumption do not provide sufficient information to deduce whether a particular model will predict high or low conductivities for real granular materials.

Models based on non-linear heat flow are generally biased below the experimental thermal conductivity, as seen from Tables 7-IV, 7-V and 7-VI. A surprising result is that the conductivities predicted by Maxwell's and Rayleigh's equations are very close for the total range of porosities and ratios of constituent conductivities. This is probably due to Rayleigh's failure to include a larger number of terms in his solution, and for this reason Meredith and Tobias' equation provides a marked improvement of the predicted values.

For the model described in this study, the effective conductivity in each case was determined by considering five or more random placements of the continuous phase in a unit cube, and finding the average of the calculated values. The variance of the calculated values was less than 0.1 for 78 cases and its highest value vas 0.587.

Whenever the variance was exceedingly high, more random placements were considered, so that a more representative average could be obtained for the effective thermal conductivity.

In Fig.(7-5) the calculated effective thermal conductivity shown in Table 7-VII, is compared to experimental data obtained by Fountain and West [3] for particulate basalt in a simulated lunar environment. The thermal conductivity of solid basalt was assumed to be a function of temperature given by:

$$k(Basalt)=0.01091+9.09 \times 10^{-6}T \quad Watt/cm-K \qquad (7-13)$$

where T is in $^{\circ}K$. Equation (7-13) is a least squares fit of the data given in Reference [64]. The effective thermal conductivity of the gaseous phase was calculated according to Equation (A-1), and the effective radiant conductivity for the transfer of heat between particle surfaces was calculated according to Equation (B-13). In both cases the effective pore size was assumed to be given by Equation (D-6). Then, the effective conductivity of the continuous phase is the sum of the gaseous conductivity and the radiant conductivity.

As indicated in Fig. (7-5), the calculated conductivities are lower than the experimental. Probably the source of error is due to two factors. First, the semi-empirical equation for the contact resistance used in this study probably predicts low values for the contact conductivity. Evidence to this effect is that calculated conductivities at low pressures, in which case heat transfer from particle to particle is a dominant mode, are generally low. A second source of error is

failure to include radiation heat transfer as a photon diffusion process. Evidence to this effect is that the discrepancy between calculated and experimental values generally increases with temperature. Nevertheless, it is seen that the model predicts fairly well the increase in slope with decreasing porosity, and the increase in slope with temperature, due to the increase of the relative influence of radiant heat transfer with decreasing porosity and increasing temperature. The maximum error of the calculated thermal conductivities is 23.6% and the mean error is 15.9%.

In Fig.(7-6) the calculated effective thermal conductivity is compared to experimental data obtained by Fountain and West [3] for particulate basalt in a simulated martian environment. In this case the gaseous conductivity and the radiant conductivity are of the order of magnitude $3 \times 10^{-5}$ and $10^{-7}$ Watt/cm$^{o}$K respectively. Consequently, radiation can be neglected. Again the predicted values are lower than the experimental, and the maximum error and mean error are 25.2% and 20.8% respectively. The slight increase of the effective thermal conductivity with temperature is due to the simultaneous increase of the conductivity of the solid and gaseous phases with temperature, and not to radiation heat transfer.

A case in which the calculated values are not in good agreement with experimental values is shown in Fig.(7-7). The experimental data in this Figure were obtained from Reference [93]. Here, experimental and calculated thermal conductivities are compared for glass spheres

in a simulated lunar environment, and the maximum and mean errors are 48.3% and 39.4% respectively. The discrepancy increases with increasing temperature. The most probable explanation for the low predicted thermal conductivities is that this case does not satisfy the assumptions stated in the development of the model. Radiation heat transfer has been incorporated in the model through the effective radiant conductivity of the voids, which accounts for the radiation heat transfer between particle surfaces. It has been necessary to make this assumption because of the lack of information about the extinction coefficient of granular materials and powders, which is required for the complete description of the radiation heat transfer process. Consequently, it has been effectively assumed that the solid particles are opaque to thermal radiation, and that the pure radiation heat transfer process can be neglected. However, there exists evidence [2,85] that this is not always the case, and for very small particles the pure radiation process is generally more effective than the conduction-radiation process. It appears that failure to account for the pure radiation process has rendered the calculated values much lower than the experimental values is this case of glass spheres.

The experimental and calculated thermal conductivities of particulate basalt in air, lead shot in air, and glass beads in air are compared in Figures (7-8), (7-9) and (7-10) respectively, as a function of pressure. It is observed that the model predicted values are generally in good agreement with the experimental values, although somewhat lower con-

ductivities are predicted at low pressures. This relatively good agreement is attributed to the choice of Equation (D-6) for the effective pore size associated with the conduction heat transfer in the voids. The maximum and mean errors corresponding to Figures (7-8),(7-9) and (7-10) are 28.4 and 19.4, 37 and 18.5, 23 and 17.6 respectively.

Table 7-VIII summarizes the mean error and the variance of percentage error for all low pressure cases.

Summarizing the comparisons between calculated and experimental thermal conductivities, it is seen that the performance of the model described in this study is sufficiently good for granular materials at atmospheric pressures. For granular materials at low pressures, the predicted thermal conductivities are generally low, but the change of the thermal conductivity with temperature and pressure is in good agreement with the changes observed in the experimental values.

The major sources of error in the calculated effective thermal conductivity values are as follows:

1. Low values for the contact conductivity predicted by Equation (C-7);

2. Failure to account for the pure radiation process;

3. Incomplete description of the particle and pore size and shape distribution by the random placement method.

The first factor is of particular importance in cases where the ratio of the constituent conductivities is large, and could explain the low calculated values at low pressures. The third factor is a manifestation of the lack of information associated with the generalized geometry of granular materials.

TABLE 7—1  COMPARISON OF CALCULATED CONDUCTIVITIES TO EXPERIMENTAL CONDUCTIVITIES

| Case (1) | Fluid Phase (2) | Solid Phase (3) | Conductivity, $(k_{cal}/m\text{-}hr - {}^{\circ}k) \times 100$ | | $k_d/k_c$ (6) | P (7) | Ref. (8) |
|---|---|---|---|---|---|---|---|
| | | | Experimental (4) | Calculated (5) | | | |
| 1 | h-Heptane 11 | Quartz 720 | 57.6 | 61.6 | 65.5 | 0.590 | 23 |
| 2 | Helium 11.5 | Quartz 720 | 63 | 61.7 | 62.6 | 0.590 | 23 |
| 3 | Hydrogen 14.7 | Quartz 720 | 74 | 73.8 | 49 | 0.590 | 23 |
| 4 | Water 54 | Quartz 720 | 180 | 152.6 | 13.3 | 0.590 | 23 |
| 5 | EtOH 29.3 | S. Steel 1793 | 172.7 | 181.2 | 61.2 | 0.505 | 36 |
| 6 | Air 2.3 | S. Steel 1793 | 22 | 24.2 | 779.6 | 0.502 | 36 |
| 7 | Glycerine 46.3 | S. Steel 1793 | 248.3 | 211.9 | 38.7 | 0.502 | 36 |
| 8 | Water 54.5 | S. Steel 1793 | 272 | 228.3 | 32.9 | 0.501 | 36 |
| 9 | Helium 15.6 | S. Steel 1785 | 117.4 | 114.4 | 114.5 | 0.500 | 21 |

TABLE 7-1   Continued

| (1) | (2) | (3) | (4) | (5) | (6) | (7) | (8) |
|---|---|---|---|---|---|---|---|
| 10 | Helium 18.5 | S. Steel 1670 | 122 | 133.5 | 90.3 | 0.500 | 21 |
| 11 | Argon 1.62 | S. Steel 1883 | 38.7 | 30.6 | 1162.3 | 0.500 | 21 |
| 12 | Argon 2.01 | S. Steel 1720 | 41.6 | 48.7 | 855.7 | 0.500 | 21 |
| 13 | Iso-Octane 12.3 | S. Steel 1793 | 80.5 | 73.3 | 145.8 | 0.476 | 36 |
| 14 | Air 2.41 | Lead 2950 | 30.4 | 27.0 | 1224.1 | 0.450 | 6 |
| 15 | Water 54.5 | Silica 973 | 216 | 191.9 | 17.9 | 0.439 | 36 |
| 16 | Air 2.25 | Quartz 947 | 26.8 | 34.5 | 420.9 | 0.438 | 35 |
| 17 | Air 2.3 | Silica 973 | 21.9 | 16.9 | 423.0 | 0.437 | 36 |
| 18 | Air 2.25 | Coal 36 | 11.8 | 8.9 | 16.0 | 0.437 | 35 |
| 19 | Hydrogen 16.6 | Coal 36 | 25.3 | 22.1 | 2.17 | 0.437 | 35 |
| 20 | EtOH 29.3 | Silica 973 | 144.6 | 122.3 | 33.2 | 0.434 | 36 |

TABLE 7-1 Continued

| (1) | (2) | (3) | (4) | (5) | (6) | (7) | (8) |
|-----|-----|-----|-----|-----|-----|-----|-----|
| 21 | EtOH 29.3 | Silica 973 | 146.5 | 124.6 | 33.2 | 0.433 | 36 |
| 22 | Air 2.3 | Silica 973 | 23.8 | 22.5 | 423.0 | 0.433 | 36 |
| 23 | Iso-Octane 12.3 | Glass 93.9 | 35.1 | 42.2 | 7.63 | 0.431 | 36 |
| 24 | Water 54.5 | Silica 973 | 218.5 | 177.5 | 17.9 | 0.430 | 36 |
| 25 | Glycerine 46.3 | Glass 93.9 | 73.2 | 61.1 | 2.03 | 0.428 | 36 |
| 26 | Iso-Octane 12.3 | Silica 973 | 94.1 | 81.9 | 79.1 | 0.428 | 36 |
| 27 | Iso-Octane 12.3 | Silica 973 | 70.9 | 78.9 | 79.1 | 0.426 | 36 |
| 28 | Air 2.3 | Silica 973 | 22.3 | 25.9 | 423.0 | 0.426 | 36 |
| 29 | Water 54.5 | Silica 973 | 210 | 159.1 | 17.9 | 0.426 | 36 |
| 30 | Air 2.3 | Silica 973 | 22.6 | 26.3 | 423.0 | 0.424 | 36 |
| 31 | Glycerine 46.3 | Silica 973 | 205.5 | 180.3 | 21.0 | 0.424 | 36 |

Table 7-1 Continued

| (1) | (2) | (3) | (4) | (5) | (6) | (7) | (8) |
|-----|-----|-----|-----|-----|-----|-----|-----|
| 32 | Air 2.41 | Steel 3850 | 44.6 | 53.2 | 1597.5 | 0.423 | 6 |
| 33 | EtOH 29.3 | Glass 93.9 | 55.4 | 41.1 | 3.2 | 0.423 | 36 |
| 34 | EtOH 29.3 | Silica 973 | 163.8 | 134.5 | 33.2 | 0.423 | 36 |
| 35 | Iso-Octane 12.3 | Silica 973 | 74.6 | 77.7 | 79.1 | 0.423 | 36 |
| 36 | Air 2.41 | Lead 2950 | 36 | 41.2 | 1224.1 | 0.420 | 6 |
| 37 | Iso-Octane 12.3 | Silica 973 | 70.6 | 66.9 | 79.1 | 0.420 | 36 |
| 38 | Helium 15.6 | MgO 2750 | 132.5 | 151.7 | 176.3 | 0.420 | 21 |
| 39 | Helium 18.6 | MgO 2160 | 152 | 127.2 | 116.1 | 0.420 | 21 |
| 40 | Air 2.68 | MgO 2820 | 33.5 | 30.5 | 1052.2 | 0.420 | 21 |
| 41 | Air 3.20 | MgO 2200 | 40.2 | 52.7 | 687.5 | 0.420 | 21 |
| 42 | Argon 2.16 | MgO 2750 | 26.8 | 19.5 | 1273.2 | 0.420 | 21 |

Table 7-1   Continued

| (1) | (2) | (3) | (4) | (5) | (6) | (7) | (8) |
|-----|-----|-----|-----|-----|-----|-----|-----|
| 43 | Argon<br>2.23 | MgO<br>2200 | 29.8 | 24.1 | 986.6 | 0.420 | 21 |
| 44 | Air<br>2.74 | $Al_2O_3$<br>2600 | 36.1 | 31.3 | 948.9 | 0.420 | 45 |
| 45 | Iso-Octane<br>12.3 | Silica<br>973 | 71.2 | 69.3 | 79.1 | 0.419 | 36 |
| 46 | EtOH<br>29.3 | Silica<br>973 | 144.2 | 114.2 | 34.2 | 0.418 | 36 |
| 47 | Air<br>2.25 | Quartz<br>947 | 29.7 | 19.4 | 420.9 | 0.416 | 35 |
| 48 | Air<br>2.3 | Glass<br>93.9 | 17.1 | 13.9 | 40.8 | 0.414 | 36 |
| 49 | Water<br>54.5 | Silica<br>973 | 230.5 | 157.7 | 17.9 | 0.414 | 36 |
| 50 | Air<br>2.41 | Steel<br>3850 | 35.1 | 29.8 | 1597.5 | 0.413 | 6 |
| 51 | Air<br>2.41 | Steel<br>3850 | 33.6 | 29.8 | 1597.5 | 0.413 | 6 |
| 52 | EtOH<br>29.3 | Silica<br>973 | 154.9 | 115.6 | 33.2 | 0.410 | 36 |
| 53 | Air<br>3.0 | Sand<br>160 | 23.1 | 16.7 | 53.3 | 0.410 | 56 |

218

Table 7-1  Continued

| (1) | (2) | (3) | (4) | (5) | (6) | (7) | (8) |
|---|---|---|---|---|---|---|---|
| 54 | Water 54.5 | Glass 93.9 | 73.1 | 69.7 | 1.72 | 0.408 | 36 |
| 55 | Air 2.41 | Steel 3850 | 36.7 | 41.6 | 1597.5 | 0.402 | 6 |
| 56 | Air 2.25 | Lead 3040 | 37.1 | 42.8 | 1351.1 | 0.400 | 35 |
| 57 | Hydrogen 16.6 | Lead 3040 | 120.7 | 128.7 | 183.1 | 0.400 | 35 |
| 58 | Water 55 | Lead 3040 | 299.5 | 273.1 | 55.3 | 0.400 | 35 |
| 59 | Glycerine 24.5 | Lead 3040 | 176 | 204.9 | 124.1 | 0.400 | 35 |
| 60 | Air 2.41 | Steel 3850 | 42.5 | 40.9 | 1597.5 | 0.394 | 6 |
| 61 | EtOH 29.3 | Copper 33200 | 327.5 | 251.3 | 1133.1 | 0.392 | 36 |
| 62 | Air 2.41 | Steel 3850 | 40.3 | 45.9 | 1597.5 | 0.391 | 6 |
| 63 | Air 2.41 | Steel 3850 | 45.6 | 48.2 | 1597.5 | 0.390 | 6 |
| 64 | Air 3.0 | Sand 160 | 29.4 | 22.4 | 53.3 | 0.390 | 56 |

Table 7-1   Continued

| (1) | (2) | (3) | (4) | (5) | (6) | (7) | (8) |
|-----|-----|-----|-----|-----|-----|-----|-----|
| 65 | Water 54.5 | Copper 33200 | 613 | 639.0 | 609.2 | 0.387 | 36 |
| 66 | Glycerine 46.3 | Copper 33200 | 607 | 529.1 | 717.1 | 0.386 | 36 |
| 67 | Glycerine 46.3 | Copper 33200 | 549 | 463.2 | 717.1 | 0.385 | 36 |
| 68 | Water 54.5 | Copper 33200 | 635 | 553.2 | 609.2 | 0.384 | 36 |
| 69 | Argon 1.46 | Lead 2950 | 25 | 29.4 | 2020.6 | 0.380 | 23 |
| 70 | Air 2.18 | Lead 2950 | 36 | 31.2 | 1353.2 | 0.380 | 23 |
| 71 | Helium 11.5 | Lead 2950 | 162 | 205.8 | 256.5 | 0.380 | 23 |
| 72 | Hydrogen 14.7 | Lead 2950 | 183 | 214.3 | 200.7 | 0.380 | 23 |
| 73 | Water 54 | Lead 2950 | 470 | 377.7 | 54.6 | 0.380 | 23 |
| 74 | Air 2.43 | Steel 3030 | 45 | 59.1 | 1246.9 | 0.380 | 58 |
| 75 | Methane 3.0 | Steel 3300 | 55.8 | 72.5 | 1100.0 | 0.380 | 58 |

Table 7-1   Continued

| (1) | (2) | (3) | (4) | (5) | (6) | (7) | (8) |
|---|---|---|---|---|---|---|---|
| 76 | $CO_2$ 1.35 | Steel 3300 | 32.4 | 42.1 | 2444.4 | 0.380 | 58 |
| 77 | Hydrogen 16.4 | Steel 3300 | 188 | 191.2 | 201.2 | 0.380 | 58 |
| 78 | Freon-12 0.78 | Glass 90 | 3.96 | 3.19 | 115.4 | 0.379 | 23 |
| 79 | Argon 1.46 | Glass 90 | 13.3 | 11.2 | 61.6 | 0.379 | 23 |
| 80 | Air 2.18 | Glass 90 | 18 | 16.2 | 41.3 | 0.379 | 23 |
| 81 | Water 54 | Glass 90 | 75.5 | 66.2 | 1.67 | 0.379 | 23 |
| 82 | Air 2.24 | Quartz 1175 | 35.7 | 41.8 | 524.6 | 0.377 | 34 |
| 83 | Air 3.0 | Sand 160 | 29.4 | 22.2 | 53.3 | 0.370 | 56 |
| 84 | Helium 13.1 | Quartz 680 | 94.5 | 72.6 | 51.9 | 0.369 | 60 |
| 85 | Helium 13.1 | Quartz 680 | 91.5 | 72.6 | 51.9 | 0.369 | 60 |
| 86 | Helium 12.2 | Quartz 830 | 97.8 | 78.0 | 68.0 | 0.369 | 60 |

Table 7-1   Continued

| (1) | (2) | (3) | (4) | (5) | (6) | (7) | (8) |
|-----|-----|-----|-----|-----|-----|-----|-----|
| 87 | Helium 12.2 | Quartz 830 | 94 | 78.0 | 68.0 | 0.369 | 60 |
| 88 | Air 2.25 | Steel 2250 | 35.6 | 29.6 | 1000.0 | 0.365 | 35 |
| 89 | Hydrogen 16.6 | Steel 2250 | 110 | 106.3 | 135.5 | 0.365 | 35 |
| 90 | Air 2.58 | $ZrO_2$ 172 | 25 | 20.2 | 66.7 | 0.360 | 45 |
| 91 | Air 2.24 | Quartz 1175 | 37.8 | 42.8 | 524.6 | 0.354 | 34 |
| 92 | Air 2.25 | Lead 3040 | 58.3 | 62.7 | 1351.1 | 0.310 | 35 |

TABLE 7-II EXPERIMENTAL AND PREDICTED THERMAL CONDUCTIVITIES
FOR VARIOUS MODELS

| CASE | EXRE | MODEL | KRUPIC. | RUSSELL | LICHT. | JEFFERSON |
|------|------|-------|---------|---------|--------|-----------|
| 1 | 0.5760 | 0.6160 | 0.4752 | 0.3965 | 0.3283 | 0.3731 |
| 2 | 0.6300 | 0.6170 | 0.4914 | 0.4132 | 0.3424 | 0.3873 |
| 3 | 0.7400 | 0.7380 | 0.5900 | 0.5174 | 0.4313 | 0.4751 |
| 4 | 1.8000 | 1.5260 | 1.4804 | 1.5330 | 1.3468 | 1.3232 |
| 5 | 1.7270 | 1.8120 | 1.5364 | 1.2773 | 1.0900 | 1.3735 |
| 6 | 0.2200 | 0.2420 | 0.1994 | 0.0958 | 0.0802 | 0.1550 |
| 7 | 2.4830 | 2.1190 | 2.1197 | 1.9338 | 1.6698 | 1.9570 |
| 8 | 2.7200 | 2.2830 | 2.3700 | 2.2294 | 1.9349 | 2.2114 |
| 9 | 1.1740 | 1.1440 | 0.9955 | 0.7184 | 0.6082 | 0.8620 |
| 10 | 1.2200 | 1.3350 | 1.1025 | 0.8403 | 0.7136 | 0.9693 |
| 11 | 0.3870 | 0.3060 | 0.1701 | 0.0781 | 0.0654 | 0.1319 |
| 12 | 0.4160 | 0.4870 | 0.2006 | 0.0967 | 0.0810 | 0.1569 |
| 13 | 0.8050 | 0.7330 | 0.9056 | 0.6081 | 0.5180 | 0.8095 |
| 14 | 0.3040 | 0.2700 | 0.3264 | 0.1327 | 0.1131 | 0.2986 |
| 15 | 2.1600 | 1.9190 | 2.1695 | 2.2576 | 2.0391 | 2.2112 |
| 16 | 0.2680 | 0.3450 | 0.2551 | 0.1267 | 0.1088 | 0.2442 |
| 17 | 0.2190 | 0.1690 | 0.2623 | 0.1299 | 0.1115 | 0.2519 |
| 18 | 0.1180 | 0.0690 | 0.0860 | 0.0908 | 0.0824 | 0.0879 |
| 19 | 0.2530 | 0.2210 | 0.2508 | 0.2619 | 0.2447 | 0.2543 |
| 20 | 1.4460 | 1.2230 | 1.5079 | 1.4039 | 1.2450 | 1.5260 |
| 21 | 1.4650 | 1.2460 | 1.5119 | 1.4073 | 1.2484 | 1.5319 |
| 22 | 0.2380 | 0.2250 | 0.2671 | 0.1313 | 0.1129 | 0.2603 |
| 23 | 0.3510 | 0.4220 | 0.3443 | 0.3838 | 0.3582 | 0.3551 |
| 24 | 2.1850 | 1.7750 | 2.2125 | 2.3022 | 2.0848 | 2.2721 |
| 25 | 0.7320 | 0.6110 | 0.6790 | 0.7060 | 0.6584 | 0.6884 |
| 26 | 0.9410 | 0.8190 | 0.9823 | 0.6648 | 0.5802 | 0.8855 |
| 27 | 0.7090 | 0.7890 | 0.8883 | 0.6683 | 0.5838 | 0.8948 |
| 28 | 0.2230 | 0.2590 | 0.2759 | 0.1339 | 0.1155 | 0.2762 |
| 29 | 2.1000 | 1.5910 | 2.2321 | 2.3224 | 2.1056 | 2.2998 |
| 30 | 0.2260 | 0.2630 | 0.2785 | 0.1347 | 0.1162 | 0.2810 |
| 31 | 2.0550 | 1.8030 | 2.0382 | 2.0673 | 1.8649 | 2.1000 |
| 32 | 0.4460 | 0.5320 | 0.3983 | 0.1433 | 0.1234 | 0.4247 |
| 33 | 0.5540 | 0.4110 | 0.5457 | 0.5898 | 0.5578 | 0.5591 |
| 34 | 1.6380 | 1.3450 | 1.5531 | 1.4422 | 1.2835 | 1.5925 |
| 35 | 0.7460 | 0.7770 | 0.8973 | 0.6737 | 0.5891 | 0.9091 |
| 36 | 0.3600 | 0.4120 | 0.3835 | 0.1443 | 0.1244 | 0.4104 |
| 37 | 0.7060 | 0.6690 | 0.9065 | 0.6792 | 0.5945 | 0.9238 |
| 38 | 1.3250 | 1.5170 | 1.4965 | 0.9027 | 0.7835 | 1.5197 |
| 39 | 1.5200 | 1.2720 | 1.5616 | 1.0549 | 0.9190 | 1.5869 |
| 40 | 0.3350 | 0.3050 | 0.4127 | 0.1603 | 0.1383 | 0.4380 |
| 41 | 0.4020 | 0.5270 | 0.4466 | 0.1907 | 0.1646 | 0.4649 |
| 42 | 0.2680 | 0.1950 | 0.3466 | 0.1294 | 0.1116 | 0.3718 |
| 43 | 0.2980 | 0.2410 | 0.3385 | 0.1333 | 0.1150 | 0.3580 |
| 44 | 0.3610 | 0.3130 | 0.4123 | 0.1638 | 0.1413 | 0.4353 |
| 45 | 0.7120 | 0.6930 | 0.9097 | 0.6810 | 0.5963 | 0.9288 |
| 46 | 1.4420 | 1.1420 | 1.5745 | 1.4601 | 1.3016 | 1.6241 |
| 47 | 0.2970 | 0.1940 | 0.2826 | 0.1348 | 0.1166 | 0.2948 |
| 48 | 0.1710 | 0.1390 | 0.1355 | 0.1197 | 0.1063 | 0.1402 |

TABLE 7-II EXPERIMENTAL AND PREDICTED THERMAL CONDUCTIVITIES FOR VARIOUS MODELS

| CASE | EXKE | MODEL | KRUPIC. | RUSSELL | LICHT. | JEFFERSON |
|------|------|-------|---------|---------|--------|-----------|
| 49 | 2.3050 | 1.5770 | 2.2934 | 2.3848 | 2.1696 | 2.3857 |
| 50 | 0.3510 | 0.2980 | 0.4221 | 0.1475 | 0.1275 | 0.4841 |
| 51 | 0.3360 | 0.2980 | 0.4221 | 0.1475 | 0.1275 | 0.4841 |
| 52 | 1.5450 | 1.1560 | 1.6100 | 1.4894 | 1.3312 | 1.6764 |
| 53 | 0.2310 | 0.1670 | 0.1981 | 0.1635 | 0.1446 | 0.2059 |
| 54 | 0.7310 | 0.6970 | 0.7396 | 0.7600 | 0.7052 | 0.7487 |
| 55 | 0.3670 | 0.4160 | 0.4506 | 0.1523 | 0.1322 | 0.5688 |
| 56 | 0.3710 | 0.4280 | 0.4104 | 0.1429 | 0.1242 | 0.5165 |
| 57 | 1.2070 | 1.2670 | 1.7518 | 1.0183 | 0.8901 | 1.8939 |
| 58 | 2.9950 | 2.7310 | 3.8028 | 3.0925 | 2.7420 | 4.0181 |
| 59 | 1.7600 | 2.0490 | 2.2712 | 1.4752 | 1.2936 | 2.4285 |
| 60 | 0.4250 | 0.4050 | 0.4731 | 0.1560 | 0.1358 | 0.6492 |
| 61 | 3.2750 | 2.5130 | 5.3789 | 1.9043 | 1.6595 | 7.1256 |
| 62 | 0.4030 | 0.4590 | 0.4820 | 0.1574 | 0.1372 | 0.6849 |
| 63 | 0.4560 | 0.4820 | 0.4850 | 0.1579 | 0.1377 | 0.6977 |
| 64 | 0.2540 | 0.2240 | 0.2199 | 0.1626 | 0.1627 | 0.2359 |
| 65 | 6.1300 | 6.3900 | 8.7746 | 3.5753 | 3.1246 | 11.1084 |
| 66 | 6.0700 | 5.2910 | 7.8344 | 3.0524 | 2.6678 | 10.2277 |
| 67 | 5.4900 | 4.6320 | 7.8784 | 3.0617 | 2.6769 | 10.3734 |
| 68 | 6.3500 | 5.5320 | 8.9197 | 3.6081 | 3.1568 | 11.5586 |
| 69 | 0.2300 | 0.2940 | 0.3300 | 0.0987 | 0.0864 | 0.5856 |
| 70 | 0.3600 | 0.3120 | 0.4492 | 0.1471 | 0.1288 | 0.7055 |
| 71 | 1.6200 | 2.0580 | 1.4818 | 0.7573 | 0.6655 | 1.7757 |
| 72 | 1.8300 | 2.1430 | 1.7469 | 0.9600 | 0.8448 | 2.0476 |
| 73 | 4.7000 | 3.7710 | 3.9764 | 3.2027 | 2.8600 | 4.3449 |
| 74 | 0.4500 | 0.5910 | 0.4908 | 0.1639 | 0.1435 | 0.7599 |
| 75 | 0.5580 | 0.7250 | 0.5874 | 0.2022 | 0.1770 | 0.8827 |
| 76 | 0.3240 | 0.4210 | 0.3180 | 0.0914 | 0.0799 | 0.6022 |
| 77 | 1.4600 | 1.9120 | 1.9507 | 1.0712 | 0.9426 | 2.2870 |
| 78 | 0.0350 | 0.0319 | 0.0767 | 0.0497 | 0.0439 | 0.0868 |
| 79 | 0.1330 | 0.1120 | 0.1132 | 0.0881 | 0.0785 | 0.1244 |
| 80 | 0.1400 | 0.1620 | 0.1437 | 0.1246 | 0.1119 | 0.1560 |
| 81 | 0.7550 | 0.6620 | 0.7286 | 0.7487 | 0.6962 | 0.7383 |
| 82 | 0.3570 | 0.4180 | 0.3651 | 0.1512 | 0.1327 | 0.4891 |
| 83 | 0.2940 | 0.2220 | 0.2266 | 0.1824 | 0.1635 | 0.2516 |
| 84 | 0.9450 | 0.7260 | 0.9818 | 0.7960 | 0.7142 | 1.0911 |
| 85 | 0.9150 | 0.7260 | 0.9818 | 0.7960 | 0.7142 | 1.0911 |
| 86 | 0.9780 | 0.7800 | 1.0204 | 0.7658 | 0.6839 | 1.1494 |
| 87 | 0.9400 | 0.7800 | 1.0204 | 0.7658 | 0.6839 | 1.1494 |
| 88 | 0.3560 | 0.2960 | 0.4712 | 0.1589 | 0.1399 | 0.8521 |
| 89 | 1.1000 | 1.0630 | 1.8384 | 1.1139 | 0.9883 | 2.2069 |
| 90 | 0.2500 | 0.2020 | 0.2215 | 0.1659 | 0.1487 | 0.2540 |
| 91 | 0.3780 | 0.4820 | 0.4156 | 0.1626 | 0.1439 | 0.7013 |
| 92 | 0.5830 | 0.6270 | 0.7508 | 0.1920 | 0.1724 | -2.5897 |

## TABLE 7-III EXPERIMENTAL AND PREDICTED THERMAL CONDUCTIVITIES FOR VARIOUS MODELS

| CASE | EXKL | MAXWELL | RAYLEIGH | W AND M | M AND T |
|---|---|---|---|---|---|
| 1 | 0.5760 | 0.3226 | 0.3213 | 0.6489 | 0.3771 |
| 2 | 0.6300 | 0.3365 | 0.3352 | 0.6736 | 0.3933 |
| 3 | 0.7400 | 0.4241 | 0.4226 | 0.8240 | 0.4951 |
| 4 | 1.8000 | 1.3371 | 1.3339 | 2.0233 | 1.5349 |
| 5 | 1.7270 | 1.0772 | 1.0733 | 2.2594 | 1.3363 |
| 6 | 0.2200 | 0.0791 | 0.0788 | 0.1919 | 0.0987 |
| 7 | 2.4830 | 1.6525 | 1.6469 | 3.2302 | 2.0490 |
| 8 | 2.7200 | 1.9161 | 1.9098 | 3.6333 | 2.3742 |
| 9 | 1.1740 | 0.6007 | 0.5983 | 1.3496 | 0.7494 |
| 10 | 1.2200 | 0.7050 | 0.7021 | 1.5492 | 0.8791 |
| 11 | 0.3870 | 0.0646 | 0.0643 | 0.1572 | 0.0807 |
| 12 | 0.4160 | 0.0800 | 0.0796 | 0.1941 | 0.1000 |
| 13 | 0.8050 | 0.5123 | 0.5097 | 1.1786 | 0.6511 |
| 14 | 0.3040 | 0.1120 | 0.1115 | 0.2764 | 0.1454 |
| 15 | 2.1600 | 2.0316 | 2.0142 | 3.3220 | 2.6230 |
| 16 | 0.2680 | 0.1077 | 0.1062 | 0.2608 | 0.1411 |
| 17 | 0.2190 | 0.1105 | 0.1089 | 0.2675 | 0.1448 |
| 18 | 0.1180 | 0.0822 | 0.0680 | 0.1305 | 0.1060 |
| 19 | 0.2530 | 0.2593 | 0.2554 | 0.2691 | 0.2859 |
| 20 | 1.4460 | 1.2368 | 1.2231 | 2.3307 | 1.6173 |
| 21 | 1.4650 | 1.2403 | 1.2264 | 2.3364 | 1.6233 |
| 22 | 0.2380 | 0.1119 | 0.1103 | 0.2708 | 0.1472 |
| 23 | 0.3510 | 0.3607 | 0.3427 | 0.4715 | 0.4537 |
| 24 | 2.1850 | 2.0778 | 2.0587 | 3.3862 | 2.7035 |
| 25 | 0.7320 | 0.7004 | 0.6968 | 0.7220 | 0.7679 |
| 26 | 0.9410 | 0.5755 | 0.5677 | 1.2462 | 0.7592 |
| 27 | 0.7090 | 0.5791 | 0.5711 | 1.2531 | 0.7652 |
| 28 | 0.2230 | 0.1144 | 0.1127 | 0.2767 | 0.1514 |
| 29 | 2.1000 | 2.0988 | 2.0788 | 3.4149 | 2.7404 |
| 30 | 0.2260 | 0.1152 | 0.1134 | 0.2784 | 0.1526 |
| 31 | 2.0550 | 1.8571 | 1.8379 | 3.1442 | 2.4365 |
| 32 | 0.4460 | 0.1223 | 0.1218 | 0.3019 | 0.1621 |
| 33 | 0.5540 | 0.5773 | 0.5677 | 0.6291 | 0.6738 |
| 34 | 1.6380 | 1.2756 | 1.2602 | 2.3939 | 1.6840 |
| 35 | 0.7460 | 0.5844 | 0.5761 | 1.2635 | 0.7742 |
| 36 | 0.3600 | 0.1234 | 0.1227 | 0.3037 | 0.1640 |
| 37 | 0.7060 | 0.5899 | 0.5813 | 1.2740 | 0.7834 |
| 38 | 1.3250 | 0.7770 | 0.7726 | 1.8045 | 1.0325 |
| 39 | 1.5200 | 0.9116 | 0.9053 | 2.0503 | 1.2111 |
| 40 | 0.3350 | 0.1371 | 0.1363 | 0.3369 | 0.1822 |
| 41 | 0.4020 | 0.1632 | 0.1620 | 0.3985 | 0.2169 |
| 42 | 0.2680 | 0.1106 | 0.1099 | 0.2723 | 0.1470 |
| 43 | 0.2580 | 0.1140 | 0.1132 | 0.2800 | 0.1515 |
| 44 | 0.3610 | 0.1401 | 0.1392 | 0.3438 | 0.1862 |
| 45 | 0.7120 | 0.5917 | 0.5830 | 1.2774 | 0.7864 |
| 46 | 1.4420 | 1.2938 | 1.2775 | 2.4228 | 1.7155 |
| 47 | 0.2570 | 0.1157 | 0.1137 | 0.2789 | 0.1542 |
| 48 | 0.1710 | 0.1056 | 0.0927 | 0.2056 | 0.1407 |

TABLE 7-III  EXPERIMENTAL AND PREDICTED THERMAL CONDUCTIVITIES
FOR VARIOUS MODELS

| CASE | EXRE | MAXWELL | RAYLEIGH | W AND M | M AND T |
|------|------|---------|----------|---------|---------|
| 49 | 2.3050 | 2.1634 | 2.1407 | 3.5011 | 2.8550 |
| 50 | 0.3510 | 0.1264 | 0.1258 | 0.3114 | 0.1689 |
| 51 | 0.3360 | 0.1264 | 0.1258 | 0.3114 | 0.1689 |
| 52 | 1.5490 | 1.3237 | 1.3058 | 2.4692 | 1.7675 |
| 53 | 0.2310 | 0.1436 | 0.1317 | 0.2922 | 0.1922 |
| 54 | 0.7310 | 0.7574 | 0.7548 | 0.7704 | 0.8167 |
| 55 | 0.3670 | 0.1312 | 0.1305 | 0.3219 | 0.1769 |
| 56 | 0.3710 | 0.1232 | 0.1224 | 0.3017 | 0.1664 |
| 57 | 1.2070 | 0.8835 | 0.8781 | 2.0414 | 1.1936 |
| 58 | 2.9950 | 2.7245 | 2.7100 | 5.5466 | 3.6783 |
| 59 | 1.7600 | 1.2842 | 1.2766 | 2.8821 | 1.7350 |
| 60 | 0.4250 | 0.1348 | 0.1341 | 0.3297 | 0.1829 |
| 61 | 3.2750 | 1.6472 | 1.6462 | 4.0117 | 2.2396 |
| 62 | 0.4030 | 0.1362 | 0.1354 | 0.3326 | 0.1853 |
| 63 | 0.4560 | 0.1366 | 0.1359 | 0.3336 | 0.1861 |
| 64 | 0.2940 | 0.1618 | 0.1463 | 0.3221 | 0.2203 |
| 65 | 6.1300 | 3.1022 | 3.1002 | 7.4618 | 4.2359 |
| 66 | 6.0700 | 2.6487 | 2.6470 | 6.3880 | 3.6196 |
| 67 | 5.4700 | 2.6579 | 2.6562 | 6.4066 | 3.6351 |
| 68 | 6.3500 | 3.1345 | 3.1325 | 7.5270 | 4.2908 |
| 69 | 0.2500 | 0.0858 | 0.0851 | 0.2086 | 0.1178 |
| 70 | 0.3800 | 0.1279 | 0.1269 | 0.3100 | 0.1756 |
| 71 | 1.0250 | 0.6610 | 0.6561 | 1.5391 | 0.9082 |
| 72 | 1.8300 | 0.8392 | 0.8329 | 1.9284 | 1.1531 |
| 73 | 4.7000 | 2.8440 | 2.8255 | 5.7066 | 3.9087 |
| 74 | 0.4500 | 0.1425 | 0.1414 | 0.3452 | 0.1957 |
| 75 | 0.5920 | 0.1758 | 0.1746 | 0.4252 | 0.2414 |
| 76 | 0.3240 | 0.0794 | 0.0788 | 0.1933 | 0.1090 |
| 77 | 1.2800 | 0.9363 | 0.9301 | 2.1519 | 1.2865 |
| 78 | 0.4396 | 0.0437 | 0.0356 | 0.0961 | 0.0601 |
| 79 | 0.1330 | 0.0781 | 0.0645 | 0.1595 | 0.1074 |
| 80 | 0.1800 | 0.1114 | 0.0932 | 0.2127 | 0.1531 |
| 81 | 0.7650 | 0.7462 | 0.7434 | 0.7569 | 0.8073 |
| 82 | 0.3570 | 0.1318 | 0.1292 | 0.3140 | 0.1815 |
| 83 | 0.2940 | 0.1627 | 0.1444 | 0.3227 | 0.2256 |
| 84 | 0.9450 | 0.7105 | 0.6894 | 1.4021 | 0.9863 |
| 85 | 0.9150 | 0.7105 | 0.6894 | 1.4021 | 0.9863 |
| 86 | 0.9750 | 0.6632 | 0.6628 | 1.3986 | 0.9443 |
| 87 | 0.9400 | 0.6632 | 0.6628 | 1.3986 | 0.9443 |
| 88 | 0.1560 | 0.1390 | 0.1374 | 0.3323 | 0.1933 |
| 89 | 1.1000 | 0.9825 | 0.9720 | 2.1721 | 1.3682 |
| 90 | 0.2500 | 0.1479 | 0.1305 | 0.3010 | 0.2070 |
| 91 | 0.3780 | 0.1431 | 0.1397 | 0.3350 | 0.2009 |
| 92 | 0.5830 | 0.1717 | 0.1693 | 0.3886 | 0.2505 |

TABLE 7-IV PERCENTAGE ERROR BETWEEN PREDICTED AND EXPERIMENTAL THERMAL CONDUCTIVITIES

| CASE | MODEL | KRUPIC. | RUSSELL | LICHT. | JEFFERSON |
|------|-------|---------|---------|--------|-----------|
| 1 | 6.544 | -17.497 | -31.156 | -43.005 | -35.217 |
| 2 | -2.064 | -22.003 | -34.411 | -45.648 | -38.520 |
| 3 | -0.270 | -20.265 | -30.082 | -41.717 | -35.802 |
| 4 | -15.222 | -17.755 | -14.833 | -25.180 | -26.487 |
| 5 | 4.922 | -11.039 | -26.041 | -36.886 | -20.470 |
| 6 | 10.000 | -9.349 | -56.450 | -63.551 | -29.558 |
| 7 | -14.660 | -14.632 | -22.120 | -32.749 | -21.183 |
| 8 | -16.066 | -12.869 | -18.037 | -28.863 | -18.697 |
| 9 | -2.555 | -15.201 | -38.807 | -48.198 | -26.578 |
| 10 | 9.496 | -9.632 | -31.120 | -41.505 | -20.550 |
| 11 | -20.930 | -56.042 | -79.813 | -83.098 | -65.923 |
| 12 | 17.067 | -51.777 | -76.743 | -80.519 | -62.283 |
| 13 | -8.544 | 12.497 | -24.456 | -35.650 | 0.561 |
| 14 | -11.184 | 7.365 | -56.360 | -62.780 | -1.770 |
| 15 | -11.157 | 0.438 | 4.517 | -5.597 | 2.372 |
| 16 | 28.731 | -4.828 | -52.734 | -59.421 | -8.894 |
| 17 | -22.831 | 19.750 | -40.704 | -49.075 | 15.039 |
| 18 | -24.576 | -27.135 | -23.054 | -30.181 | -25.482 |
| 19 | -12.648 | -0.877 | 3.520 | -3.299 | 0.497 |
| 20 | -15.422 | 4.280 | -2.910 | -13.900 | 5.534 |
| 21 | -14.949 | 3.201 | -3.936 | -14.782 | 4.568 |
| 22 | -5.462 | 12.223 | -44.828 | -52.547 | 9.384 |
| 23 | 20.228 | -1.913 | 9.337 | 2.048 | 1.173 |
| 24 | -18.764 | 1.257 | 5.364 | -4.585 | 3.987 |
| 25 | -16.530 | -7.241 | -3.548 | -10.059 | -5.959 |
| 26 | -12.965 | -6.238 | -29.354 | -38.338 | -5.901 |
| 27 | 11.283 | 25.283 | -5.736 | -17.665 | 26.210 |
| 28 | 16.143 | 23.717 | -39.951 | -48.218 | 23.853 |
| 29 | -24.238 | 6.293 | 10.593 | 0.266 | 9.517 |
| 30 | 16.372 | 23.222 | -40.412 | -48.578 | 24.345 |
| 31 | -12.263 | -0.815 | 0.600 | -9.248 | 2.188 |
| 32 | 19.283 | -10.703 | -67.878 | -72.336 | -4.772 |
| 33 | -25.812 | -1.493 | 6.461 | 0.678 | 0.919 |
| 34 | -17.888 | -5.181 | -11.956 | -21.641 | -2.775 |
| 35 | 4.155 | 20.285 | -9.690 | -21.035 | 21.868 |
| 36 | 14.444 | 6.531 | -59.916 | -65.431 | 14.011 |
| 37 | -5.241 | 28.406 | -3.801 | -15.796 | 30.848 |
| 38 | 14.491 | 12.947 | -31.872 | -40.867 | 14.695 |
| 39 | -16.316 | 2.737 | -30.597 | -39.540 | 4.401 |
| 40 | -8.955 | 23.197 | -52.144 | -58.721 | 30.738 |
| 41 | 31.095 | 11.095 | -52.554 | -59.046 | 15.645 |
| 42 | -27.239 | 29.331 | -51.730 | -58.373 | 38.737 |
| 43 | -19.128 | 13.599 | -55.256 | -61.402 | 20.151 |
| 44 | -13.296 | 14.217 | -54.630 | -60.860 | 20.570 |
| 45 | -2.669 | 27.761 | -4.355 | -16.251 | 30.443 |
| 46 | -20.804 | 9.192 | 1.253 | -9.738 | 12.628 |
| 47 | -34.680 | -4.864 | -54.624 | -60.727 | -0.736 |
| 48 | -18.713 | -20.762 | -29.995 | -37.832 | -18.003 |

TABLE 7-IV PERCENTAGE ERROR BETWEEN PREDICTED AND EXPERIMENTAL THERMAL CONDUCTIVITIES

| CASE | MODEL | KRUPIC. | RUSSELL | LICHT. | JEFFERSON |
|---|---|---|---|---|---|
| 49 | -31.583 | -0.503 | 3.461 | -5.874 | 3.499 |
| 50 | -15.100 | 25.243 | -57.989 | -63.685 | 37.913 |
| 51 | -11.310 | 25.611 | -56.114 | -62.063 | 44.070 |
| 52 | -25.371 | 3.936 | -3.846 | -14.059 | 8.225 |
| 53 | -27.706 | -14.239 | -29.205 | -37.402 | -10.851 |
| 54 | -4.651 | 1.178 | 4.053 | -3.535 | 2.415 |
| 55 | 13.351 | 22.781 | -58.500 | -63.979 | 54.998 |
| 56 | 15.364 | 10.617 | -61.477 | -66.534 | 39.226 |
| 57 | 6.628 | 45.133 | -15.632 | -26.256 | 56.913 |
| 58 | -8.415 | 26.973 | 3.256 | -8.446 | 34.159 |
| 59 | 16.420 | 29.043 | -16.181 | -26.502 | 37.983 |
| 60 | -3.765 | 11.322 | -63.295 | -68.047 | 52.760 |
| 61 | -23.267 | 64.240 | -41.854 | -49.327 | 117.577 |
| 62 | 13.896 | 19.595 | -60.938 | -65.958 | 69.961 |
| 63 | 5.702 | 6.353 | -65.374 | -69.812 | 52.996 |
| 64 | -23.810 | -25.196 | -37.908 | -44.650 | -19.776 |
| 65 | 4.941 | 43.142 | -41.676 | -49.027 | 81.213 |
| 66 | -12.834 | 29.067 | -49.713 | -56.050 | 68.496 |
| 67 | -15.628 | 43.505 | -44.231 | -51.240 | 88.952 |
| 68 | -12.882 | 40.468 | -43.180 | -50.287 | 82.026 |
| 69 | 17.660 | 32.019 | -60.505 | -65.446 | 134.239 |
| 70 | -13.333 | 24.774 | -59.126 | -64.228 | 97.181 |
| 71 | 27.037 | -8.532 | -53.251 | -58.920 | 9.610 |
| 72 | 17.164 | -4.541 | -47.538 | -53.837 | 11.893 |
| 73 | -19.638 | -15.395 | -31.857 | -39.149 | -7.556 |
| 74 | 31.333 | 0.075 | -63.569 | -68.114 | 68.862 |
| 75 | 29.028 | 5.269 | -63.759 | -68.276 | 58.193 |
| 76 | 29.538 | -1.842 | -71.802 | -75.333 | 85.873 |
| 77 | 1.792 | 3.759 | -43.022 | -49.864 | 21.650 |
| 78 | -19.444 | 93.720 | 25.497 | 10.956 | 119.219 |
| 79 | -15.789 | -14.890 | -33.762 | -40.953 | -6.454 |
| 80 | -10.000 | -25.168 | -30.779 | -37.819 | -13.344 |
| 81 | -12.313 | -3.501 | -0.836 | -7.793 | -2.214 |
| 82 | 17.587 | 2.268 | -57.645 | -62.834 | 36.997 |
| 83 | -24.490 | -22.939 | -37.951 | -44.375 | -14.405 |
| 84 | -23.175 | 3.896 | -15.770 | -24.428 | 15.459 |
| 85 | -20.456 | 7.302 | -13.008 | -21.950 | 19.244 |
| 86 | -20.245 | 4.333 | -21.702 | -30.069 | 17.524 |
| 87 | -17.021 | 8.550 | -18.536 | -27.242 | 22.275 |
| 88 | -16.454 | 32.362 | -55.374 | -60.714 | 139.360 |
| 89 | -3.364 | 67.124 | 1.244 | -5.152 | 100.628 |
| 90 | -19.200 | -11.413 | -33.646 | -40.532 | 1.610 |
| 91 | 27.513 | 9.952 | -56.975 | -61.927 | 85.528 |
| 92 | 7.547 | 28.788 | -67.062 | -70.424 | -544.204 |

TABLE 7-V PERCENTAGE ERROR BETWEEN PREDICTED AND EXPERIMENTAL THERMAL CONDUCTIVITIES

| CASE | MAXWELL | RAYLEIGH | W AND M | M AND T |
|------|---------|----------|---------|---------|
| 1 | -44.001 | -44.211 | 12.648 | -34.526 |
| 2 | -46.593 | -46.792 | 6.914 | -37.568 |
| 3 | -42.690 | -42.897 | 11.352 | -33.095 |
| 4 | -25.715 | -25.894 | 12.405 | -14.727 |
| 5 | -37.626 | -37.849 | 30.829 | -22.625 |
| 6 | -64.033 | -64.184 | -12.765 | -55.117 |
| 7 | -33.447 | -33.674 | 30.091 | -17.481 |
| 8 | -29.555 | -29.788 | 33.577 | -12.712 |
| 9 | -48.835 | -49.039 | 14.961 | -36.166 |
| 10 | -42.209 | -42.453 | 26.983 | -27.942 |
| 11 | -83.320 | -83.388 | -59.391 | -79.154 |
| 12 | -80.774 | -80.860 | -53.352 | -75.973 |
| 13 | -36.365 | -36.689 | 46.406 | -19.123 |
| 14 | -63.162 | -63.315 | -9.087 | -52.187 |
| 15 | -5.945 | -6.748 | 53.798 | 21.435 |
| 16 | -59.806 | -60.372 | -2.676 | -47.345 |
| 17 | -49.556 | -50.254 | 22.149 | -33.865 |
| 18 | -30.374 | -42.345 | 10.620 | -10.175 |
| 19 | 2.503 | 0.944 | 6.373 | 13.008 |
| 20 | -14.468 | -15.414 | 61.185 | 11.850 |
| 21 | -15.341 | -16.285 | 59.485 | 10.803 |
| 22 | -52.986 | -53.659 | 13.794 | -38.165 |
| 23 | 2.771 | -2.359 | 34.333 | 29.266 |
| 24 | -4.907 | -5.782 | 54.977 | 23.732 |
| 25 | -4.311 | -4.809 | -1.366 | 4.906 |
| 26 | -38.838 | -39.670 | 32.437 | -19.316 |
| 27 | -18.325 | -19.456 | 76.747 | 7.922 |
| 28 | -48.679 | -49.461 | 24.080 | -32.122 |
| 29 | -0.059 | -1.009 | 62.613 | 30.495 |
| 30 | -49.031 | -49.821 | 23.180 | -32.480 |
| 31 | -9.629 | -10.566 | 53.001 | 18.564 |
| 32 | -72.582 | -72.694 | -32.301 | -63.648 |
| 33 | 4.214 | 2.466 | 13.559 | 21.626 |
| 34 | -22.122 | -23.068 | 46.147 | 2.806 |
| 35 | -21.657 | -22.770 | 69.373 | 3.779 |
| 36 | -65.732 | -65.919 | -15.647 | -54.457 |
| 37 | -16.448 | -17.666 | 80.446 | 10.957 |
| 38 | -41.360 | -41.687 | 36.191 | -22.077 |
| 39 | -40.029 | -40.442 | 34.888 | -20.325 |
| 40 | -59.081 | -59.314 | 0.556 | -45.617 |
| 41 | -59.401 | -59.696 | -0.863 | -46.043 |
| 42 | -58.737 | -58.978 | 1.615 | -45.160 |
| 43 | -61.738 | -62.016 | -6.049 | -49.149 |
| 44 | -61.201 | -61.440 | -4.778 | -48.435 |
| 45 | -16.896 | -18.118 | 79.415 | 10.455 |
| 46 | -10.274 | -11.410 | 68.015 | 18.963 |
| 47 | -61.057 | -61.722 | -6.083 | -48.077 |
| 48 | -38.227 | -45.792 | 20.236 | -17.706 |

TABLE 7-V PERCENTAGE ERROR BETWEEN PREDICTED AND EXPERIMENTAL THERMAL CONDUCTIVITIES

| CASE | MAXWELL | RAYLEIGH | W AND M | M AND T |
|------|---------|----------|---------|---------|
| 49 | -6.143 | -7.128 | 51.892 | 23.863 |
| 50 | -63.990 | -64.151 | -11.296 | -51.871 |
| 51 | -62.382 | -62.550 | -7.336 | -49.723 |
| 52 | -14.542 | -15.699 | 59.409 | 14.105 |
| 53 | -37.825 | -42.998 | 26.511 | -16.795 |
| 54 | 3.607 | 3.263 | 5.388 | 11.718 |
| 55 | -64.264 | -64.440 | -12.294 | -51.810 |
| 56 | -66.795 | -67.005 | -18.691 | -55.149 |
| 57 | -26.806 | -27.246 | 69.127 | -1.111 |
| 58 | -9.032 | -9.516 | 85.196 | 22.815 |
| 59 | -27.035 | -27.464 | 63.754 | -1.421 |
| 60 | -68.288 | -68.455 | -22.433 | -56.955 |
| 61 | -49.704 | -49.735 | 22.494 | -31.614 |
| 62 | -66.210 | -66.393 | -17.468 | -54.021 |
| 63 | -70.035 | -70.198 | -26.845 | -59.191 |
| 64 | -44.973 | -50.252 | 9.564 | -25.063 |
| 65 | -49.393 | -49.426 | 21.726 | -30.899 |
| 66 | -56.364 | -56.392 | 5.238 | -40.370 |
| 67 | -51.586 | -51.618 | 16.695 | -33.786 |
| 68 | -50.637 | -50.670 | 18.535 | -32.429 |
| 69 | -65.686 | -65.952 | -16.542 | -52.881 |
| 70 | -64.476 | -64.751 | -13.881 | -51.217 |
| 71 | -59.196 | -59.502 | -4.995 | -43.939 |
| 72 | -54.144 | -54.484 | 5.377 | -36.990 |
| 73 | -39.490 | -39.882 | 21.418 | -16.836 |
| 74 | -68.335 | -68.573 | -23.300 | -56.515 |
| 75 | -68.456 | -68.713 | -23.798 | -56.735 |
| 76 | -75.504 | -75.675 | -40.353 | -66.363 |
| 77 | -59.198 | -59.528 | 14.465 | -31.567 |
| 78 | 10.252 | -10.087 | 142.802 | 51.674 |
| 79 | -41.292 | -51.476 | 19.923 | -19.231 |
| 80 | -38.133 | -48.199 | 18.180 | -14.944 |
| 81 | -1.166 | -1.531 | 0.251 | 6.931 |
| 82 | -63.085 | -63.802 | -12.035 | -49.168 |
| 83 | -44.665 | -50.889 | 9.775 | -23.251 |
| 84 | -24.615 | -27.047 | 48.375 | 4.374 |
| 85 | -22.550 | -24.655 | 53.240 | 7.797 |
| 86 | -30.453 | -32.233 | 43.003 | -3.444 |
| 87 | -27.641 | -29.493 | 48.784 | 0.459 |
| 88 | -60.963 | -61.411 | -6.648 | -45.708 |
| 89 | -10.681 | -11.640 | 97.461 | 24.381 |
| 90 | -40.838 | -47.792 | 20.392 | -17.180 |
| 91 | -62.149 | -63.042 | -11.373 | -46.845 |
| 92 | -70.554 | -70.956 | -33.346 | -57.041 |

TABLE 7-VI  AVERAGE ERROR, BIAS AND VARIANCE BETWEEN PREDICTED AND
EXPERIMENTAL THERMAL CONDUCTIVITIES

| Model | Average Error % | Average Bias % | Variance of % Error |
|---|---|---|---|
| 1. This Study | -5.78 | 15.8 | 1.63 |
| 2. Maxwell [9] | -40.59 | 41.1 | 4.99 |
| 3. Rayleigh [14] | -42.05 | 42.2 | 4.96 |
| 4. Meredith & Tobias [16] | -22.46 | 31.34 | 3.56 |
| 5. Russell [43] | -32.65 | 34.37 | 4.90 |
| 6. Jefferson [78] | 13.80 | 37.59 | 38.58 |
| 7. Krupiczka [42] | 6.76 | 17.48 | 2.63 |
| 8. Lichtenecker [24] | -40.52 | 40.82 | 4.93 |
| 9. Woodside & Messmer [23] | 19.10 | 30.12 | 6.68 |

## TABLE 7-VII  CONDUCTIVITY OF PARTICULATE BASALT IN SIMULATED LUNAR ENVIRONMENT

Conductivity (Kcal/m-hr-$^O$K)

| Solid Phase | Experimental x10$^3$ | Calculated x10$^3$ | T($^O$K) | P | Ref. |
|---|---|---|---|---|---|
| 1.078 | 1.50 | 1.46 | 180 | 0.470 | 3 |
| 1.125 | 1.82 | 1.67 | 240 | 0.470 | 3 |
| 1.156 | 2.09 | 1.86 | 280 | 0.470 | 3 |
| 1.188 | 2.42 | 2.12 | 320 | 0.470 | 3 |
| 1.219 | 2.84 | 2.28 | 360 | 0.470 | 3 |
| 1.078 | 1.17 | 1.04 | 180 | 0.540 | 3 |
| 1.125 | 1.36 | 1.20 | 240 | 0.540 | 3 |
| 1.156 | 1.53 | 1.37 | 280 | 0.540 | 3 |
| 1.188 | 1.78 | 1.46 | 320 | 0.540 | 3 |
| 1.219 | 2.06 | 1.63 | 360 | 0.540 | 3 |
| 1.078 | 0.86 | 0.69 | 180 | 0.600 | 3 |
| 1.125 | 1.01 | 0.86 | 240 | 0.600 | 3 |
| 1.156 | 1.14 | 1.00 | 280 | 0.600 | 3 |
| 1.188 | 1.31 | 1.12 | 320 | 0.600 | 3 |
| 1.219 | 1.50 | 1.24 | 360 | 0.600 | 3 |
| 1.078 | 0.51 | 0.43 | 180 | 0.721 | 3 |
| 1.125 | 0.63 | 0.57 | 240 | 0.721 | 3 |
| 1.156 | 0.77 | 0.62 | 280 | 0.721 | 3 |
| 1.188 | 0.93 | 0.71 | 320 | 0.721 | 3 |
| 1.219 | 1.10 | 0.86 | 360 | 0.721 | 3 |

TABLE 7-VIII   AVERAGE ERROR, BIAS AND VARIANCE BETWEEN PREDICTED
AND EXPERIMENTAL THERMAL CONDUCTIVITIES

| Case | Average Error % | Average Bias % | Variance of % Error |
|------|------|------|------|
| Figure 17 | -15.9 | 15.9 | 8.7 |
| Figure 18 | -20.8 | 20.8 | 2.1 |
| Figure 19 | -39.4 | 39.4 | 7.5 |
| Figure 20 | -9.4 | 19.4 | 2.4 |
| Figure 21 | 11.8 | 18.5 | 1.2 |
| Figure 22 | -17.6 | 17.6 | 1.1 |

## TABLE 7-IX MECHANICAL PROPERTIES AND DENSITY OF SOLID MATERIALS

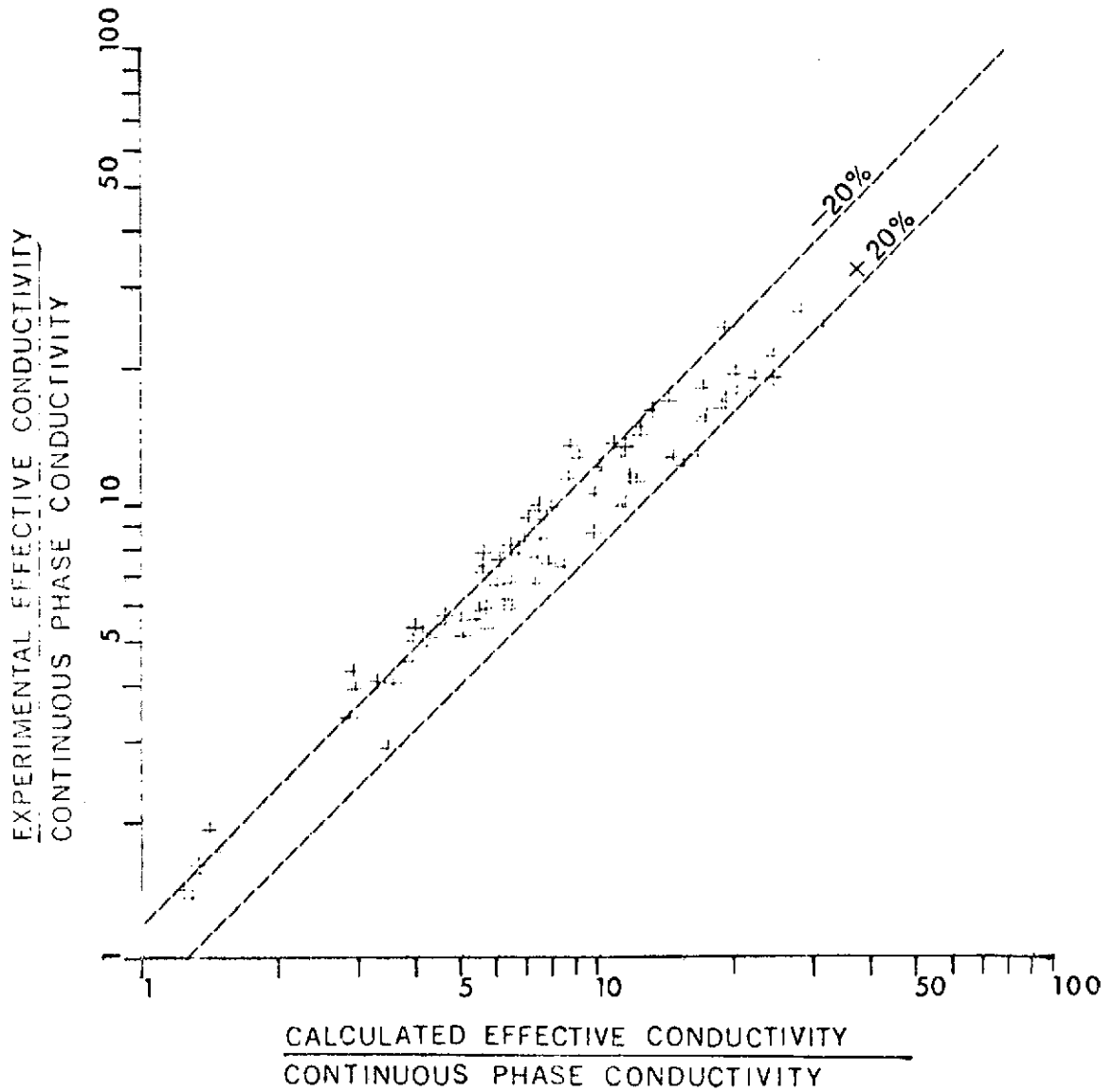| Solid | Young's Modulus Newtons/m$^2$x10$^{10}$ | Poisson's Ratio | Specific weight Newtons/m$^3$x10$^4$ |
|---|---|---|---|
| Aluminum | 6.90 | 0.33 | 2.52 |
| Basalt | 5.73 | 0.25 | 2.78 |
| Coal | 5.00 | 0.25 | 1.36 |
| Copper | 10.80 | 0.33 | 8.72 |
| Glass | 6.90 | 0.24 | 2.52 |
| Iron | 8.96 | 0.28 | 6.95 |
| Lead | 1.57 | 0.43 | 11.10 |
| MgO | 21.00 | 0.25 | 3.51 |
| Quartz (SiO$_2$) | 7.00 | 0.14 | 2.60 |
| Sand | 7.00 | 0.14 | 2.70 |
| Silica | 7.00 | 0.14 | 2.45 |
| Stainless Steel | 20.70 | 0.31 | 7.86 |
| Steel | 20.70 | 0.3 | 7.65 |

FIGURE 7-4. COMPARISON OF EXPERIMENTAL AND MODEL
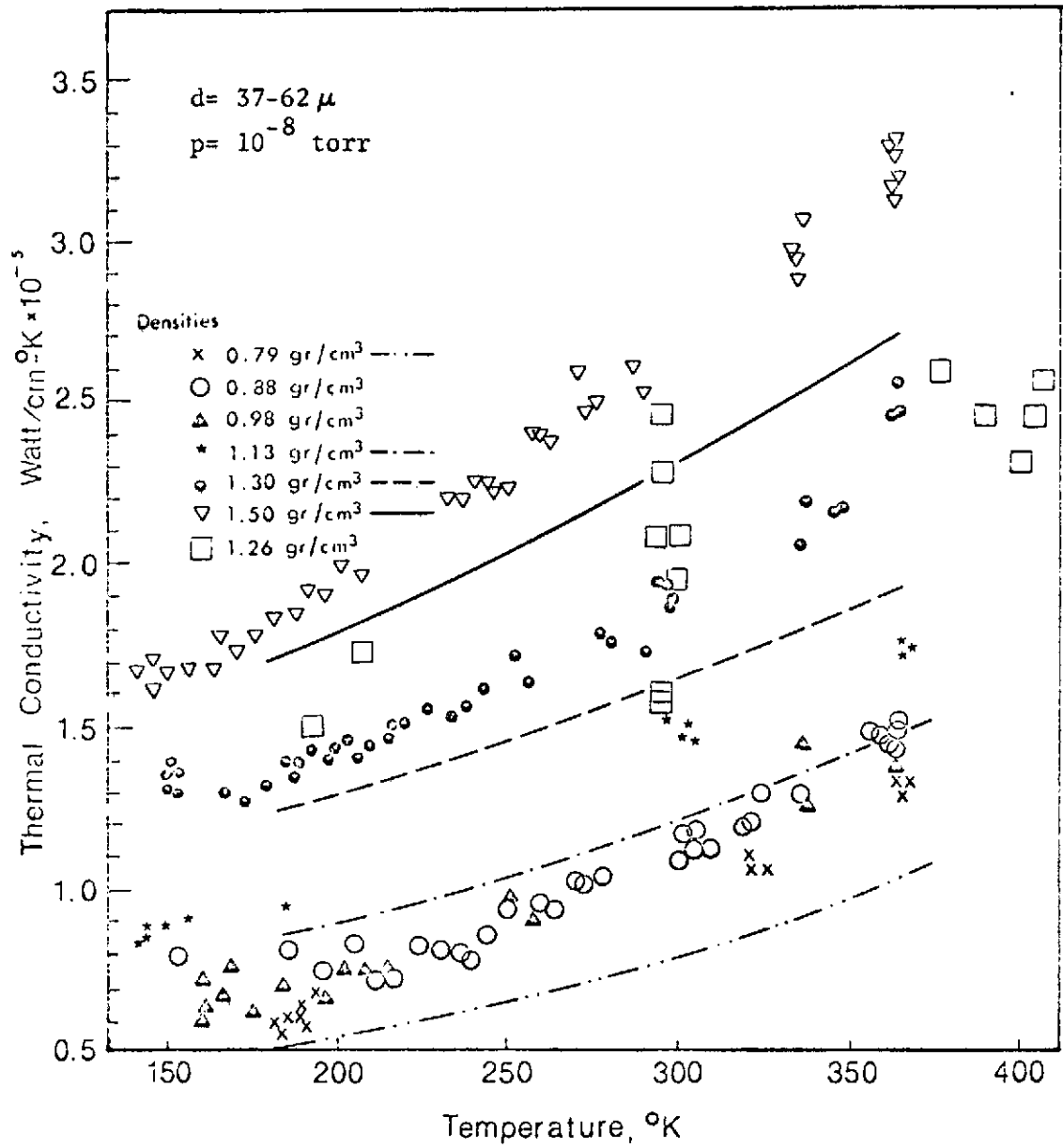PREDICTED THERMAL CONDUCTIVITIES.

FIGURE 7-5. EXPERIMENTAL AND CALCULARED CONDUCTIVITY OF PARTICULATE BASALT IN SIMULATED LUNAR ENVIRONMENT.
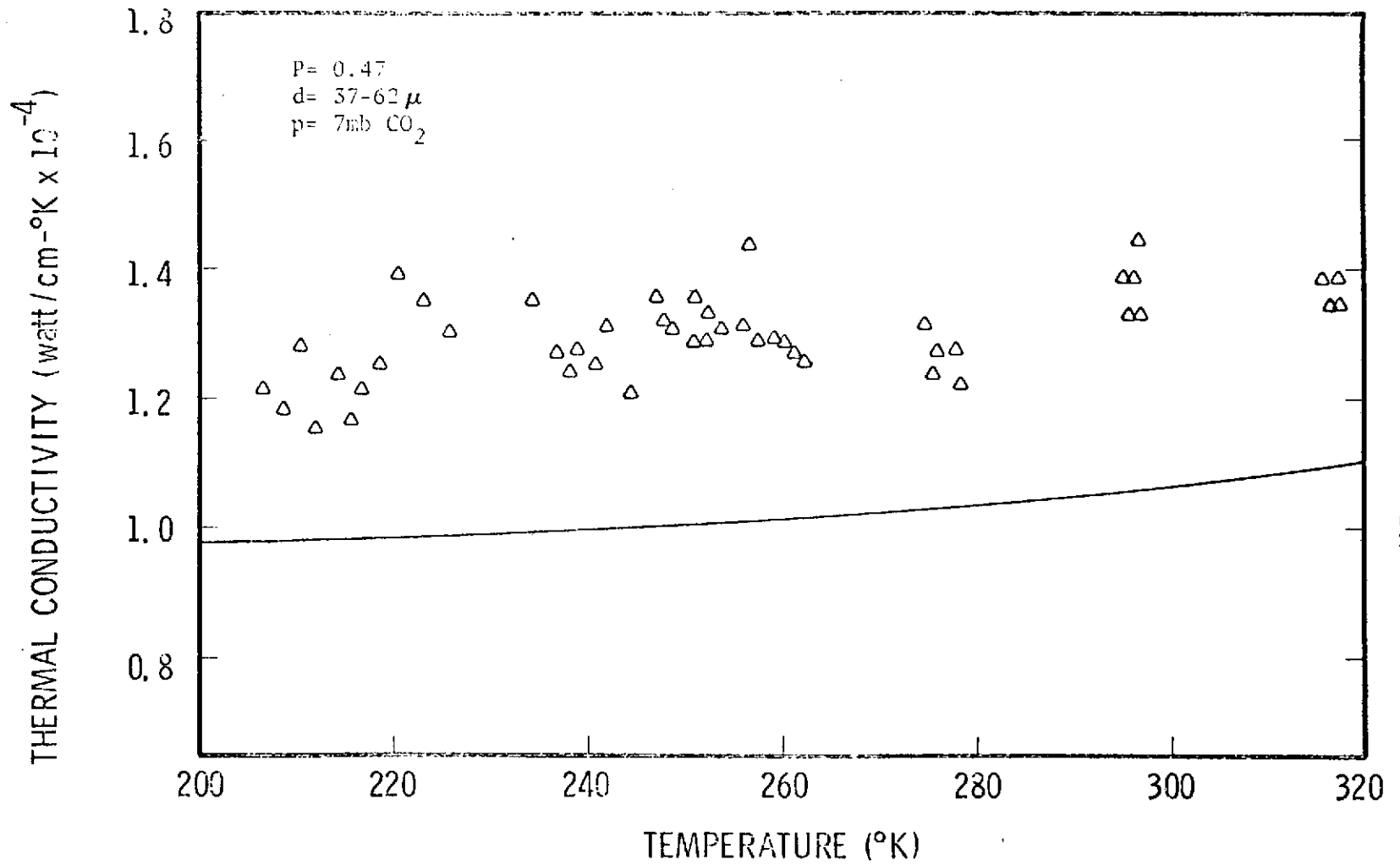
FIGURE 7-6. EXPERIMENTAL AND CALCULATED CONDUCTIVITY OF PARTICULATE BASALT IN SIMULATED MARTIAN ENVIRONMENT.
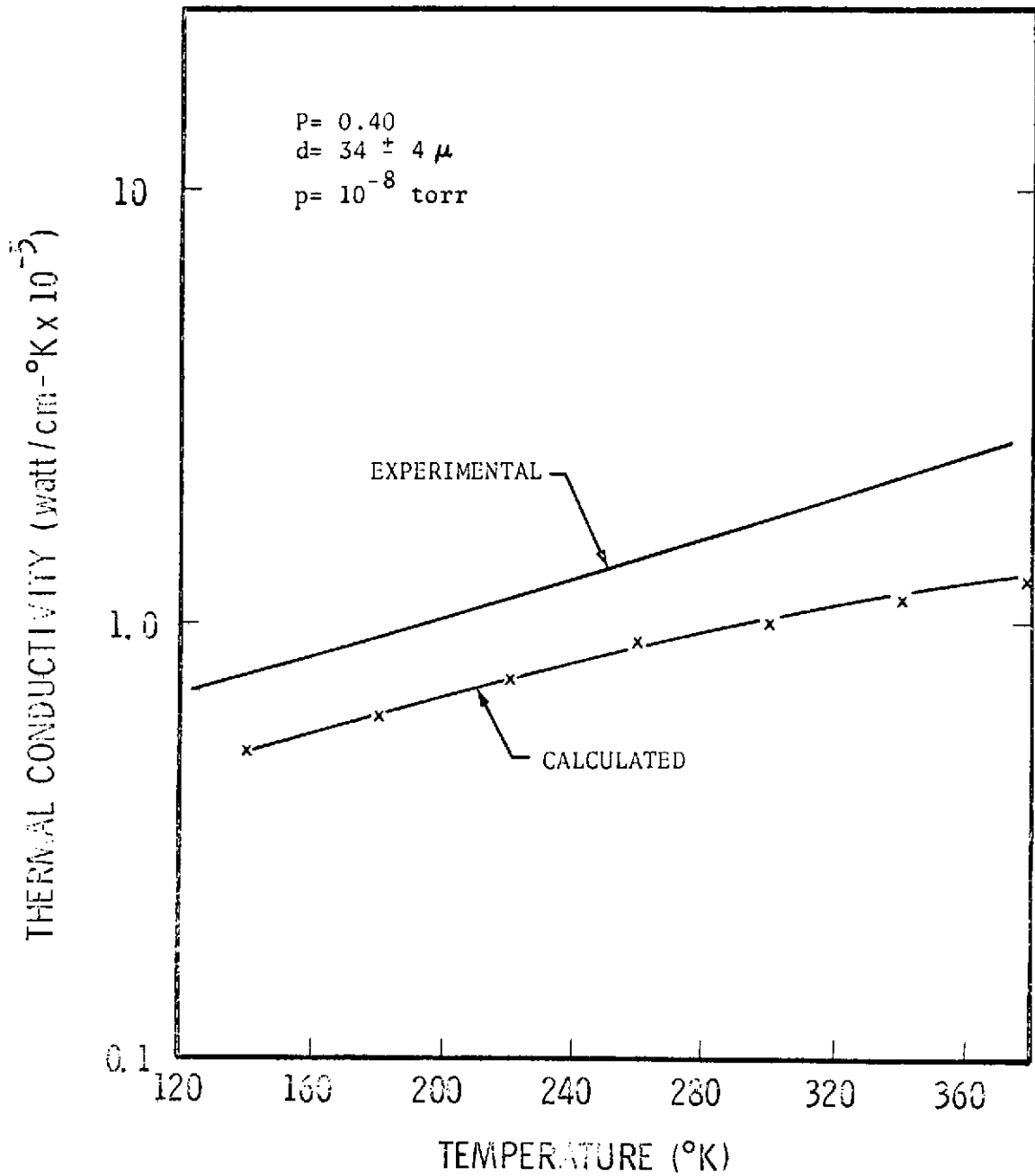
FIGURE 7-7. EXPERIMENTAL AND CALCULATED THERMAL CONDUCTIVITY OF PARTICULATE GLASS IN SIMULATED LUNAR ENVIRONMENT.
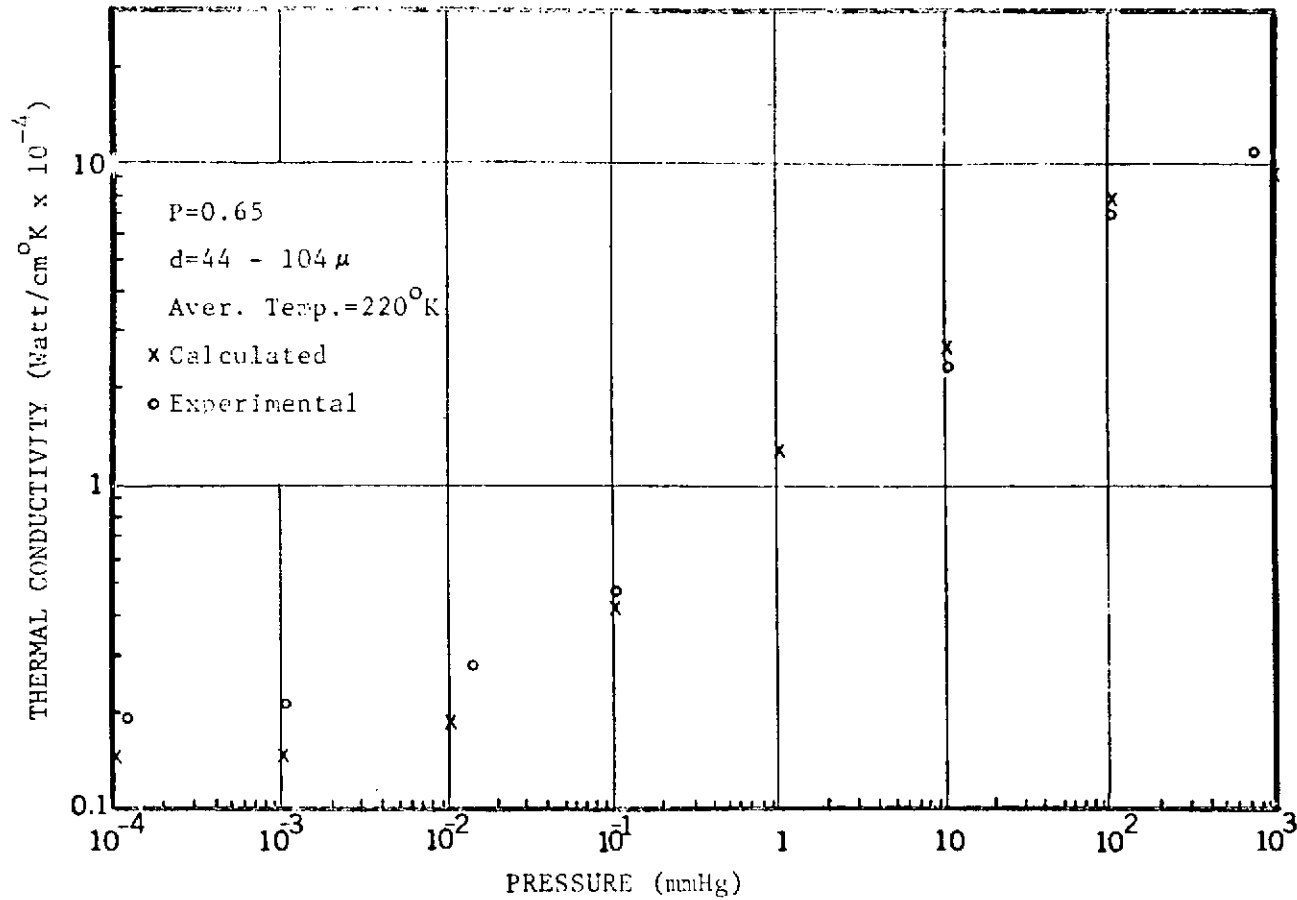
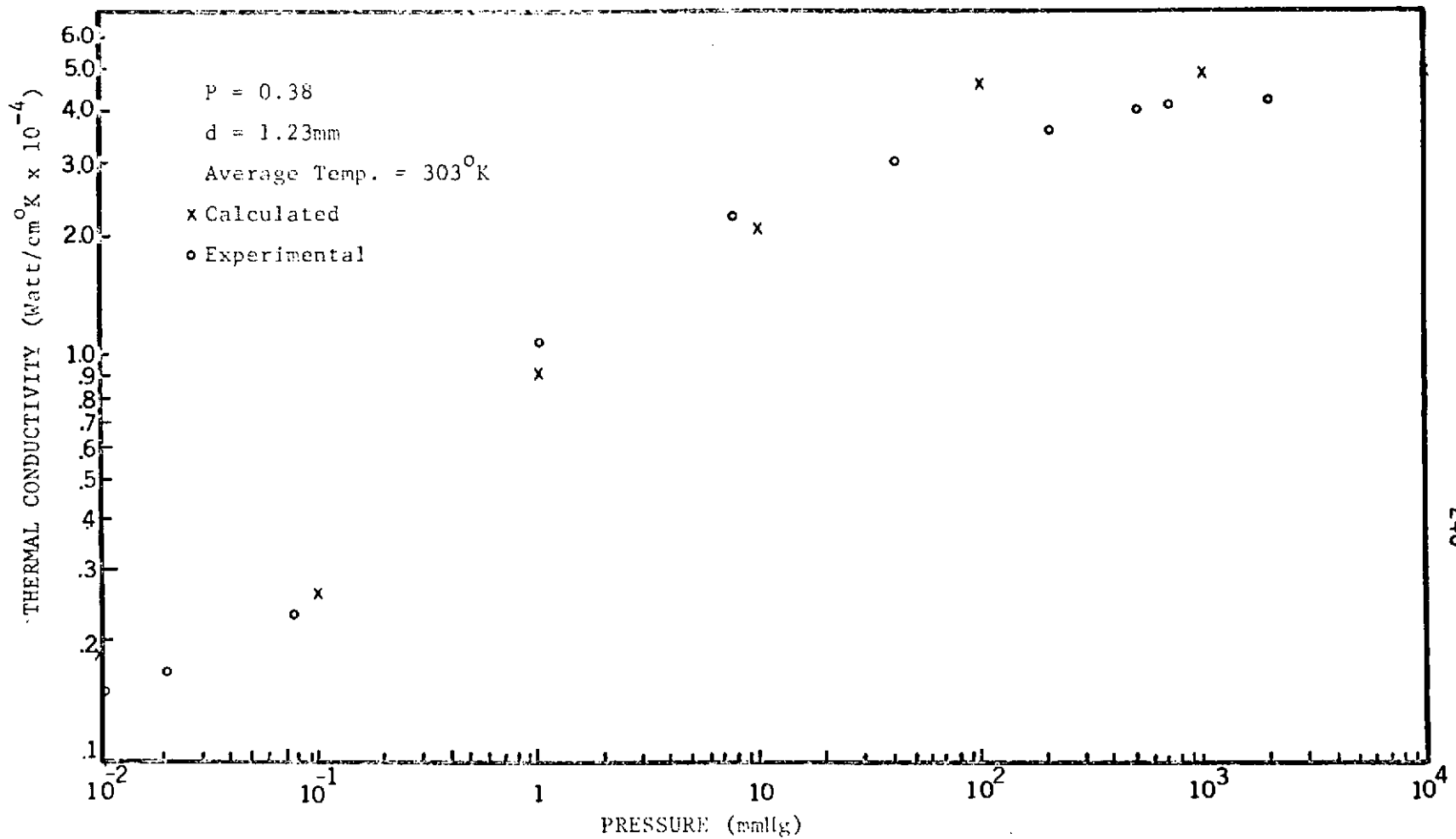FIGURE 7-8. EXPERIMENTAL AND CALCULATED THERMAL CONDUCTIVITY OF PARTICULATE BASALT IN AIR.

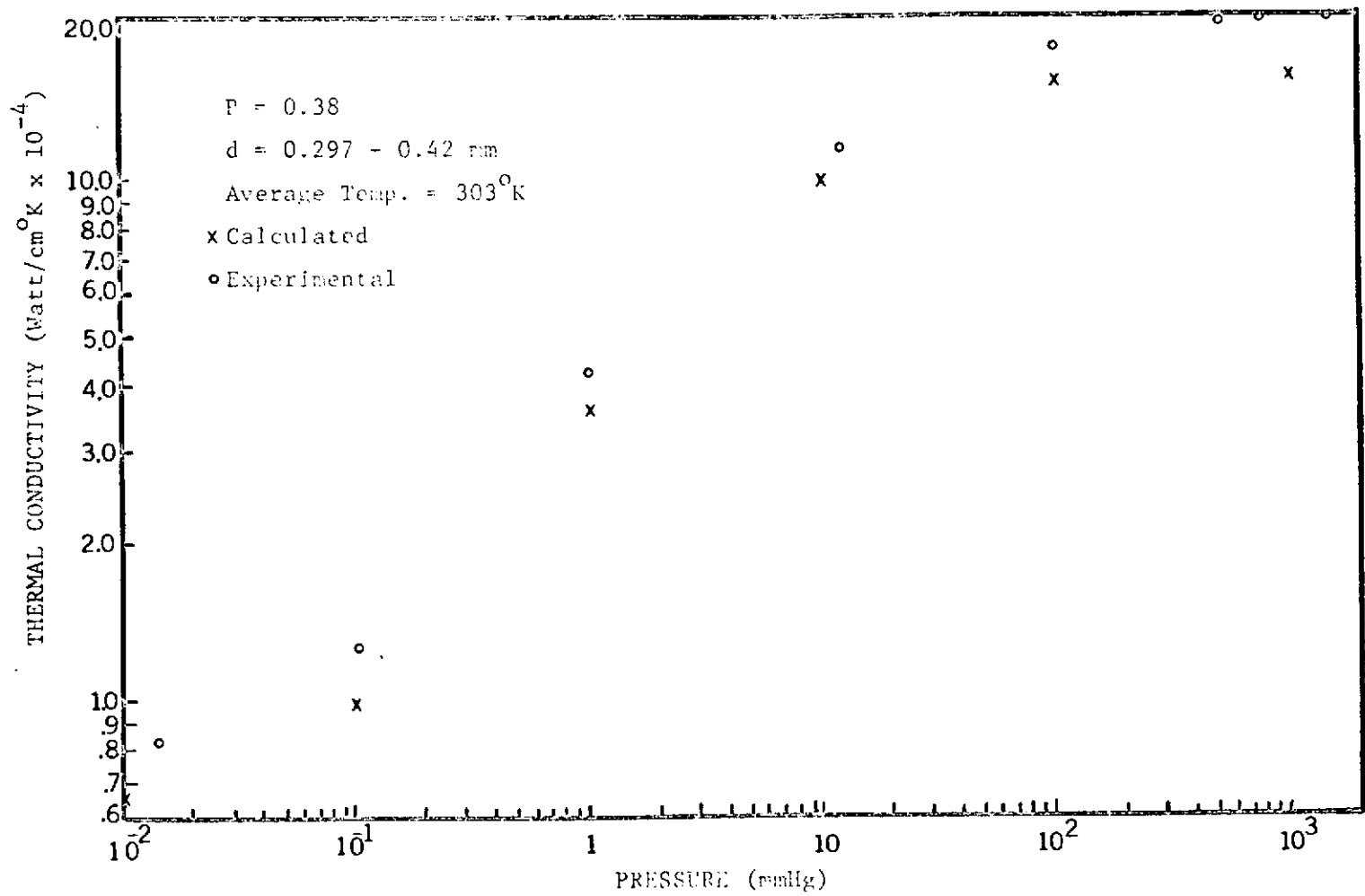FIGURE 7-9. EXPERIMENTAL AND CALCULATED THERMAL CONDUCTIVITY OF LEAD SHOT IN AIR.

FIGURE 7-10. EXPERIMENTAL AND CALCULATED THERMAL CONDUCTIVITY OF GLASS BEADS IN AIR.

# VIII. LUNAR MODEL

## Introduction

Interest in the thermal conductivity of lunar soils under lunar environmental conditions has stimulated analytical and experimental research on thermal conductivity. A problem of particular interest is the effect of lunar soil depth on the effective thermal conductivity of lunar soil samples. This section presents a model for the thermal conductivity of lunar soil as a function of soil depth as measured from the lunar surface and compares values calculated using the model with experimental data.

Before a study of thermal conductivity can be undertaken on any material the character of the material must be known. The character of the lunar surface and soil has been a mystery to man until recent years when Luna 9, Ranger 7, 8 and 9, [94] Surveyor flights [95-98] microwave and radar studies [99] and the Apollo flights have in successive steps established the character of lunar soil to some degree. The results of lunar studies to date indicate:

1. the density of the lunar outermost layer is a function of depth [100, 101].

2. the soil has a particulate structure with a mean particle size of 0.1 to 1000 m [102, 103 and 119].

3. the effective thermal conductivity as determined experimentally [105] is a function of temperature and density and below

$10^{-3}$ torr there is negligible gaseous conduction or conduction in the voids of the soil mixture.

The papers cited above suggest the lunar soil is a heterogeneous mixture and several studies on conductivity of mixtures germane to this paper can be found in the literature. The studies [45, 106 and 107] to date, however, involve the case where conduction in the gaseous voids in the mixture is not negligible whereas conduction through the points of particulate contact is neglected. The model presented herein neglects conduction in the gaseous voids and accounts for conduction at the points of particulate contact as well as radiant interchange between particles, and conduction in the particles. The model yields effective thermal conductivity values as a function of depth, temperature, porosity, particle dimension and mechanical-thermal properties of the particles.

## Mathematical Model

The model accounts for conductive and radiative transfer in the mixture. Figure (8-1) depicts these modes [85] and it is seen that conduction occurs in the solid particles and at the points of particulate contact which give rise to contact resistance. Radiative transfer occurs between adjacent particles as well as between particles viewing each other through the voids.

Consider a unit cell taken from the bed at a depth Z, which has the same average bed porosity P. The unit cell has an effective area A, and height $\Delta Z$ as shown in Figure (8-2). If the system is regarded
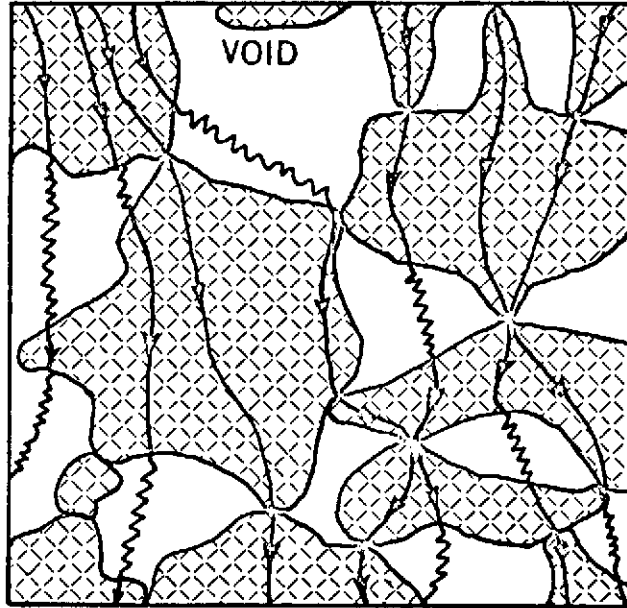
FIGURE 8-1. POSSIBLE MODES OF HEAT TRANSFER IN
LUNAR SOIL.

as homogeneous, the heat flux can be expressed by Fourier-Biot relation

$$\frac{Q}{A} = - k_e \frac{\Delta t}{\Delta Z} \qquad (8-1)$$

where $k_e$ is the effective thermal conductivity. This effective thermal
conductivity is a function of

    a.  particle size
    b.  porosity
    c.  depth below the surface
    d.  solid particle mechanical-thermal properties

The heat flux equation must account for the heat transfer modes shown
in Figure (8-1) and therefore the effective conductivity is the equivalent
of two conductances in parallel. These two parallel conductances
are

    1.  Conduction through and between solids consisting of

        a.  conduction in the solid and
        b.  conduction at the points of "particulate contact in
            series"

    2.  Radiation between surfaces.

Each of these conductances in terms of their reciprocals will be
developed and then synthesized to yield the effective thermal
conductivity. In order to obtain a simplified system which will
permit calculations of these conductances the particles will be simulated
by spheres with an effective diameter d.

## Conduction Through and Between Solids

Conduction in the Solid.

The resistance in the solid is obtained from the integration of
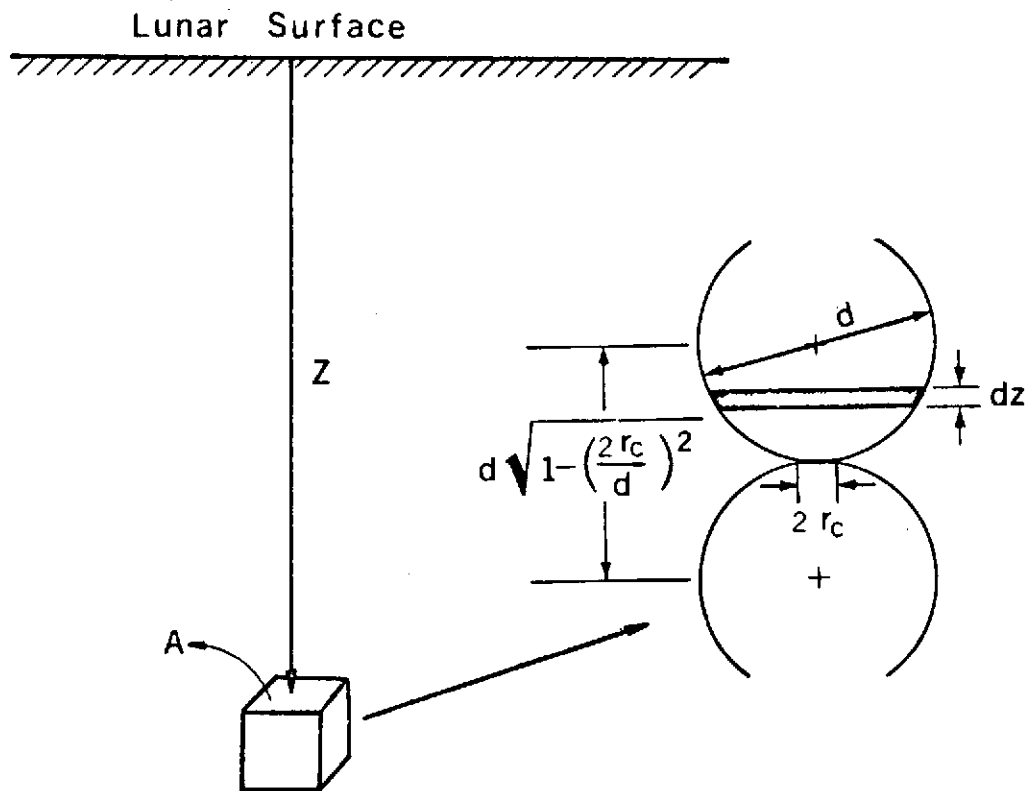the resistance through a disk of thickness dZ, as seen in Figure (8-2).

FIGURE 8-2. MODEL FOR THE STUDY OF THE THERMAL
CONDUCTIVITY OF LUNAR SOIL.

Thus

$$R_1 = \int_{-Z_1}^{Z_1} \frac{dZ}{k_s \pi (d^2/4 - Z^2)} = \frac{4}{\pi k_s d} LN \left( \frac{1 + \sqrt{1 - (2r_c/d)^2}}{1 - \sqrt{1 - (2r_c/d)^2}} \right) \quad (8-2)$$

where Z is measured normal to the contact surface from the center of the sphere and $Z_1 = \frac{d}{2} \sqrt{1 - (2r_c/d)^2}$, when deformation of the particle is neglected.

Conduction at the Points of Particulate Contact

The expression for thermal resistance at the point of particulate contact can be determined from the solution of the temperature distribution using the Hankel transformation and the analysis yields the same result as that appearing in the classical work of electric contacts [108] and will not be elaborated here. The contact resistance can be written as

$$R_c = \frac{1}{2k_s r_c} \quad (8-3)$$

where $r_c$ is the radius of the contact area and an expression for $r_c$ will be developed later. Equation (8-3) will give erroneous results if the ratio, $2r_c/d$ is large since equation (8-3) is derived based on the assumption of a semi-infinite body. This problem can be overcome by considering the analogous case of electrostatic capacitance [109] and one can write the equation for thermal contact resistance as

$$R_c = \frac{1}{2k_s r_c} (1 - \frac{2r_c}{d}) \quad (8-4)$$

The radius of the contact area must be determined. This radius is a function of the depth of the particles below the surface of the material for the case of lunar soils. The analysis to determine the radius of the contact area was made by assuming the area of contact to be small compared with the size of the spheres. This assumption is reflected in Equation (8-4) and allows one to consider the contact area to be that of the contact between two semi-infinite solids. Also, it was assumed that the spheres had smooth surfaces. Considering material deformations to be elastic under small applied loads, Hertz's equation [110],

$$r_c = \left[ \frac{3}{8} \frac{F_1 (1-\nu^2) d}{E} \right]^{1/3} \tag{8-5}$$

gives the radius of the contact area. $F_1$ is due to the weight of the particles above the contact plane. However, studies of the lunar soil density by Jones [101] show that the density is also a function of depth due to the change in material, packing and porosity. Accordingly $F_1$, will be given as

$$F_1 = A \int_0^Z \rho(Z) g \, dZ \tag{8-6}$$

where A is the effective area depending on the porosity of the material and will be determined. Substituting this relation into Equation (8-5) gives the radius of contact area as

$$r_c = \left[\frac{3d\ g(1-\nu^2)}{8E}\ A \int_0^Z \rho(Z)dZ\right]^{1/3} \tag{8-7}$$

with the contact area as an implicit function of the depth Z. However for paactical calculations the density function for relatively small depths of soil can be replaced by an average density, $\bar{\rho}$, to give

$$\frac{r_c}{d} = \left[\frac{3g\ A\ \bar{\rho}(1-\nu^2)}{8E\ d^2}\right]^{1/3} Z^{1/3} \tag{8-8}$$

Combining Equation (8-8) with Equation (8-4) yields the expression for contact resistance as

$$R_c = \frac{1}{k_s\ d}\left[\frac{1}{S} - 1\right] \tag{8-9}$$

where

$$S = 2\left[\frac{3g\ \bar{\rho}\ A\ (1-\nu^2)}{8E\ d^2}\right]^{1/3} Z^{1/3} \tag{8-10}$$

## Radiation Between Surfaces

For beds of small sized particles in a vacuum the solid conductivity is small, however the relative contribution of radiation to the heat transfer may be quite significant even at low temperature ranges (100°K - 500°K). When radiant energy impinges on particulate media, it may be reflected, transmitted through the particles or void space, absorbed by the particles and later re-radiated or scattered by the

particle surface. In the case of small particles, scattering of radiation is likely to occur. The phenomenon of absorption is intimately tied to the physical properties of the material and is influenced by the emissivity of the particle and the "absorption cross section". Similary, the transmission of energy depends on the physical characteristics of the material. The complexity of the geometry over which these transmission processes take place is one of significant difficulty in evaluating the contribution of the radiant mechanisms. However, many investigators have analyzed radiation through porous and particulate media and obtained the effective contribution of radiation made without considering the phenomena of abosrption and scattering in detail [111]. Instead an approximate analysis is considered for evaluating the radiative transport by using the "discrete model" of Wesselink [1]

$$q_r = \frac{4\sigma_b \; e(T) \; T^3}{[2 - e(T)]} \; D_p \; \frac{\Delta t}{\Delta Z} \tag{8-11}$$

where $D_p$ is the mean spacing between particles and is related to the pore size. The size of a pore is difficult to specify in a system of particles in general because of the complex shapes of these particles. Even in the simplest system comprised of uniform regularly packed spheres, there is no single dimension which will characterize the cross-section of the pore. However based on Reference [1] L can be related to the porosity of the material by

$$D_p = \frac{d}{(1-P)} \qquad (8\text{-}12)$$

which yields a radiative thermal conductivity component $k_r$, as

$$k_r = \frac{4\sigma_b\, d}{(1-P)} \; \frac{e(T)\, T^3}{[2 - e(T)]} \qquad (8\text{-}13)$$

## Effective Thermal Conductivity

The effective thermal conductivity compatible with Equation (8-1) can now be written remembering that the expressions for the resistance in each particle and the contact resistance are summed and the result is then taken in parallel with the resistance accounting for radiative transfer between particles. First the sum of the conductive resistances is written using Equation (8-2) and (8-9) to give

$$R_c = R_1 + R_c = \frac{1}{k_s d} \left[ \frac{4}{\pi} \, LN \left( \frac{1 + \sqrt{1-s^2}}{1 - \sqrt{1-s^2}} \right) + \left( \frac{1}{S} - 1 \right) \right] \qquad (8\text{-}14)$$

Equation (8-14) must be summed from 0 to Z to account for the interaction of all particles from the surface to the point in question. Thus,

$$\overline{R}_c = \frac{1}{Z} \int_0^Z R_c(Z) \; dZ \qquad (8\text{-}15)$$

gives the mean conduction resistance which yields

$$k_c = \frac{\Delta Z}{A\, \overline{R}_c(Z)} = \frac{d\sqrt{1 - s^2}}{A\, \overline{R}_c(Z)} \qquad (8\text{-}16)$$

for the conduction component of the thermal conductivity $k_e$.

The area A is determined from the unit cube shown in Figure (8-2). The porosity by definition is $1 - V_s/V$ where $V_s$ is the volume of solid material and V is the composite volume. Since $\Delta Z$ is taken as $d\sqrt{1 - s^2}$, the area of this cube is related to the porosity by

$$P = 1 - \frac{\pi}{6} \frac{d^2}{A\sqrt{1-s^2}} \tag{8-17}$$

where

$$A = \frac{1}{6} \frac{\pi d^2}{(1-P)\sqrt{1-s^2}} \tag{8-18}$$

Equations (8-16) and (8-18) result in

$$k_c = \frac{3(1-P)\ (1-c^2\ z^{2/3})\ k_s}{\left[\frac{\pi}{2}\ (\frac{3}{2c\ z^{1/3}} - 1) + (4-1.2c^2\ z^{2/3})\right]} \tag{8-19}$$

where

$$C = 2\left[\frac{q\ \bar{\rho}}{16E}\ \frac{(1-\nu^2)}{(1-P)}\right]^{1/3} \tag{8-20}$$

Combining this result with that for the expression for the radiative thermal conductivity component, Equation (8-13) yields the effective thermal conductivity $k_e$ as

$$k_e = \cfrac{3(1-P)\ (1-c^2\ z^{2/3})\ k_s}{\left[\dfrac{\pi}{2}\ (\dfrac{3}{2c\ z^{1/3}} - 1) + (4-1.2\ c^2\ z^{2/3})\right]}$$

$$+ \frac{4\sigma_b\ d}{(1-P)}\ \frac{e(T)\ T^3}{\left[2 - e(T)\right]} \tag{8-21}$$

## Application of the Model

Equation (8-21) was compared with experimental data taken with lunar soil samples from the Apollo 11 and 12 flights. Application of the model is dependent on knowing the values of certain physical properties and characteristics of the sample to be evaluated. The only property or characteristic of the lunar soil directly measured in the Apollo experiments applicable in Equation (8-21) was the sample density. Thus the values of the other properties and characteristics had to be approximated. The approximation process was based on the similarity of lunar soil to terrestrial basalt. This similarity has been demonstrated by Snoddy et al. [112], the Surveyor alpha-scattering experiments [113] and as a result of Apollo 12 [114] studies. Table 8-I compares the major and minor elements of Apollo 12 samples and terrestrial basalt and shows that there is substantive evidence to support the approximations. The properties and characteristics selected for inclusion in Equation (8-21) were

1. Solid particles density, modulus of elasticity, solid thermal
   conductivity and Poisson's ratio.

   $\rho$ = 2830 dg/m$^3$  Reference [64]

   $E$ = 2.2 x 10" N/m$^3$ calculated from data given in Reference [115]

TABLE 8-I.  COMPARISON OF MAJOR AND MINOR

ELEMENTS OF APOLLO 12 SAMPLES

AND TERRESTRIAL BASALT.

| Element Oxide | Lunar Fines % | Basalt % |
|---|---|---|
| $Si O_2$ | 47.2 | 51 |
| $Al_2O_3$ | 14.3 | 14 |
| $Fe_2O_3$ | 0.0 | 3.4 |
| $Fe\ O$ | 14.2 | 8.8 |
| $Mg\ O$ | 9.28 | 4.4 |
| $CaO$ | 10.6 | 8. |
| $Na_2O$ | 0.66 | 3.4 |
| $K_2O$ | 0.41 | 1.7 |
| $H_2O$ | 0.0 | 0.86 |
| $Ti O_2$ | 2.48 | 2.7 |
| $P_2O_5$ | 0.52 | 1.4 |
| $M_n O$ | 0.19 | 0.25 |
| $Cr_2O_3$ | 0.32 | |
| $CO_2$ | | 0.03 |
| $S$ | | 0.004 |

$$K_s = 1.324 \text{ watt/m K} \quad \text{Reference } [64]$$

$$\nu = 0.2 \quad \text{Reference } [116]$$

2. Emissivity

The hemispherical emittance as function of the temperature given by Reference [121] was used. It shows that the emissivity changes from approximately 0.98 at 80 K to 0.92 at 440 K.

3. Depth-density relationship

Matveev [100] proposed a model for the relation between the density of the outermost lunar layer and the depth as

$$\rho = \rho_\infty \left[ 1 + \left( \frac{\rho_0}{\rho_\infty} - 1 \right) \exp - \frac{Z}{Z_0} \right] \tag{8-22}$$

while Jones [101] modified this model to an approximate similar equation as

$$\rho = \rho_\infty \left/ \left[ 1 + \left( \frac{\rho_\infty}{\rho_0} - 1 \right) \exp - \frac{Z}{Z_0} \right] \right. \tag{8-23}$$

where $\rho_\infty$, $\rho_0$ and $Z_0$ are given constants [101]. Each model seems to satisfy the known physical requirements indicated by the presently available experimental data. These models together with the experimental data of Jaffe [94], Christensen et al. [97], Campbell et al. [122] were used to approximate the depth Z, for a given density.

## 4. Particle Diameter

Unfortunately, there is no method developed in the literature to specify the particle diameter to be used in conjunction with any theoretical model for the thermal conductivity of a natural sample of granular material with a diverse range of particle sizes. As an example, Figure (8-3) shows different arrangements A and B of six particles of two different sizes which will give different porosities and thermal conductivities while they give the same particle size distributions. It is an important fact that when the system of granular material is modeled theoretically, the size of the particle should be based on an experimental simulation of the natural sample. If, for example, one needs a representative particle diameter to calculate the thermal con- ductivity of a lunar sample of particle sizes from 0.1 to 1000 $\mu$m [119], one should conduct the following experiment: 1) Determine experimentally the conductivity of the lunar sample; 2) Separate the lunar sample into n samples with each of the n samples having the same particle size; 3) Determine experimentally the conductivity of each of the n samples; 4) Compare the conductivity value of the original lunar sample with each of the n samples and 5) Select a representative particle diameter for the original sample on the basis of the closest agreement of the original sample conductivity with the conductivity of one of the n samples. This diameter is then correlated to one of the statistically defined particle sizes obtained from the natural sample size-distribution data (the median, the mean, the mode, etc.). In this way, a correlation will specify the particle diameter to be used in the theoretical equation
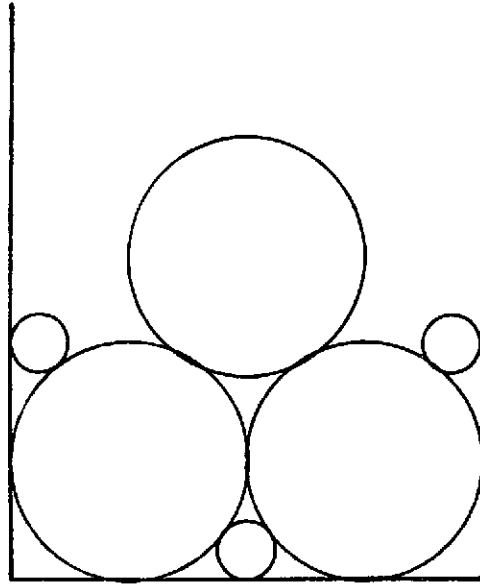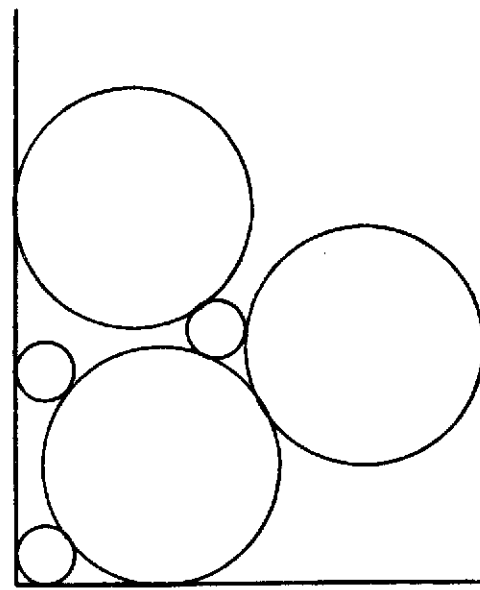
FIGURE 8-3. DIFFERENT ARANGEMENTS OF SIX PARTICLES OF TWO
DIFFERENT SIZES.

for determining the thermal conductivity of any other natural sample or material in site without the necessity of performing the previously described experiment again. The experimental values of Fountain and West [123] for basalt samples of particle sizes from 37 to 62 $\mu$m diameter and density of 1.3 g/cm$^3$, showed fairly good agreement with lunar sample data of Apollo 11 [105] at a density of 1.265 g/cm$^3$. Since the range of the particle sizes of [123] is very narrow compared to the lunar material range, an average diameter of 50 $\mu$m was used in the theoretical model. It is noted that the diameter chosen is approximately in the range of the median diameter (50%) based on a weight distribution of lunar samples analyzed by [124], [125] and [126].

Values of conductivity from equation (8-21) using the aforementioned physical properties and characteristics are compared with the data from Apollo 12 lunar soil samples in Figure (8-4). The Apollo 12 data are for sample 12001/9 having a density of 1.3 gr/cm$^3$ as determined by Cremers and Birkebak [105]. The depth at which this density most probably would occur was calculated to be 1.02 cm. This depth was based on the average value for the depth obtained using Equation (8-22) and (8-23). The data for Apollo 11 are shown in Figure (8-5) with the results of Equation (8-21). The Apollo 11 sample had a density of 1.265 gr/cm$^3$ as determined by Cremers et al. [127] and this density corresponds to a lunar soil depth of .96 cm. The model is seen to give satisfactory results.

A critical evaluation of the model requires considerable
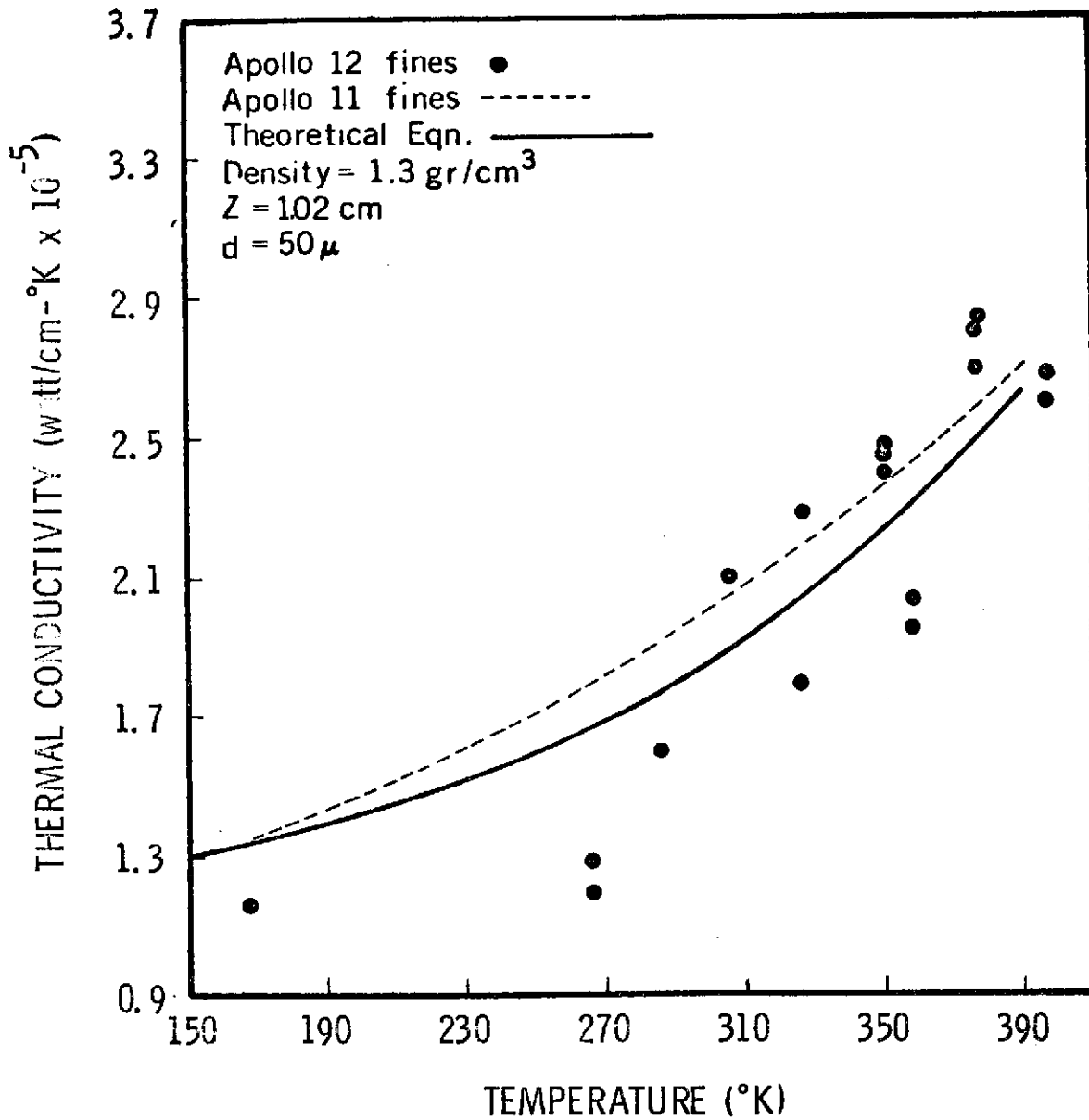
FIGURE 8-4. THERMAL CONDUCTIVITY OF APPOLO 12 FINES COMPARED WITH THE THEORY AT A DENSITY OF 1.3 GR/CM$^3$.
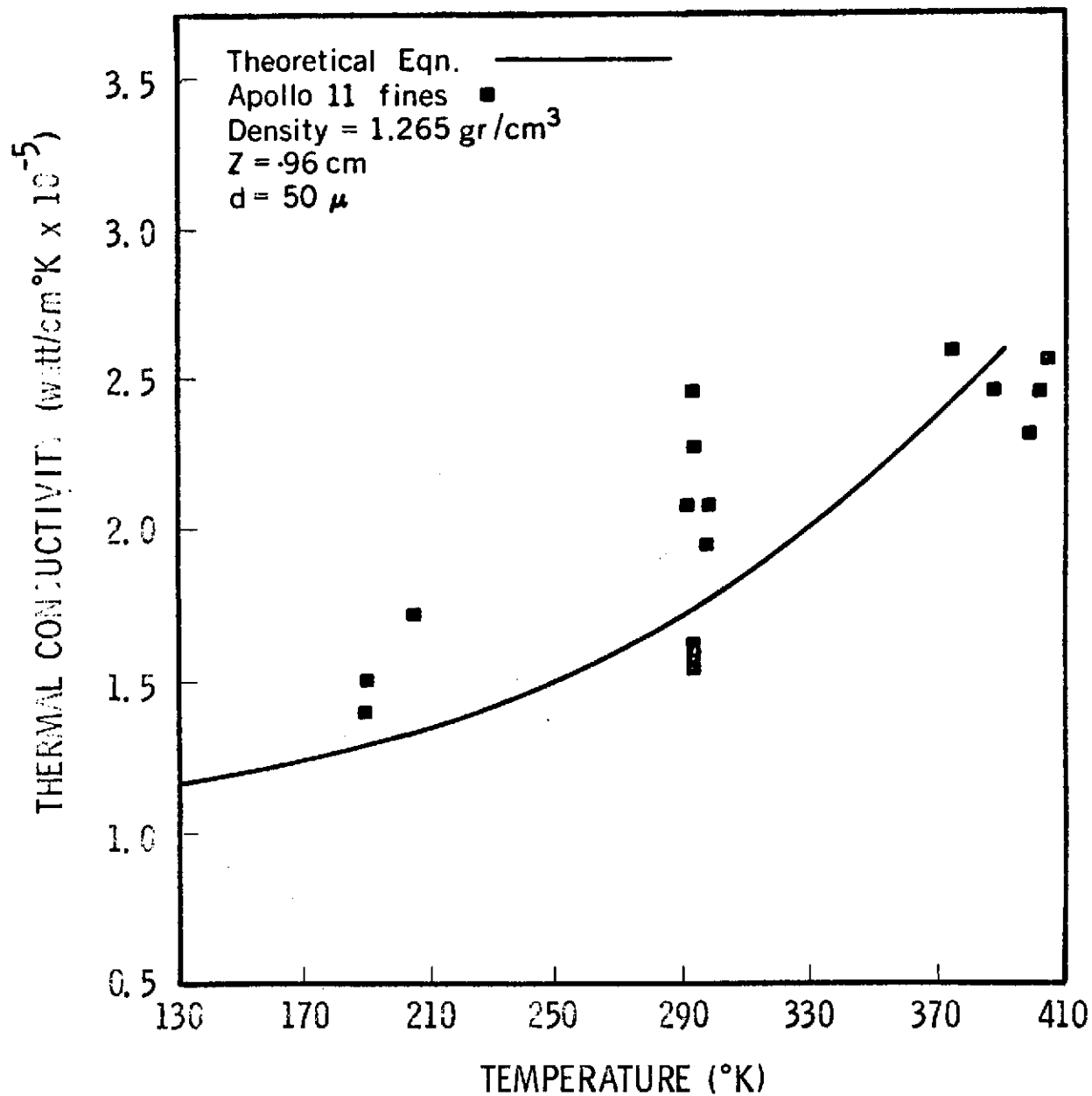
FIGURE 8-5. THERMAL CONDUCTIVITY OF APPOLO 11 FINES
COMPARED WITH THE THEORY AT A DENSITY OF
1. 265 GR/CM.

additional data. However the model can be examined from a number of viewpoints. Figures (8-6), (8-7), and (8-8) display thermal conductivity for lunar soils as a function of the variables. Figure (8-6) represents the behavior of the effective thermal conductivity at constant temperature as the depth and density increase. As one expects as the depth increases the contact area between particles increases due to the increase in the loading and consequently smaller thermal contact resistance results and in turn thermal conductivity increases. For fixed temperature, the effective thermal conductivity is plotted against the density for various depths in Figure (8-7). For high values of z and the density, the effective loading increases and in turn increases the effective conductivity of the soil. Figure (8-7) shows the thermal conductivity as a function of the temperature with the density as a parameter. As one notices from Equation (8-21) the dependance on the temperature is a consequence of radiation effects, which result in higher values of conductivity at high values of temperature. As seen from Figure (8-8) curves of different densities cross each other at different temperature. This is explained by the fact that the radiation in a system of small density (high porosity) is more effective than for a system of high density. Also the model indicates that radiation is a strong function of the particle diameter which was indicated by Watson [128]. Additionally Equation (8-21) shows that the effective thermal conductivity is dependent on the gravitational constant, g. Accordingly a lunar sample will possess higher values of thermal conductivity under the gravitational influence of earth, than it will under the lunar gravitational environment.
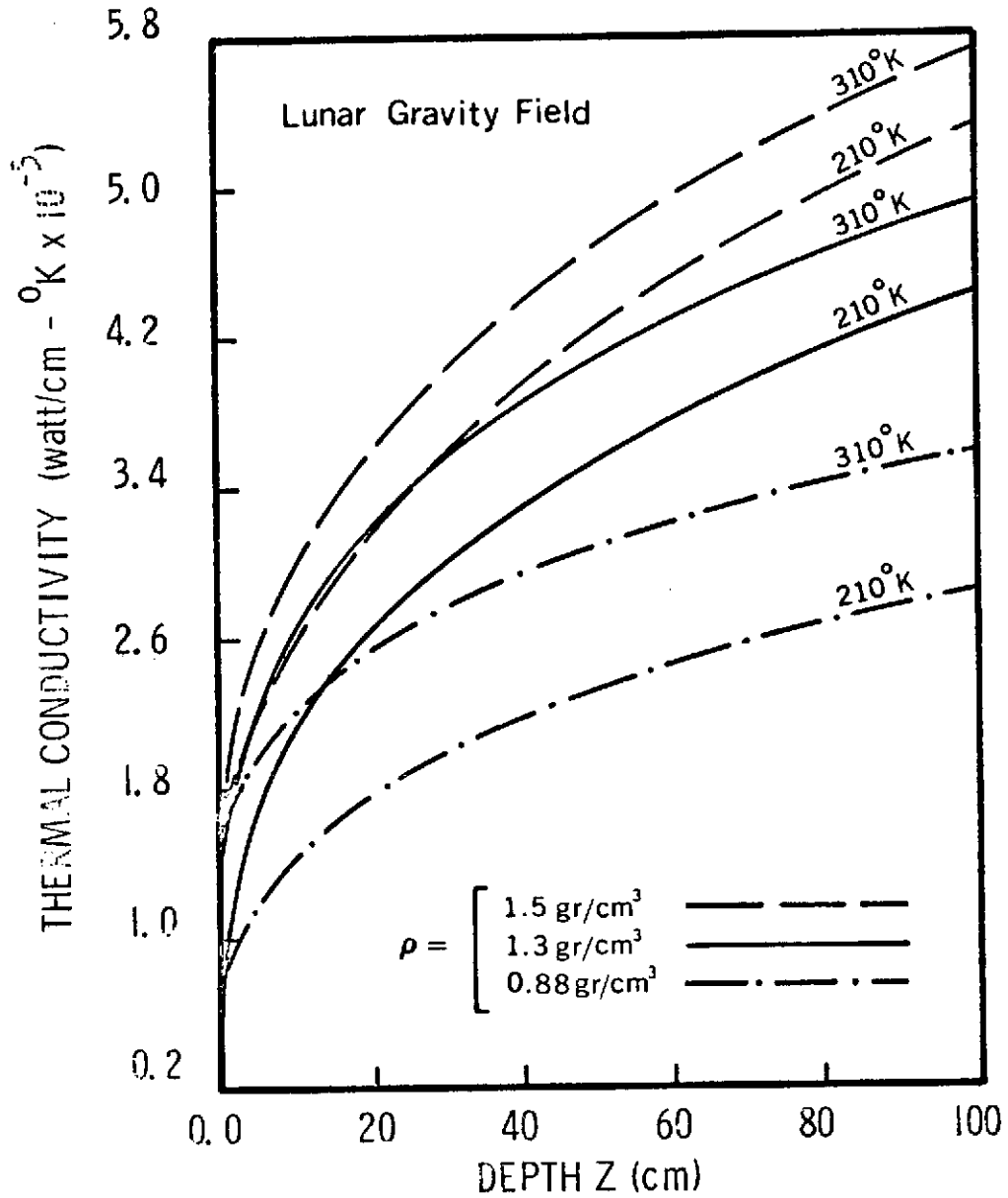
FIGURE 8-6. LUNAR CONDUCTIVITY AS A FUNCTION OF DEPTH AT CONSTANT TEMPERATURE AND DENSITY.
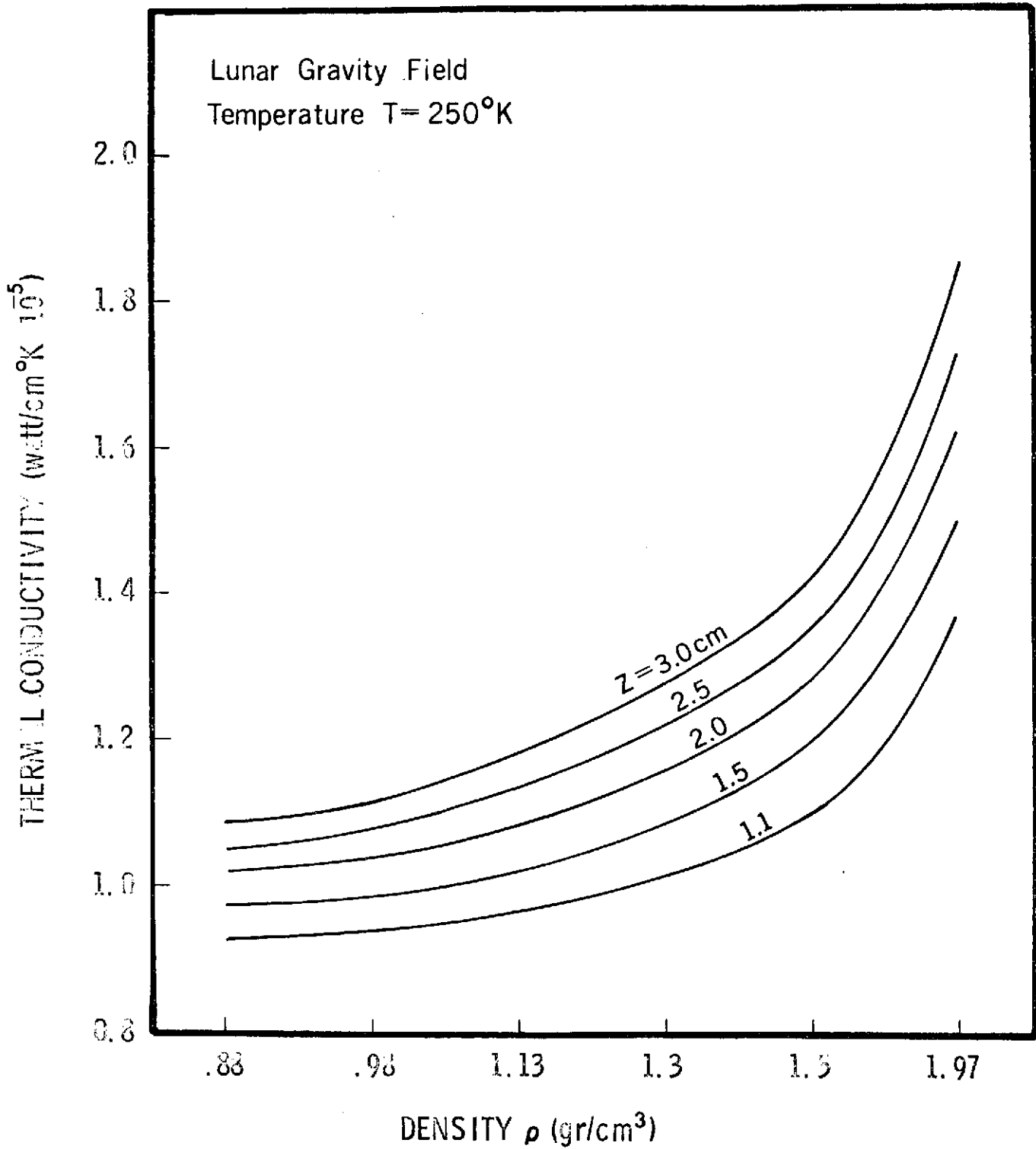
FIGURE 8-7. LUNAR THERMAL CONDUCTIVITY AS A FUNCTION OF
DENSITY AT CONSTANT TEMPERATURE OF 250 K.
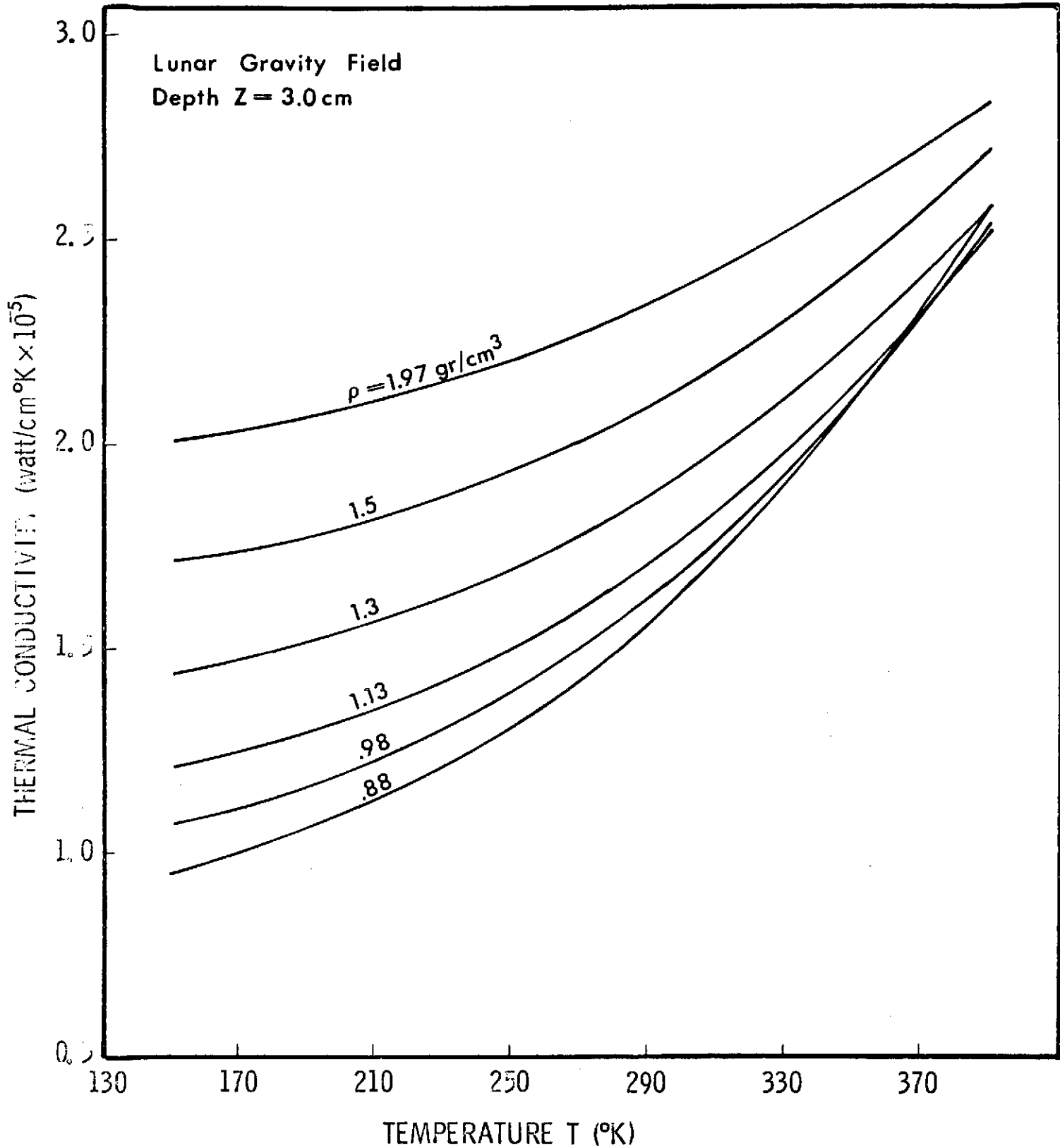
FIGURE 8-8. LUNAR THERMAL CONDUCTIVITY AS A FUNCTION OF TEMPERATURE AT CONSTANT DEPTH AND DENSITY.

The theory assumed that the particles are arranged in a simple square lattice which results in two contact areas in the direction of the heat flow, however by knowing the nature of packing of the soil, a more realistic approximation of the number of contacts can be found. With a complete analysis of the forces between particles, a more accurate estimation of the contact area can be obtained.

## IX.  GENERAL COMPARISON AND DISCUSSION

Four models have been developed in this study, each utilizing different propositions.  The parallel isotherms model, the stochastic model, and the nodular model have been applied to a wide range of granular materials at pressures ranging from atmospheric to vacuum. The lunar model has been developed and applied specifically to granular materials at a simulated lunar environment and to lunar fines.  Each of these models will now be evaluated with respect to the assumptions introduced in its development and with respect to the discrepancy between experimental and predicted thermal conductivities.

A careful review of the previously published correlations showed that the discrepancy between the analytical model and the physical granular system could be attributed to one of the following causes:

1.  Failure to account for solid to solid contact;

2.  Failure to utilize a realistic distribution of the two phases;

3.  Failure to utilize realistic heat flow assumptions.

It is thus expected that for any new model to constitute an imorovement over existing ones, these causes of failure should be eliminated. Consequently, the models presented on this study will be discussed on this basis.

The parallel isotherms model has utilized results of the packing theory to the problem of heat transfer in granular materials so that an accurate distribution of the two phases may be obtained. The description of heterogeneous materials as random mixtures of the two phases has been verified experimentally [5, 51], and has been applied by Tsao [8] to the problem of heat transfer. Two statistical parameters are introduced in the final expression for the effective conductivity, namely the mode, $\mu$, and the standard deviation, $\sigma$, of the one dimensional porosity. The mode $\mu$ is set equal to the bulk solid fraction on the basis of physical arguments. In order to determine $\sigma$, the experimental data on the effective conductivity available from the literature have been used, and have been curve fitted to obtain $\sigma$ as a function of the bulk solid fraction. Consequently in this model a realistic material distribution, as outlined in the packing theory has been introduced. In addition, good agreement between calculated and experimental thermal conductivities indicates that the unrealistic heat flow assumption has been countered by the experimentally based selection of $\sigma$.

This model has been applied to granular materials at atmospheric pressures and to basalt fines in a simulated lunar environment. For the granular materials listed in Table 6-I the average error, bias, and variance of the calculated values is 17.8%, -3.7% and 0.0236, respectively. For the data on basalt fines given by Fountain and West [3] the average error, bias and variance of the calculated values is 11.3%, -8.5% and 0.0061 respectively, as indicated in Table 9-I.

Finally, it should be noted that for granular materials at atmospheric pressures the only data required by this model is the conductivities of the constituents, and the bulk porosity of the material. At reduced pressures, the average particle diameter, the gas pressure, the gas Prandtl number, the solid emissivity and the temperature are additional required data.

The stochastic model utilizes essentially the same expressions for the distribution of the two phases in granular materials. Moreover, it is noted that the parallel isotherms and uniform heat flux assumptions are analogous to that of assuming zero and infinite resistances, respectively, normal to the direction of the bulk temperature gradient. It is then argued that since the transverse thermal conductivity of granular materials lies somewhere between the limits of zero and infinity, it follows that the true effective thermal conductivity of such materials can be represented as a weighted average of the conductivities calculated utilizing the parallel isotherms and uniform heat flux assumptions.

The standard deviation $\sigma$ is still an unknown. However it has been demonstrated that as $\sigma$ increases, both limiting conductivities approach a constant value which depends on the constituent conductivities and the bulk solid fraction only. As a result three correlations have been developed relating calculated conductivities to experimental data. The first is expressed as a correction factor for nonparallel isotherms, the second as a correction factor for nonuniform heat flux, and the third is a weighting factor for the bounding equations.

Consequently, the stochastic model introduces (1) at least point contact between particles, (2) a realistic material distribution as outlined by packing theory and (3) it overcomes the previous unrealistic heat flow assumptions. The model has been applied to granular materials at atmospheric pressures and to basalt fines in a simulated lunar environment. The comparison between predicted and experimental thermal conductivity values is summarized in Table 9-I. The input data required for the calculation of the effective conductivities are exactly the same as the data required for the parallel isotherms model.

In the nodular model developed in Chapter 7, the geometry of a unit cube of the heterogeneous mixture was characterized by the random distribution of the two phases. It was effectively assumed that no cubicle is more likely to be occupied by the solid phase than another. Further, it was noted that application of the three-dimensional Fourier conduction equation to each cubicle simply requires that the temperature of each cubicle remain constant. The cubicles were then lumped into nodes, connected with the neighboring nodes by resistances, the value of which depends on the conductivity of the neighboring nodes. Contact resistance was included in all cases, and radiant conductivity was included only for granular materials at reduced pressures. A heat balance equation was then written for each node, and this system of equations was solved by a successive overrelaxation technique, superimposing on it an iterative scheme, to determine the temperature of each node. Finally, the heat flow in each lamina perpendicular to the mean heat flow direction was determined, and the mean heat flow value in conjunction

with the Fourier-Biot law were used to find the effective thermal conductivity of the heterogeneous mixture.

It is evident that in this manner all causes contributing to the failure of previously published models have been eliminated since this model introduces (1) solid to solid contact resistance, (2) realistic distribution of the two phases based on the packing theory and (3) realistic three-dimensional heat flow as defined by the Fourier equation for steady-state heat conduction. The model has been applied to granular materials for pressures ranging from atmospheric to vacuum, and the comparison between predicted and experimental thermal conductivity values are summarized in Table 9-I. In addition to the input data required by the previous models, knowledge of the depth, density of the solid phase, Young's modulus and Poisson's ratio of the solid particles is required.

As is has already been mentioned, for granular materials "in vacuo" the modes of heat transfer are

1. Conduction in the solid particles;

2. Conduction at the contact areas between particles;

3. Radiation between particle surfaces.

The lunar model developed in Chapter 8 has synthesized these modes to yield the effective thermal conductivity. For the mathematical analysis of the model a regular array of spherical particles was assumed, and the calculation of the conduction in the solid particles was based on parallel isotherms. Further, the effect of depth on the effective thermal conductivity of granular materials was included both in the calculation

of the contact resistance, and through published expressions correlating

the density of lunar fines to the depth from the surface of the moon.

Thus, the final expressions include both the effect of lunar soil

depth and the effect of temperature on the effective thermal conductivity

of lunar fines.

The lunar model has been applied to Apollo 11 and 12 lunar fines.

Comparisons between predicted and experimental conductivity values are

summarized in Table 9-I.

Although the models presented in this study are applicable, and

have been applied to granular materials over a wide range of environ-

ments, there exists a number of limitations due to the assumptions

introduced in the development of the models. The causes of these

limitations will now be discussed.

1. Phase distribution - The geometry of three of the models has

been based on the assumption that irregular packed beds can be con-

sidered as a random mixture of the two phases. It has been shown

[49, 50, 51] that for granular materials in which the particle sizes

are not much different, and in which the particles can be approximated

by spheres, this is a valid assumption. That is, for such beds,

the distribution of the local bed properties can be approximated by

a normal distribution. For packed beds consisting of irregularly

shaped particles no generalized conclusions have been reached in the

literature concerning the distribution of the local properties. It

has been shown, however, that the geometry of packed beds of irregularly

shaped particles does not satisfy the randomness criteria when the particle size distribution is narrow [51]. It is therefore possible that the geometry of certain classes of granular materials is different than the assumed geometry.

2. **Particle size distribution** - Calculations for the unit cube size, pore size, etc. have been based on a characteristic particle size. For packed beds in which the particle size distribution is narrow, it has been assumed by all models in this study that the characteristic particle size is equal to the mean volume diameter [66]. However, no set method exists in the literature for calculating the characteristic particle size for beds having a broad particle size distribution. Further, as indicated in Chapter 8 and in Appendix F the mean volume diameter is not a satisfactory description of the characteristic particle size for such beds.

3. **Particle shape** - The geometrical parameters utilized in the development of the models such as pore size, coordination number, etc., and the equations for contact resistance have been based on equations given in the literature for randomly packed beds of equal sized spheres. It follows that none of the models presented in this study is applicable in the case of heterogeneous mixtures containing highly irregular shaped particles  such as Rashing rings, Berl saddles, etc.

4. **Solid-liquid heterogeneous mixtures at high temperatures** - The equations for the radiant conductivity used by all models have been based on the assumption that the medium in the voids is transparent.

Consequently, when the continuous phase in the voids is a liquid these equations are not valid, and radiant conductivity cannot be taken into account.

5. Convection - As indicated in the Introduction, convection heat transfer in the voids has been neglected. Consequently, the models of this study are only applicable on stagnant packed beds.

6. Anisotropy - In all models of this study, granular materials have been treated as equivalent homogeneous and isotropic single phases, so that no change in the thermal conductivity with direction is predicted. The assumption of random mixtures of the two phases justifies this treatment. It appears that for such systems, the only factor contributing to the variation of the thermal conductivity with direction is the pressure tensor, and consequently the different values of the contact resistance in the vertical and horizontal directions. This case has not been examined in this study.

7. Wall effects - As indicated in [49] and [120] both the local property variation, and the thermal conductivity of heterogeneous mixtures change at short distances from the walls of the container. Again, this case has not been examined in this study.

It can be seen that all limitations are basically due to two factors: (1) Insufficient knowledge of the geometric configuration of packed beds and (2) insufficient knowledge of the parameters associated with radiation heat transfer in packed beds. All assumptions introduced in the development of the models is an attempt to circumvent these difficulties in such a manner that the models constitute a

realistic approximation to the actual physical phenomena.

A comparison between Tables 9-I and 9-II indicates that for granular materials at atmospheric pressures the models presented in this study are generally more accurate than previously published models. This is probably due to the attempt undertaken in this study to combine a realistic geometry with realistic heat flow. It is also a strong indication that the flexible random phase distribution constitutes a better approximation to the actual geometry of granular systems than the fixed arrangement of spherical or near spherical particles utilized by previously published models.

Table 9-I also indicates that for granular materials at reduced interstitial gas pressure, thermal conductivities predicted by the models of this study are generally low. The sources of error are as follows:

1. Exclusion of pure radiation heat transfer at very low pressures;

2. Low calculated values for the contact resistance;

3. Deviation of the actual distribution of the two phases from the assumed random phase distribution.

As indicated in Appendix B, lack of experimental data on the extinction coefficient of granular materials prohibits an exact analysis of the radiation heat transfer process. As a result, only radiation heat transfer between particle surfaces has been included in the models. As indicated in [84, 85] this is a sufficiently accurate approximation when the solid particles are opaque to thermal radiation, but results in low calculated values for packed beds of particles having small

diameters. Consequently, since at very low pressures radiation is a dominant mode of heat transfer, exclusion of pure radiation heat transfer results in low calculated values for the effective thermal conductivity of packed beds.

For all models, the calculated thermal conductivities at low pressures and low temperatures are consistantly lower than the experimentally determined thermal conductivities. Since under these conditions the dominant mode of heat transfer is through contact areas between particles, the only explanation for this behavior is that the calculated values for the contact conductances are low. It should be noted that low calculated contact conductances influence the effective thermal conductivity only at low pressures and temperatures. At higher pressures and temperatures, and in particular at atmospheric pressures, the calculated effective thermal conductivity is relatively insensitive to the contact conductance.

Finally, it is noted that although at reduced pressures the calculated effective thermal conductivities are generally low, the slope of the calculated thermal conductivity versus pressure curves is in very good agreement with experimental data. Since for a major portion of these curves the only variable is the thermal conductivity of the interstitial gas, it can be concluded that Kennard's Equation (A-1) combined with the experimentally determined effective pore size given by Equation (D-6) yield accurate results for the variation of the gas conductivity with pressure. Consequently, as indicated in Appendix D, the conduction effective pore size is much smaller than the geometric pore size.

# TABLE 9-I

## AVERAGE ERROR, AVERAGE BIAS AND ERROR VARIANCE

## BETWEEN PREDICTED AND EXPERIMENTAL THERMAL

## CONDUCTIVITY VALUES FOR ALL MODELS OF THIS STUDY

|  | Average Error % | Average Bias % | Error Variance |
|---|---|---|---|
| 1. Parallel Isotherms Model | | | |
|    a.  Granular Materials at Atmospheric Pressures (Table 6-I) | 17.8 | -3.7 | 0.0236 |
|    b.  Simulated Lunar Data | 11.3 | -8.5 | 0.0061 |
| 2. Stochastic Model | | | |
|    i.  Equation (6-16) | | | |
|       a.  Granular Materials at Atmospheric Pressures (Table 6-I) | 30.1 | 25.3 | 0.0707 |
|       b.  Simulated Lunar Data | 24.8 | -22.1 | 0.0131 |
|    ii.  Equation (6-17) | | | |
|       a.  Granular Materials at Atmospheric Pressures (Table 6-I) | 27.7 | 20.9 | 0.0558 |
|       b.  Simulated Lunar Data | 25.8 | -23.4 | 0.0260 |
|    iii.  Equation (6-18) | | | |
|       a.  Granular Materials at Atmospheric Pressures (Table 6-I) | 32.3 | 23.1 | 0.0956 |
|       b.  Simulated Lunar Data | 41.8 | -17.2 | 0.0333 |
| 3. Nodular Model | | | |
|    a.  Granular Materials at Atmospheric Pressures (Table 7-I) | 15.8 | -5.8 | 0.0163 |
|    b.  Granular Materials at Reduced Pressures | 18.5 | -5.1 | 0.0157 |
|    c.  Simulated Lunar Data | 15.9 | -15.9 | 0.0870 |
|    d.  Simulated Martian Data | 20.8 | -20.8 | 0.0210 |

TABLE 9-I.  Continued

4.  Lunar Model
| | | | | |
|---|---|---|---|---|
| a. | Apollo 11 Lunar Fines | 13.7 | -6.8 | 0.0044 |
| b. | Apollo 12 Lunar Fines | 12.8 | 5.1 | 0.0090 |

# TABLE 9-II

## AVERAGE ERROR, AVERAGE BIAS AND ERROR VARIANCE BETWEEN PREDICTED AND EXPERIMENTAL THERMAL CONDUCTIVITY VALUES FOR GRANULAR MATERIALS AT ATMOSPHERIC PRESSURE (TABLE 6-I)

|  |  | Average Error % | Average Bias % | Error Variance |
|---|---|---|---|---|
| A. | Flux Law Models |  |  |  |
| 1. | Maxwell | 40.2 | -37.9 | 0.0606 |
| 2. | Lord Rayleigh | 33.7 | -24.8 | 0.0594 |
| 3. | Meredith and Tobias | 34.4 | -18.7 | 0.0416 |
| 4. | Bruggeman | 32.9 | 23.8 | 0.1540 |
| 5. | Nodular Model (this study) | 15.8 | -5.8 | 0.0163 |
| B. | Uniform Heat Flux Models |  |  |  |
| 1. | son Frey | 45.1 | -43.8 | 0.0599 |
| 2. | Woodside and Messmer | 34.8 | 20.9 | 0.0992 |
| 3. | Kanager | 18.9 | -6.7 | 0.0286 |
| 4. | Gorring and Churchill | 20.0 | -10.7 | 0.0192 |
| 5. | Willhite, Kunii & Smith | 17.8 | -3.6 | 0.0268 |
| 6. | Schumann and Voss | 25.8 | -21.1 | 0.0260 |
| 7. | Preston | 30.5 | 26.6 | 0.0875 |
| 8. | Wilhelm et al | 19.7 | -2.1 | 0.0373 |
| 9. | Krupiczka | 21.2 | 13.2 | 0.0693 |
| 10. | Equation (6-16) (this study) | 30.1 | 25.3 | 0.0707 |
| 11. | Bernstein | 686.1 | 677.9 | 85.05 |
| C. | Parallel Isotherm Models |  |  |  |
| 1. | Russell | 35.0 | -30.3 | 0.0566 |
| 2. | Woodside | 670.4 | 670.3 | 55.16 |
| 3. | Equation (5-2) (this study) | 17 8 | -3.7 | 0.0236 |
|  | Equation (6-17) (this study) | 27.7 | 20.9 | 0.0558 |

TABLE 9-II. Continued

D. Weighted Ohm's Law Models

| | | | |
|---|---|---|---|
| 1. Lichtenecker 3-D | 701.2 | 701.1 | 48.70 |
| 2. Lichtenecker 2-D | 195.0 | 194.5 | 2.98 |
| 3. Equation (6-18) (this study) | 32.3 | 23.1 | 0.0956 |

## X.   CONCLUSIONS AND RECOMMENDATIONS


The problem of predicting the effective thermal conductivity of heterogeneous mixtures has received the attention of numerous investigators over the past sixty years.  Unfortunately, the complexity of the mechanisms contributing toward heat flow is such that no truly satisfactory model has been obtained.  The continued proliferation of alternate models attests to these difficulties.  The scope of this study has been to utilize all available information on the subject and extend the analytical techniques of predicting the variable thermal conductivity of heterogeneous mixtures over as wide a range of environments as possible.

Initially a study was made of the published models with respect to the geometry and heat flow assumptions utilized by each one.  Further, a number of published equations for the effective thermal conductivity were applied to a large group of granular materials, and the results were evaluated in relation to the geometry and heat flow assumptions utilized in the development of each equation.  The results of this analysis can be summarized in that the sources of error in the predicted thermal conductivities can be attributed to one or more of the following causes:

1. Failure to account for solid to solid contact;

2. Failure to utilize a realistic distribution of the two phases;

3. Failure to utilize realistic heat flow assumptions.

It was therefore concluded that for any new model to constitute an improvement over existing ones, these causes of failure should be eliminated.

Since the possibility of assuming that the heat flow process in granular materials is approximately linear simplifies considerably the problem of heat transfer, this possibility was examined separately for random heterogeneous mixtures having a realistic phase distribution. The analysis presented in Chapter 4 resulted in the conclusion that a parallel isotherms assumption yields too high values for the effective thermal conductivity whereas a uniform heat flux assumption yields values that are too low. Also, the error in the predicted thermal conductivity increases rapidly with the ratio of the constituent conductivities. Consequently, either no assumption should be made regarding the flow of heat in granular materials, or weighting factors should be associated with the linear heat flow assumptions.

Four models have been developed in this study, each utilizing different approximations regarding the geometry and the flow of heat in granular materials. In the development of the models the most recent results of the packing theory have been used regarding the distribution of the phases, effective pore size, coordination number etc. The resulting equations enable one to calculate the effective

thermal conductivity as a function of interstitial gas pressure, temperature and loading conditions. These models have been successfully applied to large groups of granular materials and the results are summarized in Table 9-I. Comparison between Tables 9-I and 6-VII indicates that these models constitute a considerable improvement over previously published models. The error in the effective thermal conductivity values predicted by the equations developed in this study can be attributed to the following causes:

1. Exclusion of pure radiation heat transfer at very low pressures;

2. Low calculated values for the contact resistance;

3. Deviation of the actual distribution of the two phases from the assumed random phase distribution;

4. Uncertainty regarding the mean particle size in cases of granular materials having broad particle size range.

The reason it is not possible to eliminate these sources of error at this time is lack of experimental evidence. However, once more accurate expressions are found, they can be readily incorporated in the models. In spite of the above mentioned limitations to the accuracy of the models, it is now possible to predict the effective thermal conductivity of granular materials over a wide range of environments with a high degree of confidence, as attested by the successful application of the models to large groups of heterogeneous mixtures. It is evident from the discussion of the previously published models, and from the models presented in this study that the most serious drawbacks in the analysis of the thermal conductivity of heterogeneous mixtures are (a) a sufficiently accurate description

of the geometry of granular materials and (b) the radiation heat
transfer process. Since the effective thermal conductivity of granular
systems is very sensitive to the conductivity of the gaseous phase, it
is expected that knowledge of the mean void volume and void volume
distribution should provide accurate calculated thermal conductivi-
ties. Towards this end, an analysis is presented in Figure 10-1.
This analysis is based on a unit cube of a heterogeneous mixture, and
is similar to the analysis of the nodular model.

The geometry of a representative unit cube can be defined from
the sectioned void area distribution and the void volume distribution.
The mean sectioned void area and the sectioned void area distribution
are required to determine the distribution of the two phases on the
six faces of the unit cube. The mean void volume and void volume
distribution are required so that the number of voids in the unit
cube can be calculated and distributed in such a manner that the
porosity of the unit cube is equal to the bulk porosity of the
granular material. The size of the unit cube will be determined from
the particle size distribution. As a result, each cubicle in the unit
cube will be occupied either by the continuous or the discontinuous
phase.

The next step is to define the resistance between nodes. This
can be done first in terms of the conductivity of the two phases.
Then, to account for contact resistance between particles, a number
of resistances equal to the contact resistance replaces an equal number

of already determined resistances between solid cubicles. These
resistances are randomly distributed and oriented, and their number
is given by the unit cube size and the coordination number. It is
important to note at this point that the geometric parameters such
as coordination number, etc. published in the literature have been
determined for packed beds constructed of equally sized particles.
Consequently a mean particle size must be determined from the particle
size distribution of the granular material in question. However, as
indicated in Appendix F, no such procedure has been found up to now
for packed beds containing broad particle size distribution.

Once the geometry of the unit cube and the resistance between
nodes have thus been defined, it is possible to determine the tempera-
ture distribution in a manner similar to the nodular model. Then,
the conduction heat flux in the mean heat flow direction can be
determined from the summation of individual heat fluxes between cubicles.

As indicated in the Introduction, the concept of an effective
thermal conductivity consistent with the Fourier-Biot Law necessitates
that the granular materials be considered as pseudo-homogeneous systems,
in which case the volume of the granular material is assumed large
with respect to the volume of individual grains. For such granular
systems the photon mean free path is expected to be small compared
to a linear dimension of the system, and consequently only thermal
radiation in the optically thick limit need to be considered. In this
case, according to the analysis presented in Appendix B, first the
conduction heat transfer and radiation heat transfer processes can be

separated, and second the radiative heat flux can be related to the effective extinction coefficient by a simple equation. Finally, the total heat flux in granular materials is the sum of the conduction heat flux and radiation heat flux, and the effective thermal conductivity of the system can be determined from the Fourier-Biot Law.

An approximate method, similar to the one described in Figure 10-1, is presented in Figure 10-2. The only difference between the two methods is the inclusion of the radiation heat transfer process. That is, recognizing that the determination of the extinction coefficient of granular materials is an extensive and difficult task, in the method of Figure 10-2 only radiation heat transfer between particle surfaces and radiation heat transfer in solid particles are considered.

Summarizing, it has been shown that any future attempt to develop more refined models for the calculation of the effective thermal conductivity of granular materials should be based on a realistic approximation of the geometry and radiation heat transfer. In particular, it is suggested that the following experimental program be undertaken.

1. Determination of the void volume distribution and the sectioned void area distribution in terms of the particle size distribution, particle shape and porosity. The work of Debbas and Rumpf [51] is a step in the right direction, but the number of cases examined is not sufficient to justify any generalized conclusions. It is therefore suggested that experimental work, similar to the one described in Reference [51] be undertaken and extended to granular systems composed

of equal sized particles, narrow particle size distribution and broad particle size distribution.

2. Experimental work to determine the extinction coefficient of specific granular systems similar to the one described by Bastin et al [85], or experimental work to determine the radiation heat transfer in solid particles of various sizes similar to the one described by Merrill [118].

3. It is evident from Figure E-1 that the range of porosities for which the coordination number of spherical particles has been experimentally determined is too narrow to justify any of the correlations suggested in the literature. Consequently, further experimental work is required for the determination of the coordination number over a wider range of porosities. Also the coordination number of irregularly shaped particles should be determined and compared to that of spheres, so that more accurate expressions can be found for the number and distribution of contact areas in granular materials.

Experimental work on the areas mentioned above is not only essential for the analysis of the thermal conductivity of stagnant packed beds, but will also be a tremendous contribution to analytical work on fluid flow through packed beds and heat transfer in packed beds with fluid flow.

A problem that has been identified in this study is the selection of a mean particle diameter for packed beds consisting of a broad

particle size distribution. As indicated in Chapter 8 and Appendix F, the solution of this problem is solely based on experimental evidence. However, due to this problem, the majority of the models of this study have been applied to random packings of equal size spheres, and to granular materials composed of narrow particle distribution only.

Finally, it should be noted that no anisotropy of thermal conductivity has been considered in this study. However, it is possible to include the variation of the thermal conductivity in granular materials in the horizontal and vertical directions by considering the change of the contact pressure between particles in the horizontal and vertical directions. As indicated in Reference [86] the pressure tensor in a granular material can be written as

$$p_{ij} = p_0 \, \delta_{ij} + p_1 \, z_i \, z_j \tag{10-1}$$

where $p_0$, $p_1$ are constants and $z_i$ are the components of a unit vector in the direction of the applied load. It follows that the pressure in the direction of the applied load is

$$p_\nu = p_0 + p_1 \tag{10-2}$$

while in the horizontal direction it is

$$p_n = p_0 \tag{10-3}$$

When the granular material is loaded under its own weight

$$p_\nu = g \int_0^D \rho(z) \, dz \tag{10-4}$$

Assuming that the expansion of the granular material is constrained in the horizontal direction it follows that

$$p_n = \frac{\nu}{1-\nu} \, p_\nu \tag{10-5}$$

Combination of Equations (10-2) through (10-5) determines $p_\nu$ and $p_n$ in terms of density and depth. Then, $p_\nu$ can be used in the determination of the contact resistance in the direction of the applied load and $p_n$ in the determination of the contact resistance in the horizontal direction. As a result, the temperature distribution and consequently the effective thermal conductivity will be different when the mean heat flow direction is the direction of the applied load and when the mean heat flow direction is the horizontal.

It is evident that the variation of the thermal conductivity in the two directions will be significant only in the case of granular materials at low pressures because only in this case variation of the contact resistance will affect detectably the calculated effective thermal conductivity of the granular system.
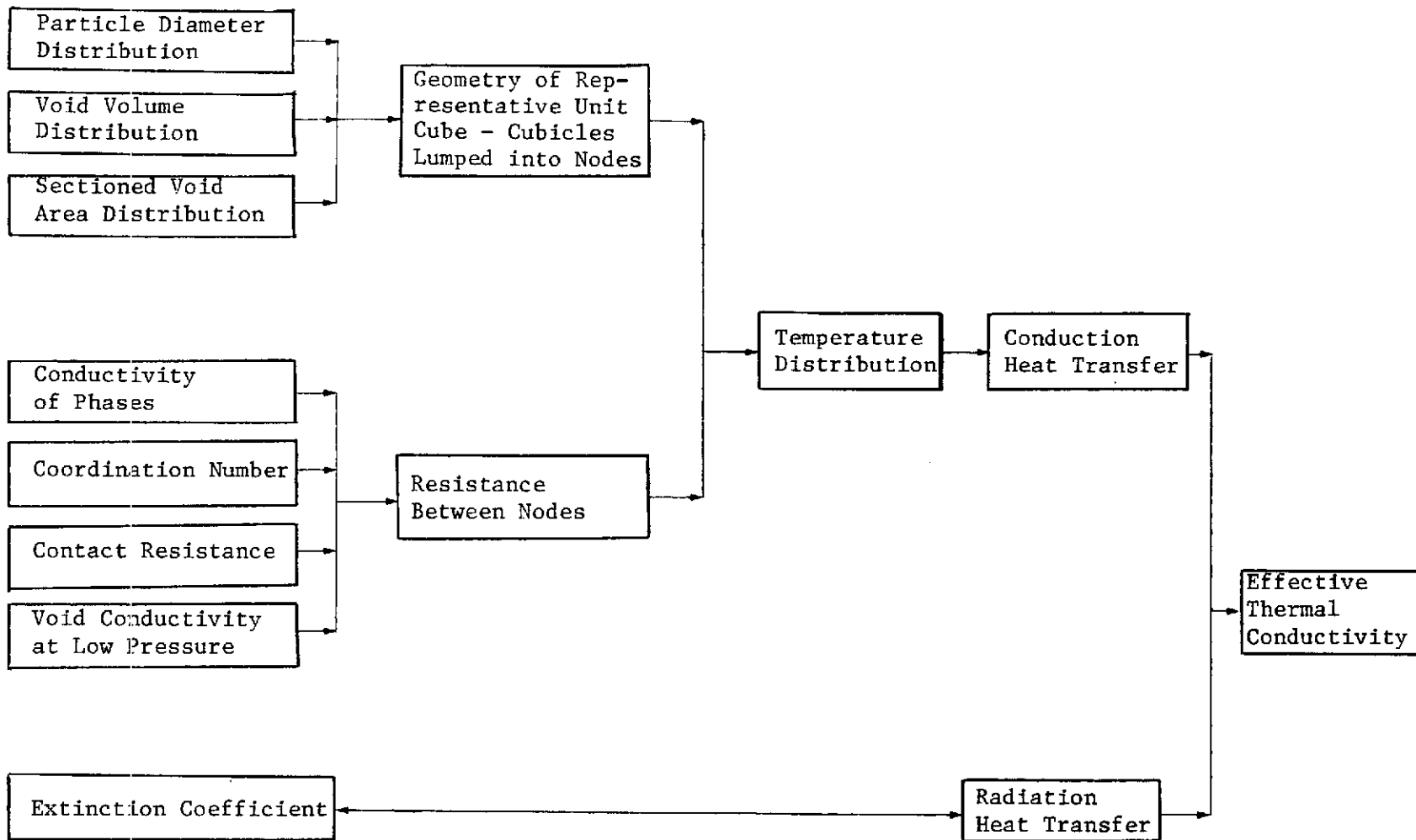
FIGURE 10-1.  FLOW CHART FOR THE CALCULATION OF THE EFFECTIVE THERMAL CONDUCTIVITY
OF GRANULAR MATERIALS.
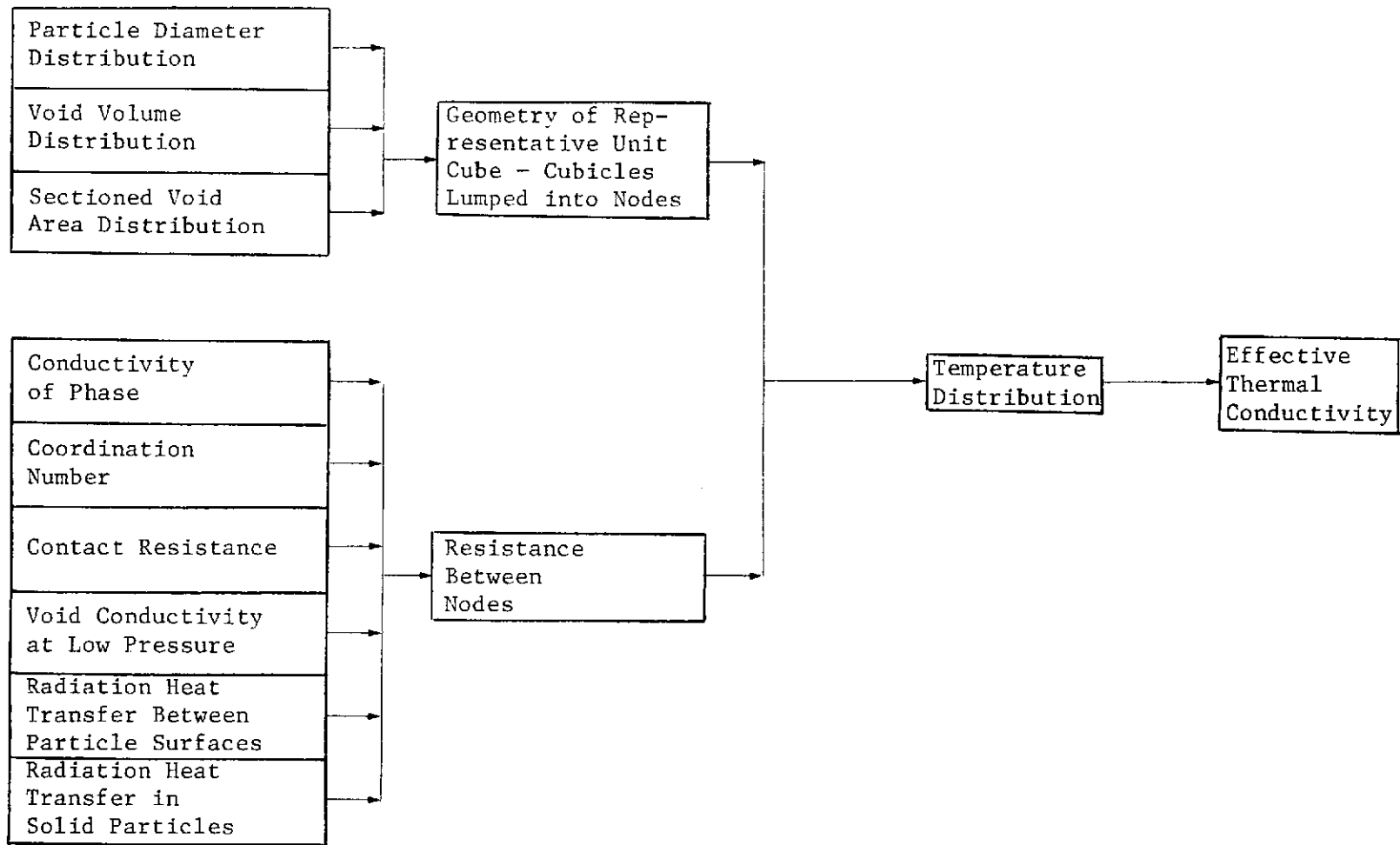
FIGURE 10-2. FLOW CHART FOR AN APPROXIMATE CALCULATION OF THE EFFECTIVE
CONDUCTIVITY OF GRANULAR MATERIALS.

# REFERENCES

1. Wesselink, A. F., "Heat Conductivity and Nature of the Lunar Surface Material," _Bulletin of the Astronomical Institutes of the Netherlands_, Vol. 10, No. 390, 351, (1948).

2. Clegg, P. E., Bastin, J. A. and Gear, A. E., "Heat Transfer in Lunar Rock," _Monthly Notices of the Royal Astronomical Society_, Vol. 133, 63, (1966).

3. Fountain, J. A. and West, E. A., "Thermal Conductivity of Particulate Basalt as a Function of Density in Simulated Lunar and Martian Environments," _Journal of Geophysical Research_, Vol. 75, No. 20, 4063, (1970).

4. Gorring, R. L. and Churchill, S. W., "Thermal Conductivity of Heterogeneous Materials," _Chemical Engineering Progress_, Vol 57, No. 7, 53, (1961).

5. Haughey, D. P. and Beveridge, G. S. G. "Local Voidage Variation in a Randomly Packed Bed of Equal Sized Spheres," _Journal of Engineering Science_, Vol 21, 905, (1966).

6. Waddams, A., "The Flow of Heat Through Granular Materials," _Journal of the Society of Chemical Industry_, Vol 63, 337, (1944).

7. Wiener, O., "The Theory of Mixtures for Fields with Constant Currents," _Akademie der Wissenschaften. Leipsiz, Math-Phys. Kl. Abhandlungen_, Vol. 32, 507, (1912).

8. Tsao, G. T., "Thermal Conductivity of Two-Phase Materials," _Industrial and Engineering Chemistry_, Vol. 53, No. 5, 395, (1961).

9. Maxwell, J. C., _A Treatise on Electricity and Magnetism_, Vol. 1, 3rd ed., Oxford University Press, London, 1892, p. 440.

10. Burgers, H. C., "The Conductivity of Diluted Air Crystal Mixtures," _Physikalische Zeitschrift_, Vol. 20, 73, (1919).

11. Fricke, H., "The Electrical Conductivity of a Suspension of Homogeneous Spheroids," _Physical Review_, Vol. 24, 515, (1924).

12. DeVries, D. A., *Physics of Plant Environment*, 2nd ed., North Holland Publishing Co., Amsterdam, 1966, p. 210.

13. Hamilton, R. L. and Crosser, O. K., "Thermal Conductivity of Heterogeneous Two-Component Systems," *Industrial and Engineering Chemistry Fundamentals*, Vol. 2, 187, (1962).

14. Rayleigh, Lord, "On the Influence of Obstacles Arranged in Rectangular Order Upon the Properties of a Medium," *Philosophical Magazine and Journal of Science*, Vol. 34, 481, (1892).

15. Runge, I., "On the Electrical Conductivity of Metallic Aggregates," *Zeitschrift fur Technische Physik-Leipzig*, Vol. 6, 61, (1925).

16. Meredith, R. E. and Tobias, C. W., "Resistance to Potential Flow Through a Cubical Array of Spheres," *Journal of Applied Physics*, Vol. 31, 1270, (1960).

17. Laubitz, M. J., "Thermal Conductivity of Powders," *Canadian Journal of Physics*, Vol. 37, 798, (1959).

18. Bruggeman, D. A. G., "Dielectric Constant and Conductivity of Mixtures of Isotropic Materials," *Annalen Physik*, Vol. 24, 636, (1935).

19. Meredith, R. E. and Tobias, C. W., "Conductivities in Emulsions," *Electrochemical Society Journal*, Vol. 108, 286, (1961).

20. Baxley, A. L. and Cooper, J. R., "Thermal Conductivity of Two Phase Systems-Part IV; Thermal Conductivity of Suspensions," University of Arkansas Experimental Station, Fayetteville, Arkansas, (1966).

21. Deissler, R. G. and Boegli, J. S., "An Investigation of Effective Thermal Conductivities of Powders in Various Gases," *Transactions of the ASME*, Vol. 80, 1417, (1958).

22. Lichteneker, K., "The Electrical Conductivity of Periodic and Random Aggregates," *Physikalische Zeitschrift*, Vol. 27, 115, (1926).

23. Woodside, W. and Messmer, J. H., "Thermal Conductivity of Porous Media in Unconsolidated Sands," *Journal of Applied Physics*, Vol. 32, 1688, (1961).

24. Lichteneker, K., "The Electrical Conductivity of Periodic and Random Aggregates," *Physikalische Zeitschrift*, Vol. 25, 169, (1924).

25. Son Frey, G. S., "The Electrical Conductivity of Binary Aggregates," *Zeitschrift fur Electrochemie*, Vol. 38, 260, (1932).

26. Schotte, W., "Thermal Conductivity of Packed Beds," _American Institute of Chemical Engineers Journal_, Vol. 6, 63, (1960).

27. Smith, W. O., "The Thermal Conductivity of Dry Soil," _Soil Science_, Vol. 53, 435, (1942).

28. Sauer, M. C., Southwick, P. F., Spiegler, K. S., and Wyllie, M. R. J., "Electrical Conductance of Porous Plugs," _Industrial and Engineering Chemistry_, Vol. 47, No. 10, 2187, (1955).

29. Yagi, S. and Kunii, D., "Studies on Effective Thermal Conductivities in Packed Beds," _American Institute of Chemical Engineers Journal_, Vol. 3, 373, (1957).

30. Kunii, D. and Smith, J. M., "Heat Transfer Characteristics of Porous Rocks," _American Institute of Chemical Engineers Journal_, Vol. 6, 71, (1960).

31. Willhite, G. P., Kunii, D., and Smith, J. M., "Heat Transfer in Beds of Fine Particles," _American Institute of Chemical Engineers Journal_, Vol. 8, No. 3, 340, (1962).

32. Masamune, S. and Smith, J. M. "Thermal Conductivity of Beds of Spherical Particles," _Industrial and Engineering Chemistry_, Vol. 2, No. 2, 136, (1963).

33. Dul'nev, G. N., "Heat Transfer Through Solid Disperse Systems," _Journal of Engineering Physics_, Vol. 9, No. 3, 399, (1965).

34. Luikov, A. V., Shashkov, A. G., Vasiliev, L. L. and Fraiman, Yu.E., "Thermal Conductivity of Porous Systems," _International Journal of Heat and Mass Transfer_, Vol. 11, 117, (1968).

35. Schumann, T. E. W. and Voss, V., "Heat Flow Through Granulated Material," _Fuel in Science and Practice_, Vol. 13, 249, (1934).

36. Preston, F. W., "Mechanism of Heat Transfer in Unconsolidated Porous Media at Low Flow Rates," Ph.D. Dissertation, Pennsylvania State University, (1957).

37. Wilhelm, R. H., Johnson, W. C., Wynkoop, R., and Collier, D. W., "Reaction Rate, Heat Transfer and Temperature Distribution in Fixed-Bed Catalytic Converters," _Chemical Engineering Progress_, Vol. 44, No. 2, p. 105, (1948).

38. Hengst, G., "The Thermal Conductivity of Powdered Thermal Insulators at High Pressure," Ph.D. Dissertation, Technische Hochschule Munchen, (1934).

39. Lyalikov, A. S., "Thermal Conductivity of Granular Materials,"
    Ph.D. Dissertation, Tomsk Polytechnic Institute, U.S.S.R., (1956).

40. Kaganer, M. G., "Thermal Insulation in Low Temperature Engineering,"
    Izd. Mashinostroenie, (1966).

41. Deissler, R. G. and Eian, C. S., "Investigation of Effective
    Thermal Conductivities of Powders," National Advisory Committee
    for Aeronautics Research Memorandum, E52C05, (1952).

42. Krupiczka, R., "Analysis of Thermal Conductivity in Granular Materials,"
    CHEMIA STOSOWANA, Vol. 2B, 183, (1966).

43. Russell, H. W., "Principles of Heat Flow in Porous Insulators,"
    Journal of the American Ceramic Society, Vol. 18, 1, (1935).

44. Bernstein, R. S., "Investigation of Natural Fuel Combustion
    Processes," Gesenergoizdat, (1948).

45. Godbee, H. W., and Ziegler, W. T., "Thermal Conductivity of
    MgO, $Al_2O_3$, and $ZrO_2$ Powders to 850°C," Journal of Applied Physics,
    Vol. 37, No. 1, 56, (1965).

46. Topper, L., "Analysis of Porous Thermal Insulating Materials,"
    Industrial and Engineering Chemistry, Vol. 47, No. 7, (1955).

47. Webb, J., "Thermal Conductivity of Soil," Nature, No. 4517,
    989, (1956).

48. Woodside, W., "Calculation of the Thermal Conductivity of Porous
    Media," Canadian Journal of Physics, Vol. 36, 815, (1958).

49. Haughey, D. P. and Beveridge, G. S. G., "Structural Properties
    of Packed Beds - A Review," Canadian Journal of Chemical Engineering,
    Vol. 47, 130, (1969).

50. Stange, K., "The Mixing of Random Systems as a Basis for Estimating
    Mixing Data," Chemic Ing. Tech. Vol. 6, 331, (1954).

51. Debbas, S. and Rumpf, H., "On the Randomness of Beds Packed with
    Spheres or Irregular Shaped Particles," Chemical Engineering Science
    Vol. 21, 583, (1966).

52. Warren, J. E. and Messmer, J. H., "Correspondence-Thermal Conductivity
    of Two Phase Materials," Industrial and Engineering Chemistry,
    Vol. 1, No. 3, 222, (1962).

53. Crane, R. A. and Vachon, R. I., "Effective Thermal Conductivity of
    Granular Materials," XII International Conference on Thermal
    Conductivity, Birmingham, Alabama, p. 99, (1972).

54. Somerton, W. H., University of California, Berkeley, California, Personal Communication.

55. Miller, I. and Freund, J. E., <u>Probability and Statistics for</u> Engineers, 1st ed., Prentice Hall, Englewood Cliffs, New Jersey, 1965, p. 245.

56. Gorring, R. L. and Churchill, S. W., "Thermal Conductivity of Heterogeneous Materials," Document 6754, American Documentation Institute, Library of Congress, Washington, D. C.

57. Verschoor, H. and Schuit, G. C. A., "Heat Transfer to Fluids Flowing Through a Bed of Granular Solids," <u>Applied Scientific</u> <u>Research</u>, Vol. 42, 97, (1950).

58. Kling, G., "The Heat Conduction of Spherical Aggragates in Still Gases," <u>Forschung</u>, Vol. 9, 28, (1938).

59. Kannuluik, W. G. and Martin, L. H., "Conduction of Heat in Powders," <u>Proceedings of the Royal Society of London</u>, A141, 144, (1933).

60. DeNee, P. B., "Thermal Conductivity of Granular Materials at Low Temperatures," Ph.D. Dissertation, Lehigh University, (1964).

61. Dul'nev, G. N., Platunov, E. S., Muratova, B. L., Sigalova, Z. V., "A Method of Determing the Thermal Conductivity of Powdered and Fibrous Insulation as a Function of Filler Gas Pressure, "<u>Inzhenerno-Fizicheskii Zhurnal</u>, Vol. 9, No. 6, 751, (1965).

62. Prins, J. A., Schenk, J., and Schram, A. J. G. L., "Heat Conduction by Powdero in Various Gaseous Atmospheres at Low Pressure," <u>Physica</u>, XVI, 4, 379, (1950).

63. Wechsler, A. E., "Thermal and Mechanical Properties of Evacuated Powders," <u>Powder Technology</u>, 3, 163, (1969-1970).

64. Wechsler, A. E. and Glaser, P. E., "Pressure Effects on Postulated Lunar Materials, " <u>Icarus</u>, 4, 335, (1965).

65. Bernett, E. C., Wood, H. L., Jaffe, L. D., Martens, H. E., "Thermal Properties of a Simulated Lunar Material in Air and in Vacuum," <u>AIAA Journal</u>, Vol. 1, No. 6, 1402, (1963).

66. Dallavalle, J. M., "<u>Micromeritics</u>", 2$^{nd}$ ed., Pitman Publishing Corporation, New York, (1948).

67. Hilsenrath, J. et. al., "Tables of Thermodynamic and Transport Properties of Air, Argon, Carbon Dioxide, Carbon Monoxide, Hydrogen, Nitrogen, Oxygen and Steam", Pergamon Press, New York, (1960).

68. Crane, R. A., "Thermal Conductivity of Randomly Packed Granular Materials," Ph.D. Dissertation, Auburn University, (1973).

69. Loeb, A. L., "Thermal Conductivity: VIII, A Theory of Thermal Conductivity of Porous Materials," Journal of The American Ceramic Society, Vol. 37, No. 2, 96, (1954).

70. Cheng, S. C. and Vachon, R. I., "The Prediction of the Thermal Conductivity of Two and Three Phase Solid Heterogeneous Mixtures," Int. J. Heat Mass Transfer, Vol. 12, 249, (1969).

71. Neville, A. M. and Kennedy, J. B., "Basic Statistical Methods for Engineers and Scientists," International Textbook Company, Scranton, Pennsylvania, (1964).

72. Trezek, G. J. and Witwer, J. G., "Finite-Difference Methods for Inhomogeneous Regions," Trans. of the ASME, Vol. 94, Series C, No 3, 321, (1972).

73. Kanager, M. G., "Contact Heat Transfer Heat Transfer in Granular Material Under Vacuum," Inzhenerno-Fizicheskii Zhurnal, Vol. 11, No. 1, 30, (1966).

74. Westlake, J. R., "A Handbook of Numerical Matrix Inversion and Solution of Linear Equations," John Wiley and Sons, Inc., (1968).

75. Argo, W. B. and J. M. Smith, "Heat Transfer in Packed Beds," Chemical Engineering Progress, Vol. 49, No. 8, 443, (1953).

76. Dul'nev, G. N. and Sigalova, Z. V., "Effective Thermal Conductivity of Granular Materials", Inzhenerno-Fizicheskii Zhurnal, Vol. 13, No. 5, (1967).

77. Jacob, Max. "Heat Transfer," Vol. I, p.85, Eighth Printing, John Wiley and Sons, Inc., (1962).

78. Jefferson, T. B. et al, "Thermal Conductivity of Graphite-Silicone Oil and Graphite-Water Suspensions," Ind. Eng. Chem., 50, 1589, (1958).

79. Kennard, E. H., "Kinetic Theory of Gases," McGraw - Hill Book Company, Inc., (1938).

80. Wachman, H. Y., "The Thermal Axxommodation Coefficient: A Critical Survey," ARS Journal, Vol. 32, No. 1, 2, (1962).

81. Chen, J. C. and Churchill, S. W., "Radiant Heat Transfer in Packed Beds," A.I.Ch.E. Journal, Vol. 9, No. 1, 35, (1963).

82. Rosseland, S., "Theoretical Astrophysics," Oxford University Press, Clarendon, England, (1936).

83. Van der Held, E. F. M., "The Contribution of Radiation to the Conduction of Heat," Appl. Sci. Research, Section A, Vol. 3, 237, (1952) ; Section A, Vol. 4, 77, (1953).

84. Troitsky, V. S., "Thermal Conductivity of Lunite as Dependent on Temperature," Nature, February 18, page 688, (1967).

85. Bastin, J. A., Clegg, P. E. and Fiedler, G., "Infrared and Thermal Properties of Lunar Rock," Science, Vol. 167, No. 3918, 728, (1970).

86. Sexl, R. U. et al "Radiative Aspects of Lunar Materials,", NAS8-25585.

87. Cooper M. G., Mikic, B. B. and Yovanovich, M. M., "Thermal Contact Conductance," Int. J. Heat Mass Transfer, Vol. 12, 279, (1969).

88. Carslaw, H. S. and Jaeger, J. C., "Conduction of Heat in Solids," Clarendon Press, Oxford, (1948).

89. Shlykov, Y. P. and Ganin, Y. A., "Thermal Resistance of Metallic Contacts," Int. J. Heat Mass Transfer, Vol. 7, 921, (1964).

90. Smith, W. O., Foote, P. D. and Busang, P. F., Phys. Rev., 34, 1271, (1929).

91. Scott, G. D., Nature, 188, 908, (1960).

92. Bernal, J. D. and Mason, J., Nature, 188, 910, (1960).

93. Fountain, J. A. and Scott, R. W., "Thermal Conductivity of a Particulate Sample in an Environment that Simulates the Planet Mars," NASA Internal Note IN-SSL-T-68 - 15, (1968).

94. Jaffe, L. D., "Lunar Surface Strength," Icarus, Vol. 6, 75, (1967).

95. Jaffe, L. D., "Lunar Surface Exploration by Surveyor Spacecraft," Journal of Geophysical Research, Vol. 72, No. 2, 773, (1967).

96. Verbalovich, T., and Jaffe, L. D., "Surveyor 3, A Preliminary Report - Summary of Result," NASA sp-146, 1967.

97. Christensen, E. M., "Surveyor 5, A Preliminary Report - Lunar Surface Mechanical Properties," NASA sp-163, 1967.

98. Christensen, E. M. et al., "Surveyor 6, A Preliminary Report - Lunar Surface Mechanical Properties," NASA sp-166, 1968.

99. Hapke, B. W., "Lunar Surface Composition Inferred from Optical Properties," Science, Vol. 159, No. 3810, 76, (1968).

100. Matveev, Y. G., Suchkin, G. L., and Troitskii, V. S., "Change of Lunite Density with Depth in the Surface Layer," Soviet Astronomy - AJ, Vol. 9, No. 4, 626, (1966).

101. Jones, B. P., "Density - Depth Model for the Lunar Outermost Layer," Journal of Geophysical Research, Vol. 73, No. 3, 7631, (1968).

102. Hapke, B. W., "On the Particle Size Distribution of Lunar Soil," Planetary Space Science, Vol. 16, 101, (1968).

103. Gorz, H. et al., "Particle Size and Shape Distributions of Lunar Fines By CESEMI," Proceedings of the Second Lunar Science Conference, Houston, Vol. 3, 2021, (1971).

104. Sparrow, E. M., and Cess, R. D., "Radiation Heat Transfer," Brooks/Cole Publishing Company, Belmont, California, 254, (1966).

105. Cremers, C. J., and Birkebak, R. C., "Thermal Conductivity of Fines from Apollo 12," Proceedings of the Second Lunar Science Conference, Houston, Vol. 3, 2311, (1971).

106. Cheng, S. C., and Vachon, R. I., "Thermal Conductivity of Packed Beds and Powder Beds," International Journal of Heat and Mass Transfer, Vol. 33, 1201, (1969).

107. Beveridge, G. S. G., and Haughely, D. P., "Axial Heat Transfer in Packed Beds," International Journal of Heat and Mass Transfer, Vol. 14, No. 8, 1093, (1971).

108. Holm, R., "Electric Contacts Handbook," Cambridge University Press, 1911.

109. Jean, J. H., "Electricity and Magnetism," Cambridge University Press, 1911.

110. See e.g. Lamb, H., "Treatise on the Mathematical Theory of Elasticity," Dover, 1957.

111. Hill, F. B., and Wilhelm, R. H., "Radiative and Conductive Heat Transfer in Quiescent Gas Solid Bed of Particles," AICHE Journal, Vol. 5, 1959.

112. Snoddy, W. E., and et al., "Infrared Emission During Simulated Lunar Eclipses," AIAA Progress in Astronautics and Aeronautics, 5469, (1967).

113. Turkevich, A. L., Franzgrote, E. J., and Paterson, J. H., "Chemical Analysis of the Moon at Surveyor 6 Landing Site," NASA sp-166, 1968.

114. Cuttitta, F. and et al., "Elemental Composition of Some Apollo 12 Lunar Rocks and Soils," Proceedings of the Second Lunar Science Conference, Houston, Vol. 2, 1217, (1971).

115. Tittmann, B. R., Housley, R. M., "Surface Elastic Wave Propagation Studies in Lunar Rocks," Proceedings of the Second Lunar Science Conference, Vol. 3, 2337, (1971).

116. Kanamori, H. et al., "Elastic Wave Velocities of Apollo 12 Rocks at High Pressures," Proceedings of the Second Lunar Science Conference, Vol. 3, 2323, (1971).

117. Chandrasekhar, S., "Radiative Transfer," Dover Publications, Inc., (1960).

118. Merrill, R. B., "Thermal Conduction Through an Evacuated Idealized Powder Over the Temperature Range of 100 to 500 K," Ph.D. Dissertation, Brigham Young University, (1968).

119. Gold, T. et al., "Some Physical Properties of Lunar Samples," Proceedings of the Second Lunar Science Conference, Houston, Vol. 3, 2173, (1971).

120. Yagi, S., and Kunii, D., "Studies of Heat Transfer Near Wall Surface in Packed Beds," AICHE Journal, Vol. 6, No. 1, 97, (1960).

121. Cremers, C. J. et al., "Thermal Characteristics of the Lunar Surface Layer," International Journal of Heat and Mass Transfer, Vol. 15, 1045, (1972).

122. Campbell, K. J., Ulrichs, J., and Gold, T., "Density of Lunar Surface," Science, Vol. 189, 973, (1968).

123. Fountain, J. A., West, E. A., "Thermal Conductivity of Particulate Basalt as a Function of Density in Simulated Lunar and Martian Environments," Journal of Geophysical Research, Vol. 75, No. 20, 4063, (1970).

124. Heywood, H., "Particle Size and Shape Distribution for Lunar Fines Sample 12057,72," Proceedings of the Second Lunar Science Conference, Houston, Vol. 3, 1989, (1971).

125. Sellers, G. A. et al., "Composition and Grain-Size Characteristics of Fines from the Apollo 12 Double-Core Tube," Proceedings of the Second Lunar Science Conference, Vol. 1, 665, (1971).

126. Quaide, W. et al., "Investigations of the Natural History of the Regolith at the Apollo 12 Site," Proceedings of the Second Lunar Science Conference, Vol. 1, 701, (1971).

127. Cremers, C. J., Birkebak, R. C., and Dawson, J. P., "Thermal Conductivity of Fines from Apollo 11," Proceedings of Apollo 11 Lunar Science Conference, Vol. 3, 2045, (1970).

128. Watson, K., "The Thermal Conductivity Measurements of Selected Silicate Powders in Vacuum from 150-350 K," Ph.D. Thesis, California Inst. of Technology, Pasadena, Calif., 1964.

# BIBLIOGRAPHY

1.  Staple, W. J., "Boundary Conditions and Conductivities Used in the Isothermal Model of Evaporation from Soil," Soil Science Society of America Proceedings, Vol. 35, No. 6, (1971).

2.  Wierenga, P. G. and DeWit, C. T., "Simulation of Heat Transfer in Soils," Soil Science Society of America Proceedings, Vol. 34, (1970).

3.  Hisakado, Terumasa, "On the Mechanism of Contact Between Solid Surfaces, (1st Report)," Bulletin of JSME, Vol. 12, No. 54, (1969).

4.  Hisakado, Terumasa, "On the Mechanism of Contact Between Solid Surfaces, (2nd Report)," Bulletin of JSME, Vol. 12, No. 54, (1969).

5.  Hisakado, Terumasa, "On the Mechanism of Contact Between Solid Surfaces, (3rd Report)," Bulletin of JSMA, Vol. 12, No. 54, (1969).

6.  Clausing, A. M. and Chao, B. T., "Thermal Contact Resistance in a Vacuum Environment," Journal of Heat Transfer, (1965).

7.  Aberdeen, J., and Laby, T. H., "Conduction of Heat through Powders and its Dependence on the Pressure and Conductivity of the Gaseous Phase," Proceedings of Royal Society of London, Vol. 113, (1927).

8.  Agrawal, M. P., and Bhandari, R. C., "Effect of Particle Shape on the Formation Resistivity Factor of Unconsolidated Porous Media," Indian J. Pure Appl. Phys., Vol. 7, (1969).

9.  Aksel'rud, G. A., "Solution of a Generalized Problem of Heat or Mass Transfer in a Bed," Inzhenerno-Fizicheskii Zhurnal, Vol. 11, No. 1, (1966).

10. Archie, G. E., "The Electrical Resistivity Log as an Aid in Determining Some Reservoir Characteristics," Petroleum Technology Proceedings, T.P. 1422, (1941).

11. Ben-Amoz, M. "The Effective Thermal Properties of two Phase Solids," Int. J. Engng. Sci., Vol. 8, (1970).

12. Fritz, W., and Kuster, W., "A Contribution to the Knowledge of Heat Conductivity of Porous Materials," Warme-Und Stoffubertragung, Bd. 3, (1970).

13. Kumar, I. J., "An Extended Variational Formulation of the Non-Linear Heat and Mass Transfer in a Porous Medium," International Journal of Heat and Mass Transfer, Vol. 14, (1971).

14. Wyllie, M. R. J., and Southwick, P. F., "An Experimental Investiga-tion of the S. P. and Resistivity Phenomena in Dirty Sands," Journal of Petroleum Technology, Vol. 44, (1954).

15. Berg, T. G., Owe, Medonald, R. L., and Trainer, R. J., Jr., "The Packing of Spheres," Power Technology, Vol. 3, (1969/70).

16. Blum, E. H., and Wilhelm, R. H., "A Statistical Geometrical Approach to Random-Packed Beds," A.I.Ch.E. - I Chem. E. Symposium Series, No. 4, (1965).

17. Bridgwater, J., Bagster, D. F. Chen, and Hallam, J. H., "Geometric and Dynamic Similarity in Particle Mixing," Powder Technology, Vol. 2, (1968/69).

18. Cahn, D. S., and D. W. Fuerstenav, "Simulation of Diffusional Mixing of Particulate Solids by Monte Carlo Techniques," Powder Technology, Vol. 1, (1967).

19. Cahn, David S., and Fuerstenav, Douglas W., "A Probabilistic Model of the Diffusional Mixing of Particulate Solids," Powder Technology, Vol. 2, (1968/69).

20. Dullien, F. A. L., Rhodes, E., and Schroeter, S. R., "Comparative Testing of Some Statistical Methods for Obtaining Particle Size Distributions," Powder Technology, Vol. 3, (1969/70).

21. McAdams, H. T., "Probability Foundations of Particle Statistics," Powder Technology, Vol. 2, (1968/69).

22. Prager, S., "Interphase Transfer in Stationary Two-Phase Media," Chemical Engineering Science, Vol. 18, (1963).

23. Roblee, L. H. S., Baird, R. M. and Tierney, J. W., "Radial Porosity Variations in Packed Beds," A.I. Ch.E. Journal, Vol. 4, No. 4, (1958).

24. Thadani, Mohan C., and Peebles, Fred N., "Variation of Local Void Fraction in Randomly Packed Beds of Equal Spheres," I & E.C. Process Design and Development, Vol. 5, No. 3, (1966).

25.  Williams, J. C., "The Properties of Non-Random Mixtures of Solid Particles," Powder Technology, Vol. 3, (1969/70).

26.  Horia, Ki-iti and Simmons, G., "Thermal Conductivity of Rock-Forming Minerals," Earth and Planetary Science Letters 6, (1969).

27.  Kinger, W. D., Francl, J., Coble, R. L., and T. Vasilos, "Thermal Conductivity: X, Data for Several Pure Oxide Materials Corrected to Zero Porosity," Journal of American Ceramic Society, Vol. 37, No. 2, (1954).

# APPENDIX A

## LOW PRESSURE EFFECTS

Figure (A-1) shows a typical pressure dependence curve of the effective thermal conductivity of a gas-powder mixture. For higher pressures (10 atm or higher depending on the nature of the gas and the particle size [37]) a large rise in the effective conductivity is noted, due to convection. When the mean free path of the gas molecules approaches the characteristic length of the gas space, the effective conductivity becomes pressure dependent, as indicated by the portion between A and B of Figure (A-1). Further reduction of the pressure does not result in any appreciable changes
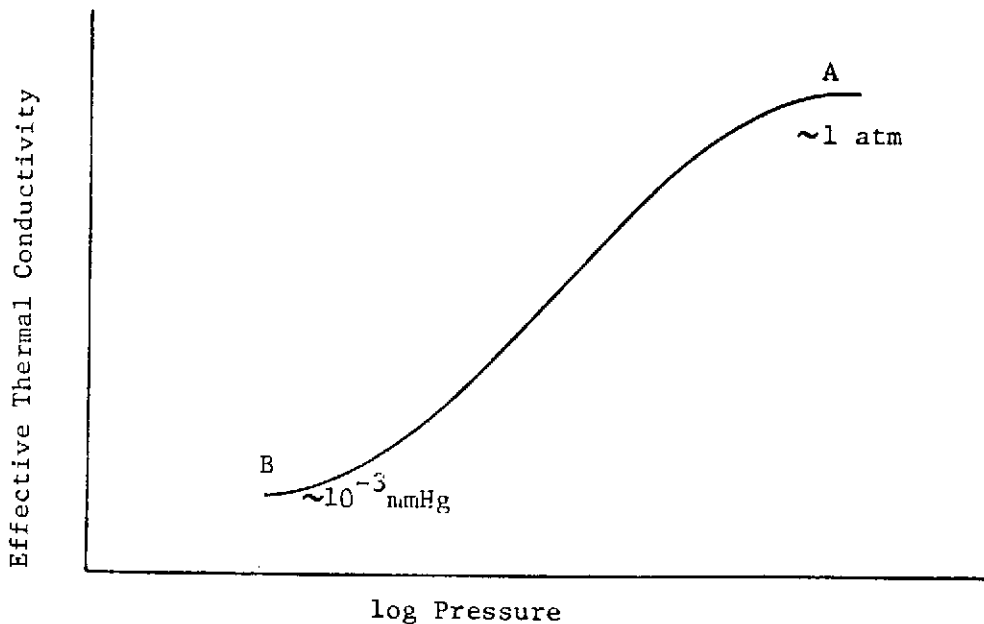


Fig. A-1. Pressure Dependence of Effective Thermal Conductivity

in the effective conductivity, since at this region the dominant

modes of heat transfer are conduction through the contact areas

between particles and radiation.

Thermal conduction in rarefied gases was first analyzed in

the pioneer works of Smoluchowski and Knudsen, as indicated by

Kennard [79]. Kennard's equation for the effective conductivity,

$k_g^*$, of a gas between two parallel plates of the same material,

separated by a relative small distance, $D_p$, is:

$$k_g^* = \frac{k_g}{1 + 2\frac{g^*}{D_p}} \tag{A-1a}$$

where $g^*$ is the temperature jump distance at one of the plates, given

by:

$$g^* = \frac{2-\alpha}{\alpha} \ \frac{2\gamma}{\gamma+1} \ \frac{1}{Pr} \ \lambda \tag{A-1b}$$

where $\alpha$ is the thermal accommodation coefficient, $\gamma$ is the ratio

of the specific heats of the gas, Pr is the Prandtl number and

$\lambda$ is the mean free path of the gas molecules. Equation (A-1)

indicates that $k_g^*$ decreases with respect to $k_g$ when $\lambda/D_p$ increases.

The principal difficulty in applying this equation lies in

evaluating the thermal accommodation coefficient, $\alpha$, and the

effective pore length, $D_p$. As indicated in [80], several attempts

have been made to predict the accommodation coefficient analytically,

but they have not proved particularly successful. Furthermore, the

accommodation coefficient is strongly influenced by parameters describing the solid surface (i.e. smoothness, impurities, etc. not reported in experimental work on the conductivity of granular materials), and experimentally determined values of $\alpha$ are not available for solids other than pure metals and alloys [80]. For this reason, most investigators of the effective conductivity of heterogeneous mixtures have either set $\alpha = 1$, effectively assuming that the solid surface is so irregular that most of the molecules struck it a number of times before escaping, or they have included $\alpha$ in an experimentally determined coefficient.

Dulnev and Sigalova [76] and Luikov et al [34] have used Equation (A-1) in the same form given by Kennard. Deissler and Boegli [21] found from their experimental data on magnesium oxide in air that the pressure at which the effective conductivity begins to vary with pressure (breakaway pressure) is 15 psia at 340°F. From this they evaluated the Knudsen number (Kn = $\lambda$/d), based on the mean particle size, to be 0.00072. Finally, arguing that Kn at the breakaway pressure must be independent of the gas, powder, temperature and pressure, they found from Equation (A-1) that the breakaway pressure in the English system of units is given by:

$$P_b = 1770 \times 10^{-24} \frac{T}{s^2 d} \tag{A-2}$$

where T is the temperature and s is the molecular diameter of the gas. Equation (A-2) seems to correlate their experimental data with

good accuracy. It is of particular importance that the value of the Knudsen number corresponding to the breakaway pressure is much less than unity, indicating that most of the heat transfer through a powder takes place in the immediate vicinity of the contact areas. Effectively, this means that the dimensions effective in transferring heat in the voids are much less than the effective geometric length of the void.

Schotte [26] and Masamune and Smith [32] found expressions for $D_p$ in terms of the porosity of the system, based on geometric considerations. They then substituted the expressions in Equation (A-1).

Woodside and Messmer [23] arguing that when the normal mean free path, $\lambda$, of the gas molecules is much larger than a characteristic pore size, then the effective mean free path, $\bar{\lambda}$, must depend on $\lambda$ as well as on $D_p$, have shown that:

$$k_g^* = k_g \cdot \frac{p\, D_p}{p\, D_p + B} \tag{A-3}$$

where

$$B = \frac{\sigma_D\, T}{\pi \sqrt{2}\, s^2}$$

$\sigma_b$ is the Boltzman constant. Equation (A-3) predicts higher values for $k_g^*$ than Equation (A-1) by a factor of roughly 2.5. It is interesting to note that also in this case the characteristic dimension

of the void space, with respect to heat conduction in the gas
occupying this space, is amaller than the mean particle diameter by
a factor of roughly 100.

Summarizing, it is seen that almost all investigators, with
the exception of [23], have used Kennard's equation to predict the
effect of pressure on the conductivity of the gaseous phase. The
principal difficulty in applying this equation lies in the determin-
ation of the thermal accommodation coefficient and $D_p$. The value
of $\alpha$ is assumed by all investigators to be unity. The determination
of $D_p$ is postponed until a later section. In Figure (A-2) the dependence
of the thermal conductivity of $CO_2$ on pressure is indicated,
according to Equations (A-1) and (A-3).
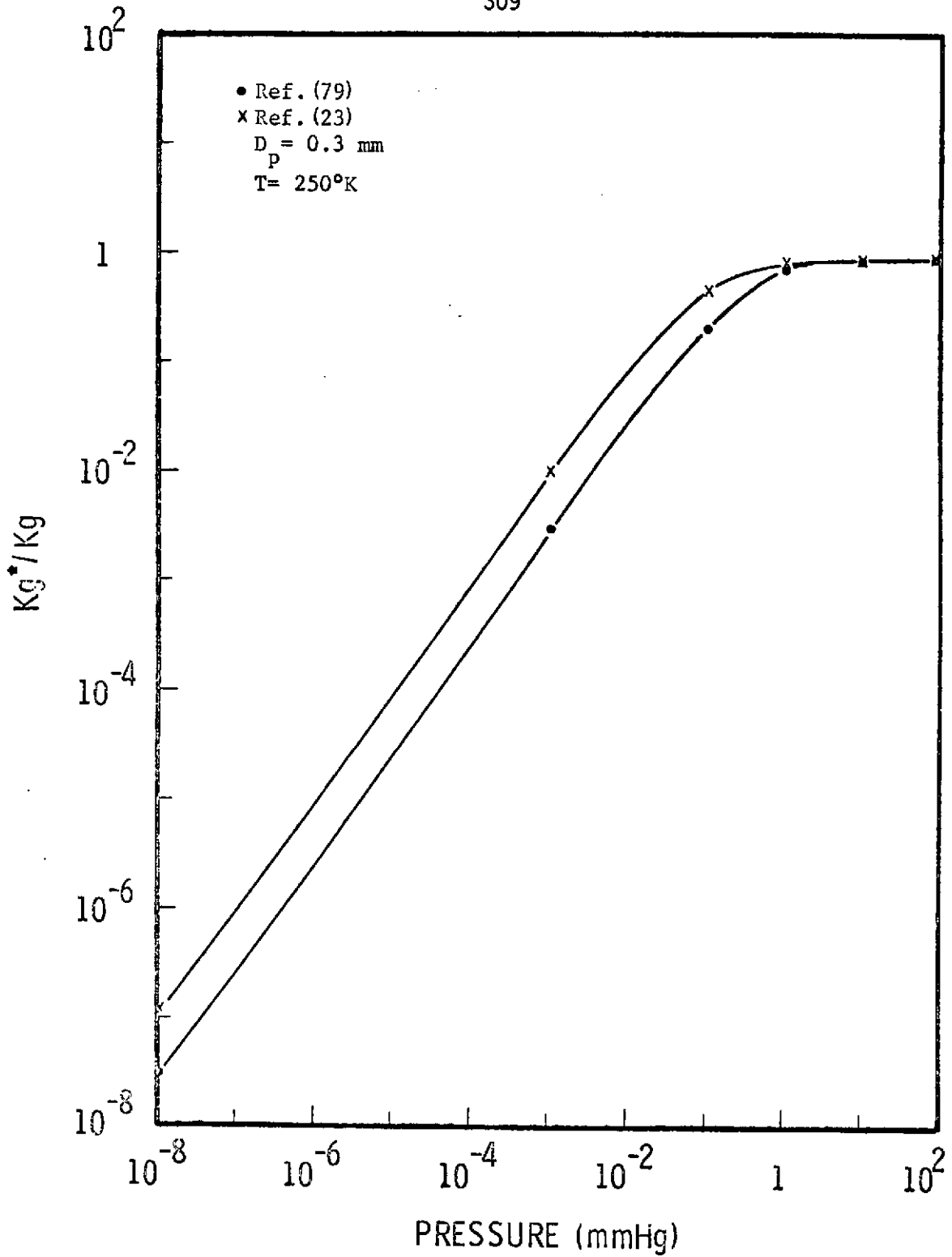
FIGURE A-2. EFFECT OF PRESSURE ON THE THERMAL CONDUCTIVITY OF $CO_2$.

# APPENDIX B

## RADIATION HEAT TRANSFER IN GRANULAR MATERIALS

Thermal radiation is known to be a dominant mode of heat transfer in evacuated granular materials, or in powders at elevated temperatures. Consequently it is no wonder that it has received considerable attention in the literature. However, due to the scarcity of information about absorption and scattering of radiation in granular materials, only approximate methods have been developed for the inclusion of radiation as a mode of heat transfer in granular materials.

According to Van der Held [83] the complete equation of Fourier, including radiant heat flux, is

$$C_p \, \rho \, \frac{\partial T_0}{\partial t} = \text{div}(k_{e_c} \, \text{grad} \, T_0) + 4 \int_0^\infty n_1^2 \, \beta_1 \, (J_1 - I_{1,T_0}) \, dl \, dV_0 \quad \text{(B-1)}$$

where $4n_1^2 \, \beta_1 \, I_{1,T_0} \, dl \, dV_0$ is the radiation emitted by a volume element $dV_0$ between the wavelengths 1 and $1 + dl$, having an absorption coefficient at these wavelengths $\beta_\lambda$ and a refractive index $n_1$. Similarly $4n_1^2 \, \beta_1 \, J_1 \, dl \, dV_0$ is the radiation absorbed by $dV_0$. $I_{1,T} \, dl$ and $J_1 \, dl$ are the black body radiation and mean irradiance respectively of a plane surface between the wavelengths 1 and $1 + dl$ at $dV_0$. In Equation (B-1) $k_{e_c}$ is the effective thermal conductivity of the medium due to conduction heat transfer only.

A second equation is required relating $J_1$ and $I_{1,T}$. This can be obtained by letting the mean irradiance of $dV_0$ be the sum of the radiation emitted and scattered by all volume elements $dV$, and reaching $dV_0$, plus the irradiance of $dV_0$ from the bounding walls. According to Van der Held [83], assuming diffuse radiation, this equation is

$$4J_{1_0} = \int_{(v)} (\beta_1 I_{1,T} + \sigma_1 J_1) \frac{e^{-T_1 r}}{\pi r^2} dV +$$

$$\int_{(s)} [e_{1,\gamma} I_{1,T} + (1-e_{1,\gamma}) J_1] \frac{e^{-t_1 r}}{\pi r^2} \cos \gamma \, dS \qquad (B-2)$$

where $\sigma_1$ is the monochromatic scattering coefficient, $\varepsilon_1 = \beta_1 + \sigma_1$ is the monochromatic scattering coefficient, $r$ is the distance between $dV_0$ and $dV$ or $dS$ (surface element on bounding walls), $e_{1,\gamma}$ is the monochromatic spectral emissivity of the walls, and $\gamma$ is the angle the distance between $dV_0$ and $dS$ makes with the normal on $dS$.

Combination of Equations (B-1) and (B-2) together with the boundary conditions determines the solutions of the heat transfer problem in granular materials. Although this system of equations appears to be quite formidable, it should be noted that the equations are very general in nature. The complexity of these equations has been reduced considerably in a number of specific situations, and these situations will now be discussed. First, however, it should be noted that the integral term in Equation (B-1) represents the net radiation heat transfer to $dV_0$, or if $\bar{q}_r$ is the radiant heat flux, the integral term is equal to $-\text{div } \bar{q}_r$. Consequently, an alternate form of Equation (B-1) is

$$C_p \, \rho \, \frac{\partial T_o}{\partial t} = \text{div} \, (k_{e_c} \, \text{grad} \, T_o) - \text{div} \, \vec{q}_r \qquad \text{(B-3)}$$

Also, the total heat flux vector within the medium will consist of the sum of the conduction and radiation contributions, and consequently is given by

$$\bar{q} = - \, k_{e_c} \, \text{grad} \, T = \bar{q}_r \qquad \text{(B-4)}$$

Assuming one-dimensional steady-state combined conduction and radiation for a medium bounded by two parallel surfaces, Equations (B-3) and (B-4) reduce to

$$k_{e_c} \, \frac{d^2 T}{dx^2} = \frac{dq_r}{dx} \qquad \text{(B-5)}$$

$$q = - \, k_{e_c} \, \frac{dT}{dx} + q_r = \text{constant} \qquad \text{(B-6)}$$

where x is the distance normal to one surface. Further assuming that the absorption and scattering coefficients are both independent of the wavelength, and that the distance between the bounding surfaces is large compared to the photon mean free path (optically thick limit), it has been shown in detail by Sparrow and Cess [104, 117] that the radiation flux can be written as

$$q_r = - \, \frac{16 \sigma_b T^3}{3 \varepsilon} \, \frac{dT}{dx} \qquad \text{(B-7)}$$

Combination of Equations (B-6) and (B-7) yields

$$q = - (k_{e_c} + \frac{16\sigma_b T^3}{3\varepsilon}) \ \frac{dT}{dx} = \text{constant} \qquad (B\text{-}8)$$

It is seen that in this specific case the conduction and radiation processes can be separated, and the total heat flux is represented as the sum of heat transfer by pure conduction and heat transfer by pure radiation. Consequently the effective conductivity of the granular material is the sum of an effective conductivity due to pure conduction and a radiant conductivity which is related to the cube of the absolute temperature. Unfortunately, no experimental data have been reported on the extinction coefficient of granular materials and powders, and consequently Equation (B-8) cannot be applied due to lack of experimental information. However, the result that the effective conductivity can be represented as the sum of two terms, one being a constant and the second related to the cube of the absolute temperature, has been extensively used in the correlation of data on evaluated granular materials.

Clegg et al [2] following a similar procedure assumed that scattering of radiation may be neglected, and using the Rosseland equation for the optically thick limit, they obtained the following equation for the radiant conductivity.

$$k_r = \frac{16}{3} \sigma_b \ \frac{T^3}{a(T)} \qquad (B\text{-}9)$$

where $\bar{a}(T)$ is the Roselland mean absorption coefficient.

Chen and Churchill [81] on the other hand represented the radiant intensity in packed beds by forward and backward fluxes, and derived the following expression for the radiant conductivity:

$$k_r = \frac{8 \, \sigma_b \, T^3}{a + 2b} \tag{B-10}$$

where a is the absorption volumetric coefficient and b is the back scattering volumetric coefficient. They also determined experimentally the values of a and b for borosilicate glass, aluminum oxide, carbon steel, and silicon carbide beds.

Another approximation is to assume one-dimensional steady-state combined conduction and radiation for a medium bounded by two parallel diffuse surfaces, where the distance between the bounding surfaces is small compared to the photon mean free path (optically thin limit). In this case, it has been shown by both Van der Held [83] and Sparrow and Cess [117] that the radiation heat flux is

$$q_r = \frac{\sigma_b (T_1^4 - T_2^4)}{(1/e_1) + (1/e_2) - 1} \tag{B-11}$$

where $T_1$ and $T_2$ are the absolute temperatures of the bounding surfaces, and $e_1$ and $e_2$ are the emissivities of the bounding surfaces. If $e_1 = e_2$ and $T_1 - T_2 = \Delta T$ is small, one can write

$$T_1^4 - T_2^4 = (T_1^2 + T_2^2)(T_1 + T_2)(T_1 - T_2) \simeq 4T^3 \, \Delta T$$

Combination of Equations (B-6) and (B-11) yields

$$q = - (k_{e_c} + \frac{4\sigma_b \, e \, T^3 \, dx}{2 - e}) \, \frac{dT}{dx} \tag{B-12}$$

Again it is seen that the conduction and radiation processes are separable. Further, this is the result for radiation transfer through a nonparticipating medium.

Equation (B-12) has been used extensively by investigators that have utilized models based on regular geometric arrangements which permit an algebraic formulation of the heat transfer processes. Russell [43], Wesselink [1], Jacob [77] and Argo and Smith [75] assumed that with respect to radiation a mixture can be treated as alternating solid and gas layers perpendicular to the heat flow. In this case, the radiant conductivity of the gas phase is given by

$$k_r = \frac{4\sigma_b \, e \, D_p \, T^3}{2 - e} \tag{B-13}$$

Some investigators have assumed that $D_p$ is equal to the particle diameter d. Others have set $D_p = d/(1-P)$.

Schotte [26] assumed spherical particles and considered that the radiation from a plane located on one side of a particle to a plane located on the far side of the particle consists of two parts. First, the radiation across the void space surrounding the particle. Second,

there is radiation from the particle surface in series with conduction through the particle. Combining these two modes, he derived the following equation for the radiant conductivity

$$k_r = \frac{1 - P}{\frac{1}{k_s} + \frac{1}{k_{r_0}}} + P \; k_{r_0} \qquad \text{(B-14a)}$$

where $k_{r_0}$ is the radiant conductivity between particle surfaces which Schotte expressed as

$$k_{r_0} = 4\sigma_b \; e \; d \; T^3 \qquad \text{(B-14b)}$$

It should be noted that when $k_s$ is much larger than $k_{r_0}$, Equation (B-14a) reduces to

$$k_r \simeq 4\sigma_b \; e \; d \; T^3 \qquad \text{(B-14c)}$$

Laubitz, on the other hand, assumed the granular material to be cubic obstacles randomly distributed in cubical volumes, and considering the probability that radiation will pass a cube without hitting an obstacle, he developed the following expression for the radiant conductivity

$$k_r = 4\sigma_b \; e \; d \; T^3 \; [1 - (1-P)^{2/3} + (1-P)^{4/3}]/(1-P) \qquad \text{(B-15)}$$

It should be noted that in all the above developments for which specific geometric configurations have been considered, it has been assumed that the particles are opaque to thermal radiation. The validity of this assumption depends on both the material of the solid phase and the size of the particles compared to the wavelength of radiation. It has been shown by Merrill [118] that glass beads less than 100$\mu$ in diameter cannot be assumed opaque to thermal radiation even at relatively low temperatures. For the case of transparent particles Merrill assumed that the radiant conductivity is equal to the conductivity of the photon gas transmitted through the particles given be

$$k_r = \frac{1}{3} C \nu \lambda_p \qquad (B-16)$$

where C is the specific heat capacity of the photon gas, is the average velocity and $\lambda_p$ is the photon mean free path. The energy density of a photon gas is given by

$$V = \frac{4}{c} \sigma_b T^4 \qquad (B-17)$$

Consequently

$$C = \frac{\partial V}{\partial T} = \frac{16}{c} \sigma_b T^3 \qquad \text{and}$$

$$k_r = \frac{16}{3} \sigma_b T^3 \lambda_p \qquad (B-18)$$

It is easily seen that Equation (B-18) is the same as the radiative component of Equation (B-8), with the exception that for the development of Equation (B-8) the heterogeneous mixture has been assumed to be a pseudo-homogeneous material whereas in Equation (B-18) only the solid phase is considered.

Rosseland [82] treated the radiation heat transfer as a diffusion of photons, and considering a random walk process, he obtained the following expression for the radiant conductivity

$$k_r = \frac{4}{3} \sigma_b \, d \, T^3 \tag{B-19}$$

Troitsky [84] and Bastin et al [85] have suggested that the conduction radiation in the voids and pure radiation processes should be considered acting in parallel, and consequently the effective radiant conductivity should be expressed as

$$k_r = \frac{4\sigma_b \, P \, D_p \, e \, T^3}{2 - e} + \frac{16}{3} \sigma_b \, \frac{T^3}{\bar{a}(T)} \tag{B-20}$$

Loeb [69] considered the case of the radiant conductivity of pores in consolidated porous media. Assuming that linear heat flow is not distrubed in the solid surrounding the pores, he derived the following expression for pores having perfect geometric shapes

$$k_r = 4\gamma \, D_p \, e \, \sigma_b \, T^3 \tag{B-21}$$

where $\gamma$ is a shape factor that depends on the geometry of the pore.

Summarizing the equations for radiant conductivity, it is seen that they can be classified into three groups.

1.  Those assuming the heterogeneous mixture to be a pseudohomogeneous material;

2.  Those based on regular geometric arrangements that permit an algebraic formulation of the radiative heat transfer processes;

3.  Those based on random walk processes.

Although the first class provides the best approximation to the interaction between pure conduction heat transfer and pure radiation heat transfer, lack of experimental work on the radiative properties of heterogeneous mixtures necessitates the application of the second class of equations. Moreover, the experimentally determined values of a and b by Chen and Churchill [81], indicate on one hand that both a and b depend on the type of bed, the solid material and the temperature, and on the other hand that is is perhaps easier to determine the effective thermal conductivity of granular materials experimentally than to determine a and b. For these reasons, at this point it is only possible to include quantitatively the conduction-radiation process in the voids in models of heterogeneous mixtures, while the pure radiation process can only be discussed qualitatively.

In Figure B-1 the values of $k_r$ predicted by various models are plotted verous temperature. In Figure B-2 models of the second and third classifications are compared to Chen and Churchill's model for an aluminum oxide bed at high temperatures.
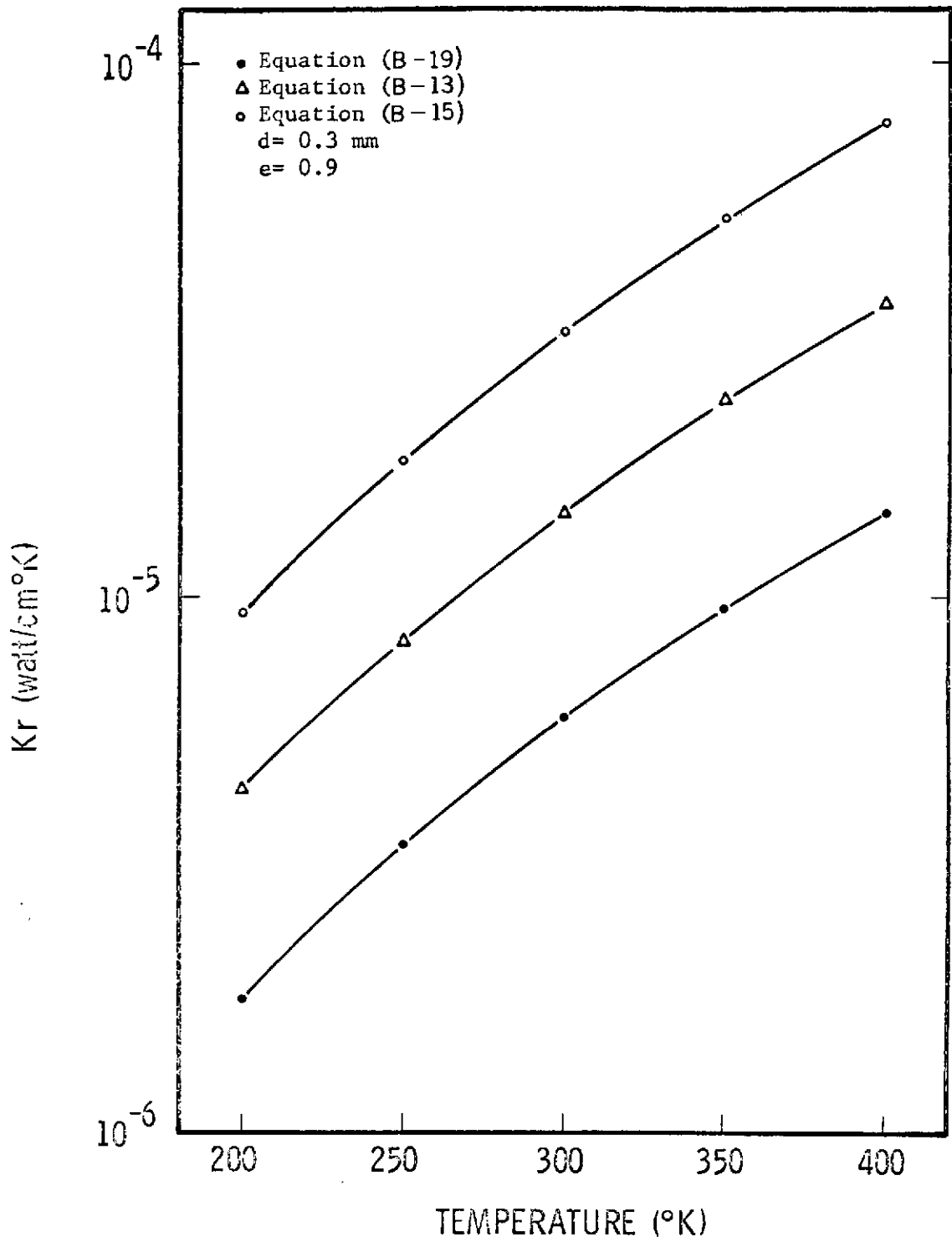
FIGURE B-1. COMPARATIVE VALUES OF Kr.
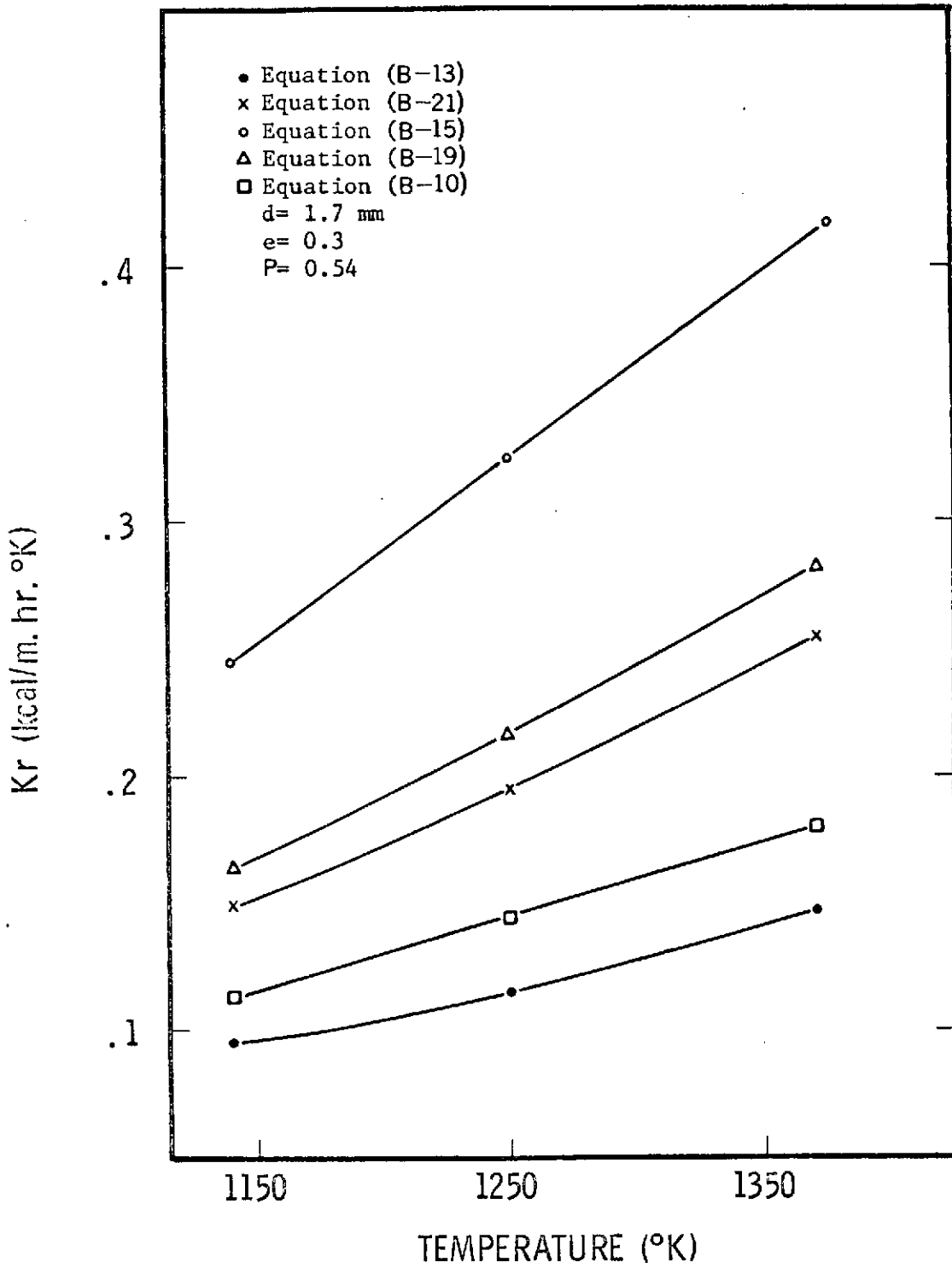
FIGURE B-2. COMPARATIVE VALUES OF Kr FOR AN ALUMINUM OXIDE BED.

# APPENDIX C

## CONTACT RESISTANCE

In accordance with [34] the heat flow from one particle to another contracts in the neighborhood of the contact area between two particles. This contraction of the heat flow lines is amplified in the case of powders under vacuum or in the case of granular materials with a high ratio of constituent conductivities, in which cases the heat flow through contact areas is a major mode of heat transfer. The importance of the contact resistance in the flow of heat in granular materials can be illustrated by the fact that it offers the only explanation as to why the heat flow through perlite at high vacuum at boundary temperatures 76 - 20°K is greater than at temperatures 70 - 4°K, as indicated in [34].

The general procedure followed in the literature is to express the action of the contact areas as a resistance to the heat flow acting between the particle temperatures. Evidently, the heat flow through the contact points depends on the contact area between particles. The expression used by almost all investigators for the radius of this area is Hertz's relation:

$$r_c = \left[ \frac{3}{4} \cdot \frac{1-\nu^2}{E} F_1 \cdot \frac{d}{2} \right]^{1/3} \qquad \text{(C-1)}$$

where d, $\nu$ and E are the diameter, Poisson's ratio and elastic constant respectively of the solid particles, and $F_1$ is the force acting on the contact area. In the case of packed beds in which pressures between particles are due to the layers above the layer under consideration, an expression has been derived for the pressure tensor in [86], the corrected form of which is:

$$P_{ij} = \frac{g}{1-\nu}\left(\int_0^D \rho(x)\, dx\right)\left[\nu\, \delta_{ij} + (1-2\nu)\, z_i z_j\right] \tag{C-2}$$

Multiplication of Equation (C-2) with the unit normal vector to the contact area gives the average pressure.

As indicated in [87] contact resistance in general depends on the following parameters: apparent contact pressure, solid thermal conductivities, surface roughness, surface waviness, interstitial fluid thermal conductivity, solid hardness, solid modulus of elasticity and mean contact temperature level. However, due to the complexity at which these parameters interact, and the difficulty to express a number of these parameters analytically, the procedure taken by many investigators is to examine the contact resistance in the case of smooth spheres, and correlate the derived expressions by experimentally determined coefficients.

Carslaw and Jaeger [88] examined the thermal resistance of a circular contact area on a semi-infinite body, and found it to be:

$$R_\infty^T = 1/4 \; r_c \; k_s \tag{C-3}$$

under the condition of constant temperature on the area having radius $r_c$, and:

$$R_\infty^q = 8/3 \; \pi^2 \; r_c \; k_s \tag{C-4}$$

under the condition of constant heat flux at the area. The values of $R_\infty^T$ and $R_\infty^q$ differ by 8 percent.

Kanager [73], considered the case of a smooth sphere, thermally insulated everywhere except at two diametrically opposite contact areas. He solved Laplace's equation for this problem, and under the assumption that the temperature of the contact area is equal to the arithetic mean of the temperatures at the center and at the periphery, he found an expression for the equivalent thermal resistance of the sphere, $R_s$. Then comparing the ratio $R_s/2 \; R_\infty^q$, he found that it increases almost linearly from 1 to 1.05 for values of $r_c/r$ from 0 to 0.1, where r is the radius of the sphere. His

conclusion was that Equations (C-3) and (C-4) provide a sufficiently accurate approximation for the contact resistance.

Luikov [34] states that in addition to the contraction of the heat flow lines, the effect of the microroughness of real particles should be included in the estimation of the contact resistance, together with the effect of any oxidizing film covering the particles. Thus, the contact resistance of granular systems can be represented as the sum of three components:

$$R_c = R_L + R_o + R_{sp} \qquad (C-5)$$

where $R_L$ is twice the expression given in Equation (C-3), $R_o$ is the resistance due to any oxidizing film, and $R_{s_p}$ is given by:

$$R_{sp} = \frac{h_r k_k}{\pi r_c^2 k_s} \qquad (C-6).$$

where $h_r$ and $k_k$ are experimentally determined coefficients depending on the height of the microroughnesses and on the thermal conductivity of the micrographs respectively. Luikov lists the recommended values for $h_r$ and $k_k$ for a number of granular material classes. Finally, he indicates that the thermal conductivity at the contact areas can be represented by:

$$k_{cr} = \frac{1}{R_c d} \qquad (C-7)$$

In the case of granular materials under externally applied loads, and in cases when particle deformations cannot be assumed elastic, the contact resistance is given in terms of the applied load, the porosity and the solid conductivity by experimentally derived correlations [34, 61, 89]. Wilhelm et al [37], have developed the following empirical equation for the effect of contact areas:

$$\log_{10} (k_{cr} \times 10^5) = 0.859 + 3.12 \left(\frac{k_s}{p}\right) \qquad (C-8)$$

where $k_{cr}$ and $k_s$ are in cal/cm sec. °C. In general the values predicted by Equation (C-8) are much higher than those predicted by Equation (C-7).

# APPENDIX D

## EFFECTIVE PORE SIZE

The equation for $k_g^*$ and $k_r$ have been expressed in terms of an effective distance between particle surfaces $D_p$, called the effective pore size. In the case of $k_g^*$, this is the mean distance gas molecules travel from the surface of one particle to that of another, when the molecular mean free path is large. It follows that this parameter is significant both for the geometric characterization of the granular material, as well as for the heat transfer process.

The initial investigations on the characteristics of packings were concerned with systematic arrangements of spheres [66]. By this method, in order to determine the effective pore size for a range of porosities, it was assumed that the spacing of spheres in rhombohedral array is increased by assuming a halo of thickness $\delta$ around each sphere, and $\delta$ is adjusted to the observed porosity. Dul'nev et al [61] considered this case, and found that the effective pore size is given by:

$$D_p = 4.2 \, d \, (A - 2/3) \tag{D-1}$$

where: $A = [0.74/(1-P)]^{1/3}$

Haughey and Beveridge [5] investigated both analytically and experimentally the case of randomly packed beds of equal-sized spheres for loose packed (P = 0.3812 - 0.4), poured packed (P = 0.364) and close packed (P = 0.3587) beds. Then, they generalized their results for a wide range of porosities. The reported expressions for the mean void hydraulic diameter and for the mean void equivalent hole volume are respectively as follows:

$$(D_p)_h = \frac{2}{3} \ d \ P/(1-P) \qquad (D-2)$$

$$V_h = \frac{\pi}{6} \ d^3 \ P/(1-P) \qquad (D-3)$$

Debbas and Rumpf [51] studied the randomness of beds packed with spheres or irregular shaped particles by means of a statistical approach. Their results are similar to those of Haughey and Beveridge, however the range of porosities examined is not wide enough to allow extrapolation to a wider range of porosities. Nevertheless, an important conclusion that can be reached by the results of both papers is that the local mean voidage is normally distributed, and that beds packed with spheres or irregular particles are in general subject to a statistical analysis. Effectively, it has been shown that in such beds all particles of the same size and shape have the same probability to occupy each unit volume of the mixture. The approach taken by Debbas and Rumpf appears to be very promising with respect to the geometric characterization of

granular materials, but the limited number of experimental data prohibits any generalized conclusions.

The equations presented up to this point have been obtained from geometric considerations. However, as indicated in a previous section, for powders under reduced pressures, most of the heat transfer through the voids takes place in the vicinity of the contact areas. This means that the dimensions effective in conducting heat through the voids are much less than the effective geometric length of the void. To account for this phenomenon, Masamune and Smith [32] considered the volume occupied by pendular rings around the contact points between particles, and derived the following expression for the conduction effective pore size:

$$(D_p)_c = n \, d \, [(\sec \theta - 1)^2 \, (1 - (\tfrac{\pi}{2} - \theta) \tan \theta)] \qquad \text{(D-4)}$$

$$n = 6.93 - 5.51 \, \frac{P - 0.260}{0.476 - 0.260}$$

$$\theta = \cos^{-1} (1 - \frac{1}{n})$$

Dul'nev et al [61] have reported the following equation for $(D_p)_c$ based on the kinetic theory of gases:

$$(D_p)_c = d \, \frac{1.14 \, P - 0.14}{6(1 - P)} \qquad \text{(D-5)}$$

Another approach is to correlate the experimentally determined values for the breakaway pressure to Equation (A-1). Effectively, the pressure at which the effective thermal conductivity of a granular material is reduced by 5 percent was determined from a number of experimental data in the region A of Figure A-1. Subsequently, the value of $k_g^*/k_g$ required to attain this decrease in $k_e$ was calculated, and from Equation (A-1) the corresponding value of $(D_p)_c$ was determined. The experimental data were taken from References [21, 32, 58, 59, 61, 62, 63]. The least squares fit of $(D_p)_c/d$ as a function of P is:

$$\frac{(D_p)_c}{d} = \frac{0.2177 \; P - 0.051}{1 - P} \qquad (D\text{-}6)$$

for

$$0.3 < P < 0.7$$

The values of $D_p/d$ predicted by the equations discussed in this section are plotted in Figure D-1 as a function of P.

(1) Ref. [5]
(2) Ref. [5]
(3) Eq. (D-2)
(4) Eq. (D-1)
(5) Eq. (D-4)
(6) Eq. (D-5)
(7) Eq. (D-6)
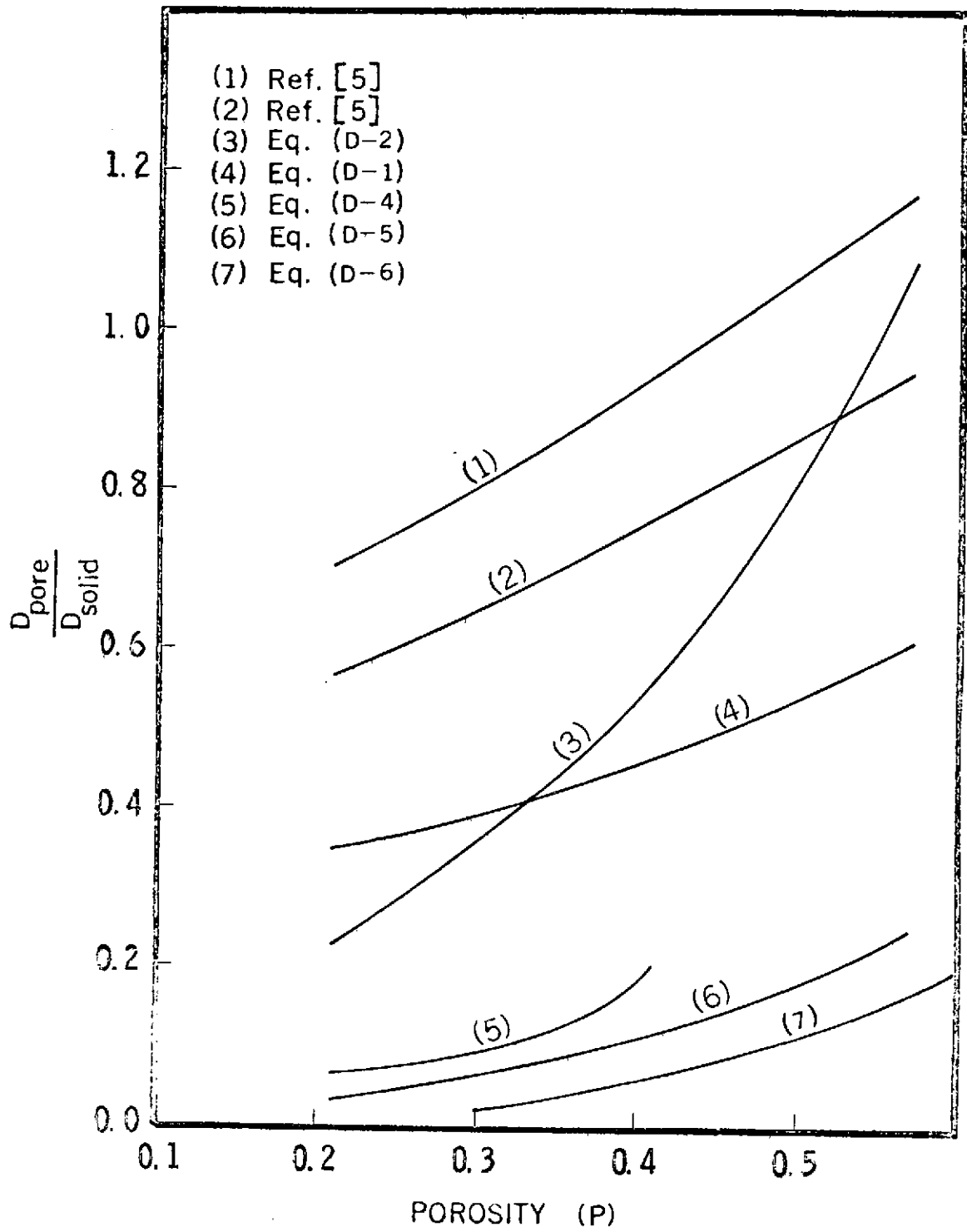
FIGURE D-1. EQUIVALENT PORE SIZE OF GRANULAR MATERIALS.

## APPENDIX E

## COORDINATION NUMBER

It is evident that the heat flux through contact areas depends on the number of contacts each particle has with its neighbors, or the coordination number n [5]. This number is known for regular packings of spheres and is 6 for cubic packing ( P = 0.476), 8 for orthorhombic packing ( P = 0.3954), 10 for tetragonal-sphenoidal packing ( P = 0.3019), and 12 for rhombohedral packing ( P = 0.2595). In addition to these fixed values, extensive experimental work has been done [49, 90, 91, 92] to find the coordination number for random packed beds of spheres, as indicated in Figure E-1. However, almost all of the experimental work has been carried out for loose random and close random beds, and consequently in order to find a relation between n and P extrapolation beyond the experimental data is required.

Dul'nev et al [61] have proposed the following equation:

$$n = 11.6 \ ( \ 1 - P \ ) \tag{E-1}$$

represented by curve 5 in Figure E-1. However it is seen that the predicted values of n are too high at large porosities.

Willhite et al [31] used the results of Smith et al [90] and proposed the following equation:

$$n = 6 \cdot \frac{5.01 - 8.42 \ P}{1.91 - 1.91 \ P} \tag{E-2}$$

However, as noted in [49], this equation is in good agreement with the experimental results of Smith et al, but not with recent experimental data.

Kunii and Smith [30] considered the packed bed to be composed of spheres in the most open packed state and in the closest packed state, and taking into account the frequency and orientation of each cell, they derived the following semi-empirical relationship for the coordination number:

$$n = 13.86 - 51.0 \ (P - 0.26) \tag{E-3}$$

This equation is represented by curve 2 in Figure E-1, and it is seen that it overpredicts n for low values of P.

Haughey and Beveridge [5, 49] examined the distribution of the number of sphere centers found in spherical shells at varying distances from a given sphere, and for a random bed of spheres they developed the following expression for the coordination number:

$$n = 22.47 - 39.39 \ P \tag{E-4}$$

This equation is represented by curve 3 in Figure E-1, and it is seen that it provides the best fit to experimental data.

It should be noted that all equations and experimental data presented in Figure 8 are based on randomly or regularly packed

beds of spheres. However, all heat transfer models, in which contact resistance has been included, have utilized one of these equations for the coordination number. In this study Equation (E-4) has been used, with the reservation that although its application has been extended to mixtures of non-uniform particles, no better expression has been found for real physical systems.
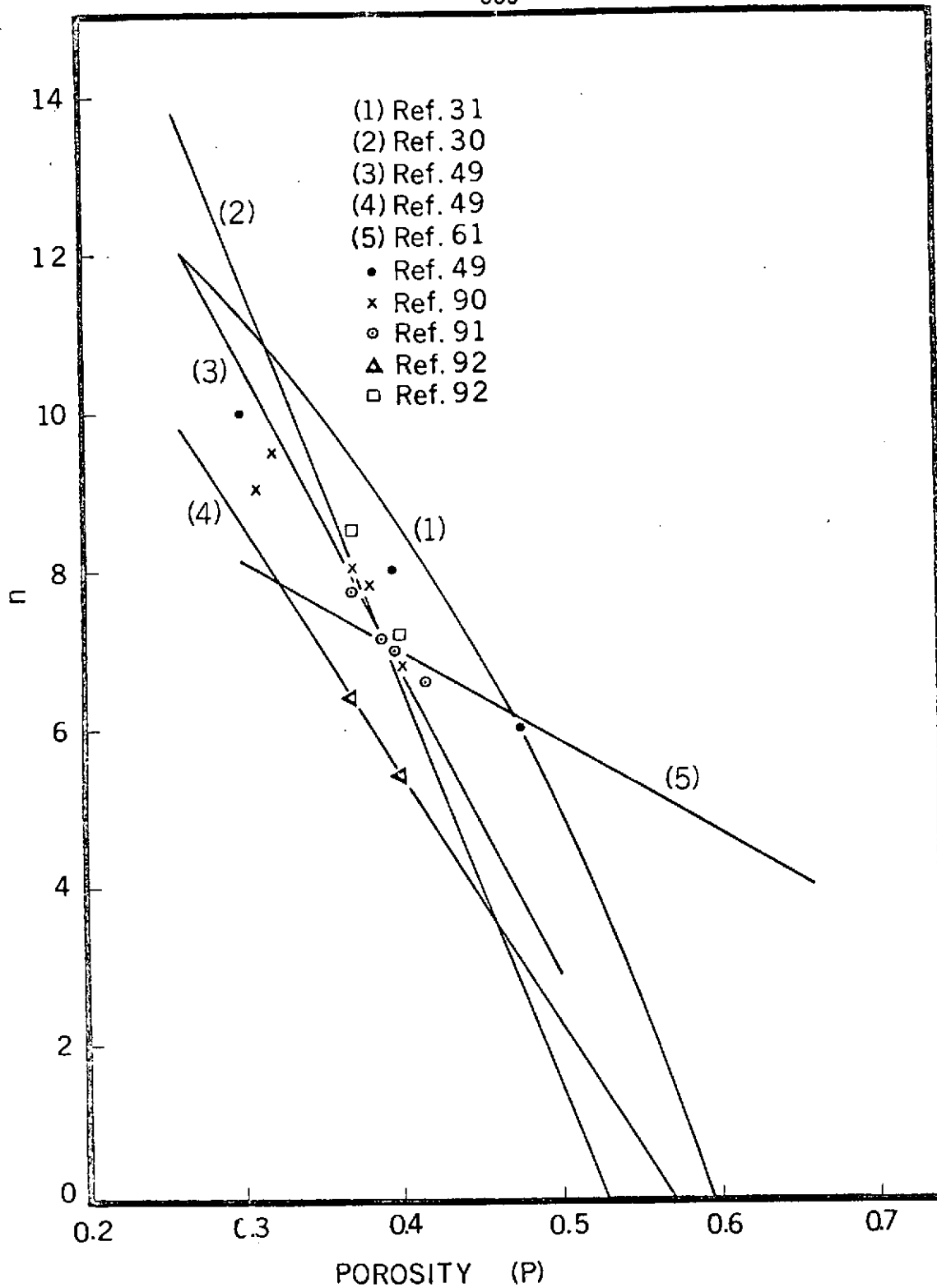
FIGURE E-1. CO-ORDINATION NUMBER.

# APPENDIX F

## PACKING THEORY

One of the most significant complications in the development of
a model that predicts reasonably well the effective thermal conductivity
of heterogeneous materials is the construction of the geometry of such
a model. This complication arises from the large number of parameters
associated with the structural properties of packed beds, as indicated
in an excellent review of the subject by Haughey and Beveridge [49].

In general, the structural properties of packed beds are charac-
terized either by a single representative dimension, or through a
distribution described by mean, variance, skewness, etc. In this study
the first approach has been utilized. Moreover, the equations presented
for the effective pore size and coordination number are based on
random packings of equal sized spheres. This approach has been
necessitated by the fact that most experimental and statistical work
in the literature is referred to this type of packings. Even for this
simplified case, it can be seen from Figures D-1 and E-1 that the effec-
tive pore size and coordination number suggested by various investigators
differ greatly.

Most practical applications involve a particle size variation
between 2 and 100 fold. The mixing of smaller particles into a bed

of larger particles produces two opposing effects. On one hand, the smaller particles tend to increase the voidage by forcing the larger particles apart thus increasing the size of voids between particles, on the other hand the smaller particles tend to decrease the voidage by filling the voids between larger particles. The characteristics of such packed beds do not depend only on the particle shape, and size ratio but also on the amount of each size fraction present. Consequently, from the same particle size distributions, packed beds having a wide range of voidages can be obtained. As indicated in [49, 50, 51, 66] very little information exists about the characteristics of packed beds involving large particle size variations. Consequently, a great degree of ambiguity exists whether a volume mean particle size together with the associated effective pore size calculated from the expressions given in Appendix D provide a sufficiently accurate description of the packed bed. This is especially important in the case of evacuated powders, in which case both particle size and effective pore size are primary parameters in the calculation of the effective thermal conductivity. In particular, for lunar fines the particle size range is from $0.1\mu m$ to approximately $800\mu m$ [119], with most of the particles in the lower size range, and the porosity is assumed to be approximately 0.5. At present, the selection of a particular mean volumetric particle size for the calculation of the effective conductivity is highly speaclative, since no experimental data exist on the local voidage variation for similar packings to compare calculated values.

Evidently, description of packed beds utilizing the local property variations provides a much better approximation to the geometry than characterization of the beds by a single representative dimension. At present, the mean and variance of local properties has been determined in the literature with a satisfactory degree of confidence only for loose packed, poured packed, and close packed random beds of equal sized spheres [5]. Utilization of these data in any future model will probably provide a further refinement to the predicted effective thermal conductivity values of heterogeneous mixtures.

APPENDIX G

FORTRAN IV COMPUTER

PROGRAMS

```
C     THERMAL CONDUCTIVITIES PREDICTED BY FOLLOWING MODELSO
C     1. RUSSELL  2. BERNSTIEN  3. WOODSIDE  4. CRANE AND VACHON
C     (EQUATION 5-2)
      IMPLICIT REAL*4(A-Z)
      INTEGER*4 I,INDEX
      COMMON KC, KD, L, MU, PD, SIGMA, T  ,KE,Q ,CK
      DIMENSION SUM(10),PLOT1(173),PLOT2(173),PLOT3(173),PLOT4(173),
     *Y(173),XLAB(5),YLAB(5),GLAB(5),DATLAB(5)
       DATA SUM,INDEX/10*0.0,0/
      EXTERNAL F
      SUM1BI=0.
      SUM2BI=0.
      SUM3BI=0.
      SUM4BI=0.
      SUMSQ1=0.
      SUMSQ2=0.
      SUMSQ3=0.
      SUMSQ4=0.
      SUMK1E=0.
      SUMK2E=0.
      SUMK3E=0.
      SUMK4E=0.
       PI=3.14159
      READ(5,5)XLAB,YLAB,GLAB,DATLAB
    5 FORMAT(20A4)
  1   WRITE(6,100)
100 FORMAT(1H1,////////////////,25X,'DATA',17X,'EFFECTIVE THERMAL CONDU
     $CTIVITY (KCAL/M-HR-K) X 100 ',//,25X,'CASE',1X ,
     $'  EXPERIMENTAL  ','      RUSSELL    ','     BERNSTEIN    ',
     $'    WOODSIDE    ','      CRANE &    ',/,30X,
     $'                ','                ','                ',
     $'                ','     VACHON     ',/)
  2   READ(5,3,END=6) KC,KD,PD,EXKE,CASE,CASE1,CASE2,MV,MR
  3   FORMAT(4F10.5,3A4,2(F5.0))
      INDEX=INDEX+1
      Y(INDEX)=ALOG10(EXKE/KC)
      E=1.0-PD
      MU=1.0-PD
      IF (MV.GE.1) CALL VACUUM
      SIGMA=0.32248*PD-0.092543*PD**2
      CALL QG10(0.,1.,F,INTF)
      KE=1./INTF
      IF (MR.GE.1) CALL RAD
      CE=KE/KC
      CXKE=EXKE/KC
      DIF=(CE-CXKE)/CXKE
      K4=KE
      PLOT4(INDEX)=ALOG10(K4/KC)
```

```
C       BERNSTEIN
        EP=E
        IF(PD.GE.0.5) GO TO 44
        K2=KC*(4.0*PD/(1.0+KC/KD)+KD/KC*(1.0-2.0*PD))
        GO TO 46
   44   K2=KC*(4.0*EP/(1.0+KC/KD)+(2.0*PD-1.0))
   46   CONTINUE
        PLOT2(INDEX)=ALOG10(K2/KC)
C       WOODSIDE
        RATIO=PI/6.0
        IF(EP.GE.RATIO) EP=RATIO
        A=SQRT(1.0+4.0/(PI*(KD/KC-1.0)*(6.0*EP/PI)**(2./3.)))
        IF(A.LE.1.00001)A=1.00001
        K3=KC/(1.0-(6.0*EP/PI)**(1./3.)*(1.0-(A-1.0/A)*ALOG((A+1.)/(A-1.)
     *      ))
        K3=K3*2.0
        PLOT3(INDEX)=ALOG10(K3/KC)
C       RUSSELL
        R1=2.0/3.0
        K1=KC*(E**R1+KC/KD*(1.0-E**R1))/(E**R1-E+KC/KD*(1.0-E**R1+E))
        PLOT1(INDEX)=ALOG10(K1/KC)
        WRITE(6,200)INDEX,EXKE,K1,K2,K3,K4
  200   FORMAT(/,25X,I4,4X,5(F10.5,6X))
        BK1=((K1-EXKE)/EXKE)*100.
        BK2=((K2-EXKE)/EXKE)*100.
        BK3=((K3-EXKE)/EXKE)*100.
        BK4=((K4-EXKE)/EXKE)*100.
        K1OFF=ABS(BK1)
        K2OFF=ABS(BK2)
        K3OFF=ABS(BK3)
        K4OFF=ABS(BK4)
        SUM1BI=SUM1BI+BK1
        SUM2BI=SUM2BI+BK2
        SUM3BI=SUM3BI+BK3
        SUM4BI=SUM4BI+BK4
        SQK1ER=K1OFF**2
        SQK2ER=K2OFF**2
        SQK3ER=K3OFF**2
        SQK4ER=K4OFF**2
        SUMSQ1=SUMSQ1+SQK1ER
        SUMSQ2=SUMSQ2+SQK2ER
        SUMSQ3=SUMSQ3+SQK3ER
        SUMSQ4=SUMSQ4+SQK4ER
        SUMK1E=SUMK1E+K1OFF
        SUMK2E=SUMK2E+K2OFF
        SUMK3E=SUMK3E+K3OFF
        SUMK4E=SUMK4E+K4OFF
        GO TO 2
```

```
    6 BOCASE=FLOAT(INDEX)
      AVBI1=SUM1BI/BOCASE
      AVBI2=SUM2BI/BOCASE
      AVBI3=SUM3BI/BOCASE
      AVBI4=SUM4BI/BOCASE
      T1ERAV=SUMK1E/BOCASE
      T2ERAV=SUMK2E/BOCASE
      T3ERAV=SUMK3E/BOCASE
      T4ERAV=SUMK4E/BOCASE
      T1ERVA=((SUMSQ1/BOCASE)-T1ERAV**2)/10000.
      T2ERVA=((SUMSQ2/BOCASE)-T2ERAV**2)/10000.
      T3ERVA=((SUMSQ3/BOCASE)-T3ERAV**2)/10000.
      T4ERVA=((SUMSQ4/BOCASE)-T4ERAV**2)/10000.
      WRITE(6,573)AVBI1,AVBI2,AVBI3,AVBI4,T1ERAV,T2ERAV,T3ERAV,T4ERAV,T1
     *ERVA,T2ERVA,T3ERVA,T4ERVA
  573 FORMAT(3X,8F8.2,4F12.4)
      GO TO 621
      CALL ORIGIN(2.5,3.5,1)
       CALL GRAPH(173,Y,PLOT1,3,-7,-5.,-5.,2.,0.,2.,0.,XLAB,YLAB,GLAB,
     *DATLAB)
       CALL ORIGIN(8.5,0.,1)
       CALL GRAPH(173,Y,PLOT2,3,-7,-5.,-5.,2.,0.,2.,0.,XLAB,YLAB,GLAB,
     *DATLAB)
       CALL ORIGIN(8.5,0.,1)
       CALL GRAPH(173,Y,PLOT3,3,-7,-5.,-5.,2.,0.,2.,0.,XLAB,YLAB,GLAB,
     *DATLAB)
       CALL ORIGIN(8.5,0.,1)
       CALL GRAPH(173,Y,PLOT4,3,-7,-5.,-5.,2.,0.,2.,0.,XLAB,YLAB,GLAB,
     *DATLAB)
       CALL ORIGIN(8.5,0.,1)
  621 CONTINUE
      STOP
      END
      FUNCTION F(P)
      REAL MU,KC,KD,INTF,KE,LAMMA,KBOLTZ,K,KNUDSN,L,KR
      COMMON KC, KD, L, MU, PO, SIGMA, T  ,KE,Q ,CK
      X=SIGMA*SQRT(2.0)
      FNORM=ERF((1.0-MU)/X)-ERF((0.-MU)/X)
      P2=(ERF((1.0-MU)/X)-ERF((P-MU)/X))/FNORM
      F=1.0/(KC+(KD-KC)*P2)
      RETURN
      END
```

```
      SUBROUTINE VACCUM
      REAL MU,KC,KD,INTF,KE,LAMMA,KBOLTZ,K,KNUDSN,L,KR
      COMMON KC, KD, L, MU, PD, SIGMA, T  ,KE,Q ,CK
      READ(5,4)T,PRESS,DIAG,K,PR,L,A
4     FORMAT(7E10.0)
      KBOLTZ=1.3804E-23
      PI=3.14159
      C1=.495
      CH=PRESS*1.333224E+7
      CH=PRESS
      WRITE(6,100) CH,DIAG, A, PR, K, L
100   FORMAT(6E11.4)
      LAMMA=KBOLTZ*T/(SQRT(2.)*CH*PI*DIAG**2)*10.0**5
      G=((2.-A)/A)*4.*C1*K/(K+1.)*LAMMA/PR
      KNUDSN=LAMMA/L
      PORE=L*(0.74/MU)**2/43.
      KC=CK/(1.+2.*G/PORE)
      WRITE(6,101) LAMMA,G,KNUDSN,KC
101   FORMAT(4E11.4)
      RETURN
      END
```

```
      SUBROUTINE RAD
      REAL MU,KC,KD,INTF,KE,LAMMA,KBOLTZ,K,KNUDSN,L,KR
      COMMON KC,  KD,  L,  MU,  PD,  SIGMA,  T   ,KE,Q ,CK
      READ(5,1)T,EP
    1 FORMAT (2F10.5)
      EP=0.95
      SIGMAR=5.668E-8
      D=L
      KR=4.0*EP*SIGMAR*D*T**3/((2.0-EP))
      KE=KE+KR
      RETURN
      END
```

```
C     COMPUTER PROGRAM FOR THE NODULAR MODEL
      INTEGER CASE
      REAL KS,KG,KE,KC,KD
      DIMENSION N(N1+2,N1+2,N1+2),R(N1+2,N1+2,N1+2),T(N1+2,N1+2,N1+2),TK
     *(6,N1+2,N1+2,N1+2)
      DIMENSION D(3),C(6)
      N1
      N2=N1+2
      N3=N1+1
      N4=N1-1
      IY=3
      YFL=0.0
      ITEST=0
    1 READ(5,3,END=1000)KS,KG,P,EXKE,CASE
    3 FORMAT(4F10.5,A5)
      READ(5,159)DIAM,POISON,YOUNG,DENS,DEPTH,COEF1,COEF2
  159 FORMAT(E8.3,F4.3,2E8.3,F4.3,F5.4,F4.2)
      WRITE(6,4)
    4 FORMAT(///)
      ITEST=ITEST+1
      M1=N1**3
      M2=N2**3
      M=0
      PORES=P*FLOAT(M2)
      LPORES=PORES
      DO 2 I=1,N2
      DO 2 J=1,N2
      DO 2 K=1,N2
      N(I,J,K)=0
    2 CONTINUE
   20 IA=0
   21 IA=IA+1
      IX=IY
      CALL RANDU(IX,IY,YFL)
      D(IA)=YFL*FLOAT(N2)
      IF(IA-3)21,22,22
   22 CONTINUE
      I1=D(1)
      I2=D(2)
      I3=D(3)
      I=I1+1
      J=I2+1
      K=I3+1
      LA=N(I,J,K)
      IF(LA-1)23,20,20
   23 N(I,J,K)=1
      M=M+1
      IF(M-LPORES)20,24,24
```

```
   24 CONTINUE
      WRITE(6,340)M
  340 FORMAT(3X,'M=',I4)
      A=0.5
      DO 5 K=2,N3
      DO 6 I=1,N2
      DO 6 J=1,N2
    6 T(I,J,K)=A
      A=A+1.
    5 CONTINUE
      DO 38 K=2,N3
      DO 38 I=2,N3
      DO 38 J=2,N3
      IF(N(I,J,K))7,7,8
    7 B=1.
      GO TO 9
    8 B=0.
    9 IF(I-2)202,202,160
  160 IF(N(I-1,J,K))202,11,12
   11 C(1)=1.0
      GO TO 203
   12 C(1)=0.
  203 TK(1,I,J,K)=((B*KS+(1.-B)*KG)*(C(1)*KS+(1.-C(1))*KG))/(0.5*(B*KS+(
     *1.-B)*KG)+0.5*(C(1)*KS+(1.-C(1))*KG).)
      GO TO 13
  202 TK(1,I,J,K)=0.
   13 IF(I-N3)161,204,204
  161 IF(N(I+1,J,K))204,14,15
   14 C(2)=1.0
      GO TO 205
   15 C(2)=0.
  205 TK(2,I,J,K)=((B*KS+(1.-B)*KG)*(C(2)*KS+(1.-C(2))*KG))/(0.5*(B*KS+(
     *1.-B)*KG)+0.5*(C(2)*KS+(1.-C(2))*KG))
      GO TO 16
  204 TK(2,I,J,K)=0.
   16 IF(J-2)206,206,162
  162 IF(N(I,J-1,K))206,17,18
   17 C(3)=1.0
      GO TO 207
   18 C(3)=0.
  207 TK(3,I,J,K)=((B*KS+(1.-B)*KG)*(C(3)*KS+(1.-C(3))*KG))/(0.5*(B*KS+(
     *1.-B)*KG)+0.5*(C(3)*KS+(1.-C(3))*KG))
      GO TO 19
  206 TK(3,I,J,K)=0.
   19 IF(J-N3)163,208,208
  163 IF(N(I,J+1,K))208,30,31
   30 C(4)=1.0
      GO TO 209
```

```
   31 C(4)=0.
  209 TK(4,I,J,K)=((B*KS+(1.-B)*KG)*(C(4)*KS+(1.-C(4))*KG))/(0.5*(B*KS+(
     *1.-B)*KG)+0.5*(C(4)*KS+(1.-C(4))*KG))
      GO TO 32
  208 TK(4,I,J,K)=0.
   32 IF(K-2)210,210,350
  350 IF(N(I,J,K-1))210,33,34
   33 C(5)=1.0
      GO TO 211
   34 C(5)=0.
  211 TK(5,I,J,K)=((B*KS+(1.-B)*KG)*(C(5)*KS+(1.-C(5))*KG))/(0.5*(B*KS+(
     *1.-B)*KG)+0.5*(C(5)*KS+(1.-C(5))*KG))
      GO TO 35
  210 TK(5,I,J,K)=0.
   35 IF(K-N3)351,212,212
  351 IF(N(I,J,K+1))212,36,37
   36 C(6)=1.0
      GO TO 213
   37 C(6)=0.
  213 TK(6,I,J,K)=((B*KS+(1.-B)*KG)*(C(6)*KS+(1.-C(6))*KG))/(0.5*(B*KS+(
     *1.-B)*KG)+0.5*(C(6)*KS+(1.-C(6))*KG))
      GO TO 38
  212 TK(6,I,J,K)=0.
   38 CONTINUE
      PRES=DEPTH*(1.-P)*DENS
      RSP=0.93*(DIAM/2.)*((((1.-(POISUN**2))*PRES)/(YOUNG*((1.-P)**2)))*
     **0.3333)
      HR=COEF1*DIAM
      KC=RSP/((0.5+((HR*COEF2)/(3.14*RSP)))*DIAM)
      CONTR=KC*KS
  185 IF(ITEST-1)186,186,187
  186 CONTAC=95.*(22.47-(39.39*P))
      GO TO 191
  187 IF(ITEST-3)188,188,189
  188 CONTAC=100.*(22.47-(39.39*P))
      GO TO 191
  189 IF(ITEST-6)190,190,191
  190 CONTAC=110.*(22.47-(39.39*P))
  191 CONTINUE
      IF(CONTAC)158,157,157
  158 CONTAC=0.
  157 CONTINUE
      LCONT=CONTAC
      WRITE(6,325)LCONT,CONTR
  325 FORMAT(3X,'LCONT=',I4,' CONTR=',E10.5)
      NUM=0
      NTEST=0
  302 IA=0
```

```
      NTEST=NTEST+1
300 IA=IA+1
      IX=IY
      CALL RANDU(IX,IY,YFL)
      D(IA)=YFL*FLOAT(N1)
      IF(IA-3)300,301,301
301 CONTINUE
      I1=D(1)
      I2=D(2)
      I3=D(3)
      I=I1+2
      J=I2+2
      K=I3+2
      IF(N(I,J,K))302,303,302
303 IF(N(I-1,J,K))304,305,304
305 IF(TK(1,I,J,K)-CONTR)306,304,306
306 IF(I-2)330,330,70
330 TK(1,I,J,K)=CONTR
      GO TO 71
 70 TK(2,I-1,J,K)=CONTR
      TK(1,I,J,K)=CONTR
 71 NUM=NUM+1
304 IF(N(I+1,J,K))307,309,307
309 IF(TK(2,I,J,K)-CONTR)331,307,331
331 IF(I-N3)72,308,308
308 TK(2,I,J,K)=CONTR
      GO TO 73
 72 TK(1,I+1,J,K)=CONTR
      TK(2,I,J,K)=CONTR
 73 NUM=NUM+1
307 IF(N(I,J-1,K))310,311,310
311 IF(TK(3,I,J,K)-CONTR)332,310,332
332 IF(J-2)80,80,74
 80 TK(3,I,J,K)=CONTR
      GO TO 75
 74 TK(4,I,J-1,K)=CONTR
      TK(3,I,J,K)=CONTR
 75 NUM=NUM+1
310 IF(N(I,J+1,K))313,314,313
314 IF(TK(4,I,J,K)-CONTR)315,313,315
315 IF(J-N3)76,81,81
 81 TK(4,I,J,K)=CONTR
      GO TO 77
 76 TK(3,I,J+1,K)=CONTR
      TK(4,I,J,K)=CONTR
 77 NUM=NUM+1
313 IF(N(I,J,K-1))316,318,316
318 IF(TK(5,I,J,K)-CONTR)319,316,319
```

```
319  IF(K-2)82,82,83
 82  TK(5,I,J,K)=CONTR
     GO TO 84
 83  TK(5,I,J,K)=CONTR
     TK(6,I,J,K-1)=CONTR
 84  NUM=NUM+1
316  IF(N(I,J,K+1))321,322,321
322  IF(TK(6,I,J,K)-CONTR)86,321,86
 86  IF(K-N3)323,87,87
 87  TK(6,I,J,K)=CONTR
     GO TO 85
323  TK(6,I,J,K)=CONTR
     TK(5,I,J,K+1)=CONTR
 85  NUM=NUM+1
     IF(NTEST-15000)321,321,100
321  IF(NUM-LCONT)302,324,324
324  CONTINUE
     DO 88 J=2,N3
     DO 88 K=2,N3
     TK(1,2,J,K)=0.
     TK(2,N3,J,K)=0.
 88  CONTINUE
     DO 89 I=2,N3
     DO 89 K=2,N3
     TK(3,I,2,K)=0.
     TK(4,I,N3,K)=0.
 89  CONTINUE
     DO 90 I=2,N3
     DO 90 J=2,N3
     TK(5,I,J,2)=0.
     TK(6,I,J,N3)=0.
 90  CONTINUE
     WRITE(6,500)NUM
500  FORMAT(3X,'NUM=',I4)
502  WRITE(6,501)NTEST
501  FORMAT(3X,'NTEST=',I5)
     L1=0.
101  L1=L1+1
     SR=0.
     DO 10 K=3,N1
     DO 10 I=2,N3
     DO 10 J=2,N3
     R(I,J,K)=TK(1,I,J,K)*(T(I-1,J,K)-T(I,J,K))+TK(2,I,J,K)*(T(I+1,J,K)
    *-T(I,J,K))+TK(3,I,J,K)*(T(I,J-1,K)-T(I,J,K))+TK(4,I,J,K)*(T(I,J+1,
    *K)-T(I,J,K))+TK(5,I,J,K)*(T(I,J,K-1)-T(I,J,K))+TK(6,I,J,K)*(T(I,J,
    *K+1)-T(I,J,K))
     STK=0.
     DO 40 L=1,6
```

```
      TTK=TK(L,I,J,K)
      STK=STK+TTK
  40 CONTINUE
      T(I,J,K)=T(I,J,K)+1.2*(R(I,J,K)/STK).
      SR=SR+ABS(R(I,J,K)/STK)
  10 CONTINUE
      WRITE(6,103)SR
 103 FORMAT(3X,'SR=',E10.4)
      IF(L1-50)150,150,100
 150 IF(SR-5.)102,102,101
 102 CONTINUE
      WRITE(6,104)L1
 104 FORMAT(3X,'L1=',I4)
      AVHEAT=0.
      DO 44 K=2,N1
      THEAT=0.
      DO 45 I=2,N3
      DO 45 J=2,N3
  51 HEAT=(TK(6,I,J,K))*(T(I,J,K+1)-T(I,J,K))
      THEAT=THEAT+HEAT
  45 CONTINUE
      WRITE(6,52)K,THEAT
  52 FORMAT(3X,'K=',I2,'    THEAT=',E10.4)
      AVHEAT=AVHEAT+THEAT
  44 CONTINUE
      KE=AVHEAT/900.
      RATIO=KS/KG
      OFF=((KE-EXKE)/EXKE)*100.
      WRITE(6,105)CASE,KS,KG,P,RATIO,KE,EXKE,OFF
 105 FORMAT(3X,'CASE=',A5,'  KS=',F10.5,'  KG=',F10.5,'  P=',F5.3,'  RA
     *TIO=',F8.2,'  KE=',F10.5,'  EXKE=',F10.5,'  OFF=',F7.2)
 100 CONTINUE
      GO TO 1
1000 STOP
      END
```

<br>

351

```
C      CALCULATION OF EFFECTIVE THERMAL CONDUCTIVITY OF GRANULAR MATER-
C      IALS AT ATMOSPHERIC PRESSURES EXK=EXPERIMENTAL COND., KC=COND. OF
C      CONTINUOUS(GAS OR LIQUID) PHASE, KD=COND. OF DISCONTINUOUS (SOLID)
C      PHASE, P=POROSITY, F=VOLUME FRACTION OF SOLID PHASE, K1=EFF. COND.
C      BY MODEL, K2=BY KRUPICZKA, K3=BY RUSSELL, K4=BY LICHTENECKER AND
C      SON FREY, K5=BY JEFFERSON, K6=BY MAXWELL, K7=BY RAYLEIGH, K8= BY
C      WOODSIDE AND MESSMER, K9=BY MEREDITH AND TOBIAS.
       INTEGER CASE
       REAL K1,K2,K3,K4,K5,K6,K7,K8,K9,KC,KD,KS,KG,K1P,K1BIAS,K2BIAS,K3BI
      *AS,K4BIAS,K5BIAS,K6BIAS,K7BIAS,K8BIAS,K9BIAS
       DIMENSION BK1(100),BK2(100),BK3(100),BK4(100),BK5(100),BK6(100),BK
      *7(100),BK8(100),BK9(100),VOLF(100),KC(100),KD(100),EXK(100),RK(100
      *),RK1(100),RK2(100),RK3(100),RK4(100),RK5(100),RK6(100),RK7(100),R
      *K8(100),RK9(100),POR(100),K1BIAS(100),K2BIAS(100),K3BIAS(100),K4BI
      *AS(100),K5BIAS(100),K6BIAS(100),K7BIAS(100),K8BIAS(100),K9BIAS(100
      *),K1(100),K2(100),K3(100),K4(100),K5(100),K6(100),K7(100),K8(100),
      *K9(100)
       NOCASE=92
       SUM1BI=0.
       SUM2BI=0.
       SUM3BI=0.
       SUM4BI=0.
       SUM5BI=0.
       SUM6BI=0.
       SUM7BI=0.
       SUM8BI=0.
       SUM9BI=0.
       SUMSQ1=0.
       SUMSQ2=0.
       SUMSQ3=0.
       SUMSQ4=0.
       SUMSQ5=0.
       SUMSQ6=0.
       SUMSQ7=0.
       SUMSQ8=0.
       SUMSQ9=0.
       SUMK1E=0.
       SUMK2E=0.
       SUMK3E=0.
       SUMK4E=0.
       SUMK5E=0.
       SUMK6E=0.
       SUMK7E=0.
       SUMK8E=0.
       SUMK9E=0.
       DO 35 I=1,NOCASE
       READ(5,4)KS,KG,P,EXKE,CASE,K1P
     4 FORMAT(4F10.5,A5,F10.5)
```

```
      READ(5,159)DIAM,POISON,YOUNG,DENS,DEPTH,COEF1,COEF2
  159 FORMAT(E8.3,F4.3,2E8.3,F4.3,F5.4,F4.2)
      K1(I)=K1P/100.
      EXK(I)=EXKE
      VOLF(I)=1.-P
      POR(I)=P
      F=1.-P
      C=KG
      D=KS
      KC(I)=KG
      KD(I)=KS
      K2(I)=KG*((KS/KG)**(.280-(.757*ALOG10(P))-(.057*ALOG10(KS/KG))))
      FP=(1.-P)**.6667
      FQ=(1.-P)**.33333
      R=KG/KS
      K3(I)=KG*(FP+R*(1.-FP))/(FP-1.+P+R*(2.-P-FP))
      K4(I)=KG*(1.-FQ+FP+R*(1.-FQ))/(1.-FQ+R)
      W=2.*KG+KS-2.*(1.-P)*(KG-KS)
      Z=2.*KG+KS+F*(KG-KS)
      K6(I)=C*W/Z
      B=F**3.3333*1.569*(C-D)/(4.*C+3.*D)
      K7(I)=C*(W-B)/(Z-B)
      K8(I)=C*((((F+0.03)**2*D)/(0.03*D+F*C))+0.97-F)
    6 X=(D/C-1.)/(D/C+2.)
      K9(I)=(2.+2.*F*X)*(2.+F*(2.*X-1.))/((2.-X*F)*(2.-F*(X+1.)))*C
      XN=.403/FQ-.5
      XK=C*D*(2.*D/(D-C)**2*ALOG(D/C)-2./(D-C))
      XP=.7854/(1.+2.*XN)**2
      K5(I)=C*(1.-XP)+XP*(.5+XN)*XK*C/(.5*C+XN*XK)
      K1BIAS(I)=(((K1(I)-EXKE)/EXKE)*100.)
      K2BIAS(I)=(((K2(I)-EXKE)/EXKE)*100.)
      K3BIAS(I)=(((K3(I)-EXKE)/EXKE)*100.)
      K4BIAS(I)=(((K4(I)-EXKE)/EXKE)*100.)
      K5BIAS(I)=(((K5(I)-EXKE)/EXKE)*100.)
      K6BIAS(I)=(((K6(I)-EXKE)/EXKE)*100.)
      K7BIAS(I)=(((K7(I)-EXKE)/EXKE)*100.)
      K8BIAS(I)=(((K8(I)-EXKE)/EXKE)*100.)
      K9BIAS(I)=(((K9(I)-EXKE)/EXKE)*100.)
      BK1(I)=ABS(K1BIAS(I))
      BK2(I)=ABS(K2BIAS(I))
      BK3(I)=ABS(K3BIAS(I))
      BK4(I)=ABS(K4BIAS(I))
      BK5(I)=ABS(K5BIAS(I))
      BK6(I)=ABS(K6BIAS(I))
      BK7(I)=ABS(K7BIAS(I))
      BK8(I)=ABS(K8BIAS(I))
      BK9(I)=ABS(K9BIAS(I))
      RK1(I)=K1(I)/C
```

```
      RK2(I)=K2(I)/C
      RK3(I)=K3(I)/C
      RK4(I)=K4(I)/C
      RK5(I)=K5(I)/C
      RK6(I)=K6(I)/C
      RK7(I)=K7(I)/C
      RK8(I)=K8(I)/C
      RK9(I)=K9(I)/C
      RK(I)=D/C
      SUM1BI=SUM1BI+K1BIAS(I)
      SUM2BI=SUM2BI+K2BIAS(I)
      SUM3BI=SUM3BI+K3BIAS(I)
      SUM4BI=SUM4BI+K4BIAS(I)
      SUM5BI=SUM5BI+K5BIAS(I)
      SUM6BI=SUM6BI+K6BIAS(I)
      SUM7BI=SUM7BI+K7BIAS(I)
      SUM8BI=SUM8BI+K8BIAS(I)
      SUM9BI=SUM9BI+K9BIAS(I)
      SQK1ER=BK1(I)**2
      SQK2ER=BK2(I)**2
      SQK3ER=BK3(I)**2
      SQK4ER=BK4(I)**2
      SQK5ER=BK5(I)**2
      SQK6ER=BK6(I)**2
      SQK7ER=BK7(I)**2
      SQK8ER=BK8(I)**2
      SQK9ER=BK9(I)**2
      SUMSQ1=SUMSQ1+SQK1ER
      SUMSQ2=SUMSQ2+SQK2ER
      SUMSQ3=SUMSQ3+SQK3ER
      SUMSQ4=SUMSQ4+SQK4ER
      SUMSQ5=SUMSQ5+SQK5ER
      SUMSQ6=SUMSQ6+SQK6ER
      SUMSQ7=SUMSQ7+SQK7ER
      SUMSQ8=SUMSQ8+SQK8ER
      SUMSQ9=SUMSQ9+SQK9ER
      SUMK1E=SUMK1E+BK1(I)
      SUMK2E=SUMK2E+BK2(I)
      SUMK3E=SUMK3E+BK3(I)
      SUMK4E=SUMK4E+BK4(I)
      SUMK5E=SUMK5E+BK5(I)
      SUMK6E=SUMK6E+BK6(I)
      SUMK7E=SUMK7E+BK7(I)
      SUMK8E=SUMK8E+BK8(I)
      SUMK9E=SUMK9E+BK9(I)
   35 CONTINUE
      WRITE(6,1)
    1 FORMAT('1',/////15X,'TABLE II. EXPERIMENTAL AND PREDICTED THERMAL
```

```
     *CONDUCTIVITIES')
      WRITE(6,60)
  60 FORMAT(35X,'FOR VARIOUS MODELS')            *
      WRITE(6,3)
   3 FORMAT(//15X,'CASE',4X,'EXKE',4X,'MODEL',3X,'KRUPIC.',2X,'RUSSELL'
     *,3X,'LICHT.',1X,'JEFFERSON')
      DO 36 I=1,48
      WRITE(6,7)I,EXK(I),K1(I),K2(I),K3(I),K4(I),K5(I)
   7 FORMAT(16X,I2,1X,6F9.4)
  36 CONTINUE
      WRITE(6,1)
      WRITE(6,60)
      WRITE(6,3)
      DO 37 I=49,92
      WRITE(6,2)I,EXK(I),K1(I),K2(I),K3(I),K4(I),K5(I)
   2 FORMAT(16X,I2,1X,6F9.4)
  37 CONTINUE
      WRITE(6,61)
  61 FORMAT('1',/////14X,'TABLE III. EXPERIMENTAL AND PREDICTED THERMAL
     * CONDUCTIVITIES')
      WRITE(6,60)
      WRITE(6,33)
  33 FORMAT(//15X,'CASE',5X,'EXKE',4X,'MAXWELL',2X,'RAYLEIGH',3X,'W AND
     * M',3X,'M AND T')
      DO 38 I=1,48
      WRITE(6,30)I,EXK(I),K6(I),K7(I),K8(I),K9(I)
  30 FORMAT(16X,I2,1X,5F10.4)
  38 CONTINUE
      WRITE(6,61)
      WRITE(6,60)
      WRITE(6,33)
      DO 39 I=49,92
      WRITE(6,31)I,EXK(I),K6(I),K7(I),K8(I),K9(I)
  31 FORMAT(16X,I2,1X,5F10.4)
  39 CONTINUE
      WRITE(6,40)
  40 FORMAT('1',/////15X,'TABLE IV. PERCENTAGE ERROR BETWEEN PREDICTED
     *AND EXPERIMENTAL')
      WRITE(6,41)
  41 FORMAT(31X,'THERMAL CONDUCTIVITIES')
      WRITE(6,42)
  42 FORMAT(//15X,'CASE',5X,'MODEL',5X,'KRUPIC.',4X,'RUSSELL',4X,'LICHT
     *.',3X,'JEFFERSON')
      DO 43 I=1,48
      WRITE(6,44)I,K1BIAS(I),K2BIAS(I),K3BIAS(I),K4BIAS(I),K5BIAS(I)
  44 FORMAT(16X,I2,1X,5F11.3)
  43 CONTINUE
      WRITE(6,40)
```

```
      WRITE(6,41)
      WRITE(6,42)
      DO 45 I=49,92
      WRITE(6,46)I,K1BIAS(I),K2BIAS(I),K3BIAS(I),K4BIAS(I),K5BIAS(I)
 46   FORMAT(16X,I2,1X,5F11.3)
 45   CONTINUE
      WRITE(6,62)
 62   FORMAT('1',//////15X,'TABLE V. PERCENTAGE ERROR BETWEEN PREDICTED A
     *ND EXPERIMENTAL')
      WRITE(6,41)
      WRITE(6,47)
 47   FORMAT(//19X,'CASE',5X,'MAXWELL',4X,'RAYLEIGH',5X,'W AND M',5X,'M
     *AND T')
      DO 48 I=1,48
      WRITE(6,49)I,K6BIAS(I),K7BIAS(I),K8BIAS(I),K9BIAS(I)
 49   FORMAT(20X,I2,1X,4F12.3)
 48   CONTINUE
      WRITE(6,62)
      WRITE(6,41)
      WRITE(6,47)
      DO 50 I=49,92
      WRITE(6,51)I,K6BIAS(I),K7BIAS(I),K8BIAS(I),K9BIAS(I)
 51   FORMAT(20X,I2,1X,4F12.3)
 50   CONTINUE
      WRITE(6,12)
 12   FORMAT('1',2X,115H                        MEAN AND VARIANCE OF PERCENTAGE
     *ERROR BETWEEN MODEL PREDICTED AND EXPERIMENTAL THERMAL CONDUCTIVIT
     *Y)
      WRITE(6,13)
 13   FORMAT(24X,5HMODEL,5X,7HKRUPIC.,5X,7HRUSSELL,6X,6HLICHT.,3X,9HJEFF
     *ERSON,6X,7HMAXWELL,4X,8HRAYLEIGH,3X,9HWO AND MS,5X,7HM AND T)
      BOCASE=NOCASE
      AVBI1=SUM1BI/BOCASE
      AVBI2=SUM2BI/BOCASE
      AVBI3=SUM3BI/BOCASE
      AVBI4=SUM4BI/BOCASE
      AVBI5=SUM5BI/BOCASE
      AVBI6=SUM6BI/BOCASE
      AVBI7=SUM7BI/BOCASE
      AVBI8=SUM8BI/BOCASE
      AVBI9=SUM9BI/BOCASE
      T1ERAV=SUMK1E/BOCASE
      T2ERAV=SUMK2E/BOCASE
      T3ERAV=SUMK3E/BOCASE
      T4ERAV=SUMK4E/BOCASE
      T5ERAV=SUMK5E/BOCASE
      T6ERAV=SUMK6E/BOCASE
      T7ERAV=SUMK7E/BOCASE
```

```
      T8ERAV=SUMK8E/BOCASE
      T9ERAV=SUMK9E/BOCASE
      T1ERVA=((SUMSQ1/BCCASE)-T1ERAV**2)/10000.
      T2ERVA=((SUMSQ2/BOCASE)-T2ERAV**2)/10000.
      T3ERVA=((SUMSQ3/BOCASE)-T3ERAV**2)/10000.
      T4ERVA=((SUMSQ4/BOCASE)-T4ERAV**2)/10000.
      T5ERVA=((SUMSQ5/BCCASE)-T5ERAV**2)/10000.
      T6ERVA=((SUMSQ6/BOCASE)-T6ERAV**2)/10000.
      T7ERVA=((SUMSQ7/BOCASE)-T7ERAV**2)/10000.
      T8ERVA=((SUMSQ8/BOCASE)-T8ERAV**2)/10000.
      T9ERVA=((SUMSQ9/BCCASE)-T9ERAV**2)/10000.
      WRITE(6,16)AVBI1,AVBI2,AVBI3,AVBI4,AVBI5,AVBI6,AVBI7,AVBI8,AVBI9
   16 FORMAT(6X,6HAVGERR,6X,9F12.5)
      WRITE(6,14)T1ERAV,T2ERAV,T3ERAV,T4ERAV,T5ERAV,T6ERAV,T7ERAV,T8ERAV
     *,T9ERAV
   14 FORMAT(6X,6HAVBIAS,6X,9F12.5)
      WRITE(6,15)T1ERVA,T2ERVA,T3ERVA,T4ERVA,T5ERVA,T6ERVA,T7ERVA,T8ERVA
     *,T9ERVA
   15 FORMAT(6X,6HVARERR,7X,9F12.5)
      WRITE(6,17)
   17 FORMAT(///45X,34H DIMENSIONLESS CONDUCTIVITY RATIOS)
      WRITE(6,18)
   18 FORMAT(//131H        KC        KD        P      KD/KC      MODEL
     *KRUPIC.   RUSSELL    LICHT.  JEFFERSON  MAXWELL   RAYLEIGH WO AND
     *MS   M AND T                    )
      DO 20 I=1,NCCASE
   19 FORMAT(13F10.4)
   20 WRITE(6,19)KC(I),KD(I),POR(I),RK(I),RK1(I),RK2(I),RK3(I),RK4(I),RK
     *5(I),RK6(I),RK7(I),RK8(I),RK9(I)
      STOP
      END
```

```
C        THERMAL CONDUCTIVITIES PREDICTED BY FOLLOWING
C        MODELSO  1. SON FREY  2. WOODSIDE AND MESSMER
C        3. HENGST  4. GORRING AND CHURCHILL
         IMPLICIT REAL*4(A-Z)
         INTEGER*4 I,INDEX,IERO,IERR1,IER
         DIMENSION SUM(10),PLOT1(173),PLOT2(173),PLOT3(173),PLOT4(173),
        *Y(173),XLAB(5),YLAB(5),GLAB(5),DATLAB(5)
          DATA SUM,INDEX/10*0.0,0/
         SUM1BI=0.
         SUM2BI=0.
         SUM3BI=0.
         SUM4BI=0.
         SUMSO1=0.
         SUMSO2=0.
         SUMSO3=0.
         SUMSO4=0.
         SUMK1E=0.
         SUMK2E=0.
         SUMK3F=0.
         SUMK4E=0.
          PI=3.14159
         READ(5,5)XLAB,YLAB,GLAB,DATLAB
       5 FORMAT(20A4)
    1    WRITE(6,100)
   100 FORMAT(1H1,///////////////////,25X,'DATA',17X,'EFFECTIVE THERMAL CONDU
        $CTIVITY (KCAL/M-HR-K)  X 100 ',//,25X,'CASE',1X ,
        $'  EXPERIMENTAL  ','      SON FREY    ','     WOODSIDE        ',
        $'       HENGST     ','      GORRING &   ',/,30X,
        $'                  ','                  ','  & MESSMER       ',
        $'                  ','     CHURCHILL    ',/)
    2    READ(5,3,END=6) KC,KD,PD,EXKE,CASE,CASE1,CASE2
    3    FORMAT(4F10.5,3A4)
         INDEX=INDEX+1
         Y(INDEX)=ALOG10(EXKE/KC)
         E=1.0-PD
C        SONFREY  EQ
         R7=1.0/3.0
          R8=KC/KD
         K1=KC*(1.0-E**R7+E+R8*(E**R7-E))/(1.0-E**R7+R8*E**R7)
         PLOT1(INDEX)=ALOG10(K1/KC)
C        WOODSIDE & MESSMER  EQ
         K2=KC*((E+0.03)**2*KD/(0.03*KD+E*KC)+0.97-E)
         PLOT2(INDEX)=ALOG10(K2/KC)
C        HENGST
         N=11.6*E
         K3=KC*(N*E*KD/(2.0*(KD-KC))*(KD/(KD-KC)*ALOG(KD/KC)-1.0))
         PLOT3(INDEX)=ALOG10(K3/KC)
C        GORRING & CHURCHILL
```

```
      X=1.0
      C=10.*PD/PI
      IF(PD.LE.0.314159) GO TO 4
      C=(3.0*PI/(5.0*PI-20.0*PD))**1.5
      X=1.0/C**(1.0/3.0)
    4 B=(KC/(C*(KD-KC)))**(1.0/3.0)
      K4=KC*(PI/(6.0*(1.0-KC/KD)*C*B)*(ALOG(SQRT(B**2-B*X+X**2)/(B+X))
     *       +SQRT(3.0)*ATAN((2.0*X-B)/(SQRT(3.0)*B))-SQRT(3.)*ATAN
     *(-1.0/SQRT(3.0))                     )+1.0-PI*X**2/4.)
      KH=EXKE
      IF(K4.GT.EXKE) KH=K4
      SUM(4) = SUM(4) + ((K4-EXKE)/KH)**2
      PLOT4(INDEX)=ALOG10(K4/KC)
      WRITE(6,200)INDEX,EXKE,K1,K2,K3,K4
  200 FORMAT(/,25X,I4,4X,5(F10.5,6X))
      BK1=((K1-EXKE)/EXKE)*100.
      BK2=((K2-EXKE)/EXKE)*100.
      BK3=((K3-EXKE)/EXKE)*100.
      BK4=((K4-EXKE)/EXKE)*100.
      K1OFF=ABS(BK1)
      K2OFF=ABS(BK2)
      K3OFF=ABS(BK3)
      K4OFF=ABS(BK4)
      SUM1BI=SUM1BI+BK1
      SUM2BI=SUM2BI+BK2
      SUM3BI=SUM3BI+BK3
      SUM4BI=SUM4BI+BK4
      SQK1ER=K1OFF**2
      SQK2ER=K2OFF**2
      SQK3ER=K3OFF**2
      SQK4ER=K4OFF**2
      SUMSQ1=SUMSQ1+SQK1ER
      SUMSQ2=SUMSQ2+SQK2ER
      SUMSQ3=SUMSQ3+SQK3ER
      SUMSQ4=SUMSQ4+SQK4ER
      SUMK1E=SUMK1E+K1OFF
      SUMK2E=SUMK2E+K2OFF
      SUMK3E=SUMK3E+K3OFF
      SUMK4E=SUMK4E+K4OFF
      IF(INDEX.EQ.14) GO TO 1
      IF(INDEX.EQ.28) GO TO 1
      IF(INDEX.EQ.42) GO TO 1
      IF(INDEX.EQ.56) GO TO 1
      IF(INDEX.EQ.70) GO TO 1
      IF(INDEX.EQ.84) GO TO 1
      IF(INDEX.EQ.98) GO TO 1
      IF(INDEX.EQ.112) GO TO 1
      IF(INDEX.EQ.126) GO TO 1
```

```
      IF(INDEX.EQ.140) GO TO 1
      IF(INDEX.EQ.154) GO TO 1
      GO TO 2
   6  BOCASE=FLOAT(INDEX)
      AVBI1=SUM1BI/BOCASE
      AVBI2=SUM2BI/BOCASE
      AVBI3=SUM3BI/BOCASE
      AVBI4=SUM4BI/BOCASE
      T1ERAV=SUMK1E/BOCASE
      T2ERAV=SUMK2E/BOCASE
      T3ERAV=SUMK3E/BOCASE
      T4ERAV=SUMK4E/BOCASE
      T1ERVA=((SUMSQ1/BOCASE)-T1ERAV**2)/10000.
      T2ERVA=((SUMSQ2/BOCASE)-T2ERAV**2)/10000.
      T3ERVA=((SUMSQ3/BOCASE)-T3ERAV**2)/10000.
      T4ERVA=((SUMSQ4/BOCASE)-T4ERAV**2)/10000.
      WRITE(6,573)AVBI1,AVBI2,AVBI3,AVBI4,T1ERAV,T2ERAV,T3ERAV,T4ERAV,T1
     *ERVA,T2ERVA,T3ERVA,T4ERVA
  573 FORMAT(3X,8F8.2,4F12.4)
      GO TO 621
      CALL ORIGIN(2.5,3.5,1)
       CALL GRAPH(173,Y,PLOT1,3,-7,-5.,-5.,2.,0.,2.,0.,XLAB,YLAB,GLAB,
     *DATLAB)
      CALL ORIGIN(8.5,0.,1)
       CALL GRAPH(173,Y,PLOT2,3,-7,-5.,-5.,2.,0.,2.,0.,XLAB,YLAB,GLAB,
     *DATLAB)
      CALL ORIGIN(8.5,.1,1)
       CALL GRAPH(173,Y,PLOT3,3,-7,-5.,-5.,2.,0.,2.,0.,XLAB,YLAB,GLAB,
     *DATLAB)
      CALL ORIGIN(8.5,.1,1)
       CALL GRAPH(173,Y,PLOT4,3,-7,-5.,-5.,2.,0.,2.,0.,XLAB,YLAB,GLAB,
     *DATLAB)
      CALL ORIGIN(8.5,.1,1)
  621 CONTINUE
      STOP
      END
```

```
C      THERMAL CONDUCTIVITY PREDICTED BY FOLLOWING
C      MODELSO  1. WILLHITE, KUNII AND SMITH  2. SCHUMANN
C      AND VOSS  3. PRESTON  4  KRUPICZKA
       IMPLICIT REAL*4(A-Z)
       INTEGER*4 I,INDEX
       DIMENSION SUM(10),PLOT1(173),PLOT2(173),PLOT3(173),PLOT4(173),
      *Y(173),XLAB(5),YLAB(5),GLAB(5),DATLAB(5)
        DATA SUM,INDEX/10*0.0,0/
       SUM1BI=0.
       SUM2BI=0.
       SUM3BI=0.
       SUM4BI=0.
       SUMSQ1=0.
       SUMSQ2=0.
       SUMSQ3=0.
       SUMSQ4=0.
       SUMK1E=0.
       SUMK2E=0.
       SUMK3E=0.
       SUMK4E=0.
        PI=3.14159
       READ(5,5)XLAB,YLAB,GLAB,DATLAB
     5 FORMAT(20A4)
   1    WRITE(6,100)
 100 FORMAT(1H1,////////////////,25X,'DATA',17X,'EFFECTIVE THERMAL CONDU
     $CTIVITY (KCAL/M-HR-K) X 100 ',//,25X,'CASE',1X ,
     $'  EXPERIMENTAL  ',' '     WILLHITE,   ',' '     SCHUMANN     ',
     $'      PRESTON     ',' '    KRUPICZKA   ',/,30X,
     $'                  ',' '  KUNII & SMITH ',' '     & VOSS     ',
     $'                  ',' '                ',/)
   2  READ(5,3,END=6) KC,KD,PD,EXKE,CASE,CASE1,CASE2
   3  FORMAT(4F10.5,3A4)
      INDEX=INDEX+1
      Y(INDEX)=ALOG10(EXKE/KC)
      E=1.0-PD
C     WILLHITE, KUNII,& SMITH
      N=3.0*(5.01-8.42*PD)/(1.91-1.91*PD)
      IF(N.LE.1.0) N=1.0
      THETA=ARSIN(SQRT(1.0/N))
      GAMMA=0.5
      ALPHA=1.0/(2.0*N)*(1.0-KC/KD)**2/(ALOG(KD/KC-
     *  (KD/KC-1.0)*COS(THETA))-(1.0-KC/KD)*(1.0-COS(THETA)))
      K1=KC*(1.0+E*(1.0-KC/KD)+GAMMA/ALPHA*(1.0-KC/KD)**2*E)
      KH=EXKE
      IF(K1.GT.EXKE) KH=K1
      SUM(1) = SUM(1) + ((K1-FXKE)/KH)**2
      PLOT1(INDEX)=ALOG10(K1/KC)
C  SHUMANN
```

```
      IF(PD.GE.0.5) GO TO 31
      KE=KEXP
      M=.2
   30 Y1=M*(M+1.)*ALOG((1.+M)/M)-M-PD
      IF(ABS(Y1).LT..0005)GO TO 40
      YP=(2.0*M+1.0)*ALOG((1.0+M)/M)-2.0
      M=M-Y1/YP
      GO TO 30
   31 M=10000.
   40 K2=KC*PD**3+KC*(1.-PD**3)*KD/(KC+M*(KC-KD))*(1.0+M*(1.0+M)*(KC-KD)
     */(KC+M*(KC-KD))*ALOG(KC*(1.0+M)/(M*KD)))
      PLOT2(INDEX)=ALOG10(K2/KC)
C     PRESTON
      K3=1.88574*K2**0.959
      PLOT3(INDEX)=ALOG10(K3/KC)
C     KRUPICZKA
      K4=KC*(KD/KC)**(0.280-0.757*ALOG10(PD)-0.057*ALOG10(KD/KC))
      PLOT4(INDEX)=ALOG10(K4/KC)
      WRITE(6,200)INDEX,EXKE,K1,K2,K3,K4
  200 FORMAT(/,25X,I4,4X,5(F10.5,6X))
      BK1=((K1-EXKE)/EXKE)*100.
      BK2=((K2-EXKE)/EXKE)*100.
      BK3=((K3-EXKE)/EXKE)*100.
      BK4=((K4-EXKE)/EXKE)*100.
      K1OFF=ABS(BK1)
      K2OFF=ABS(BK2)
      K3OFF=ABS(BK3)
      K4OFF=ABS(BK4)
      SUM1BI=SUM1BI+BK1
      SUM2BI=SUM2BI+BK2
      SUM3BI=SUM3BI+BK3
      SUM4BI=SUM4BI+BK4
      SQK1ER=K1OFF**2
      SQK2ER=K2OFF**2
      SQK3ER=K3OFF**2
      SQK4ER=K4OFF**2
      SUMSQ1=SUMSQ1+SQK1ER
      SUMSQ2=SUMSQ2+SQK2ER
      SUMSQ3=SUMSQ3+SQK3ER
      SUMSQ4=SUMSQ4+SQK4ER
      SUMK1E=SUMK1E+K1OFF
      SUMK2E=SUMK2E+K2OFF
      SUMK3E=SUMK3E+K3OFF
      SUMK4E=SUMK4E+K4OFF
      IF(INDEX.EQ.14) GO TO 1
      IF(INDEX.EQ.28) GO TO 1
      IF(INDEX.EQ.42) GO TO 1
      IF(INDEX.EQ.56) GO TO 1
```

```
      IF(INDEX.EQ.70) GO TO 1
      IF(INDEX.EQ.84) GO TO 1
      IF(INDEX.EQ.98) GO TO 1
      IF(INDEX.EQ.112) GO TO 1
      IF(INDEX.EQ.126) GO TO 1
      IF(INDEX.EQ.140) GO TO 1
      IF(INDEX.EQ.154) GO TO 1
      IF(INDEX.EQ.168) GO TO 1
      GO TO 2
    6 BOCASE=FLOAT(INDEX)
      AVBI1=SUM1BI/BOCASE
      AVBI2=SUM2BI/BOCASE
      AVBI3=SUM3BI/BOCASE
      AVBI4=SUM4BI/BOCASE
      T1ERAV=SUMK1E/BOCASE
      T2ERAV=SUMK2E/BOCASE
      T3ERAV=SUMK3E/BOCASE
      T4ERAV=SUMK4E/BOCASE
      T1ERVA=((SUMSQ1/BOCASE)-T1ERAV**2)/10000.
      T2ERVA=((SUMSQ2/BOCASE)-T2ERAV**2)/10000.
      T3ERVA=((SUMSQ3/BOCASE)-T3ERAV**2)/10000.
      T4ERVA=((SUMSQ4/BOCASE)-T4ERAV**2)/10000.
      WRITE(6,573)AVBI1,AVBI2,AVBI3,AVBI4,T1ERAV,T2ERAV,T3ERAV,T4ERAV,T1
     *ERVA,T2ERVA,T3ERVA,T4ERVA
  573 FORMAT(3X,8F8.2,4F12.4)
      GO TO 621
      CALL ORIGIN(2.5,3.5,1)
       CALL GRAPH(173,Y,PLOT1,3,-7,-5.,-5.,2.,0.,2.,0.,XLAB,YLAB,GLAB,
     *DATLAB)
       CALL ORIGIN(8.5,0.,1)
       CALL GRAPH(173,Y,PLOT2,3,-7,-5.,-5.,2.,0.,2.,0.,XLAB,YLAB,GLAB,
     *DATLAB)
       CALL ORIGIN(8.5,0.,1)
       CALL GRAPH(173,Y,PLOT3,3,-7,-5.,-5.,2.,0.,2.,0.,XLAB,YLAB,GLAB,
     *DATLAB)
       CALL ORIGIN(8.5,0.,1)
       CALL GRAPH(173,Y,PLOT4,3,-7,-5.,-5.,2.,0.,2.,0.,XLAB,YLAB,GLAB,
     *DATLAB)
       CALL ORIGIN(8.5,0.,1)
  621 CONTINUE
      STOP
      END
```

```
C     THERMAL CONDUCTIVITIES PREDICTED BY FOLLOWING
C     MODELS 0  1. EQUATION 6-16  2. EQUATION 6-17
C     3. EQUATION 6-18  4. LICHTENECKER 3-D
      IMPLICIT REAL*8 (A-Z)
      INTEGER*4 I,INDEX
        COMMON MU,SIGMA,KC,KD
      DIMENSION SUM(10),PLOT1(173),PLOT2(173),PLOT3(173),PLOT4(173),
     *Y(173),XLAB(5),YLAB(5),GLAB(5),DATLAB(5),PLOT5(173),PLOT6(173)
       DATA SUM,INDEX/10*0.0,0/
      MU=0.499
        PI=3.141592653589793
      SIGMA=10.0D0
      SUM4BI=0.
      SUMSQ4=0.
      SUMK4E=0.
      READ(5,190)XLAB,YLAB,GLAB,DATLAB
 190  FORMAT(20A4)
  1   WRITE(6,100)
 100  FORMAT(1H1,////////////////,25X,'DATA',17X,'EFFECTIVE THERMAL CONDU
     $CTIVITY (KCAL/M-HR-K) X 100 ',//,25X,'CASE',1X ,
     $'  EXPERIMENTAL ','  EQUATION 6-16 ','  EQUATION 6-17 ',
     $'  EQUATION 6-18 ','   LICHTENKER   ',/)
  5 READ(5,3,END=6) KC,KD,PD,EXKE,CASE,CASE1,CASE2
  3   FORMAT(4F10.5,3A4)
      INDEX=INDEX+1
      Y(INDEX)=DLOG10(EXKE/KC)
      E=1.0-PD
      IF(PD.GE.0.5) MU=0.51
      EPSI=1.0D0-PD
        X=SIGMA*DSQRT(2.0D0)
      FN1=X*DSQRT(PI)/2.0D0
        IF(PD.LT.0.5)GO TO 12
        IF(PD.GT.0.5)GO TO 21
      X1=(1.0D0-MU)/X
      X2=(0.0D0-MU)/X
      FN=FN1*(DERF(X1)-DERF(X2))
      CALL DQG32(0.0D0,1.0D0,F,INTF)
        KE1=INTF/FN
      CALL DQG32(0.0D0,1.0D0,F2,REMN)
 12 DO 11 I=1,6
 50 CALL DQG32(0.0D0,1.0D0,F1,ANSW)
      X1=(1.0D0-MU)/X
      X2=(0.0D0-MU)/X
      FN=FN1*(DERF(X1)-DERF(X2))
        BNSW=1.0D0-ANSW/FN
      IF(BNSW.LE.PD) GO TO 11
      MU=MU+10.0D0**(-I)
      GO TO 50
```

```
   11 MU=MU-10.0D0**(-I)
      GO TO 7
   21 DO22 I=1,6
    9 CALL DQG32(0.0D0,1.0D0,F1,ANSW)
      X1=(1.0D0-MU)/X
      X2=(0.0D0-MU)/X
      FN=FN1*(DERF(X1)-DERF(X2))
         BNSW=1.D0-ANSW/FN
      IF(BNSW.GE.PD) GO TO 22
      MU=MU-10.0D0**(-I)
      GO TO 9
   22 MU=MU+10.0D0**(-I)
      GO TO 7
         KE2=FN/REMN
      PLOT5(INDEX)=DLOG10(KE1/KC)
      PLOT6(INDEX)=DLOG10(KE2/KC)
      RK = KD/KC
      FO=DEXP(-2.4006+0.83611*DLOG(RK)-0.0036959*DLOG(RK)**2+12.426*PD
     *         -16.278*PD**2-3.0926*DLOG(RK)*PD+0.0019151*DLOG(RK)**3
     *         -0.034069*DLOG(RK)**2*PD+3.3197*DLOG(RK)*PD**2
     *         +2.5768*PD**3)
      FINF=DEXP(6.038+0.28697*DLOG(RK)-0.0796930*DLOG(RK)**2-42.035*PD
     *         +94.701*PD**2-0.91135*DLOG(RK)*PD+0.0029629*DLOG(RK)**3
     *         +0.0040281*DLOG(RK)**2*PD+0.80897*DLOG(RK)*PD**2
     *         -69.049*PD**3)
      FW=1.5287+0.064259*DLOG(RK)-0.0064623*DLOG(RK)**2-6.1759*EPSI
     *         +11.059*EPSI**2+0.22176*DLOG(RK)*EPSI+0.00015041*DLOG(RK)
     *      **3-0.0042453*DLOG(RK)**2*EPSI-0.10971*DLOG(RK)*EPSI**2
     *         -7.2252*EPSI**3
      IF(FW.GE.1.0)FW=1.0
      IF(FW.LE.0.0)FW=0.0
      K3=KE2-FW*(KE2-KE1)
      PLOT3(INDEX)=DLOG10(K3/KC)
      K2=KE1*FO
      PLOT2(INDEX)=DLOG10(K2/KC)
         K1=KE2*FINF
      PLOT1(INDEX)=DLOG10(K1/KC)
C     LICHTENKER   EQ
      K=1.5*(KD-KC)/((2.0*DSQRT(KD)+DSQRT(KC))*(2.0*DSQRT(KC)+
     *      DSQRT(KD)))
      K4=(KC**(PD*(1.0-K*E)))*(KD**(E*(1.0+K*PD)))
      PLOT4(INDEX)=DLOG10(K4/KC)
      BK4=((K4-EXKE)/EXKE)*100.
      K4OFF=DABS(BK4)
      SUM4BI=SUM4BI+BK4
      SQK4ER=K4OFF**2
      SUMSQ4=SUMSQ4+SQK4ER
      SUMK4E=SUMK4E+K4OFF
```

```
       GO TO 5
  6 BOCASE=FLOAT(INDEX)
    AVBI4=SUM4BI/BOCASE
    T4ERAV=SUMK4E/BOCASE
    T4ERVA=((SUMSQ4/BOCASE)-T4ERAV**2)/10000.
    WRITE(6,576)AVBI4,T4ERAV,T4ERVA
576 FORMAT(3X,3F20.5)
    WRITE(6,200)INDEX,EXKE,K1,K2,K3,K4
200 FORMAT(/,25X,I4,4X,5(F10.5,6X))
    WRITE(6,572)BK1,BK2,BK3
572 FORMAT(3X,'BK1=',F7.2,'   BK2=',F7.2,'   BK3=',F7.2)
    WRITE(6,573)AVBI1,AVBI2,AVBI3,T1ERAV,T2ERAV,T3ERAV,T1ERVA,T2ERVA,T
   *3ERVA
573 FORMAT(3X,9F12.4)
    CALL ORIGIN(2.5,3.5,1)
     CALL GRAPH(-173,Y,PLOT1,3,-7,-5.,-5.,2.,0.,2.,0.,XLAB,YLAB,GLAB,
   *DATLAB)
    CALL ORIGIN(8.5,0.,1)
     CALL GRAPH(-173,Y,PLOT2,3,-7,-5.,-5.,2.,0.,2.,0.,XLAB,YLAB,GLAB,
   *DATLAB)
    CALL ORIGIN(8.5,.1,1)
     CALL GRAPH(-173,Y,PLOT3,3,-7,-5.,-5.,2.,0.,2.,0.,XLAB,YLAB,GLAB,
   *DATLAB)
    CALL ORIGIN(8.5,.1,1)
     CALL GRAPH(-173,Y,PLOT4,3,-7,-5.,-5.,2.,0.,2.,0.,XLAB,YLAB,GLAB,
   *DATLAB)
    CALL ORIGIN(8.5,.1,1)
    STOP
    END
    DOUBLE PRECISION FUNCTION F(P)
    IMPLICIT REAL*8 (A-Z)
       COMMON MU,SIGMA,KC,KD
       F=DEXP(-0.5D0*((P-MU)/SIGMA)**2)*KC*KC/(P*(KC-KD)+KD)
       RETURN
       END
    DOUBLE PRECISION FUNCTION F1(P)
    IMPLICIT REAL*8 (A-Z)
       COMMON MU,SIGMA,KC,KD
       F1=P*DEXP(-0.5D0*((P-MU)/SIGMA)**2)
       RETURN
       END
    DOUBLE PRECISION FUNCTION F2(P)
    IMPLICIT REAL*8 (A-Z)
       COMMON MU,SIGMA,KC,KD
       F2=DEXP(-0.5*((P-MU)/SIGMA)**2)/(KC+(KD-KC)*P)
       RETURN
       END
```

```
C     THERMAL CONDUCTIVITY PREDICTED BY THE FOLLOWING
C     MODELSO  1. MAXWELL  2. RAYLEIGH  3. MEREDITH
C     AND TOBIAS  4. BRUGGEMAN
      IMPLICIT REAL*4(A-Z)
      INTEGER*4 I,INDEX
      DIMENSION SUM(10),PLOT1(173),PLOT2(173),PLOT3(173),PLOT4(173),
     *Y(173),XLAB(5),YLAB(5),GLAB(5),DATLAB(5)
      DATA SUM,INDEX/10*0.0,0/
      SUM1BI=0.
      SUM2BI=0.
      SUM3BI=0.
      SUM4BI=0.
      SUMSQ1=0.
      SUMSQ2=0.
      SUMSQ3=0.
      SUMSQ4=0.
      SUMK1E=0.
      SUMK2E=0.
      SUMK3E=0.
      SUMK4E=0.
      PI=3.14159
      READ(5,5)XLAB,YLAB,GLAB,DATLAB
    5 FORMAT(20A4)
    1 WRITE(6,100)
  100 FORMAT(1H1,/////////////////,25X,'DATA',17X,'EFFECTIVE THERMAL CONDU
     $CTIVITY (KCAL/M-HR-K) X 100 ',//,25X,'CASE',1X ,
     $'  EXPERIMENTAL ',' MAXWELL  ','  RAYLEIGH  ',
     $'  MEREDITH  ','  BRUGGEMAN  ',/,30X,
     $'  ','  ',' ',
     $'  & TOBIAS  ','  ',' ',/)
    2 READ(5,3,END=6) KC,KD,PD,EXKE,CASE,CASE1,CASE2
    3 FORMAT(4F10.5,3A4)
      INDEX=INDEX+1
      Y(INDEX)=ALOG10(EXKE/KC)
      E=1.0-PD
C     MAXWELL  EQ
      K1=KC*(KD+2.0*KC-2.0*E*(KC-KD))/(KD+2.0*KC+E*(KC-KD))
      PLOT1(INDEX)=ALOG10(K1/KC)
C     RAYLEIGH  EQ
      R1=(2.0*KC+KD)/(KC-KD)
      R2=(3.0*KC-3.0*KD)/(4.0*KC+3.0*KD)
      R3=10.0/3.0
      K2=KC*(R1-2.0*E-0.525*R2*E**R3)/(R1+E-0.525*R2*E**R3)
      PLOT2(INDEX)=ALOG10(K2/KC)
C     MEREDITH & TOBIAS
      K3=KC*(4.0*KC+2.0*KD-2.0*E*(KC-KD))/(4.0*KC+2.0*KD+E*(KC-KD))
     *    *(4.0*KC+2.0*KD-E*(4.0*KC-KD))/(4.0*KC+2.0*KD-E*(KC+2.0*KD))
      PLOT3(INDEX)=ALOG10(K3/KC)
```

```
C      BRUGGEMAN
       KEFF=EXKE
 10    Y1=(KEFF-KD)/(KC-KD)*(KC/KEFF)**(1./3.)-PD
       IF(ABS(Y1).LT..0005)GO TO 20
       YP=1./(KC-KD)*(KC/KEFF)**(1./3.)-(1./3.)*(KEFF-KD)/(KC-KD)*(KC**(1
      *./3.))/(KEFF**(4./3.))
       KEFF=KEFF-(Y1/YP)
       IF(KEFF.LE.0.0) KEFF=1.0E-8
       GO TO 10
 20    K4=KEFF
       PLOT4(INDEX)=ALOG10(K4/KC)
       WRITE(6,200)INDEX,EXKE,K1,K2,K3,K4
200    FORMAT(/,25X,I4,4X,5(F10.5,6X))
       BK1=((K1-EXKE)/EXKE)*100.
       BK2=((K2-EXKE)/EXKE)*100.
       BK3=((K3-EXKE)/EXKE)*100.
       BK4=((K4-EXKE)/EXKE)*100.
       K1OFF=ABS(BK1)
       K2OFF=ABS(BK2)
       K3OFF=ABS(BK3)
       K4OFF=ABS(BK4)
       SUM1BI=SUM1BI+BK1
       SUM2BI=SUM2BI+BK2
       SUM3BI=SUM3BI+BK3
       SUM4BI=SUM4BI+BK4
       SQK1ER=K1OFF**2
       SQK2ER=K2OFF**2
       SQK3ER=K3OFF**2
       SQK4ER=K4OFF**2
       SUMSQ1=SUMSQ1+SQK1ER
       SUMSQ2=SUMSQ2+SQK2ER
       SUMSQ3=SUMSQ3+SQK3ER
       SUMSQ4=SUMSQ4+SQK4ER
       SUMK1E=SUMK1E+K1OFF
       SUMK2E=SUMK2E+K2OFF
       SUMK3E=SUMK3E+K3OFF
       SUMK4E=SUMK4E+K4OFF
       GO TO 2
  6    BOCASE=FLOAT(INDEX)
       AVBI1=SUM1BI/BOCASE
       AVBI2=SUM2BI/BOCASE
       AVBI3=SUM3BI/BOCASE
       AVBI4=SUM4BI/BOCASE
       T1ERAV=SUMK1E/BOCASE
       T2ERAV=SUMK2E/BOCASE
       T3ERAV=SUMK3E/BOCASE
       T4ERAV=SUMK4E/BOCASE
       T1ERVA=((SUMSQ1/BOCASE)-T1ERAV**2)/10000.
```

```
      T2ERVA=((SUMSQ2/BOCASE)-T2ERAV**2)/10000.
      T3ERVA=((SUMSQ3/BOCASE)-T3ERAV**2)/10000.
      T4ERVA=((SUMSQ4/BOCASE)-T4ERAV**2)/10000.
      WRITE(6,573)AVBI1,AVBI2,AVBI3,AVBI4,T1ERAV,T2ERAV,T3ERAV,T4ERAV,T1
     *ERVA,T2ERVA,T3ERVA,T4ERVA
  573 FORMAT(3X,8F8.2,4F12.4)
      GO TO 621
      CALL ORIGIN(2.5,3.5,1)
        CALL GRAPH(173,Y,PLOT1,3,-7,-5.,-5.,2.,0.,2.,0.,XLAB,YLAB,GLAB,
     *DATLAB)
      CALL ORIGIN(8.5,0.,1)
        CALL GRAPH(173,Y,PLOT2,3,-7,-5.,-5.,2.,0.,2.,0.,XLAB,YLAB,GLAB,
     *DATLAB)
      CALL ORIGIN(8.5,0.,1)
        CALL GRAPH(173,Y,PLOT3,3,-7,-5.,-5.,2.,0.,2.,0.,XLAB,YLAB,GLAB,
     *DATLAB)
      CALL ORIGIN(8.5,0.,1)
        CALL GRAPH(173,Y,PLOT4,3,-7,-5.,-5.,2.,0.,2.,0.,XLAB,YLAB,GLAB,
     *DATLAB)
      CALL ORIGIN(8.5,0.,1)
  621 CONTINUE
      STOP
      END
```

```
C     THERMAL CONDUCTIVITIES CALCULATED BY THE
C     FOLLOWING MODELS 1. WILHELM ET AL  2. LICH-
C     TENECKER 2-D  3. KANAGER
      IMPLICIT REAL*4(A-Z)
      INTEGER*4 I,INDEX
      DIMENSION SJM(10),PLOT(172),Y(172),XLAB(5),YLAB(5),GLAB(5),DATLAB(
     *5),PLOT1(172),PLOT2(172),PLOT3(172)
      DATA SJM,INDEX/10*0.0,0/
      SJM3I1=0.
      SJM3I2=0.
      SJM3I3=0.
      SJMSQ1=0.
      SJMSQ2=0.
      SJMSQ3=0.
      SJMK1E=0.
      SJMK2E=0.
      SJMK3E=0.
      PI=3.14159
      READ(5,5)XLAB,YLAB,GLAB,DATLAB
    5 FORMAT(20A4)
    2 READ(5,3,END=5) KC,KD,PD,EKKE,CASE,CASE1,CASE2
    3 FORMAT(4F10.5,3A4)
      INDEX=INDEX+1
      Y(INDEX)=ALOG10(EKKE/KC)
      E=1.0-PD
C     WILHELM ET AL
      IF(PD.GE.0.5) GO TO 31
      M=.2
   30 Y1=M*(M+1.)*ALOG((1.+M)/M)-M-PD
      IF(ABS(Y1).LT..0005)GO TO 40
      Y2=(2.0*M+1.0)*ALOG((1.0+M)/M)-2.0
      M=M-Y1/Y2
      GO TO 30
   31 M=10000.
   40 K7=(KC*PD**3+KC*(1.-PD)**3)*KD/((KC+M*(KC-KD))*(1.0+M*(1.0+M)*(KC-KD)
     */(KC+M*(KC-KD)))*ALOG(KC*(1.0+M)/(M*KD)))
      K8=(10.**.859)*(10.**(3.12*(KD/(100.*360.*PD))))*.0036
      K1=100.*K8+K7
      PLOT1(INDEX)=ALOG10(K1/KC)
C     LICHTENECKER
      K2=(KC**PD)*(KD**E)
      PLOT2(INDEX)=ALOG10(K2/KC)
C     KANAGER
      V=11.5*E
      A=KD-KC
      K3=((V*E*KC*KD)/(2.*A))*(((KD/A)*ALOG(KD/KC))-1.)
      PLOT3(INDEX)=ALOG10(K3/KC)
      BK1=(((K1-EKKE)/EKKE)*100.)
```

```fortran
      BK2=((K2-EXKE)/EXKE)*100.
      BK3=((K3-EXKE)/EXKE)*100.
      K1DFF=ABS(BK1)
      K2DFF=ABS(BK2)
      K3DFF=ABS(BK3)
      SUM1BI=SUM1BI+BK1
      SUM2BI=SUM2BI+BK2
      SUM3BI=SUM3BI+BK3
      SQK1ER=K1DFF**2
      SQK2ER=K2DFF**2
      SQK3ER=K3DFF**2
      SUMSQ1=SUMSQ1+SQK1ER
      SUMSQ2=SUMSQ2+SQK2ER
      SUMSQ3=SUMSQ3+SQK3ER
      SUMK1E=SUMK1E+K1DFF
      SUMK2E=SUMK2E+K2DFF
      SUMK3E=SUMK3E+K3DFF
      WRITE(5,203)INDEX,EXKE,BK1,BK2,BK3
  203 FORMAT(3X,'CASE=',I3,'   EXKE=',F10.5,'   DFF1=',F7.2,'   DFF2=',F
     *7.2,'   DFF3=',F7.2)
      GO TO 2
    5 BOCASE=FLOAT(INDEX)
      AVBI1=SUM1BI/BOCASE
      AVBI2=SUM2BI/BOCASE
      AVBI3=SUM3BI/BOCASE
      T1ERAV=SUMK1E/BOCASE
      T2ERAV=SUMK2E/BOCASE
      T3ERAV=SUMK3E/BOCASE
      T1ERVA=T1ERVA
      T1ERVA=((SUMSQ1/BOCASE)-T1ERAV**2)/10000.
      T2ERVA=((SUMSQ2/BOCASE)-T2ERAV**2)/10000.
      T3ERVA=((SUMSQ3/BOCASE)-T3ERAV**2)/10000.
      WRITE(6,573)AVBI1,AVBI2,AVBI3,T1ERAV,T2ERAV,T3ERAV,T1ERVA,T2ERVA,T
     *3ERVA
  573 FORMAT(3X,6F10.2,3F14.4)
      STOP
      END
```